UNIVERSITÉ DE NEUCHÂTEL

Hydrogen-bonded Metalla-assemblies

Thèse présentée à la Faculté des Sciences,

Pour l'obtention du grade de Docteur ès Sciences

Fan ZHANG

Titulaire d'un Master de Chimie supramoléculaire de l'Université de Strasbourg, France

Membres du jury :

Prof. Bruno THERRIEN	Directeur de thèse, Université de Neuchâtel
Prof. Robert DESCHENAUX	Rapporteur interne, Université de Neuchâtel
Prof. David MONCHAUD	Rapporteur externe, Université de Bourgogne

Institut de Chimie de l'Université de Neuchâtel

Soutenue le 09/10/2018

UNIVERSITÉ DE NEUCHÂTEL

Faculté des Sciences
Secrétariat-décanat de Faculté
Rue Emile-Argand 11
2000 Neuchâtel – Suisse
Tél : + 41 (0)32 718 21 00
E-mail : secretariat.sciences@unine.ch

IMPRIMATUR POUR THESE DE DOCTORAT

La Faculté des sciences de l'Université de Neuchâtel autorise l'impression de la présente thèse soutenue par

Madame Fan ZHANG

Titre:

"Hydrogen-bonded Metalla-assemblies"

sur le rapport des membres du jury composé comme suit:

- Prof. associé, Bruno Therrien, directeur de thèse, Université de Neuchâtel, Suisse
- Prof. Robert Deschenaux, Université de Neuchâtel, Suisse
- Dr David Monchaud, CNRS, Université de Dijon, France

Neuchâtel, le 15 novembre 2018

Le Doyen, Prof. P. Felber

P. Fel

Remerciements

C’est grâce à l’aide de nombreuses personnes que j’ai pu mener ce travail doctoral à son terme. De ce fait, mes souhaits les plus chers seront de remercier vivement toutes les personnes de l’institut de chimie à l’université de Neuchâtel.

Je souhaite en premier lieu adresser mes plus sincères remerciements à mon directeur de thèse, le Professeur Bruno THERRIEN, pour m’avoir accueillie dans son laboratoire en tant que doctorante, pour le temps qu’il m’a consacré tout au long de cette thèse, pour ses conseils et sa guidance, pour la confiance qu’il m’a accordé, ainsi que pour son soutien financier.

Je remercie l’entreprise « Cytrozene Paris » pour m’avoir apporté son soutien financier, ce qui m’a permis de finir ma thèse.

Mes remerciements vont également à Professeur Robert DESCHENAUX et Professeur David MONCHAUD pour avoir accepté de faire partie de mon jury de thèse.

Je souhaiterais exprimer ma gratitude aux Professeur Robert DESCHENAUX, Professeur Stephan VON REUSS et Professeur Edith JOSEPH.

Je souhaiterais exprimer ma gratitude à mon époux Minghui YUAN pour son soutien quotidien et dans le domaine de la chimie.

J’adresse également mes remerciements à tous les collègues que j’ai rencontrés dans notre groupe : Marie GASCHARD, Vidya MANNANCHERRIL, Dr. Cristina ALVARINO BOUZA, Dr. Bing SUN, Dr. Thomas CHEMINEL, Dr. David STIBAL.

Je tiens également à remercier Dr. SUTOUR Sylvain Aime Roger pour son aide lors des analyses de RMN.

Je remercie également les collègues de l’institut de chimie: Mathilde MONACHON, Magdalena ALBELDA BERENGUER, Lidia MATHYS, Celia BERGAME, Rocio RIVERA SANCHEZ, Dr. Siva BANDI, Giau LE Hoang, Yassine CHADI Ahmed, Aurelien BILLOT.

Enfin, mes remerciements vont à ma famille qui m’a apporté le soutien économique pour étudier et vivre à l’étranger, ainsi qu’à mes amis en Chine et ici, qui m’accompagnent dans ma vie.

Abstract

Hydrogen bonds are the most utilized non-covalent interactions in biological systems, due to their directionality, stability, reversibility and diversity. The weak strength of hydrogen-bond can be modified by combining several hydrogen bonds in the same unit, like in the melamine·cyanuric/barbituric acid rosette-type system.

Arene ruthenium metalla-assemblies have showed a great biological potential. Inspired by the combination of hydrogen bonding and metal complexation from the group of de Mendoza, we have recently prepared a series of hydrogen-bonded metalla-assemblies. Therefore, to further investigate hydrogen-bonded metalla-assemblies, we used the melamine/barbituric rosette-type system with piano-stool complexes or dinuclear metalla-clips. The introduction of a pyridyl group on the barbituric acid moiety or the melamine moiety allows coordination of metals at the periphery of the rosette.

New rosette-type metalla-assemblies have been prepared and characterized. Neutral and cationic trinuclear rosette-type metalla-assemblies have been synthesized, as well as hetero-hexanuclear rosette-type metalla-assemblies. Coordination of dinuclear metalla-clips has produced cationic hexanuclear metalla-assemblies. Overall, rosette-type assemblies with piano-stool complexes offer great opportunities in the field of supramolecular chemistry.

Keywords

Rosettes, Hydrogen bonds, Ruthenium, Rhodium, Iridium, Piano-stool complexes, Metalla-clips, Metal coordination, Self-assembly.

Mots Clés

Rosette, Liaison hydrogène, Ruthénium, Rhodium, Iridium, Métallo-clip, Complexe tabouret-de-piano, Chimie de coordination, Auto-assemblage.

Table of Contents

Chapter 7

Chapter 1

Introduction

1.1 Hydrogen bonding

1.1.1 Definition

Hydrogen bonds are the most important interactions in supramolecular chemistry, and it is widely used in chemical, biological and physical science. The term ‘‘hydrogen

bond'' was first mentioned by Bernal in 1935,[1] followed by Huggins in 1936.[2] The first definition was given by Pauling in 1939,[3] only then the hydrogen-bond theory started to display an important role in the understanding of some natural substances, such as water, proteins, sugars and so on. Since the 1970s, many researchers have changed their focusing field from theoretical chemistry to biochemistry and materials science.[4-5] And in 1997, the IUPAC defined hydrogen bonds in the ''Compendium of Chemical Terminology''.[6] Then the definition of hydrogen bonds was updated and detailed in 2011. The new definition says: '*The hydrogen bond is an attractive interaction between a hydrogen atom from a molecule or a molecular fragment X-H in which X is more electronegative than H, and an atom or a group of atoms in the same or a different molecule, in which there is evidence of bond formation.*'[7] Until now, there are almost 100 years of history about ''hydrogen bond'' interactions, but it is still a growing research area.

The hydrogen-bonded system generally contains three parts (Figure 1). Hydrogen atom is necessary and it connects to an atom D (donor) by a covalent bond and is attracted at the same time by another atom A (acceptor). The dipole-dipole interaction between the hydrogen atom and atom A is defined as ''Hydrogen bonding''.[8] Atoms D and A are electronegative atoms, their electronegativity is larger than that of hydrogen. Examples are C, N, O, S and Cl with electronegativity of respectively C: 2.55, H: 2.20, N: 3.04, O: 3.44, S: 2.58, Cl: 3.16.[9] In such systems, atom D can be considered as the ''donor'', due to its strong electronegativity, the electrons around the hydrogen atom are pulled towards D, giving a partially negative charge to atom D (δ^-) and a partially positive charge to the hydrogen atom (δ^+).[10] Generally, atom A is an atom or an anion, or a fragment (A-B), with a lone pair of electrons. This lone pair attracts the hydrogen atom, therefore atom A can be considered as the ''acceptor''.[7] Therefore hydrogen-bonded systems are generally expressed as D-H···A systems.

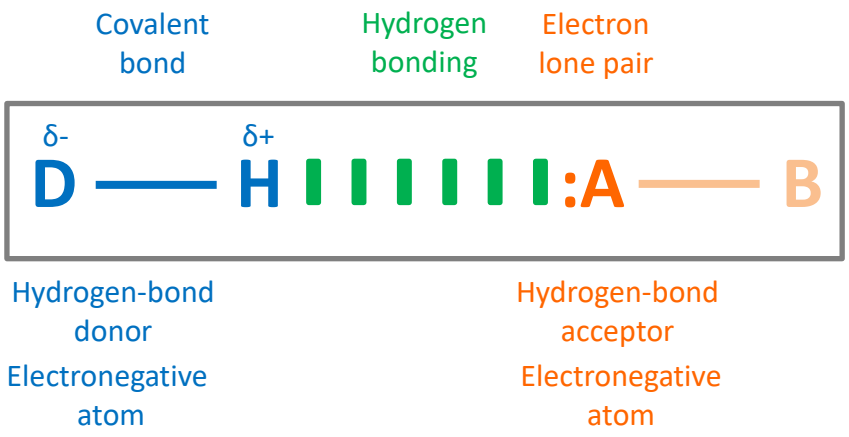

Figure 1: Components of a hydrogen-bonded system

1.1.2 Properties and characteristics

Hydrogen bonds have special properties in comparison with other non-covalent interactions, such as directionality, reversibility, stability and diversity. Several characteristics of hydrogen bonds will now be introduced.

The orientation of hydrogen bonds is defined from the hydrogen-bond donor towards the hydrogen-bond acceptor, so it can be determined for each hydrogen-bond donor/acceptor pairs. Another important factor is the D-H···A angle. This angle is usually equal or close to 180 °, and should preferably be more than 110 °. For example, the hydrogen-bond angle of the hydrogen fluoride dimer is 171.21 °(Figure 2).[7]

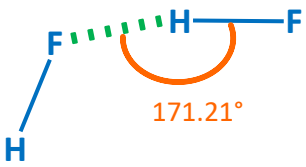

Figure 2: Representation of hydrogen bond in the hydrogen fluoride dimer

Hydrogen bonds are much weaker than other non-covalent interactions, except for ‘van der Waals’ interactions. Furthermore, covalent bonds are almost ten times stronger than hydrogen bonds.[11] So the hydrogen bond has been defined as a relatively weak interaction, but it has a wide range of interaction strengths. Depending on various

strengths, a classification of hydrogen bonds was proposed by Jeffrey.[12] This classification can help us to analyze hydrogen bonds qualitatively in different structures.

Hydrogen bonds were divided into three types by Jeffrey (Table 1), a strong interaction with a strength of 14 – 40 kcal mol^{-1}, a moderate interaction with a strength of 4 – 15 kcal mol^{-1} and a weak interaction with a strength of less than 4 kcal mol^{-1}. The strong hydrogen bond is similar to a covalent bond; its bond length is close to the bond length of DH. The shape of strong hydrogen bonds is almost linear, for example the $[F\cdots H\cdots F]^-$ has a strength of 38.6 kcal mol^{-1} with a D-H···A angle of 171.21 °.[13] This type of hydrogen bonds is usually formed between a strong acid and a good hydrogen-bond acceptor, or a strong base and a good hydrogen-bond donor. Moderate hydrogen bonds form between neutral hydrogen-bond donor and neutral hydrogen-bond acceptor *via* electron lone pairs.[9] Hydrogen bonds formed by acids, alcohols, phenols and hydrates in biological molecules show moderate interaction. The bond length of moderate hydrogen bonds is longer than that of D-H, and their shape is slightly bent, like the [O-H···O=C], and [O-H···O-H].[14] Then weak hydrogen bonds are electrostatic, with a bond length two or three times longer than that of D-H. The shape of weak hydrogen bonds is non-linear. Normally, weak hydrogen bonds can form between weak hydrogen-bond donor and strong hydrogen-bond acceptor (C-H···O=C), strong hydrogen-bond donor and weak hydrogen-bond acceptor (O-H···C=C), or weak hydrogen-bond donor and weak hydrogen-bond acceptor (C≡C-H···C≡C). These weak hydrogen bonds always play a role of stabilizing the molecular structures.

From another point of view, we can observe that the stronger the hydrogen bond is, the shorter the distance between hydrogen atom and hydrogen-bond acceptor are, and also that the shape of hydrogen bonds is closer to linear. Through this rule, we can better characterize hydrogen bonds.[12]

	Strong	Moderate	Weak
D-H···A interaction	Mainly covalent	Mainly electrostatic	Electrostatic
Bond lengths	$d_{DH} \approx d_{HA}$	$d_{DH} < d_{HA}$	$d_{DH} << d_{HA}$
d_{HA} (Å)	1.2 – 1.5	1.5 – 2.2	2.2 – 3.2
d_{DA} (Å)	2.2 – 2.5	2.5 – 3.2	3.2 – 4.0
Bond angles [°]	175 – 180	130 – 180	90 – 150
Bond energy (kcal mol^{-1})	14 – 40	4 – 15	< 4
^{1}H NMR chemical shift downfield (ppm)	14 – 22	< 14	–
Examples	➢ Gas-phase dimers with strong acids or strong bases ➢ Acid salts ➢ Proton sponges ➢ Pseudohydrates ➢ HF complexes	➢ Acids ➢ Alcohols ➢ Phenols ➢ Hydrates ➢ All biological molecules	➢ Gas-phase dimers with weak acids or weak bases ➢ Minor components of 3-center bonds ➢ C – H···O/N bonds ➢ O/N – H···π bonds

Table 1: Classification and properties of hydrogen bonds

Solvent is a factor that cannot be ignored in any interacting systems, especially in hydrogen-bonded systems. The hydrogen-bonding interaction strongly depends on the solvent. In other words, the strength of hydrogen bonds will be influenced in protic and polar solvents such as water. Hydrogen bonds are easy to break in these solvents. Hunter's group studied a hydrogen-bonded system between perfluoro-*tert*-butyl alcohol and tri-*n*-butylphosphine oxide, and its association constants in different solvents were published (Figure 3).[15] Results showed that their association constants in carbon

tetrachloride and cyclohexane were better than those in other polar solvents, because of limited competitions with hydrogen bonds for nonpolar solvents.

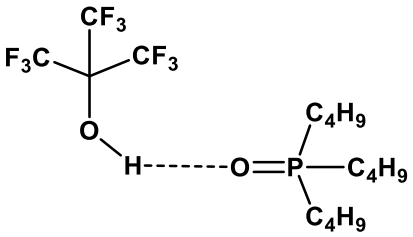

Solvents	Association constants (K_a in M^{-1})
DMSO	6.8×10^{-1}
Acetonitrile	1.6×10^{2}
THF	2.4×10^{2}
Nitromethane	1.5×10^{3}
$CHCl_3$	2.7×10^{3}
CCl_4	7.6×10^{4}
Cyclohexane	$>10^{5}$

Figure 3: Association constants in different solvents of the hydrogen-bonded system perfluoro-*tert*-butyl alcohol and tri-*n*-butylphosphine oxide[15]

Therefore, most hydrogen-bonded systems are analyzed in chloroform, toluene and cyclohexane.[16] However, the poor solubility of some hydrogen-bonded systems in these solvents can be problematic. In 2008, the strength of hydrogen-bonded assemblies was increased by Rehm and Schmuck, through combinations with other interactions such as hydrophobic contacts, metal-ligand interactions or ion-pair formations,[17] thus offering the possibility to use other solvents to study hydrogen-bonded systems.

As we know, hydrogen bonds are relatively weak interactions, the most direct method to increase its strength is the combination of several hydrogen bonds together.[18] Therefore, a wide range of double, triple and quadruple hydrogen-bonded systems has been synthesized and studied. The cooperativity gives a much stronger system than single hydrogen bond.[10]

The strength of the single hydrogen bond depends on the basicity of the hydrogen-bond donor and the acidity of the hydrogen-bond acceptor.[19] However, for multi-hydrogen-bonded systems, the strength can be increased by multiplying hydrogen bonds.[20] Some examples are listed in Figure 4, we can see that UPy dimer with four

hydrogen bonds is more stable than G-C with three hydrogen bonds, and G-C is more stable than A-T with two hydrogen bonds.

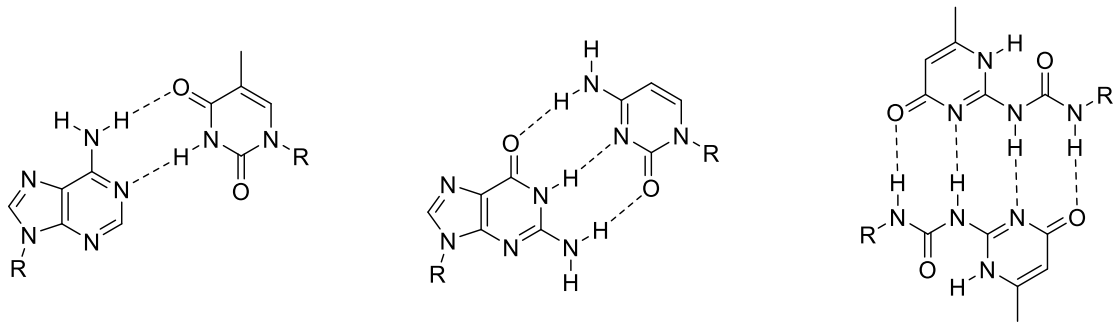

A-T G-C Upy dimer

$K_a = 10^2$ м$^{-1}$ $K_a = 10^4 – 10^5$ м$^{-1}$ $K_a > 10^6$ м$^{-1}$

Figure 4: Multi-hydrogen-bonded systems and their association constants

The number of hydrogen bonds is not the unique factor affecting the strength of multi-hydrogen-bonded systems. Intramolecular hydrogen bonds, preorganizations, secondary interactions, tautomerizations and electronic substituent effects cannot be ignored.

In recent years, scientists are more attracted by triple and quadruple hydrogen-bonded systems, because they are good linkers for constructing supramolecular assemblies. Secondary interactions exist almost in all triple and quadruple hydrogen-bonded systems. Therefore we need to study these secondary interactions.

Secondary electrostatic interactions were identified by the group of Jorgensen in 1990.[21] Due to partial charges on adjacent atoms, attractions and repulsions occur and have an effect on the stability of the multi-hydrogen-bonded system.[22] The strength of a multi-hydrogen-bonded system will be stronger, if there is more attractive secondary electrostatic interactions. On the contrary, the higher the number of secondary repulsions is, the weaker the strength will be. Thus DDD-AAA array with only attractive interactions is more stable than the ADA-DAD and AAD-DDA arrays (Figure 5).[23]

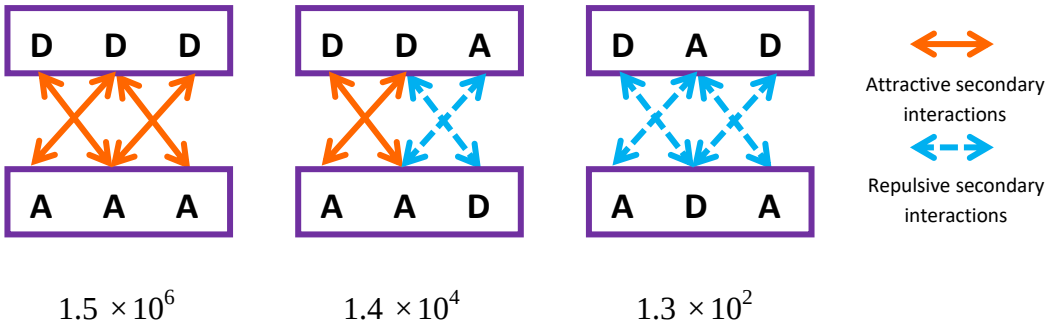

Figure 5: Arrangements of triple hydrogen-bonded systems and their predicted stability constants (in M^{-1}) in chloroform

The same rule can be applied in quadruple hydrogen-bonded systems. In six quadruple hydrogen-bonded dimers, four of them are complementary arrays and two of them are self-complementary arrays (Figure 6). Through studies of multi-hydrogen-bonded systems, Schneider predicted that the primary interaction increases the stability by -8.0 kJ mol^{-1}, the attractive secondary interaction gives -2.9 kJ mol^{-1} and the repulsive secondary interaction weakened the system by +2.9 kJ mol^{-1}.[23]

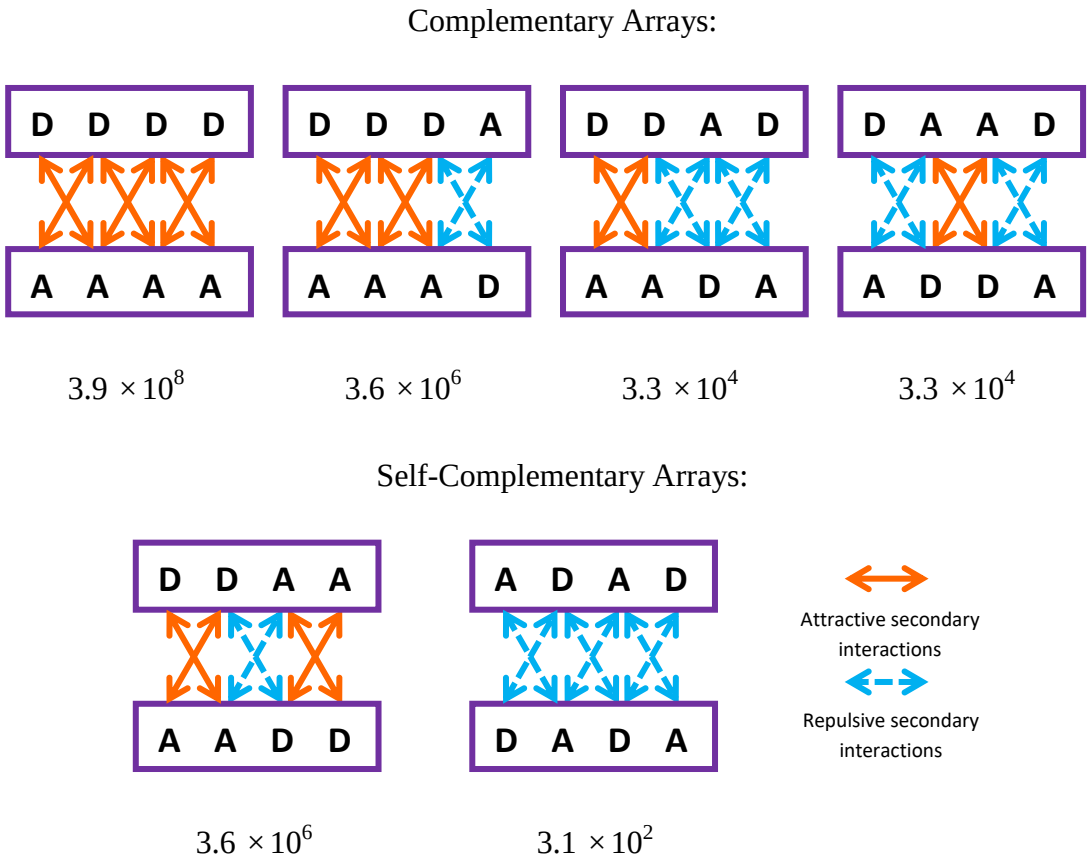

Figure 6: Arrangements of quadruple hydrogen-bonded systems and their predicted stability constants (in M^{-1}) in chloroform[18]

1.1.3 Hydrogen-bonded complexes in biological chemistry

The idea of exploiting hydrogen bonds in supramolecular chemistry comes from nature. In nature, the most evident example is water (Figure 7). The oxygen atom in a water molecule provides two lone pairs of electrons that can form two hydrogen bonds with other water molecules. Therefore, four hydrogen bonds are obtained for each water molecule.

The crystal structure of ice is affected by hydrogen bonds. Because of cavities in the open hexagonal lattice of ice, the density of ice is less than the density of water. That is the reason why ice always floats on liquid water.

The boiling point of water is also affected by hydrogen bonds. As we all know, the boiling point of water is 100 ℃. It is higher than the boiling point of fluorhydric acid which has only two hydrogen bonds within one molecule of fluorhydric acid. To reach the gas state, they need to break their hydrogen bonds. Therefore they have relatively

high boiling points compared to similar molecules without hydrogen bonds, such as hydrogen sulfide and methane.[24]

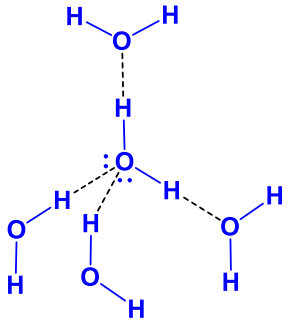

Figure 7: Tetrahedrally-placed hydrogen bonds in water molecules

When we mention hydrogen bonds, we have to mention DNA and proteins (Figure 8).[25] Two strands of DNA are held together by hydrogen bonds and π-π stacking interactions, thus giving a stable double helical structure of DNA. Hydrogen bonds are observed between either adenine and thymine, or guanine and cytosine, which are the four basic components of DNA. These mutually complementary hydrogen-bonded pairs are called Watson-Crick base pairs, and were first identified in 1953.[26] The G-C pair with three hydrogen bonds is more stable than the A-T pair with only two hydrogen bonds, as mentioned previously. The mainly used hydrogen bond is N-H···O/N with a length of about 2.8 – 2.9 Å. In total, the G-C pair has the same length as the A-T pair. Therefore, they form a perfect double helix self-assembly.[27]

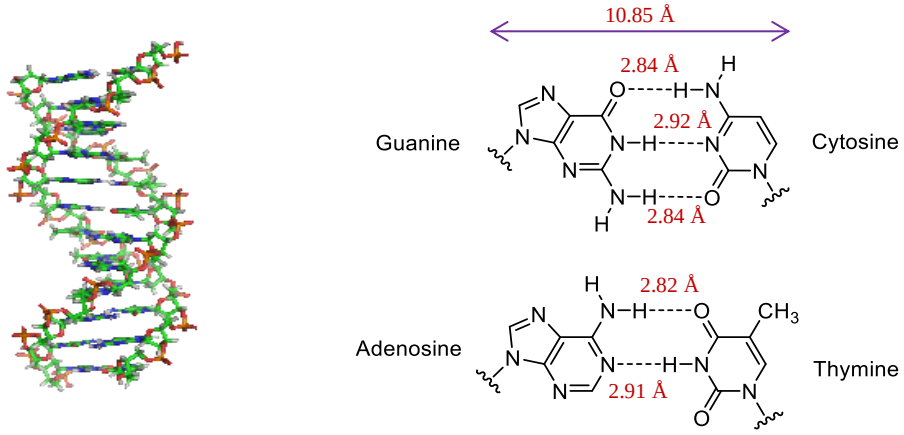

Figure 8: The DNA double helix, G-C and A-T pairs

The first structure of a protein was published by the group of Pauling in 1951 (Figure 9).[28] In the protein secondary structures, the most basic structure motifs are α helices and β sheets. They are constituted by repeating N-H···O=C hydrogen bonds.[29]

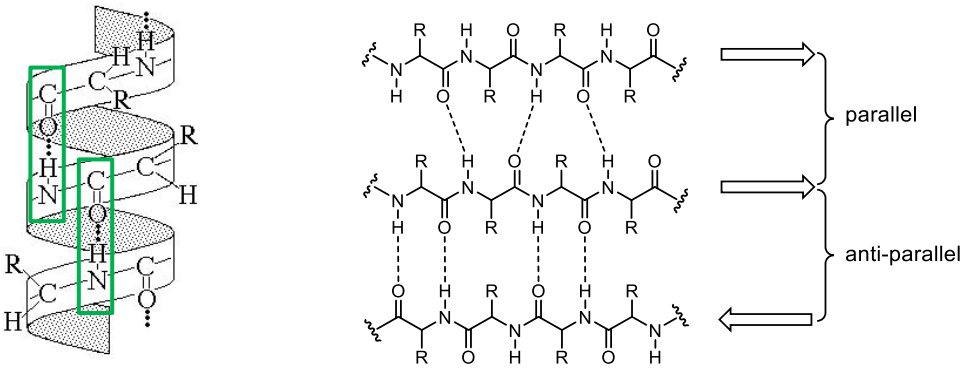

α helix β sheets

Figure 9 : Structures of α helix[30] and β sheets

In addition, the interesting structure of G-quadruplex was detected with crystallographic methods by the group of Gellert in 1962 (Figure 10).[31] Four guanines are associated through eight hydrogen bonds to form a square planar structure called quartet of guanines.[32] Each guanine possesses two hydrogen-bond donors and two hydrogen-bond acceptors, thus they can link each other in a tetrameric way. The cooperativity improves an average energy for hydrogen bonds from 0.22 to 0.42 eV in G-quartet.[33] Furthermore, the presence of a cation like potassium in the middle can stabilize this structure.[34]

In fact, G-rich repetitive sequences do not exist as quartet of guanines, they exist in biological systems as a more complicated structure. Three quartets of guanines superimposed from top to bottom to form the G-quadruplex by π-π stacking interactions. These stacked tetrads align themselves to generate a right-handed helical twist. These G-rich repetitive sequences are mainly located at the end of chromosomes and a protein, with a reverse transcriptase activity.[35] Its formation can inhibit telomerase activity of cancer cells.

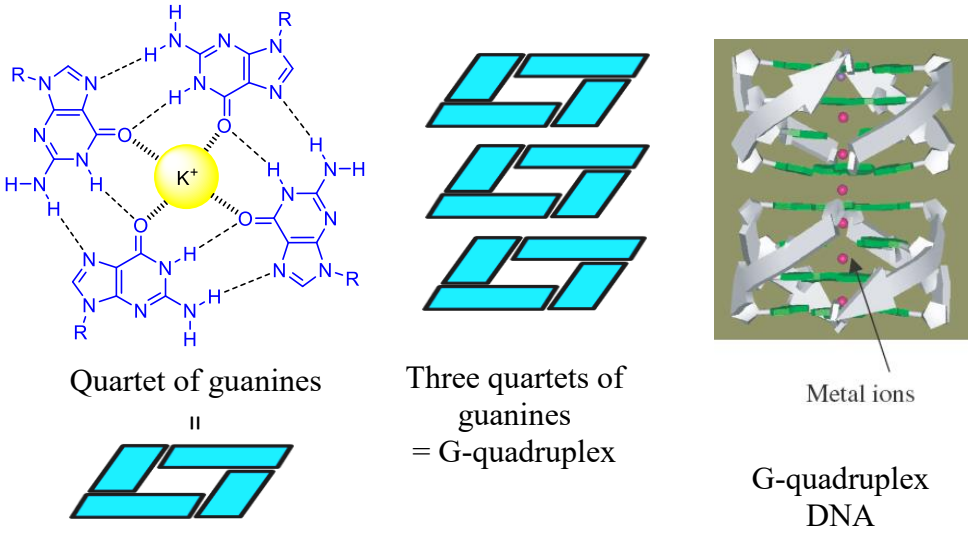

Figure 10: Structure of G-quadruplex[35]

1.1.4 Hydrogen-bonded complexes in synthetic chemistry

Inspired from biomolecules, novel designs of hydrogen-bonded assemblies can give numbers of novel applications. In the 1980s and the 1990s, a wide range of hydrogen-bonded assemblies was synthesized through designing multi-hydrogen-bonded modules. Heterocycles containing nitrogen and cycles with nitrogen functional groups were mainly used to design hydrogen-bonded modules, for example, compounds based on amides,[36-37] ureas,[38-39] imides,[40-41] and so on.

Triple hydrogen-bonded systems can be formed between pyridine-2,6-diyldiacetamide and uracil (Scheme 1). On this basis, tartaric acid linked bidentate derivative **1** and uracil bidentate derivative **2** were synthesized by Lehn's group.[42] The spontaneous association between these two complementary units promoted the formation of a polymolecular entity **3**. Liquid crystalline properties were shown by polymer **3**, but not for compounds **1** or **2** alone.[43]

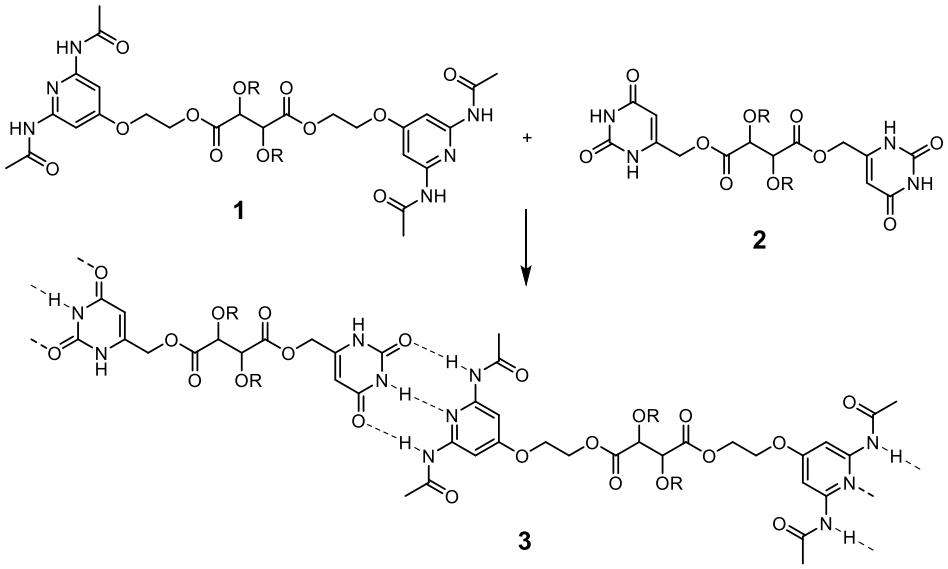

Scheme 1: Self-assembly of the poly-supramolecular species **3**

In 1988, a receptor of barbiturates including two 2,6-diamidopyridine units was synthesized by the group of Hamilton (Figure 11).[44] Two triple hydrogen-bonded systems were incorporated in this receptor, thus the selectivity for the barbiturate family of drugs was increased. The binding strength between the receptor and the substrate reached up to 10^5 M^{-1}.[45] Hamilton's receptor is a successful example in supramolecular chemistry, and has extensive applications in the domain of supramolecular polymers. In summary, the combination of several hydrogen-bonded systems in one molecule makes the whole system more stable, and supplies the lack of strengths for ADA-DAD arrays. This structure will be introduced in more detail later.

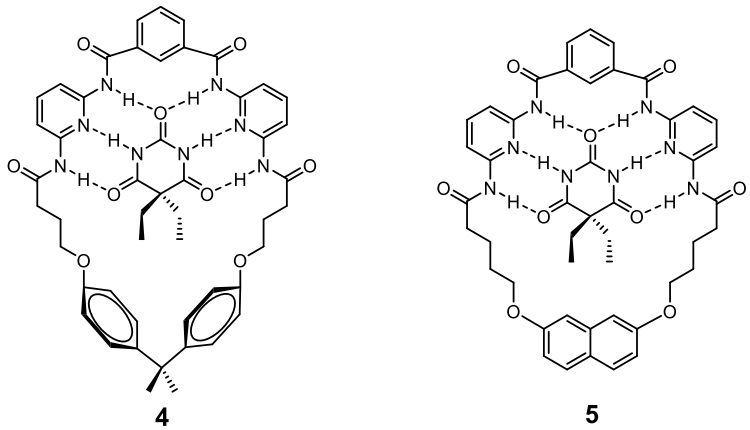

Figure 11: Hydrogen bonds between Hamilton's receptors and barbital

In 2008, 5-membered heterocycles were used to replace 6-membered rings for the formation of DDA arrays by the group of Hisamatsu[46] and the group of Wilson (Figure 12).[47] This replacement avoids influences from intramolecular hydrogen-bonded interactions on the formation of compounds containing DDA-AAD arrays. Then, the group of Wilson found that the stability of hydrogen-bonded compounds was modified by changing the substituents in each array. The stability of hydrogen-bonded compounds could reach up to 8×10^4 M^{-1}.[48]

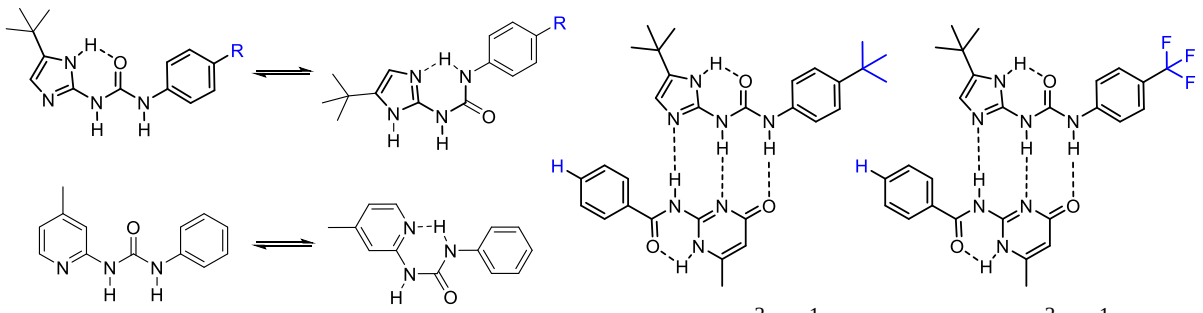

Figure 12: DDA-AAD hydrogen-bonded systems and their association constants

The DDD-AAA hydrogen-bonded system is the most stable one, but their complicated structures are difficult to synthesize. Some examples are known (Figure 13):[49-51] among them, the most stable one was synthesized by the group of Leigh through protonated diaminopyridine as DDD arrays. The stability constant of this compound reached 3×10^{10} M^{-1}.[52]

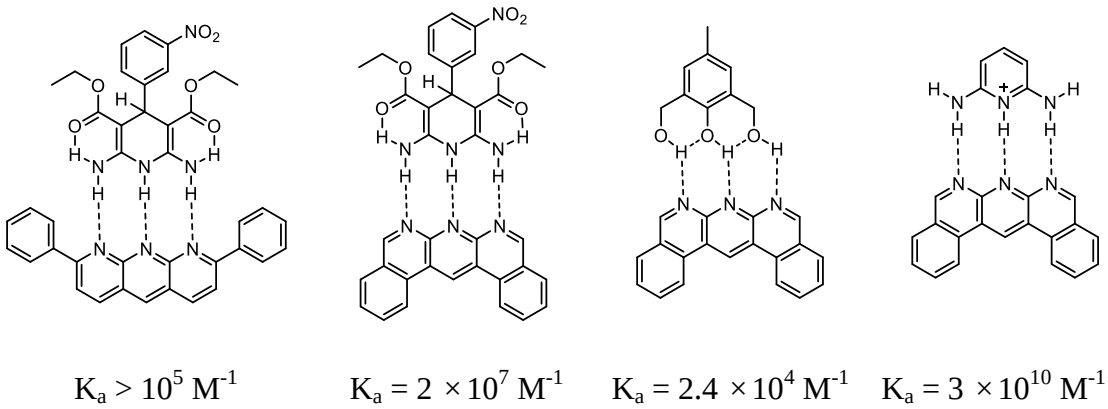

Figure 13: DDD-AAA hydrogen-bonded systems and their association constants

Six combinations of quadruple hydrogen-bonded systems can be designed. Among them, DDDD-AAAA, DDDA-AAAD and DDAD-AADA arrays have been rarely published, due to their synthetic difficulties and scarce applications.

The DADA-ADAD hydrogen-bonded system is considered as the least stable system, because of six additional repulsions according to Jorgensen's theory of secondary interactions. A series of DADA-ADAD hydrogen-bonded systems was synthesized by the group of Meijer. When they designed their hydrogen-bonded system, they found that two amides with the *trans* configuration were replaced by amides with *cis* configuration in compound **6**, because of electrostatic repulsions between carbonyl groups and nitrogen atoms in the triazine ring (Scheme 2). Thus only dimer **7** was found and analyzed, and its dimeric constant was only 37 M^{-1}.[53]

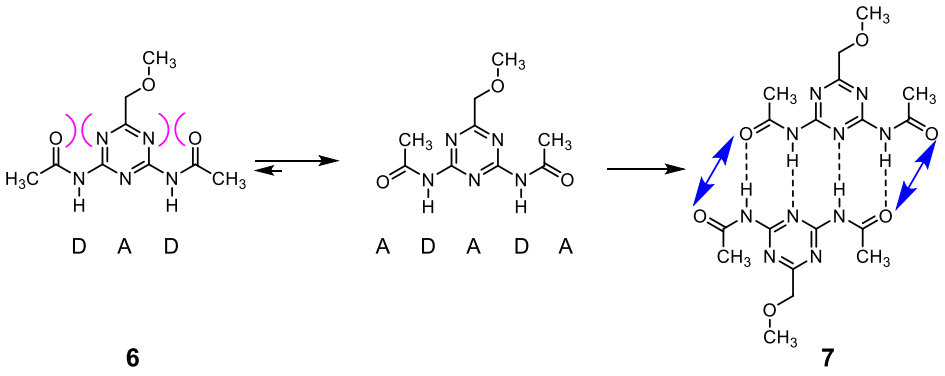

Scheme 2: Conformational equilibrium of diacylated 2,4-diaminotriazines **6** and the dimer **7** with additional repulsive electrostatic interactions

Subsequently, an amide group was removed to form a DADA array, see compound **8** (Figure 14). An intramolecular hydrogen-bonding interaction was used to preorganize arrays in dimers **9** and **10**, thus their dimeric constants were significantly improved.[54]

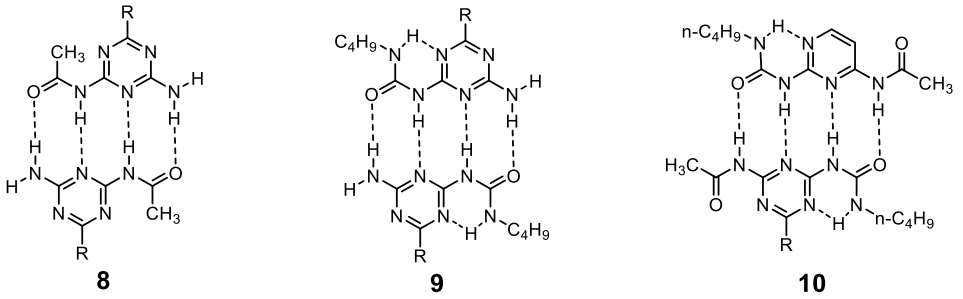

Figure 14: Quadruple hydrogen-bonded systems synthesized by the group of Meijer

In the case of the deazapterin (DeAP) **11** hydrogen-bonded system, the group of Zimmerman found that the presence of 2,7-diamido-1,8-naphthyridines (**14**) broke the dimeric system of DeAP and formed new DAAD-ADDA systems with **14** (Figure 15).[55] The group of Zimmerman developed a series of DAAD-ADDA systems based on **14**. For example, the system formed between butylurea of guanosine (UG) **12** which used imidazole in place of the pyridine ring in DeAP **11**[56-57] and ureido-7-deazaguanine (DeUG) **13** which used pyrrole in place of the pyridine ring in DeAP **11**.[58] When UG and DeUG are alone, their dimeric constants are small, 230 M^{-1} for UG **12** and 880 M^{-1} for DeUG **13**. However, they can form stable heterodimers with DAN **14**, their association constants can reach 3×10^8 M^{-1} for **12-14** dimer and 1.9×10^8 M^{-1} for **13-14** dimer. The structure of **13-14** dimer was confirmed by X-ray spectroscopy and showed a zipper-like hydrogen-bonded assembly.[59]

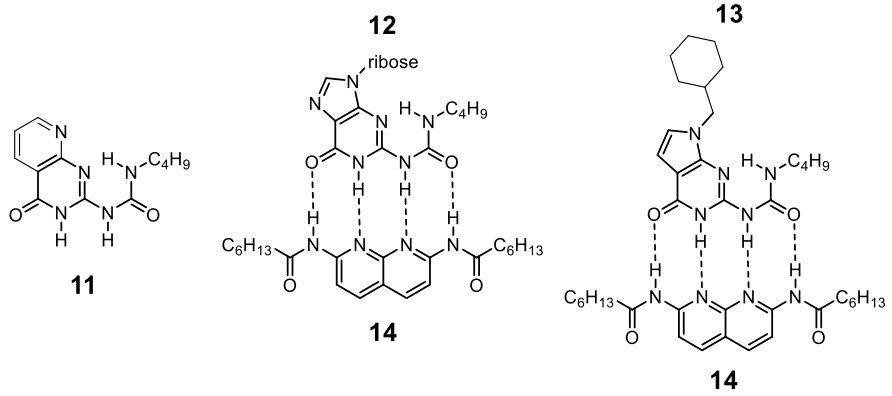

Figure 15: The DeAP **11**, quadruple hydrogen-bonded heterodimers based on UG **12**, DeUG **13** and DAN **14**

Recently, the DDAA-AADD array is the most widely developed system in all quadruple hydrogen-bonded systems. This array has only one secondary repulsion, thus it has a relatively stable structure, and involves a relatively simple synthesis. In numerous DDAA-AADD arrays, the UPy (ureidopyrimidinone) dimer is the most successful one (Figure 16). The intramolecular hydrogen-bonded interaction is used to fix and form favorable dimers. Therefore, the dimeric constant of UPy is more than 10^7 M^{-1}.[60] Different substituents were added and thereby improved solubility and functionality to the dimeric systems.[39, 61] UPy systems were widely used in supramolecular and material sciences, due to their excellent performance.[62]

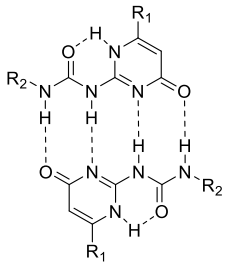

R_1 = CH_3; *n*-$C_{13}H_{27}$; C_6H_5; *p*-NO_2-C_6H_4; CF_3.

R_2 = *n*-C_4H_9; *t*-C_4H_9; C_6H_5; *p*-NO_2-C_6H_4; *p*-NEt_2-C_6H_4; *n*-$C_{18}H_{37}$.

$K_d > 10^7\ M^{-1}$

Figure 16: UPy dimers with different substituents

1.1.5 Combinations of hydrogen bonds and metal coordinations

Metal-ligand and hydrogen bonds are two effective methods to establish supramolecular architectures and to control molecular self-assemblies.[63] The combination of hydrogen bonds and metal coordinations was already demonstrated and used in the 1990s.[64-66]

The UPy dimer was also used to form supramolecular structures with metal coordinations by the genius idea from the group of De Mendoza (Figure 17).[67] Square planar *cis*-coordinated Pd(II) species were chosen for the formation of neutral cyclic arrangements based on the pioneer work of Fujita and Stang.[68-69] Upon mixing equimolecular amounts of Pd(II) complexes and UPy dimers with two coordinated sites, neutral molecular squares and triangles were formed. This work reminds us that

structural changes, steric factors and solubility issues need to be considered for the design of molecular architectures.

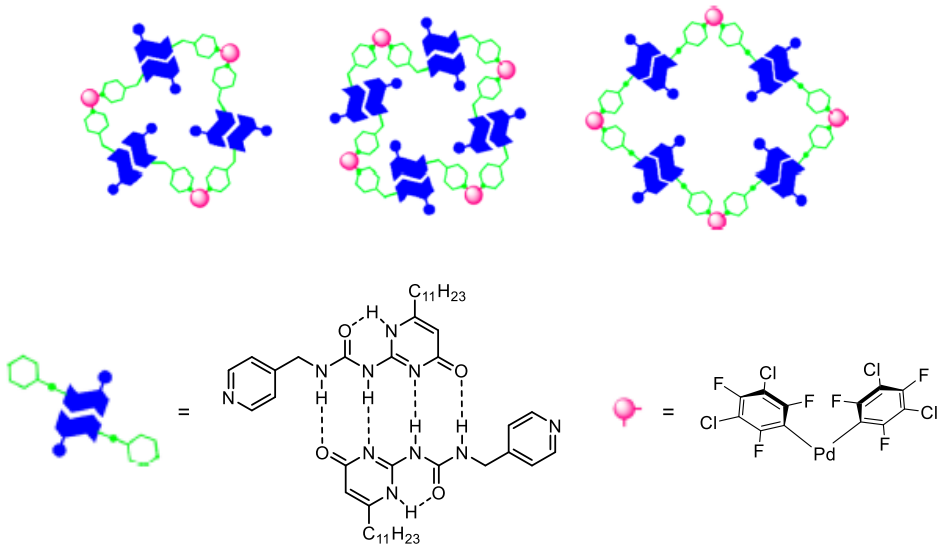

Figure 17: Structures of Pd (II) cyclic aggregates: propeller-shaped triangle, propeller-shaped square, tubular-shaped tetramer[67]

The UPy dimer also serves an important role in the formation of supramolecular polymers. A fast and easy synthesis was used to establish complicated structures by the group of Stang, where bis (phosphine) Pt(II) rhomboidal or hexagonal metallacycles were connected by UPy dimers to form linear chains or cross-linked supramolecular polymers (Figure 18).[70] In this synthesis, the number of steps was reduced due to the contribution of hydrogen-bonded interactions.[71]

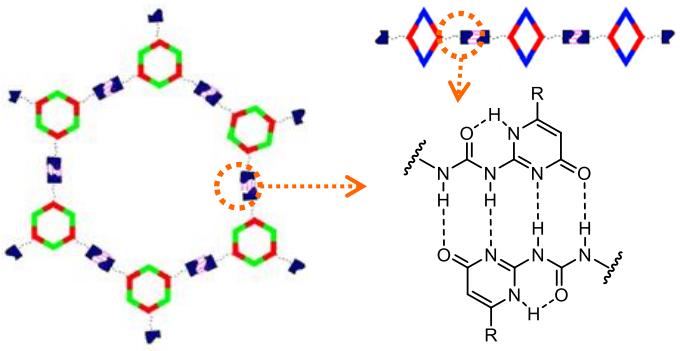

Figure 18: Representations of the linear supramolecular polyrhomboid and the cross-linked supramolecular hexagonal network[70]

Thus 2-ureido-4-[1*H*]-pyrimidinone (UPy) being the most popular, this scaffold was chosen by our team to design arene ruthenium metalla-assemblies (Figure 19). Several cationic arene ruthenium cages were synthesized, characterized and investigated by rotating frame overhauser effect NMR measurements.[72] The arene ruthenium rectangles remained stable in solution owing to the DDAA hydrogen-bonded array of ureido-pyrimidone dimers. These successful examples demonstrate that even monodentate ligands can be considered as scaffold for designing supramolecular assemblies.[73]

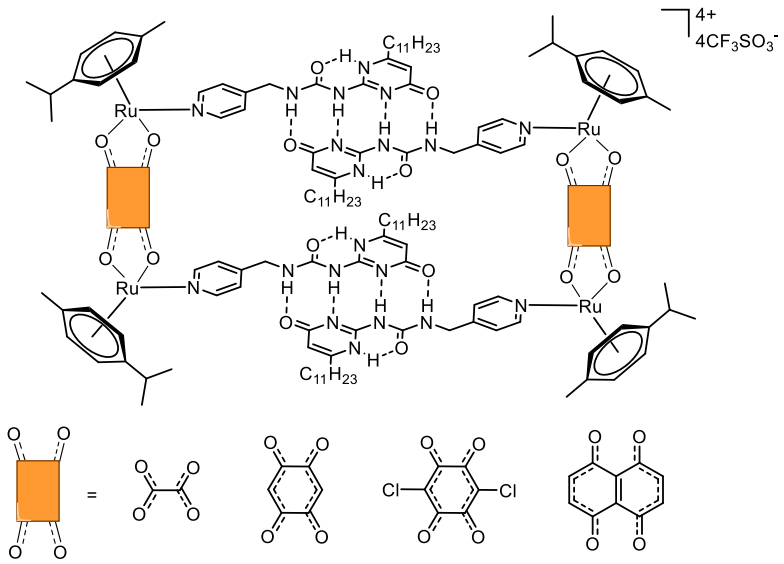

Figure 19: Structures of synthesized cationic arene ruthenium cages

1.1.6 Melamine•cyanuric/barbituric acid self-assemblies

The melamine·cyanuric acid (M·CA) lattice was formed by the reaction between melamine with DAD hydrogen-bonded arrays and cyanuric acid with ADA hydrogen-bonded arrays.[74] These two components were mixed in a 1:1 ratio leading to a stable, insoluble complex (Figure 20).[75] Three types of aggregates are contained in this lattice: cyclic rosettes,[76-77] linear tapes[78-79] and crinkled tapes.[80]

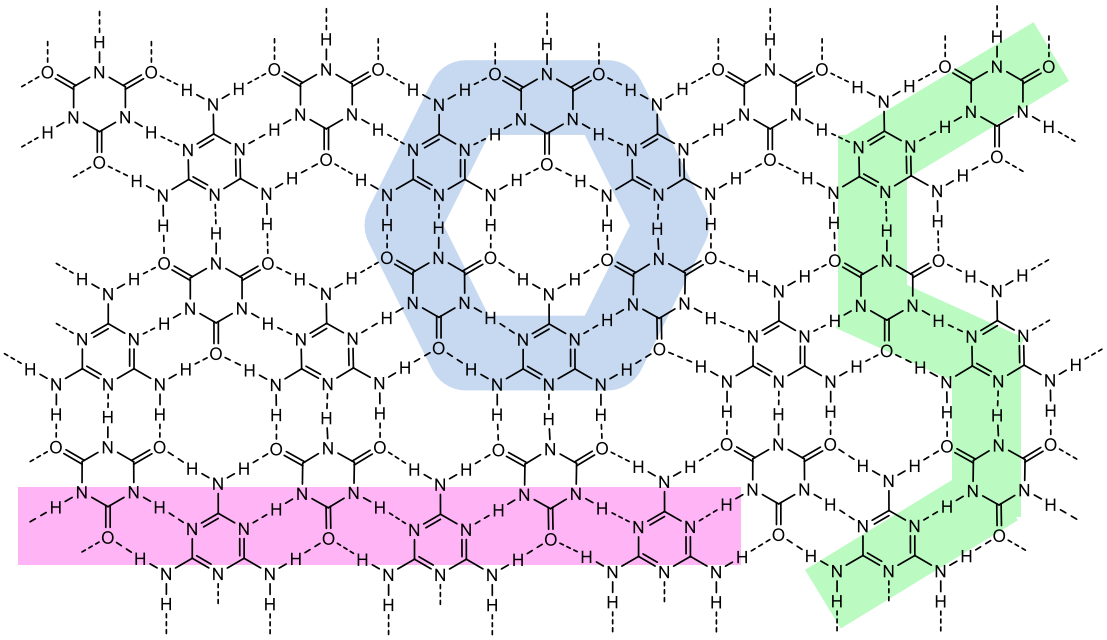

Figure 20: Structure of melamine·cyanuric acid lattice

The melamine·cyanuric acid/barbituric acid (M·CA/BA) pair was widely investigated by the group of Whitesides.[75, 81-82] Two concepts were demonstrated for the preferential formation of cyclic rosettes (Figure 21).[83] The covalent preorganization concept connected three melamines by a central 'hub' spacer and formed a cap upon the rosette.[75] The peripheral crowding concept used melamines with sterically bulky substituents as walls to promote the formation of single rosette.[76] The most widely used substituent is *tert*-butylphenyl that provides favorable steric interaction to form rosette structures.[84]

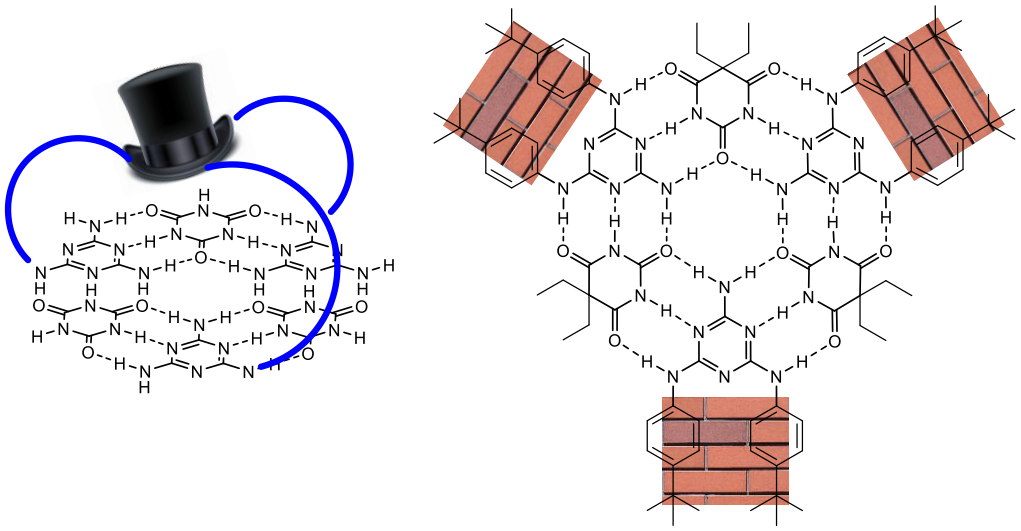

Figure 21: Rosette structures forming selectively by covalent preorganization or by peripheral crowding

In 2001, a theoretical model for the self-assembly of melamine and cyanuric/barbituric acid derivatives into rosettes and tapes was reported by the group of Timmerman.[85] All possible stereoisomeric tape structures were considered for the calculations. Their studies showed that the internal energy of the rosette structure was affected sensitively through changes in parameters, thus impacting the tape/rosette ratio. After the investigation of these calculations, the concept of peripheral crowding was questioned and the concentration ratio was suggested to be the key element.[86]

The tape-like structures possess undefined shape and size, and limited solubility. However, these disadvantages do not exist for rosette motifs. Therefore, rosettes are more attractive than tape-like structures for scientists in the field.[10] The six-membered rosette with complementary hydrogen-bonded pairs can be formed between heterocyclic motifs M and CA/BA, which is hold together by 18 hydrogen bonds through complementary centrosymmetric ADA-DAD hydrogen-bonded arrays. M·CA/BA rosettes were extensively studied by the groups of Whitesides,[83] Timmerman[10] and Yagai.[87]

One of the most well-known rosette was the one formed between *N,N'*-bis(4-*tert*-butylphenyl) melamine (ME) and barbital (BA) that was synthesized by the group of Whitesides in 1994 (Scheme 3).[80] One equivalent of ME was mixed with one equivalent of BA in chloroform, to form the rosette $(ME)_3 \cdot (BA)_3$. In this system,

concentrations of both reactants need to be higher than 4 mM, if not, the disassembly of rosette $(ME)_3 \cdot (BA)_3$ will occur in solution. Similar observations were made for another hydrogen-bonded trimer synthesized by the group of Zimmerman in 1992.[88] Rosette $(ME)_3 \cdot (BA)_3$ demonstrated a better solubility than each reactant in chloroform which is a nonpolar and aprotic solvent. The self-assembly of $(M)_3 \cdot (CA/BA)_3$, which is led by polar hydrogen bonds, prefers the formation of soluble rosettes over insoluble tapes.

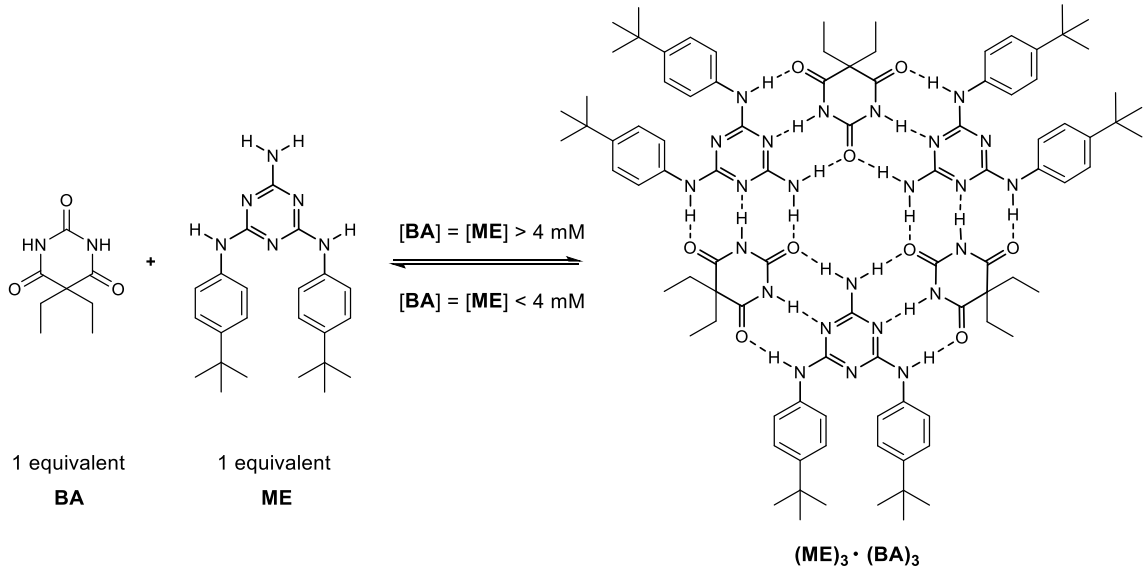

Scheme 3: Self-assembly of rosette $(ME)_3 \cdot (BA)_3$

A series of analytic methods was used by the group of Whitesides to comfirm the structure of the rosette. ^{1}H NMR is the most direct method, signals of hydrogen bonds can be observed in the spectrum. Vapor pressure osmometry (VPO) can be used to predict the average molecular weight of the rosettes.[89] Another method to determine the molecular weight of rosettes is gel permeation chromatographic (GPC). But this method was unsuccessful for the molecular weight determination of rosette $(ME)_3 \cdot (BA)_3$, because of its good thermodynamic stability.[80] Crystals of rosette $(ME)_3 \cdot (BA)_3$ were obtained through slow evaporation of a solution containing ME/BA (1:1) in isopropyl alcohol/toluene (1:1), and the X-ray structure was determined (Figure 22).

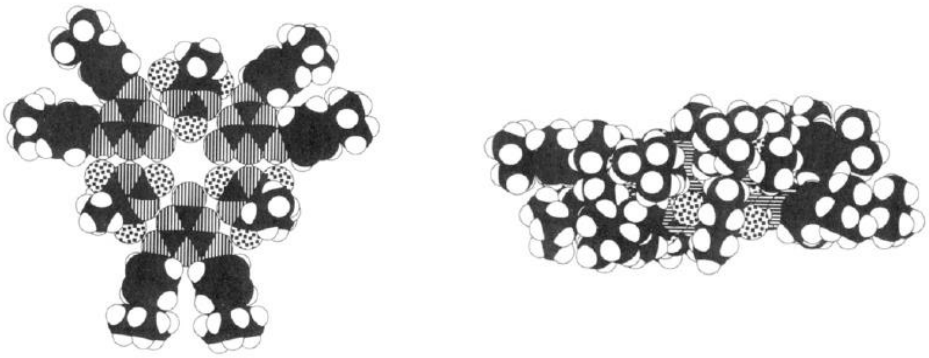

Figure 22: X-ray crystal structure and packing structure of $(ME)_3 \cdot (BA)_3$ rosette [80]

In 1997, four aggregates based on $(M)_3 \cdot (CA)_3$ rosettes were synthesized and characterized by the group of Whitesides (Figure 23).[90] Zinc tetraphenyl porphyrin units (ZnTPP) were added at the periphery of the rosettes by coordination to the imidazole groups. Aggregates with ZnTPP were demonstrated to be more stable than aggregates with free imidazole groups.

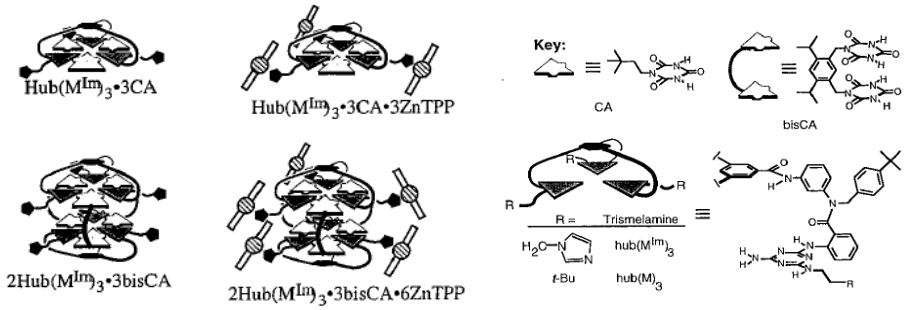

Figure 23: Structures of aggregates with free imidazoles or ZnTPP[90]

In the same year, the metalla-dendrimer associated with $(M)_3 \cdot (BA)_3$ was constructed by the group of Reinhoudt (Figure 24).[91] 2-D NOESY experiments were used to confirm the structure of the rosette, strong cross signals were found between the three hydrogen bonds in the rosette. This was the first nanosized assembly formed by the combination of hydrogen bonds and metal coordinations.

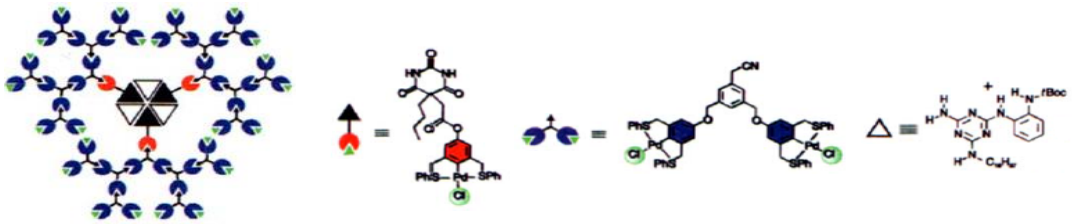

Figure 24: Structure of the discrete rosette with palladium coordination[91]

In 2004, gold atoms were inserted into the double rosette structure through phosphane addition at the periphery of the melamine unit (Figure 25).[92] Six Au(I)Cl moieties were incorporated into hydrogen-bonded rosette assemblies. This rosette was extremely stable in the solid state.

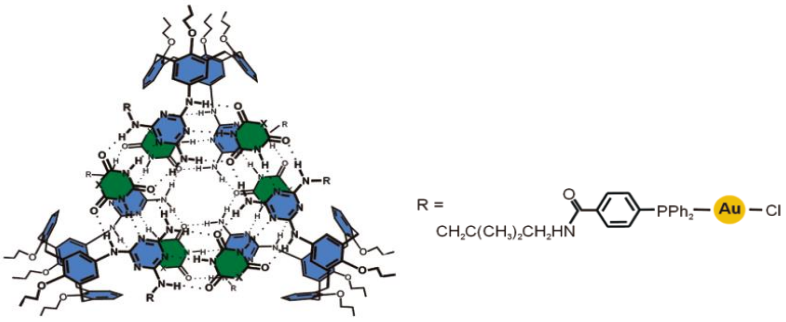

Figure 25: Structure of double rosettes containing six Au(I) atoms[92]

In the same year, free porphyrin and Zn(II) porphyrin derivatives were prepared by the group of Li (Figure 26).[93] The presence of large porphyrins stabilized the rosettes. Therefore, these porphyrin rosettes were found to be more stable than the rosette initially synthesized by the group of Whitesides. The results show that rosette $(M)_3 \cdot (CA/BA)_3$ can be used to generate supramolecular receptors by binding large molecules at the periphery.

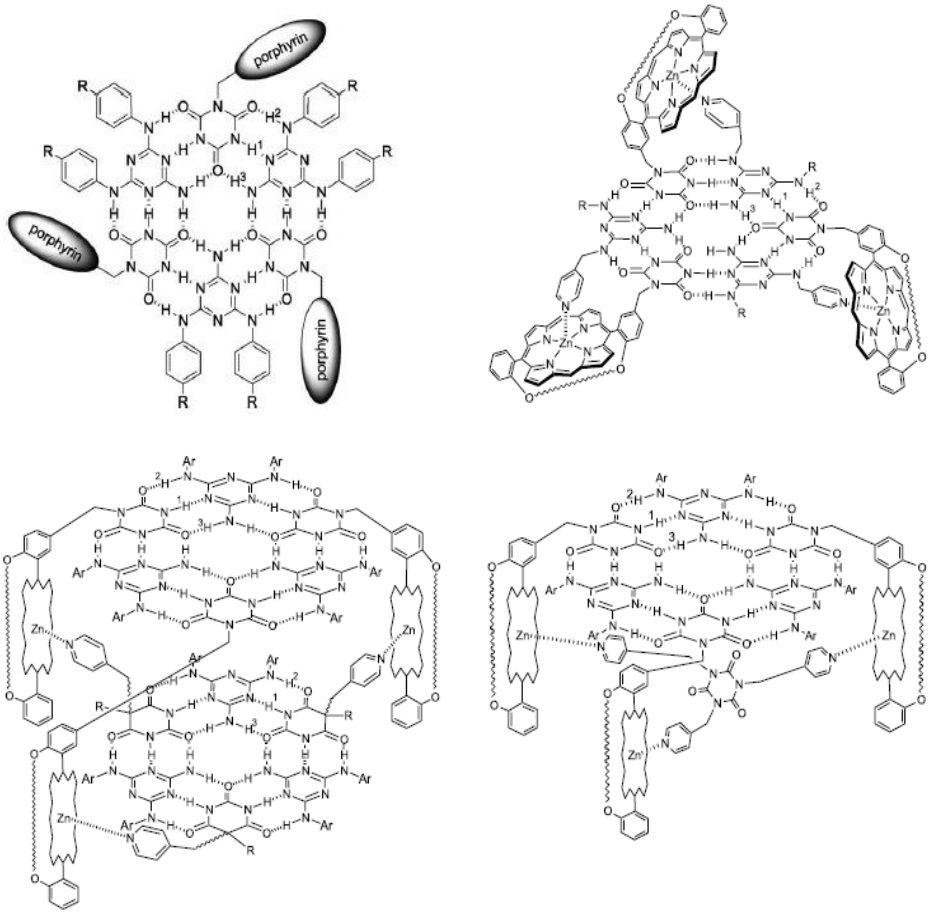

Figure 26: Structures of rosettes with porphyrins[93]

Three strategies were used to add Zn(II) porphyrins around rosettes. The first one was by connecting the porphyrin to the CA structure (Figure 27). The second method used the coordination of Zn(II) over the melamine or BA unit through the addition of pyridines. These ideas are extremely useful for our design of hydrogen-bonded metalla-assemblies.

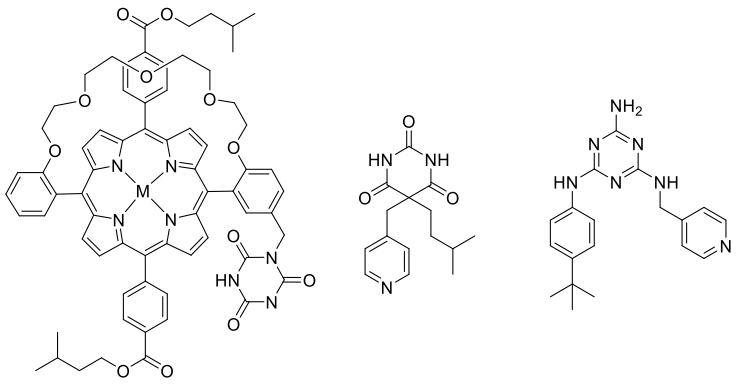

Figure 27: Key molecules for the coordination of Zn(II) porphyrins to $(ME)_3 \cdot (BA)_3$ rosettes

All above mentioned examples show the feasibility of the combination between $(M)_3{\cdot}(CA/BA)_3$ rosettes and metal coordinations.

Stimuli-responsive properties were found for several $(M)_3{\cdot}(CA/BA)_3$ rosettes with π-conjugated systems, due to the possibility of dynamically rearranging hydrogen-bonded patterns.[87]

Photoswitching properties were first found in the M·BA assembly by the group of Kitamura in 2003 (Scheme 4).[94] The isomerization of azobenzenes through UV-irradiation suppressed transformation from soluble cyclic rosette into insoluble tape-like polymers. Owing to the thermodynamic stability of rosette **15** in solution, the stability was further increased upon the photoisomerization of the azobenzene groups.

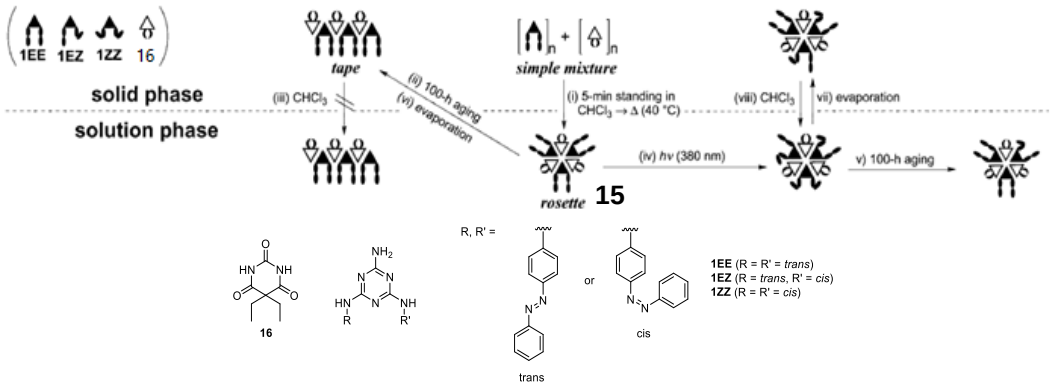

Scheme 4: Transformation of rosette **15** by UV-irradiation[94]

Soon after, a more complicated rosette **16** with azobenzenes accompanying the *E* → *Z* isomerization through photoirradiation was synthesized by the same group (Figure 28).[95] This rosette **16** is stable in chloroform, toluene and methylcyclohexane.

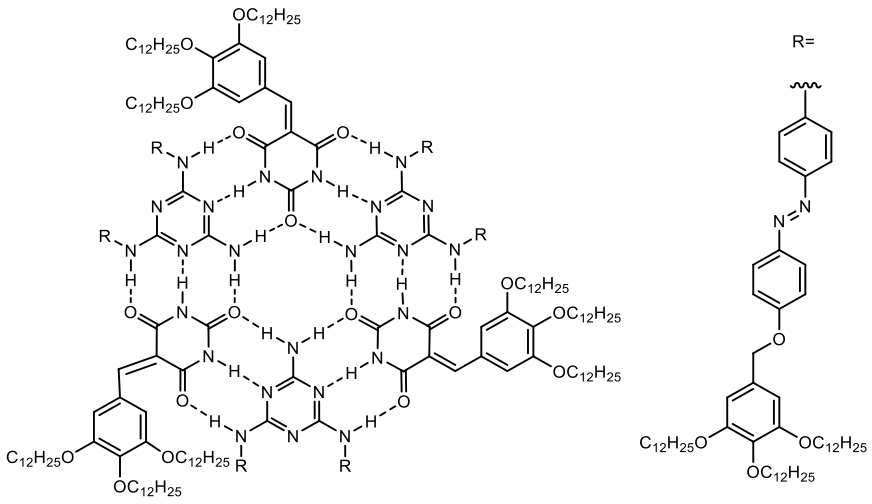

16

Figure 28: Structure of rosette **16**

Another disk-shaped aggregate with azobenzene was investigated by the same group in 2005 (Scheme 5).[96] The columnar aggregate of rosette **17** in cyclohexane was dissociated and reformed through *trans-cis* isomerization by UV-irradiation of the azobenzene group.

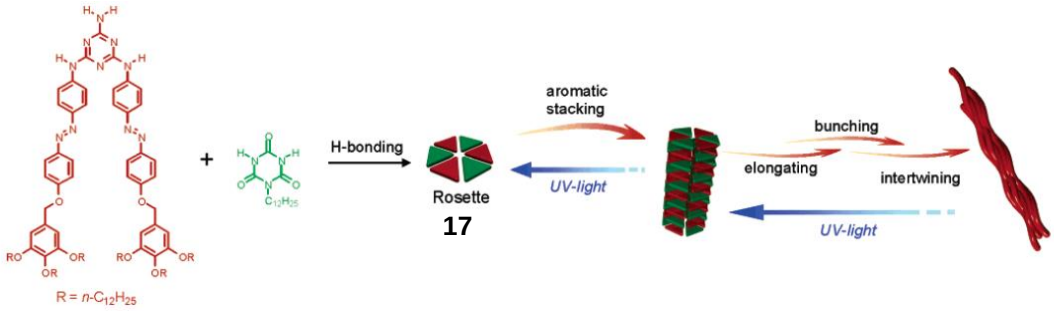

Scheme 5: Formation of aggregates on the basis of rosette **17**[96]

Heating-induced rosette-type assembly was explored by the group of Yagai in 2012 (Figure 29).[97] Perylene 3,4,9,10-tetracarboxylic acid bisimide (PBI) was added to the cyanuric acid part for the formation of rosette **18**. The transformation from columnar assemblies of rosettes to lamellar assemblies of linear tapes occurred by increasing the temperature.

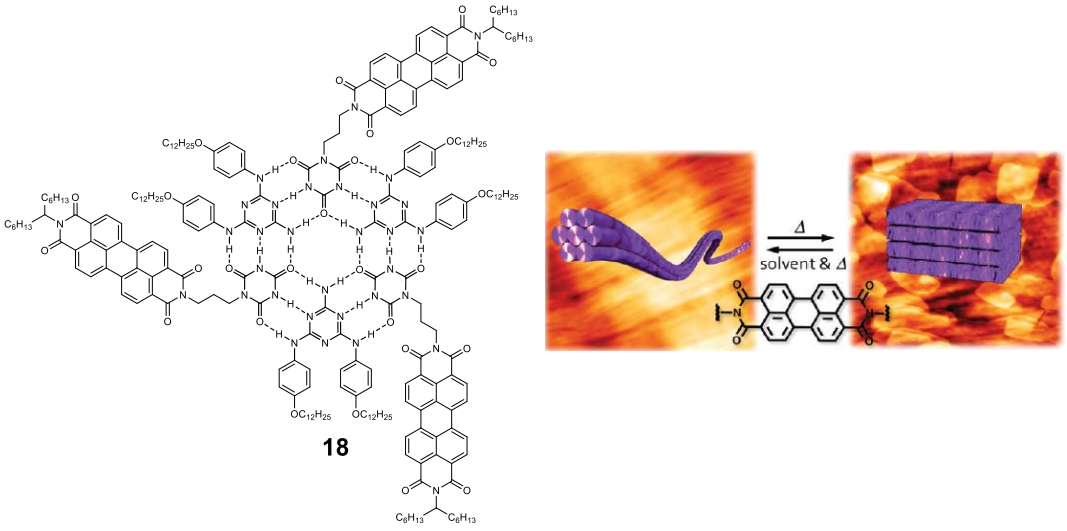

Figure 29: Thermoresponsive aggregates of rosette **18**[97]

These stimuli-responsive self-assemblies mentioned above can be used for the design of smart nanomaterials.

Rosette **19** was formed by a collaborative work of Yagai and Ajayaghosh (Scheme 6).[98] A self-organisation in aliphatic solvent between the melamine-derivative **20** with the substituent oligo(*p*-phenyleneethynylene) (OPE) and cyanurate **21** provides the desired rosette **19**. Toroidal nanoobjects were detected by atomic force microscopy (AFM). This rosette system may possibly be used for the design of artificial light-harvesting nanodevices.

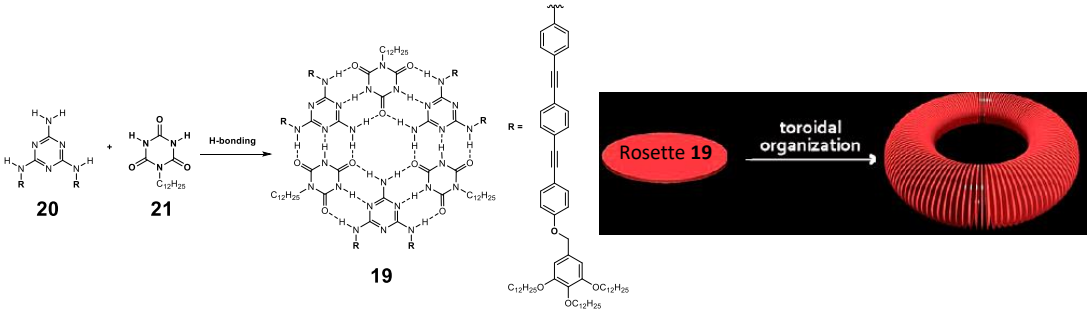

Scheme 6: Formation of rosette **19**[98]

1.2 Supramolecular chemistry

1.2.1 General introduction

In 1987, Jean-Marie Lehn, Donald J. Cram and Charles J. Pedersen won the Nobel Prize in chemistry for their contributions in supramolecular chemistry. Since this Nobel Prize, the field of supramolecular chemistry has become more and more widely investigated and applied.[99] In 2016, James Fraser Stoddart, Bernard L. Feringa and Jean-Pierre Sauvage were awarded the Nobel Prize in Chemistry for molecular machines based on supramolecular chemistry.[100] And after nearly thirty years of development, supramolecular chemistry has now evolved to supramolecular science. This interdisciplinary science covers chemical, physical, biological and material areas.[101]

A definition of supramolecular chemistry was provided by Lehn in the book "Supramolecular chemistry-concepts and perspectives": '*Beyond molecular chemistry based on the covalent bond there lies the field of supramolecular chemistry, whose goal it is to gain control over the intermolecular bond.*' This means that the supramolecular chemistry based on molecular interactions is focused on the synthesis of complicated system associating two or more molecules, owing to its highest efficiency and selectivity.[102]

1.2.2 Tools of supramolecular chemistry

Molecules that are held together by non-covalent interactions are called supramolecules. Non-covalent interactions are normally weaker than covalent interactions (250 – 800 kJ mol^{-1}), but their cooperativities can help them to form stable supramolecular complexes. A list of non-covalent interactions is provided in Table 2 with their relative strengths.[103-104]

Interaction	Strength (kJ mol^{-1})
Ion - ion	200 – 300
Ion - dipole	50 – 200
Dipole – dipole	5 – 50
Hydrogen bonding	4 – 120
Cation - π	5 – 80
π - π	0 – 50
Van der Waals	< 5
Hydrophobic	< 50
Coordination bonding	50 – 150

Table 2: Summary of supramolecular interactions

1.2.3 Categories of supramolecular chemistry

Supramolecular chemistry can be divided in two categories: host-guest chemistry and self-assembly.[104]

The concept of 'host-guest chemistry' was first proposed by Cram in 1974, while investigating enzymatic systems.[105] The substrate selectivity of enzymes can be simulated to design complexes composed of organic compounds. To design host-guest systems, matching sizes, shapes and electronic properties that can provide strong bindings between hosts and guests are crucial.[106]

Some common supramolecular host molecules have been found since 1967. A series of crown ethers was synthesized by the group of Pedersen and their cavity size was controlled by the number of repetitive motifs (Figure 30).[107-108] Then cryptands were synthesized by the group of Lehn in 1969.[109-110] Spheroids were synthesized and investigated by the group of Cram.[111] Soon after, complexation rates and equilibria were investigated between host molecules and ions.[112]

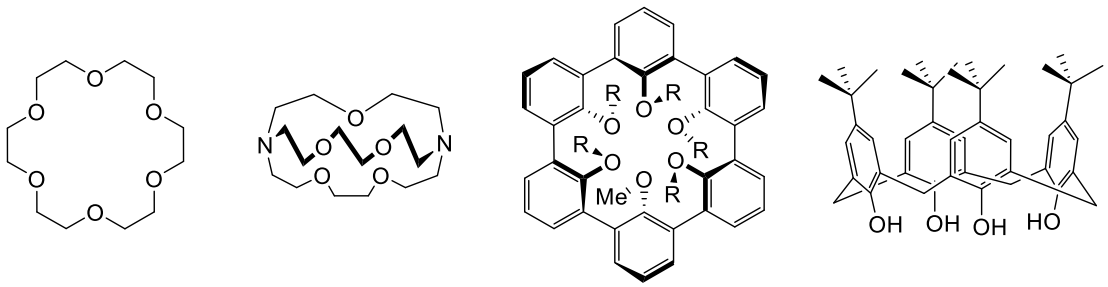

Figure 30: Typical supramolecular host molecules

Obviously, supramolecular interactions can be used in host-guest systems. For example, Van der Waals interactions can be increased by extending the contact surface between the host and the guest. Acceptors or donors of hydrogen bonds can be inserted into host molecules, and guest molecules can be attracted by adding complementary sites (Scheme 7). Ion dipole interactions were the first interactions used in host-guest systems.[108] The electrostatic interaction between two ions can also be used in such system. Additionally, combinations of several interactions are common to obtain stable complexes.

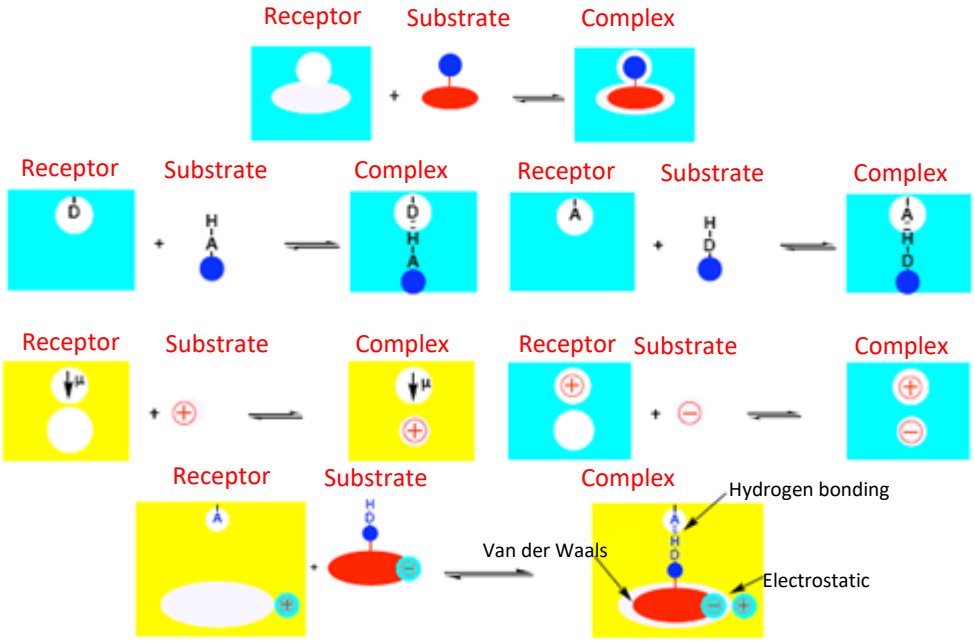

Scheme 7: Supramolecular interactions used in host-guest systems[113]

Self-assembly was first defined as the convergent process from which a supramolecular species forms spontaneously from its components.[114] Then self-assembly was redefined by the group of Steed in 2009 "*as the spontaneous and reversible association of molecules or ions to form larger, more complex supramolecular entities according to the intrinsic information contained in the molecules themselves*".[9] But self-asembly is not only confined to supramolecular chemistry, it is ubiquitous throughout life.

The first self-assembling macrocycle formed upon coordination chemistry was reported by the group of Maverick in 1984 (Figure 31).[115] This work showed how simple self-assemblies can be formed when using metal coordinations. Soon after, another macrocycle was synthesized by the same group.[116]

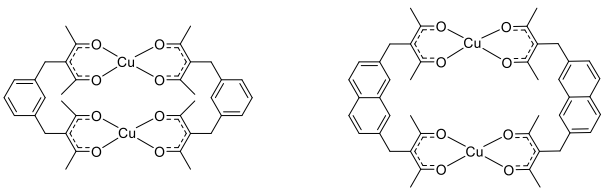

Figure 31: Self-assemblies synthesized by the group of Maverick

Then Saalfrank's tetrahedral iron-malonate assembly was published in 1993 (Figure 32).[117] Pyridyl ligands were used as skeletons for most of this study. For example, Lehn's cylindrical box was based on copper (I) and coordination of 2,2'-bipyridine.[118] Fujita and Ogura's square box was based on palladium (II) and coordination of 4,4'-bipyridine,[119] which can be extended into cubes. A supramolecular cube was formed through the combination of eight octahedral metal 'corners' and twelve ligand 'edges' by the group of Thomas in 1998.[120] Thus, the brilliant value of self-assemblies was demonstrated for the formation of large complexes.

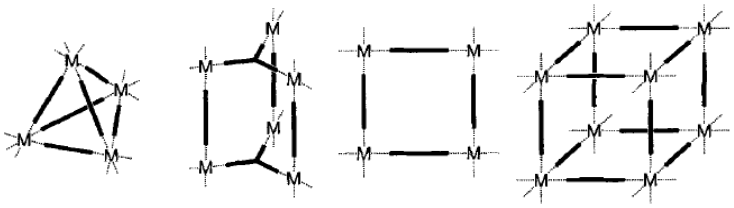

Figure 32: Self-assemblies with different sizes and shapes[121]

Multiple hydrogen-bonding interactions have been demonstrated to be useful for the formation of closed self-assembled spherical molecules or capsules.[122] Reversible dimerization was used for the formation of bowl-shaped molecules through the presence of hydrogen bonds. A relatively large bowl-shaped molecule was synthesized by the group of Rebek in 1996 (Figure 33).[123] Glycoluril units were used to provide two donors and two acceptors groups for self-complementary structures. When three glycoluril units were attached to a triphenylene core, two molecules could be assembled by twelve hydrogen bonds, thus forming a large capsule (**22**). Some aromatic guests like cyclohexane were encapsulated in the cavity of this bowl-shaped capsule.

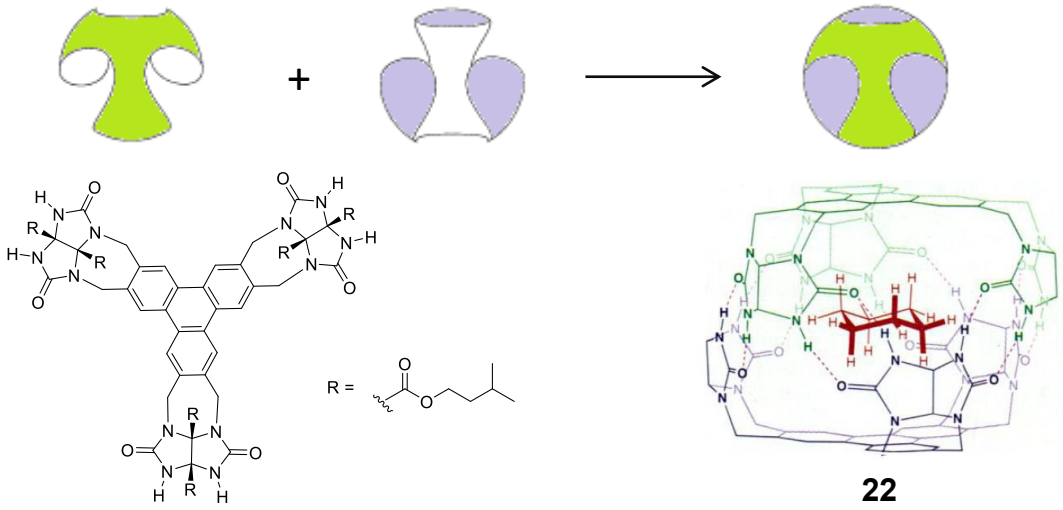

Figure 33: Structure of a bowl-shaped assembly **22**[123]

Self-assembling capsules were defined by the group of Rebek in 1997 ‘‘*as receptors with enclosed cavities that are formed by the reversible noncovalent interaction of two or more, not necessarily identical, subunits*’’.[124] Utilizations of non-covalent reversible interactions can offer opportunities for ‘catch-and-release’ of a guest to control drug delivery or reactivity.[125] Therefore, a series of capsules was self-assembled through hydrogen bonds.

One common example is capsules formed by calixarenes. A self-assembling heterodimeric system was reported by the group of Reinhoudt (Figure 34). The tetrasubstituted calixarene with pyridyl groups and the other calixarene with carboxylic acid groups were combined through four hydrogen bonds.[126]

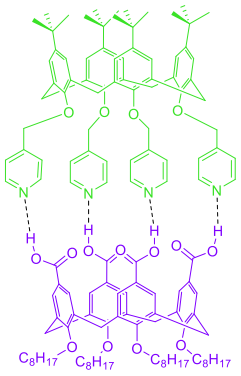

Figure 34: Structure of calixarenes based capsule

Another example was the supramolecular capsule constructed by resorcinarene-based cavitands functionalized with acetamido groups, which was reported by the group of Aakeroy in 2011 (Figure 35).[127] In this case, chelating effects at the cavitands were created to avoid the formation of co-products from polymerization. Two *c*-pentyltetra(2-acetamidopyridyl-5-ethynyl) cavitands were held together by three self-complementary NH···O=C hydrogen bonds to give this capsule. In their investigation, three ethanol molecules, two methanol, and one toluene were trapped in the cavity of this capsule.

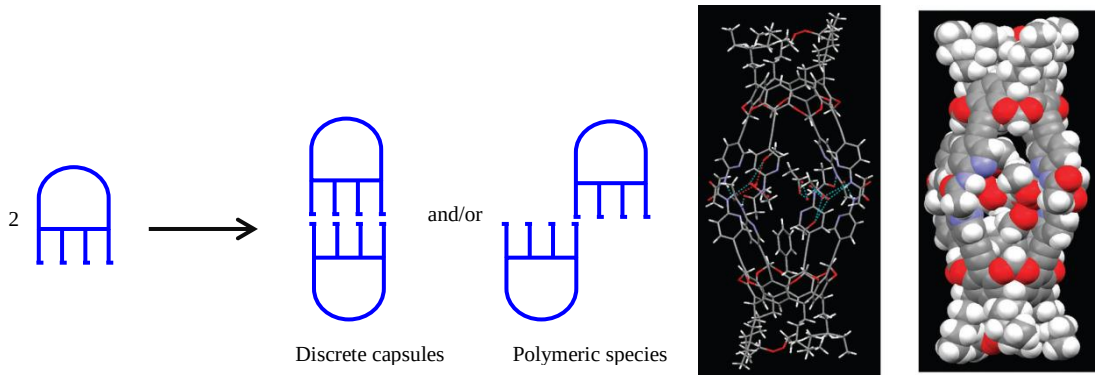

Figure 35: Assembly of two cavitands and crystal structures of a resorcinarene-based capsule[127]

1.3 Coordination chemistry

1.3.1 Element ruthenium

Ruthenium, derived from the latinised name of Russia, was discovered by Karl Karlovitch Klaus in 1844. It was the last 'platinum metal' to be discovered.[128] Ruthenium is a rare transition metal, it is only the 74th most abundant metal on Earth.

Ruthenium has the symbol Ru, molecular weight 101.07 g/mol,[129] and atomic number 44. It is in group 8 and period 5 in the periodic table with its electronic configuration [Kr] $4d^7$ $5s^1$.[130] Ruthenium has a wide range of oxidation states from -II {$[Ru(CO)_4]^{2-}$} to +VIII (RuO_4).[131] Principal oxidation states for ruthenium are +II and +III. Ruthenium (III) is the best-known oxidation state, and its complexes are generally octahedral {$[Ru(H_2O)_6]^{3+}$} and distorted tetrahedral $[Ru_2(CH_2SiMe_3)_6]$. Ru(II) is the second most common oxidation state. It forms complexes with ligands based on group 15 or 16 elements. Ru(II) complexes are normally octahedral {$[Ru(bpy)_3]^{2+}$}, pseudo-tetrahedral [(arene)$RuCl_2(PPh_3)$] and trigonal bipyramidal $[RuHCl(PPh_3)_3]$, apart from complexes like $[RuCl_2(PPh_3)_3]$, which are square pyramidal because of their stereochemically blocked coordination positions.[132] Ruthenium containing complexes have potential applications in catalytic chemistry, biology and medicine.

1.3.2 Mononuclear arene ruthenium complexes

Mononuclear arene ruthenium complexes with a piano-stool structure are the most studied complexes in the large family of ruthenium (Figure 36), [133] they possess potential biological applications. In this type of complexes, the arene can be considered as the seat of the piano-stool and the other three ligands as the legs. Because arenes are able to occupy three coordination sites, the three remaining sites are available for different ligands.[134] Because of their structural similarity, this type of complexes can also be called half-sandwich complexes. In such complexes, the arenes prevent oxidation from Ru(II) to Ru(III). Furthermore, arenes with extended ring systems can potentially interact with DNA.[135] The other coordination sites can be used to introduce desired properties.[133] Normally, ligands with N-, O-, S-, or P-donor groups are easily introduced, labilities of these ligands offer more possibilities in self-assemblies[136] and catalytic processes.[137] In particular, chelate ligands can increase the stability of the complexes and modulate the electronic properties of the metal center.[138]

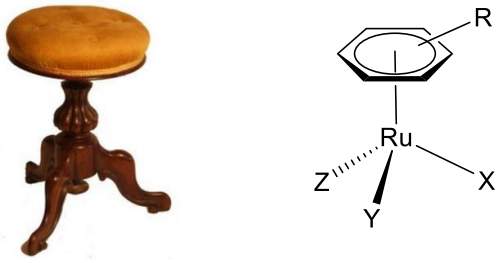

Figure 36: Piano-stool and the typical structure of mononuclear arene ruthenium complexes

The first arene ruthenium complex $[(\eta^6\text{-mesitylene}]_2Ru](BPh_4)_2$ was synthesized by Fischer and Böttcher in 1957 through a redox reaction from $RuCl_3$ and Al.[139] In 1967, the synthesis of $[(\eta^6\text{-}C_6H_6)RuCl_2]_x$ was reported by Winkhaus and Singer. This polymeric complex was obtained from $RuCl_3{\cdot}nH_2O$ (Scheme 8), the most common precursor in the synthesis of arene ruthenium complexes. $[(\eta^6\text{-}C_6H_6)RuCl_2]_x$ is a red powder, poorly defined chemically but very versatile synthesized.[140-141] Subsequently, a dimeric structure was suggested by Zelonka and Baird.[142] Soon after, a series of brown, diamagnetic complexes with the general formula $[(\eta^6\text{-arene})RuCl_2]$ were prepared through methanolic or ethanolic $RuCl_3$ with the appropriate cyclohexa-1,3-diene or cyclohexa-1,4-diene. The para-cymene complex was demonstrated by osmometry to be dimeric in chloroform.[143] Eventually, Bennett confirmed the dimeric structure of $[(\eta^6\text{-}C_6H_6)Ru(\mu\text{-Cl})Cl]_2$ in 1974, where two Ru(II) are linked by two chloride bridges (Scheme 8).[144]

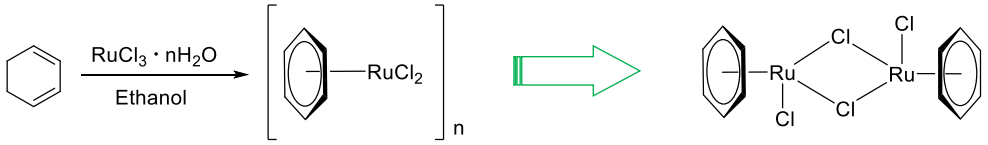

Scheme 8: Synthesis and structure of benzene ruthenium complex

Meanwhile the most common procedure to prepare standard dimeric arene ruthenium complexes with chloride bridges was found by the same group. The reaction between $RuCl_3{\cdot}nH_2O$ and a cyclohexadiene derivative in $EtOH/H_2O$ can give different arene ruthenium complexes.[144] Another procedure implies arene exchange, a method that can be used to synthesize ruthenium complexes with electronically rich arenes.[145] Starting from dinuclear arene ruthenium complexes, the electronically rich arenes can

replace the original arenes at high temperature to form the desired arene ruthenium dimers (Scheme 9).

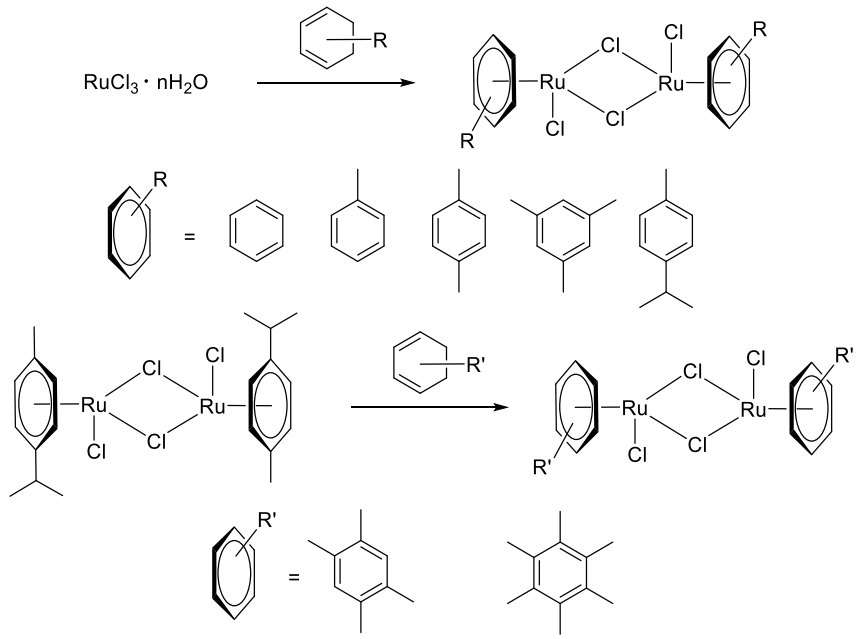

Scheme 9: Methods to synthesize chloro-bridged arene ruthenium complexes

A wide range of half-sandwich piano-stool complexes was synthesized using dinuclear chloride-bridged arene ruthenium complexes $[(\eta^6\text{-arene})Ru(\mu\text{-}Cl)Cl]_2$ as the reactant (Scheme 10). Because of the easy cleavage of the chloride bridges, especially in coordinating solvents, solvated monomeric derivatives can be formed.[146]

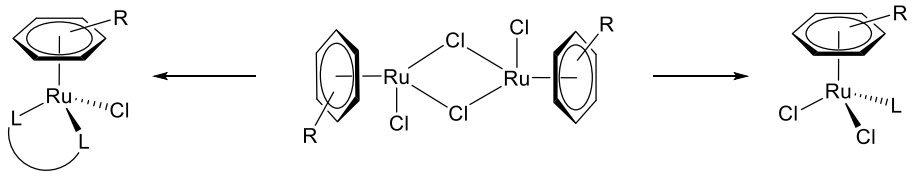

Scheme 10: Methods to synthesize half-sandwich piano-stool complexes

The biological potential of arene ruthenium complexes has been extensively investigated by the groups of Dyson[147] and Sadler.[148-149] In their early studies, RAPTA-C and RM175 were considered as promising compounds for anticancer applications.[149]

The RAPTA family is characterized by their half-sandwich piano-stool structure (Figure 37). Their unique properties are obtained by the coordination of the monodentate PTA (1,3,5-triaza-7-phosphaadamantane) ligand. PTA is an hydrophilic ligand, thus water solubility can be increased.[150] The first RAPTA complex was [Ru(cym)Cl_2(PTA)] abbreviated as RAPTA-C.[151] Although a poor anticancer activity was observed *in vitro*, an *in vivo* study showed promising antimetastatic activities.[152] The number and weight of solid lung metastases were reduced in mice bearing the MCa mammary carcinoma. Then several new RAPTA complexes were reported and investigated for anticancer activities *in vitro*.[153] Further studies of RAPTA-C showed anti-tumor activities in human ovarian and colorectal carcinomas, where an inhibition of angiogenesis was observed.[154-155]

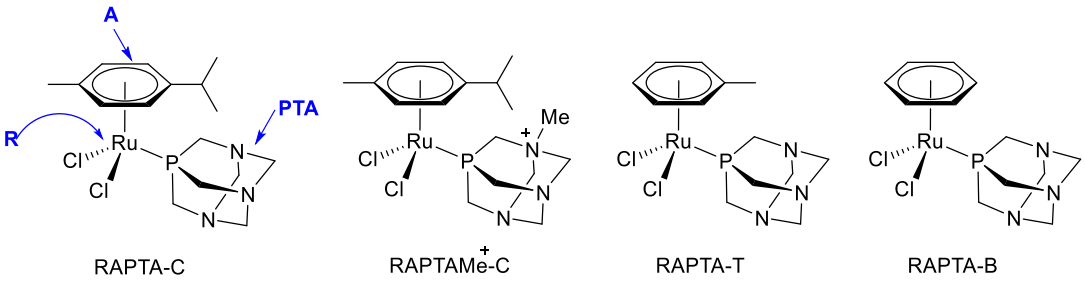

Figure 37: Structures of RAPTA complexes

The half-sandwich arene ruthenium complexes, abbreviated as RM or HC, have been synthesized by the group of Sadler in 2001[156] (Figure 38), and their biological properties investigated by the same group in 2002.[157] This type of arene ruthenium complexes is bonded by a chelate diamine ligand and a labile ligand.[158] RM175 and HC29 have both shown good activities *in vitro* in human ovarian cancer cells, which is comparable to carboplatin. In this family, the most active complex is HC11, which allows an activity comparable to cisplatin. During their investigations, the presence of a stable ligand (chelate), a more hydrophobic arene ligand (possibly to enhance cellular penetration) and a labile ligand, were identified as necessary components to design active anticancer complexes.[157]

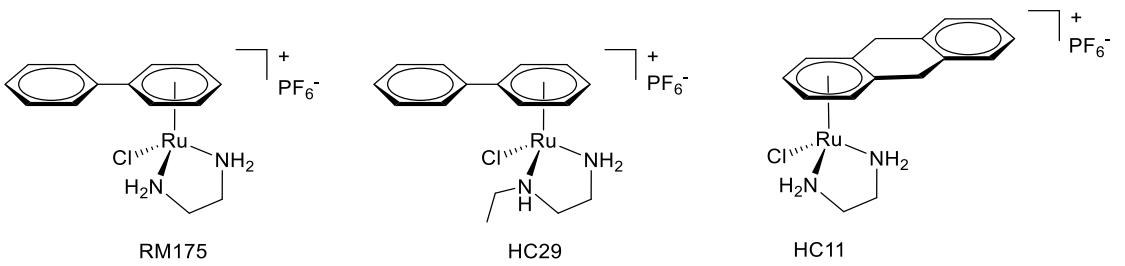

Figure 38: Structures of arene ruthenium complexes with chelate diamine ligands

1.3.3 Dinuclear arene ruthenium clips

Dinuclear arene ruthenium clips bridged by OO∩OO or ON∩NO have been widely used by our group to construct more complicated supramolecular structures, such as metalla-rectangles, metalla-prisms and metalla-cubes. Since the first OO∩OO clip and its arene ruthenium metalla-rectangle was synthesized by Süss-Fink in 1997 (Scheme 11),[159] our group developed metalla-cages via the strategy used in this paper. The activation of metalla-clips can be achieved by adding silver triflate, thus the chloride ligands are abstracted to form silver chloride, which is then removed by filtration. The dicationic intermediate with coordinations of solvent molecules can easily react with pyridyl-based ligands.[160] One of the dicationic intermediates with coordinations of methanol has been isolated and characterized.[161]

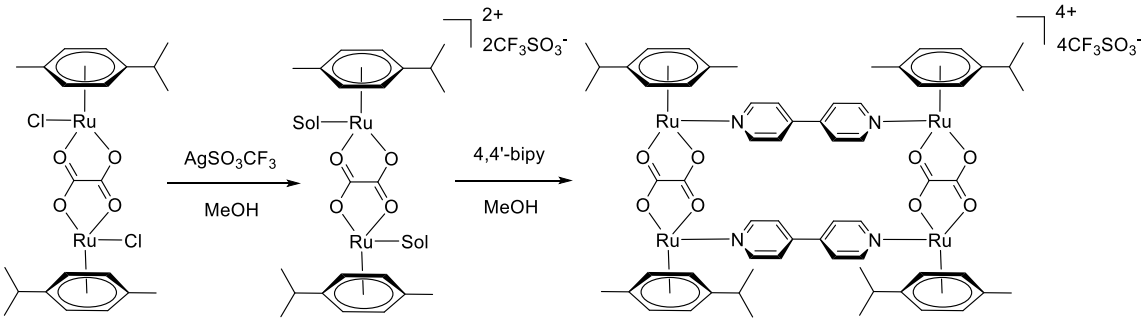

Scheme 11: Synthesis of arene ruthenium metalla-rectangle $[(cym)_4Ru_4(C_2O_4)_2(bpy)_2](4CF_3SO_3)$

The general synthetic method to prepare arene ruthenium clips uses chloride-bridged arene ruthenium complex $[(\eta^6\text{-arene})Ru(\mu\text{-Cl})Cl]_2$ as starting materials. The activation of this complex is performed by cleavage of two chloride bridges, and one equivalent of the desired quinone ligand can replace two chloride bridges (Scheme 12).

Quinones with a weak reactivity need the addition of sodium acetate to react. Another type of bridges is ON∩NO bridges, which can be synthesized with the same reactant and desired ON∩NO ligands in the presence of weak bases [diisopropylethylamine (DIPEA) or NEt_3].

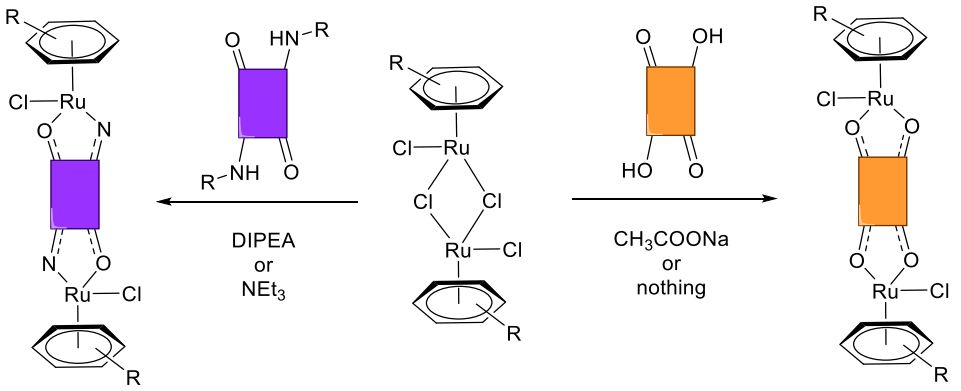

Scheme 12: Method to synthesize arene ruthenium clips with OO∩OO or ON∩NO bridges

Another type of clips with two carboxylic acid bridges was synthesized by the group of Severin in 2010 (Scheme 13).[162] Their synthesis is similar to ours with the same reactant and the presences of two equivalents of the desired carboxylic acid ligands and silver acetate.

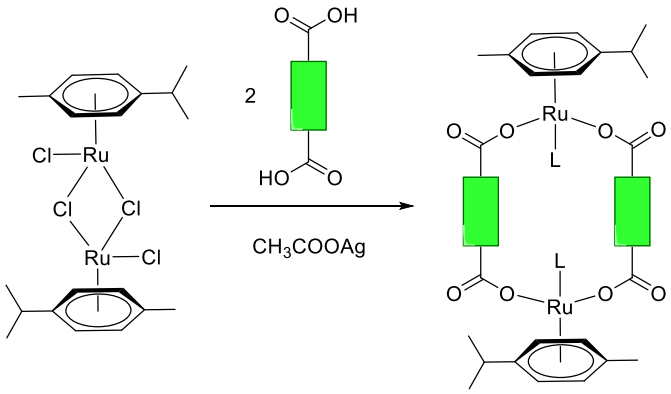

Scheme 13: Method to synthesize arene ruthenium clips with carboxylic acid bridges

Several OO∩OO bridged arene ruthenium clips have been used in our group[160], such as $[Ru_2(\eta^6\text{-arene})_2(oxalato)Cl_2]$,[159] $[Ru_2(\eta^6\text{-arene})_2(dhbq)Cl_2]$ (dhbq: 2,5-dihydroxy-1,4-benzoquinonato),[163] $[Ru_2(\eta^6\text{-arene})_2(dchq)Cl_2]$ (dchq: 2,5-dichloro-1,4-benzoquinonato),[164] $[Ru_2(\eta^6\text{-arene})_2(dhnq)Cl_2]$ (dhnq: 5,8-dihydroxy-1,4-

naphthoquinonato),[165] $[Ru_2(\eta^6\text{-arene})_2(dhaq)Cl_2]$ (dhaq: 9,10-dihydroxy-1,4-anthraquinonato),[166] and $[Ru_2(\eta^6\text{-arene})_2(dhtq)Cl_2]$ (dhtq: 6,11-dihydroxynaphthacene-5,12-dionato).[167] To increase the size of the assembly and to encapsulate various 'guest' compounds, arene ruthenium clips possess different lengths (Figure 39).

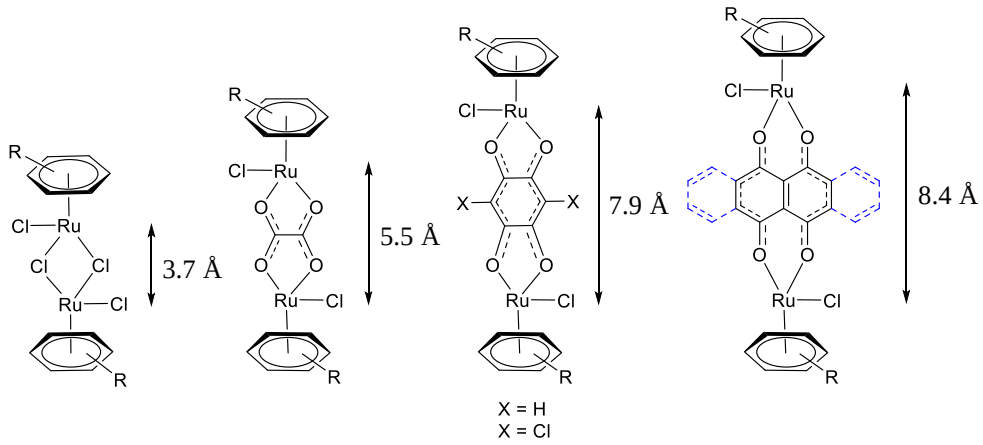

Figure 39: OO∩OO bridged dinuclear arene ruthenium clips

The ON∩NO derivatives show similar properties,[168] but offer more synthetic possibilities to insert functional groups. Some arene ruthenium cationic cages formed by these clips showed great selectivity for cancerous cells.[169] Thus developments of this type of clips are necessary for biological optimization.[169] Some ON∩NO arene ruthenium clips were synthesized by our group and others, such as $[Ru_2(cym)_2(\mu\text{-L})Cl_2]$ [H_2L: diethyl-1,2-diazenedicarboxylate, N,N'-bis(2-hydroxyethyl)oxamide, N,N'-bisethanediamide,[169] dihexyloxalamide or dioctyloxalamide][170] (Figure 40).

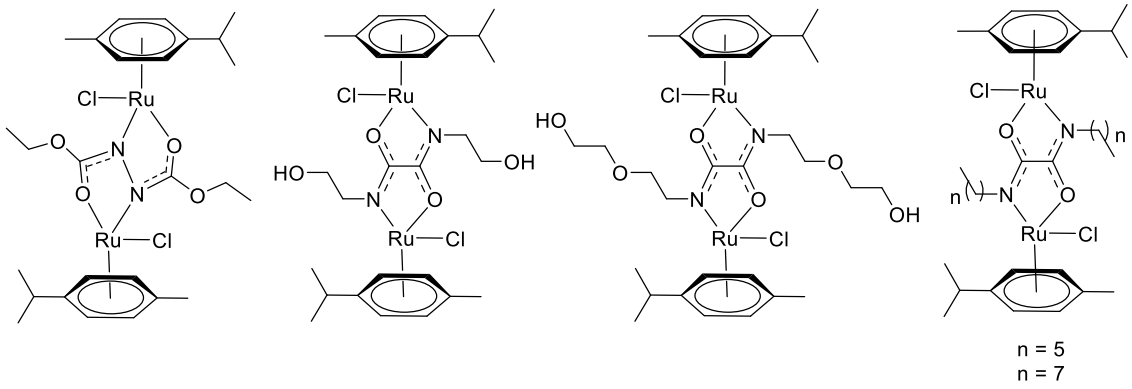

Figure 40: ON∩NO bridged dinuclear arene ruthenium clips

Dicarboxylate-bridged ruthenium clips opened a new domain for the synthesis of arene ruthenium cages (Figure 41). They can be used to synthesize neutral arene ruthenium cages and offer access to more complex molecular architectures.[171] The dicarboxylate spacers were chosen owing to the lability of the carboxylate donor groups and their flexible coordination geometries.[172] Furthermore, one of them prepared from 3,6-dimethoxynaphtalene-2,7-dicarboxylic acid can reach a length of 10.9 Å and its metalla-prism can encapsulate two coronene molecules.[162]

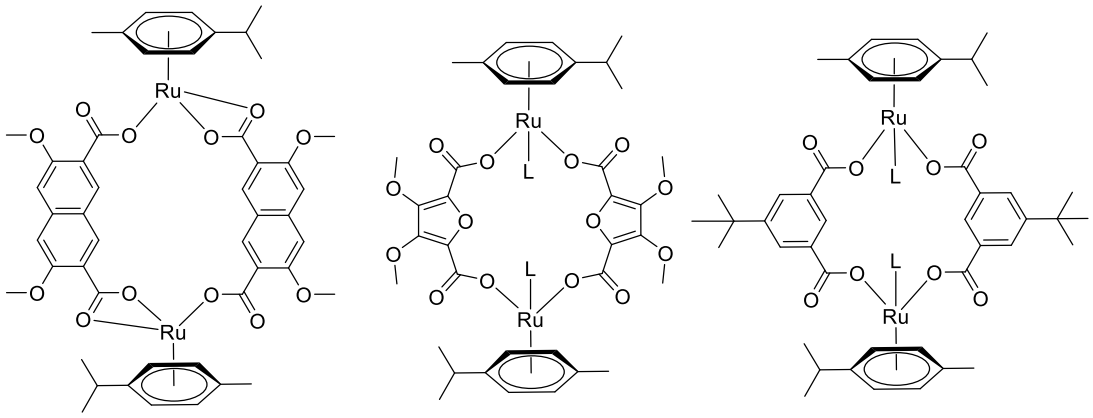

Figure 41: Dicarboxylate-bridged dinuclear arene ruthenium clips

1.3.4 Multinuclear arene ruthenium complexes

From dinuclear arene ruthenium clips, different metalla-rectangles, metalla-prisms and metalla-cubes can be synthesized through metal-ligand coordinations. Coordination-driven supramolecular complexes were principally pioneered by the groups of Fujita[136] and Stang.[173] The Pd(II) square complexes were quantitatively synthesized by the group of Fujita in 1990.[119] The geometry of transition metal centers and the rigidity of electron-rich organic ligands are two important features to design this type of supramolecular metalla-cages.[174] It took five years, to extend 2D supramolecular structures to 3D structures.[175] These Pd(II) M_6L_4 octahedral 3D structures showed high solubility in water, strong bindings with 'guest' molecules through hydrophobic interactions, and large cavities,[136] which inspired many groups, including ours.

The desired 2D and 3D supramolecular assemblies are obtained by combining the appropriate building blocks. Different pyridyl spacers, which were widely used by the groups of Fujita[176] and Stang[177-178] to form Pd(II) or Pt(II) metalla-assemblies,

were chosen by our group for the design of arene-ruthenium metalla-cages (Table 3). Pyridyl spacers play a crucial role to determine the geometry of the arene ruthenium metalla-assembly. For example, linear bipyridyl ligands have two coordination sites at a 180 ° angle, thus arene ruthenium rectangles are formed by the combination of two bipyridyl ligands with two arene ruthenium clips. A wide range of multinuclear arene ruthenium cages was reported by our group.[179]

Arene Ruthenium Clips	**Spacer ligands Structures**	**Angle**	**Metalla-cages**
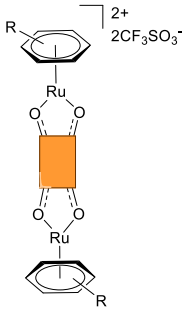	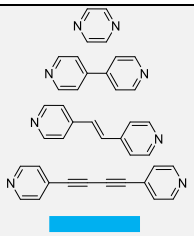	180 °	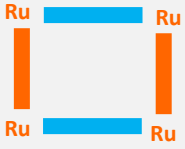 Metalla-rectangle
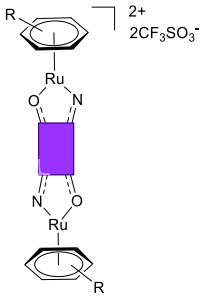	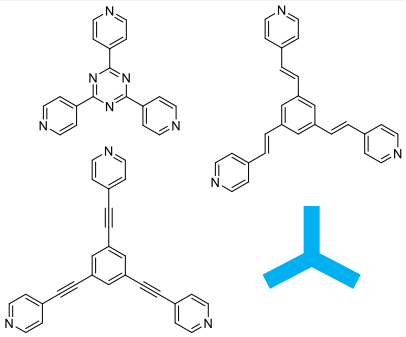	120 °	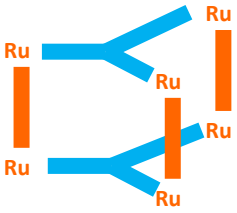 Metalla-prism
	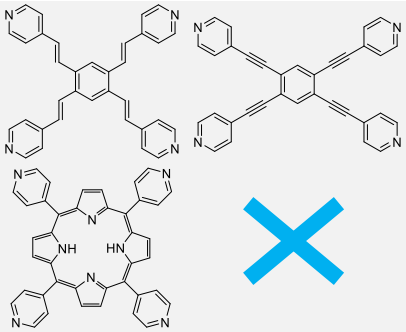	90 °	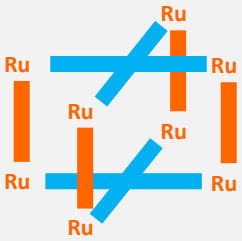 Metalla-cube

Table 3: Strategies for syntheses of metalla-cages from arene ruthenium clips with spacer ligands

A series of metalla-rectangles with the general formula $[Ru_4(\eta^6\text{-arene})_4(OO\cap OO)_2(N\cap N)_2](CF_3SO_3)_4$ (η^6-arene = para-cymene, hmb; OO∩OO = dobq, dClobq; N∩N = pyrazine (pyr), 4-4'-bipyridine (bpy), 1,2-bis(4-pyridyl)ethylene (bpe)) was synthesized by our group.[180] Their anticancer activities were tested against the A2780 ovarian cancer cell line. The metalla-rectangle

$[Ru_4(hmb)_4(dobq)_2(bpe)_2](CF_3SO_3)_4$ showed the best activity (Figure 42). Importantly, these metalla-rectangles showed good selectivity towards tumor cells over normal cells. In addition, the formation mechanisms of such metalla-rectangles were also investigated.[181]

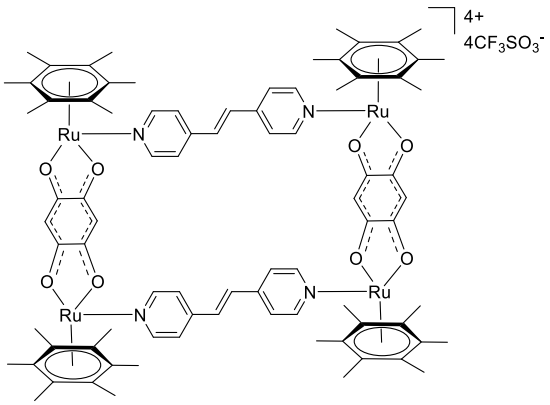

Figure 42: Structure of metalla-rectangle $[Ru_4(hmb)_4(dobq)_2(bpe)_2](CF_3SO_3)_4$

The first arene ruthenium metalla-prism synthesized by our group was the oxalato-bridged para-cymene ruthenium prism.[182] Then the chloro-bridged para-cymene ruthenium prism was synthesized.[183] But no guest molecule could be encapsulated in these two prisms, because of a limited length between the two tpt panels. To overcome this limitation, the dobq-bridged para-cymene ruthenium prism was synthesized and showed good ability for encapsulations.[184] A series of encapsulations was achieved,[185] and the encapsulation was realized during the synthesis of the prism.

A ‘‘Trojan horse’’ strategy was suggested for cancer treatment, as non water soluble drugs were encapsulated in the hydrophobic cavity of the metalla-prisms for transport and release into cancer cells (Scheme 14).[186] Metalla-prisms were isolated as trifluoromethanesulonate salts, thus presenting good solubility in water. [187-188]

In their biological tests, the cytotoxicity of the prism was increased after encapsulations of complexes $[Pt(acac)_2]$, $[Pd(acac)_2]$ or pyrenyl derivatives. And highly cytotoxic systems were obtained through changing functional groups at the edge of the pyrenyl compounds.[189]

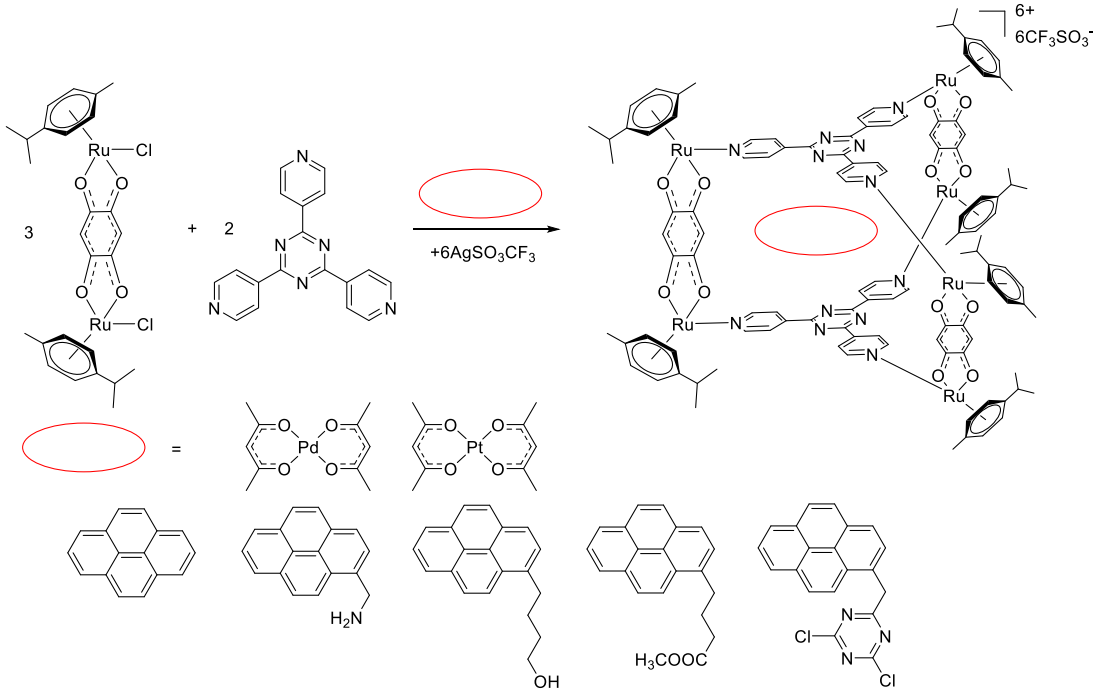

Scheme 14: Synthesis of the dobq-bridged para-cymene ruthenium prism with encapsulations of pyrenyl derivatives or complexes

Arene ruthenium metalla-cubes, larger than metalla-prisms, were synthesized to increase the size of the metalla-assemblies. The metalla-cube $[Ru_8(cym)(dhnq)_4(tpvb)_2](CF_3SO_3)_8$ (tpvb: 1,2,4,5-tetrakis[2-(4-pyridyl)vinylbenzene]) can be used to encapsulate porphin, a photosensitizer (Figure 43).[190] This system showed hypochromism properties towards the photosensitizer inside the cavity. Thus the phototoxic effect can be hidden during encapsulation.[191]

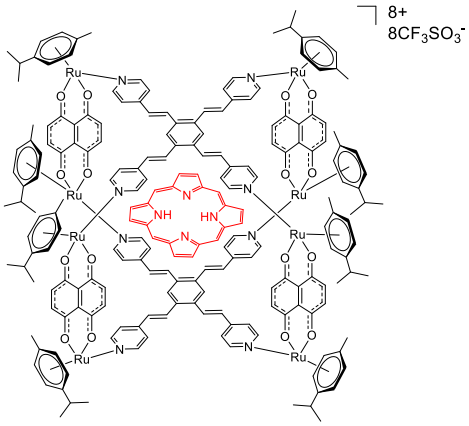

Figure 43: Encapsulated porphin in the cavity of metalla-cube $[Ru_8(cym)(dhnq)_4(tpvb)_2](CF_3SO_3)_8$

1.3.5 Cyclopentadienyl rhodium/iridium complexes

Rhodium and iridium are both rare elements, they are members of the 'Platinum-group metals' with ruthenium, palladium, osmium and platinum, owing to their similar chemical and physical properties.[192] Rhodium has the symbol Rh, molecular weight 102.91 g/mol, and atomic number 45. It is in group 9 and period 5 of the periodic table with the electronic configuration [Kr] $4d^8$ $5s^1$. Iridium has the symbol Ir, molecular weight 192.22 g/mol, and atomic number 77. It is also in group 9 but in the next period 6 of the periodic table with the electronic configuration [Xe] $4f^{14}$ $5d^7$ $6s^2$. Rhodium and Iridium have a wide range of oxidation states from -III ($[M(CO)_3]^{3-}$) to +VI ($[MF_6]$).[132] In my thesis, only complexes with Rh(III) and Ir(III) were synthesized.

The chemistry of cyclopentadienyl rhodium/iridium complexes is similar to that of arene ruthenium complexes.[193] The most common cyclopentadienyl derivative is the 1,2,3,4,5-pentamethylcyclopentadiene (Cp*) rhodium/iridium complexes. In these complexes, the rhodium and the iridium possess six coordination sites, three of them are occupied by the cyclopentadienyl derivative. The other three coordination sites can be coordinated by ligands of various properties.[194]

Like the synthesis of mononuclear arene ruthenium complexes, mononuclear cyclopentadienyl rhodium/iridium complexes are obtained from the dinuclear chloride-bridged cyclopentadienyl rhodium/iridium complexes $[(Cp^*)M(\mu\text{-}Cl)Cl]_2$ (M = Rh or Ir) (Scheme 15). As mentioned previously, the pentamethylcyclopentadienyl derivative was selected owing to its good stability. The dinuclear chloride-bridged pentamethylcyclopentadienyl rhodium/iridium complexes $[(Cp^*)M(\mu\text{-}Cl)Cl]_2$ (M = Rh or Ir) are easy to prepare and give high yields and pure products.[195]

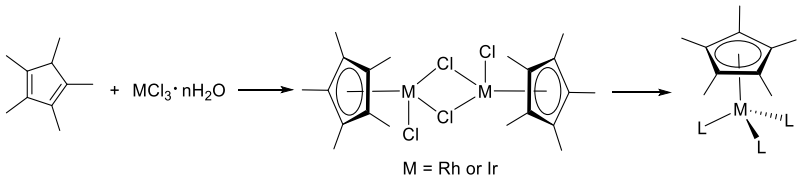

Scheme 15: Synthesis of mononuclear pentamethylcyclopentadienyl rhodium/iridium complexes

Rhodium (III) and iridium (III) complexes have showed relatively inert anticancer activities, until a bioactive iridium (III) complex [(Cp*)Ir(ppy)Cl] (ppy: 2-

phenylpyridine) was reported by the group of Sadler in 2011 (Figure 44).[196] This complex with a C,N-bidentate ligand showed significant cytotoxicity towards A2780 cell line, owing to its strong nucleobase binding ability and high hydrophobicity.[197] Later on, one iridium complex with a N,O-bidentate ligand (ketoiminate) was synthesized and showed activity comparable to cisplatin against HT-29 and MCF 7 cell lines. Another iridium (III) complex with an O,O-bidentate ligand (2-hydroxy-1,4-napthoquinone) was synthesized by the group of McGowan. This complex showed more anticancer properties than that of the reactants.[198] For mononuclear cyclopentadienyl rhodium complexes, the neutral complex [(Cp*)Rh(pmp)Cl] (pmp: 2-[(propylimino)methyl]phenol) was synthesized by the group of Smith in 2013. It showed only moderate cytotoxicity.[199]

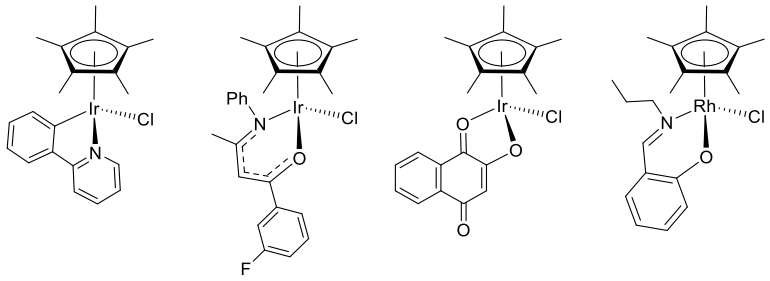

Figure 44: Structures of pentamethylcyclopentadienyl iridium and rhodium complexes

Dinuclear cyclopentadienyl rhodium/iridium clips bridged by OO∩OO ligands have been used by our group to construct metalla-assemblies. Their preparations are similar to those of arene ruthenium complexes bridged by OO∩OO ligands. From $[(Cp^*)M(\mu\text{-}Cl)Cl]_2$ (M = Rh or Ir), the corresponding OO∩OO ligands can be introduced to obtain rhodium/iridium clips (Scheme 16). The activation of rhodium/iridium clips can be achieved by adding silver triflate. The dicationic intermediate obtained can be used for the formation of metalla-cages.

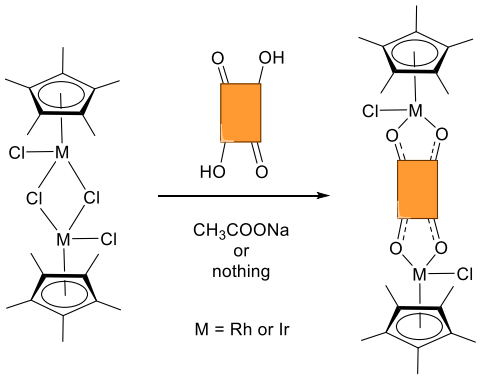

Scheme 16: Synthesis of pentamethylcyclopentadienyl rhodium/iridium clips with OO∩OO bridges

Because of moderate anti-cancer activities of rhodium and iridium complexes, our group has tried to increase their antiproliferative activities by preparing a range of thiolato-bridged dinuclear pentamethylcyclopentadienyl rhodium/iridium complexes (Figure 45).[194, 200] Both neutral thiolato-bridged rhodium/iridium complexes and cationic thiolato-bridged rhodium/iridium complexes showed good antiproliferative activities and cytotoxicity in the nanomolar range. The cytotoxicity of these complexes was strongly affected by the substituents connected to the thiolato-bridges. However, their poor selectivity was problematic.

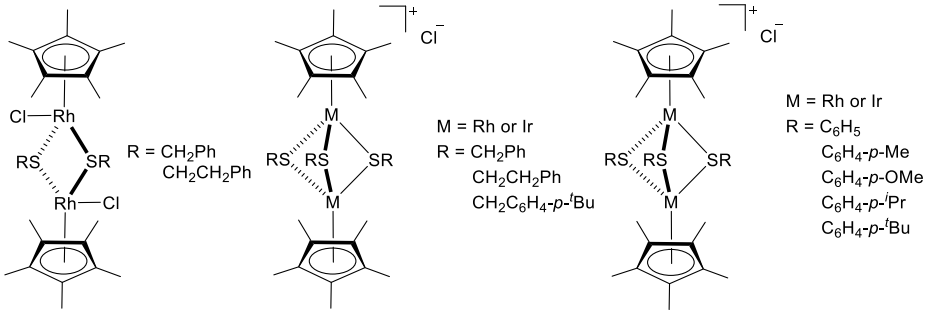

Figure 45: Structures of thiolato-bridged pentamethylcyclopentadienyl rhodium/iridium complexes

After the successful synthesis of arene ruthenium metalla-cages, cyclopentadienyl rhodium/iridium analogues were synthesized, and their antiproliferative activity evaluated. A series of rhodium/iridium metalla-rectangles was reported by our group in 2013 (Figure 46).[201] They showed high cytotoxicity.

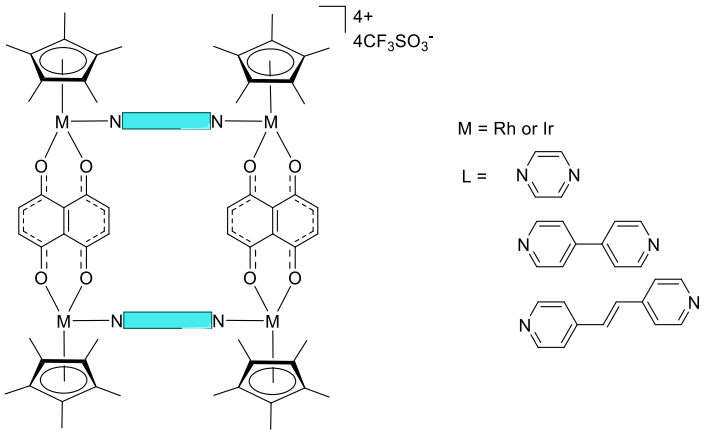

Figure 46: Structures of cyclopentadienyl rhodium/iridium metalla-rectangle

In 2014, rhodium/iridium metalla-prisms containing lipophilic side chains were synthesized (Figure 47).[202] These cationic metalla-prisms showed excellent activities *in vivo* in tumor-induced C57L6/J mice, and also some selectivity. Furthermore, the Rh (III) metalla-prism showed higher potential than the Ir (III) metalla-prism for reducing tumors and inducing apoptosis in tumor cells.

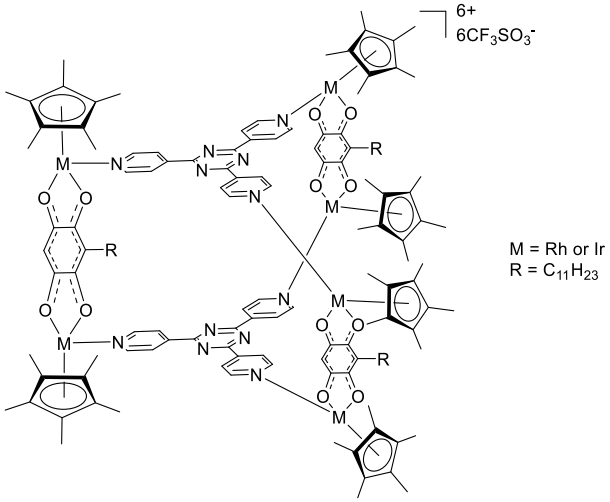

Figure 47: Structures of cyclopentadienyl rhodium/iridium metalla-prisms

Similarly, a series of metalla-cubes containing lipophilic side chains was synthesized to increase the size of metalla-cages (Figure 48).[203] All metalla-cubes showed antiproliferative activities and IC_{50} values in the nanomolar range. The Rh (III) metalla-cube interacted with ctDNA and induced apoptosis in cancer cells. Thus, the Rh

(III) metalla-cube showed the strongest activity in comparison to the Ir (III) analogues and Ru (II) metalla-cubes.

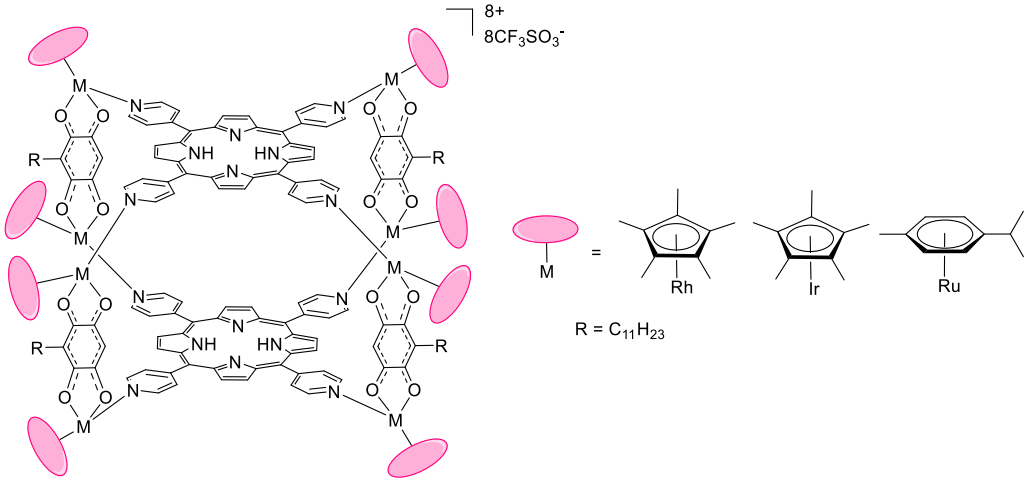

Figure 48: Structures of metalla-cubes with lipophilic side chains

1.4 Aim of this thesis

Hydrogen bonds are widely used in biological systems, thus being biocompatible. The diversity of hydrogen bonds can offer more possibilities for designing supramolecular complexes than only coordination chemistry. On the other hand, we have developed metalla-assemblies based on ruthenium (II), osmium (II), rhodium (III) and iridium (III) for nearly 15 years, and a large range of metalla-assemblies based on these four metals has been synthesized, characterized and evaluated as anticancer agents. Some of them possess promising potential to become anti-tumor drugs.

The combination of hydrogen bonds and Ru(II), Rh(III) or Ir(III) metalla-assemblies can open new directions. This combination was already tested by Dr. Appavoo-Gupta who associated arene ruthenium complexes with UPy dimers. Thus the aim of my thesis is to synthesize and analyze Ru(II), Rh(III) or Ir(III) metalla-assemblies based on melamine/barbituric acid hydrogen-bonded rosette system, for the design of large complexes. The idea is to add pyridyl substituents on the rosette system to achieve metal-ligand coordinations. This work is divided in three parts: The first part consists of adding three mononuclear metal complexes at the periphery of hydrogen-bonded rosette systems that are not only neutral but also cationic. The second part comprises the design and addition of different mononuclear metal complexes in similar

systems, while the last part shows our attempts to form double-decker rosette systems by addition of dinuclear metal complexes.

Chapter 2

Coordination of piano-stool complexes to a hydrogen-bonded rosette-type assembly

2.1 General introduction

"Unity is strength" can be considered the motto of supramolecular chemistry. The multiplication of weak interactions allows complex structures to form and to remain stable in solution, despite the fragility of each individual interaction. Typical noncovalent interactions (< 20 kcal mol^{-1}) include ionic, hydrophobic, hydrogen-bond, and metal-coordination.[204-205] In nature, these interactions are crucial for biological

processes and essential for building up large molecules, such as DNA, enzymes, or proteins. Inspired by nature, chemists are using noncovalent interactions to generate structural complexity and to develop chemical systems.[206-209]

In recent years, coordination-driven self-assembly has been exploited to prepare esthetical and functional complex structures.[177, 210-212] Those including arene ruthenium units have shown great promises,[160-161, 213-214] especially for biological applications.[134, 215-216] Until recently, these arene ruthenium metalla-assemblies were held together by covalent and multiple metal-coordination bonds.[160-161, 213-214] However, last year our group inserted quadruple self-complementary hydrogen-bonding motifs to generate a new type of arene ruthenium metallacycle.[72-73] Yet, this self-complementary approach was somehow limiting in terms of structural diversity, and therefore, the use of hetero hydrogen-bond-pairing systems can, in principle, offer more possibilities.

Among non-self-complementary hydrogen-bonding motifs, melamine·cyanuric acid/barbituric acid pairing is one of the most studied triple-hydrogen-bonding systems.[10, 98, 217-218] As demonstrated by Whitesides, controlled formation of rosette-type assemblies over tapelike structures can be achieved by steric constraints.[76] Indeed, it was shown that the combination of the crowded *N,N'*-bis(4-*tert*-butylphenyl)melamine (ME) with 5,5-diethylbarbituric acid (BA) formed an $(ME)_3$ $(BA)_3$ rosette-type structure exclusively (Figure 49), an arrangement that was confirmed by single-crystal X-ray diffraction structure analysis.[76] This elegant strategy allows synthetic modifications on both the melamine and the barbituric acid units.[90-92]

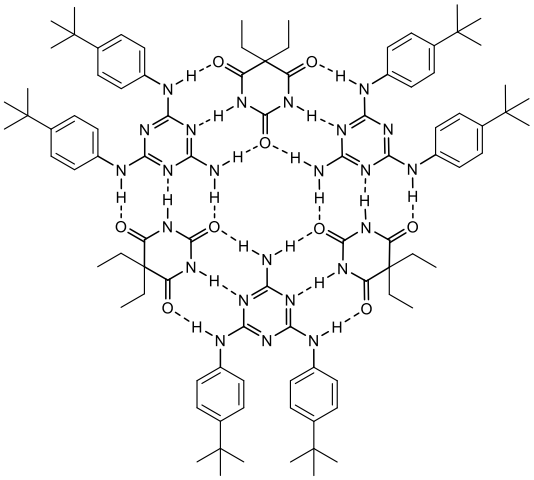

Figure 49 : Rosette-type structure developed by Whitesides using *N,N'*-bis(4-*tert* butylphenyl)melamine and 5,5-diethylbarbituric acid

In our search to develop new strategies to synthesize supramolecular arene ruthenium assemblies, we have introduced a pyridyl coordination site to a barbituric acid unit, with a view to obtaining metal-coordinated rosette-type systems. Arene ruthenium complexes, as well as the pentamethylcyclopentadienyl iridium/rhodium analogues, have been coordinated to the new rosette. These assemblies are either neutral or ionic, depending on the nature of the piano-stool complex used. This simple strategy opens up new perspectives in the field of coordination driven self-assembly of piano-stool complexes, and to the development of complex structures.

2.2 Synthesis

2.2.1 Synthesis of rosette-type ligands

In this section, two building blocks were used to prepare the $(ME)_3{\cdot}(BApy)_3$ rosettes [ME: *N,N'*-bis(4-*tert*-butylphenyl)melamine; BApy: 5-butyl-5-(pyridine-4-ylmethyl)pyrimidine-2,4,6-trione]. The synthesis of these ligands can be divided in three parts. The first part was the formation of BApy which was obtained in two synthetic steps, starting from diethyl 2-butylmalonate and 4-(chloromethyl)pyridine. Then the ME derivative was also obtained in two synthetic steps, starting from 4-(*tert*-butyl)aniline and cyanuric chloride. The final part was the formation of the $(ME)_3{\cdot}(BApy)_3$ rosette starting from melamine (ME) and the barbituric acid derivative containing a pyridyl group (BApy) (Scheme 17).

The synthesis of $(ME)_3{\cdot}(BApy)_3$ was performed in chloroform to facilitate hydrogen-bonding interactions. To prepare the hydrogen-bonded rosettes-type assembly, another important factor is the concentration of reactants. Concentrations of ME and BApy need to be higher than 4 mM, otherwise assembly/disassembly of the rosette-type complex might occur.[80]

Initially, *N,N'*-bis(4-methylphenyl)melamine was used to make a rosette, but this derivative was not soluble in chloroform, even in the presence of BApy. When we tried with *N,N'*-bis(4-*tert*-butylphenyl)melamine, the two reactants were almost insoluble in chloroform. But the rosette was well soluble in chloroform. Therefore, the solubility of the reactants needs to be considered for the design of rosette-type assemblies.

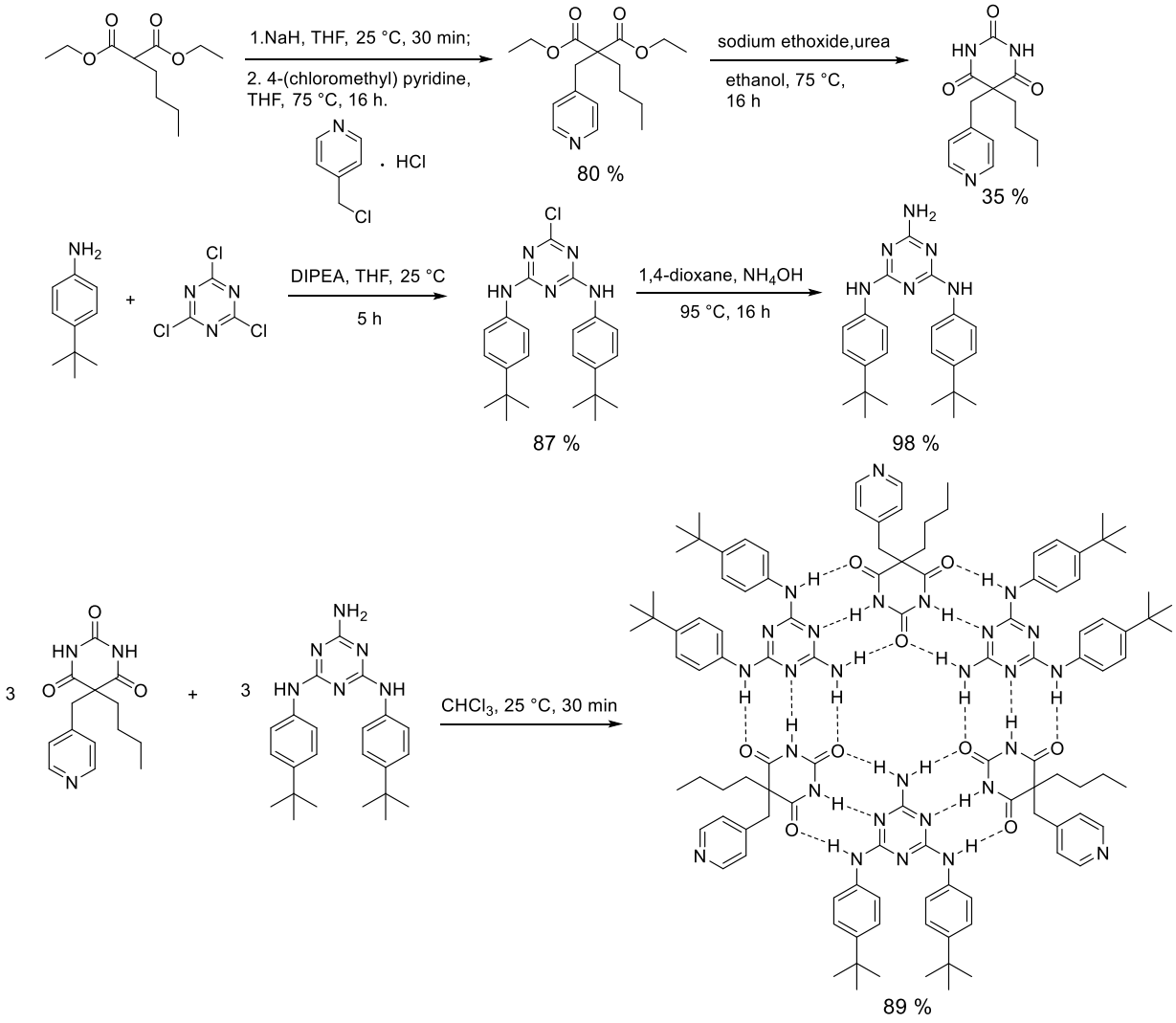

Scheme 17: Synthesis of the rosette-type assembly $(ME)_3{\cdot}(BApy)_3$

2.2.2 Synthesis of neutral trinuclear hydrogen-bonded metalla-assemblies

The three pyridyl groups at the periphery of $(ME)_3{\cdot}(BApy)_3$ can be used to coordinate metal centers. Addition of 1.5 equivalent of $[Ru(cym)Cl_2]_2$ (cym: para-cymene), $[Rh(Cp^*)Cl_2]_2$ or $[Ir(Cp^*)Cl_2]_2$ (Cp*: pentamethylcyclopentadienyl) to a solution of $(ME)_3{\cdot}(BApy)_3$ in chloroform afforded the corresponding metal-containing rosettes $(ME)_3{\cdot}(BApyRu)_3$, $(ME)_3{\cdot}(BApyRh)_3$ or $(ME)_3{\cdot}(BApyIr)_3$ [Ru: $Ru(cym)Cl_2$, Rh: $Rh(Cp^*)Cl_2$, Ir: $Ir(Cp^*)Cl_2$]. An excellent yield, around 90 %, was obtained for this reaction (Scheme 18).

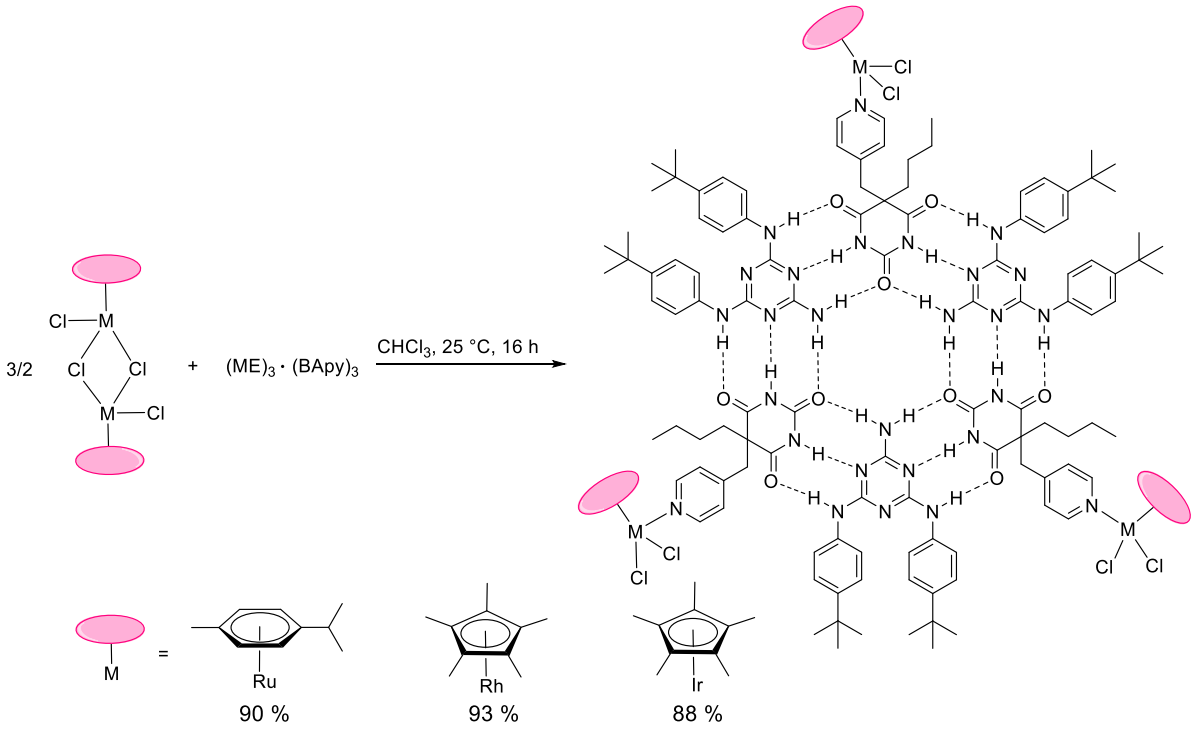

Scheme 18: Synthesis of neutral trinuclear hydrogen-bonded rosettes

Coordination of the BApy unit to the metal centers can also be performed prior to the rosette formation. Indeed, the reaction of $[Ru(cym)Cl_2]_2$ or $[Rh(Cp^*)Cl_2]_2$ with BApy afforded the mononuclear complexes BApyRu or BApyRh, respectively. We first used methanol as solvent, but the product showed impurities. Thus, a solvent effect cannot be ignored in this step. Then addition of ME to the solution of BApyRu or BApyRh in chloroform afforded the corresponding metal-containing rosettes $(ME)_3{\cdot}(BApyRu)_3$ or $(ME)_3{\cdot}(BApyRh)_3$ also in excellent yields (Scheme 19). This method consumes more energy in comparison with the previous method, thus being preferable.

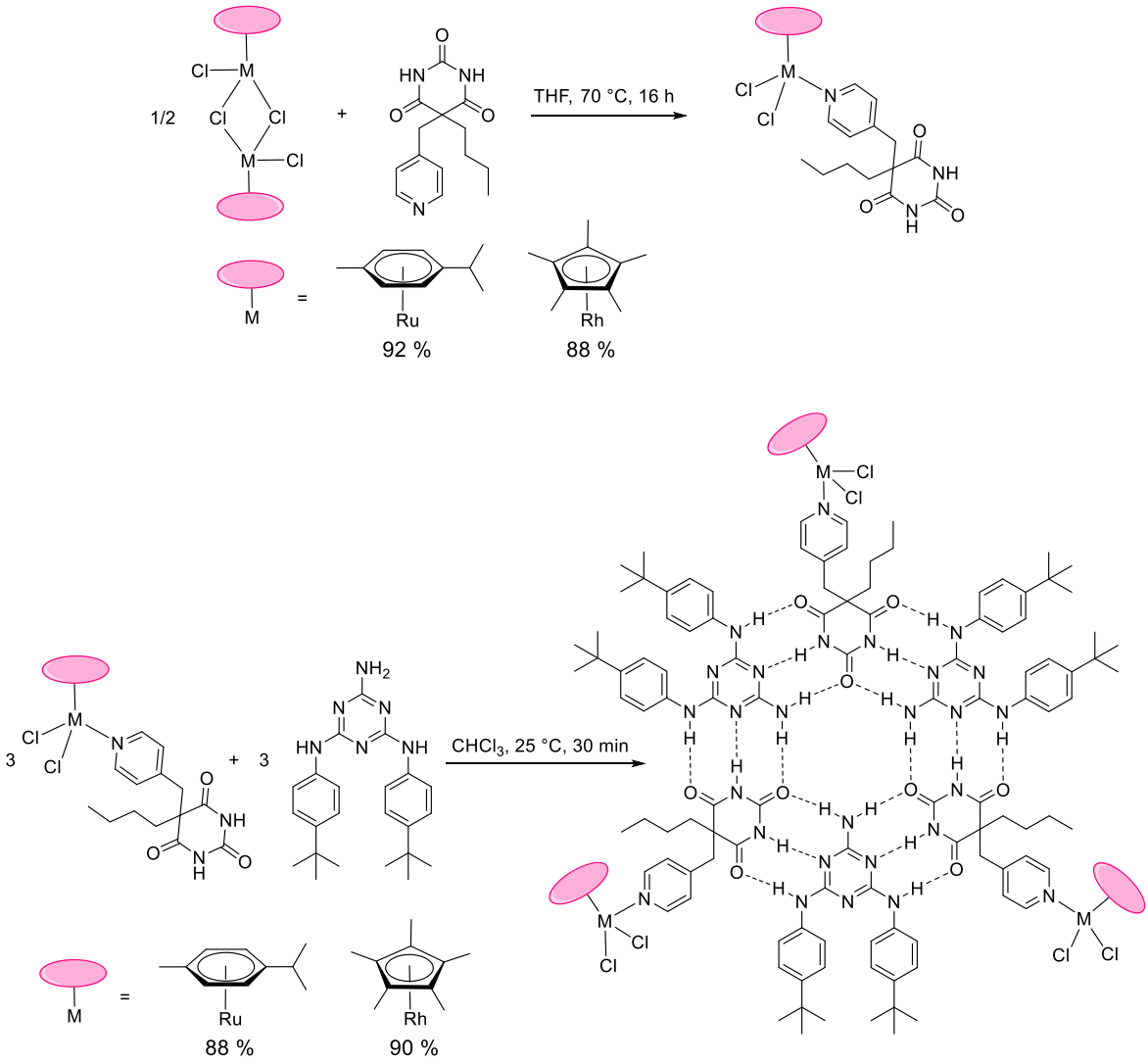

Scheme 19: Synthesis of neutral trinuclear hydrogen-bonded metalla-assemblies $(ME)_3 \cdot (BApyM)_3$ from BApyRu or BApyRh and ME

2.2.3 Synthesis of cationic trinuclear hydrogen-bonded metalla-assemblies

Coordination of triphenylphosphine to the metal centers affords the half-sandwich complexes $[Ru(cym)Cl_2(PPh_3)]$, $[Rh(Cp^*)Cl_2(PPh_3)]$ and $[Ir(Cp^*)Cl_2(PPh_3)]$ respectively (PPh_3: triphenylphosphine). Addition of silver triflate affords the intermediate complexes $[Ru(cym)(PPh_3)(Sol)Cl](CF_3SO_3)$, $[Rh(Cp^*)(PPh_3)(Sol)Cl](CF_3SO_3)$, and $[Ir(Cp^*)(PPh_3)(Sol)Cl](CF_3SO_3)$, which is accompanied by precipitation of silver chloride (Scheme 20).

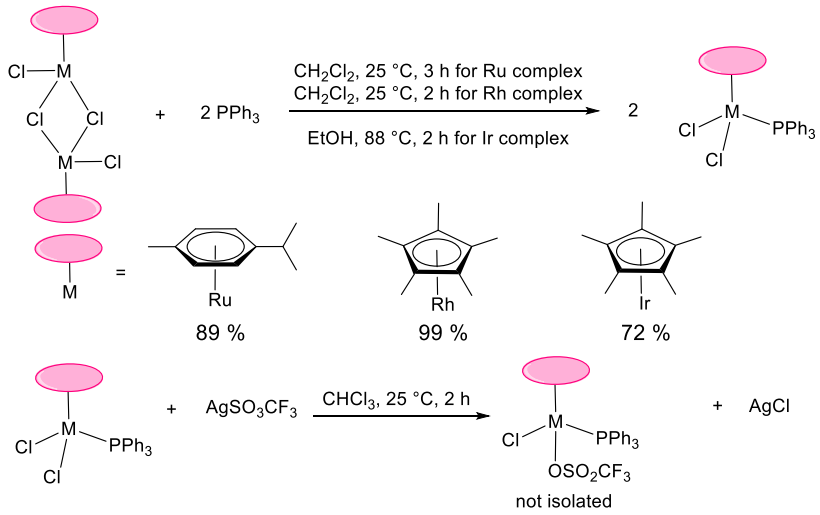

Scheme 20: Synthesis of triflate derivatives

These cationic mononuclear complexes can also react with the $(ME)_3{\cdot}(BApy)_3$ rosette to generate the cationic trinuclear assemblies $\{(ME)_3{\cdot}[(BApy)Ru(cym)(PPh_3)Cl]_3\}^{3+}$, $\{(ME)_3{\cdot}[(BApy)Rh(Cp^*)(PPh_3)Cl]_3\}^{3+}$ and $\{(ME)_3{\cdot}[(BApy)Ir(Cp^*)(PPh_3)Cl]_3\}^{3+}$ respectively (Scheme 21).

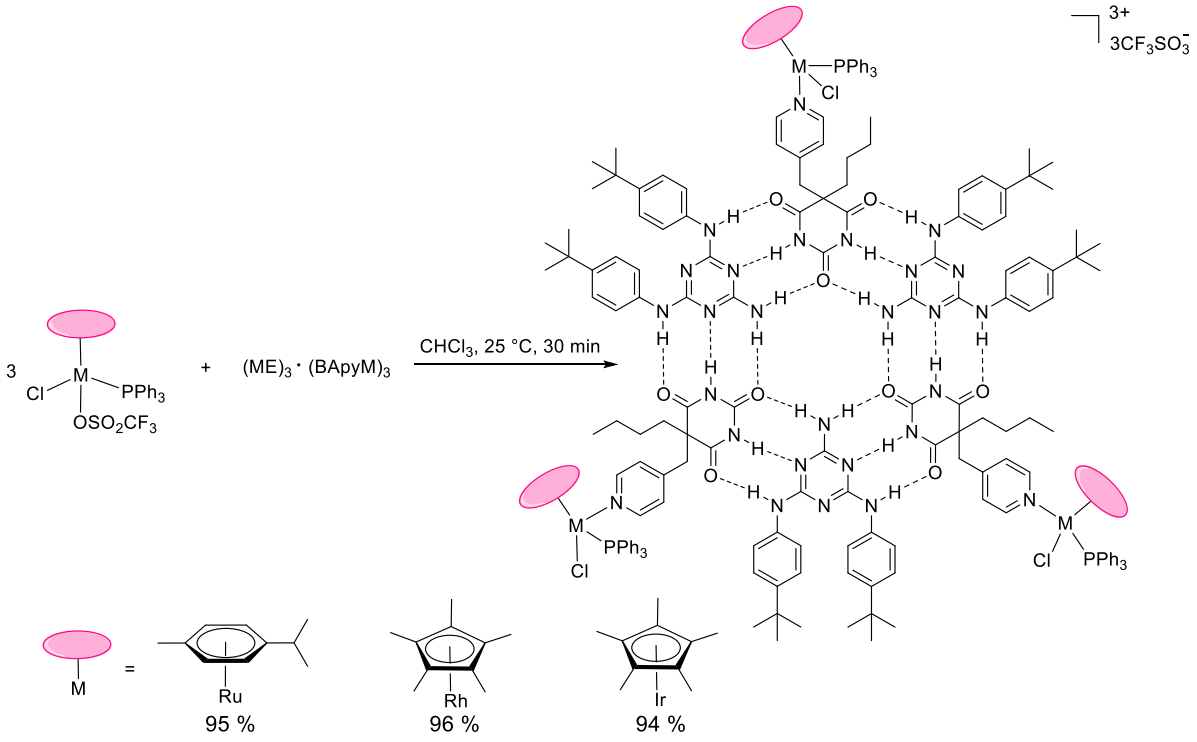

Scheme 21: Synthesis of cationic trinuclear hydrogen-bonded metalla-assemblies.

2.3 Characterizations

2.3.1 Proton and carbon NMR spectroscopy

All synthesized rosettes were fully characterized by NMR spectroscopy. By comparing spectra of ME and BApy with the $(ME)_3 \cdot (BApy)_3$ rosette (Figure 50), the most evident signal is at 14.0 ppm which is the NH signals of the BApy units confirming the formation of rosette-type assemblies. This NH signals are shifted by ca. 2.4 ppm, while for the ME units, the signals are shifted by ca. 2.5 ppm (NH) and ca. 1.9 ppm (NH_2), respectively. On the other hand, the protons of the butyl, pyridyl, and *tert*-butylphenyl groups are almost unaffected, being all located at the periphery of the rosette.

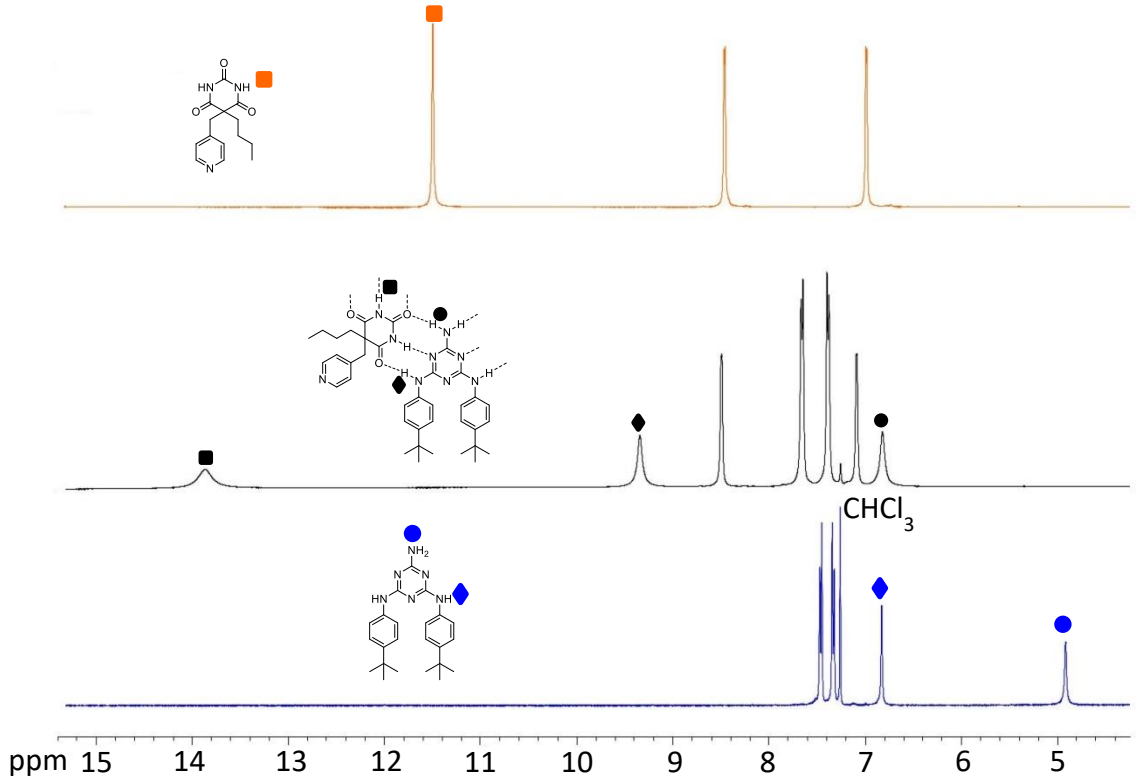

Figure 50: ^{1}H NMR spectra of BA, $(ME)_3 \cdot (BApy)_3$, and ME, with an emphasis on the chemical shifts of the different NH protons ($CDCl_3$, 25 ℃)

The coordination of the pyridyl group to the metal centers only slightly influences the ^{1}H NMR chemical shift of the pyridyl protons (Figure 51). The most important shift is observed for the signals of the H_α protons of the pyridyl group (0.4

ppm). Similarly, the most affected carbon atoms as indicated by the ^{13}C NMR signals of the BApyRu and BApyRh complexes are those adjacent to the nitrogen atom of the pyridyl groups (Figure 52). Other proton and carbon signals are almost unaffected or only slightly shifted.

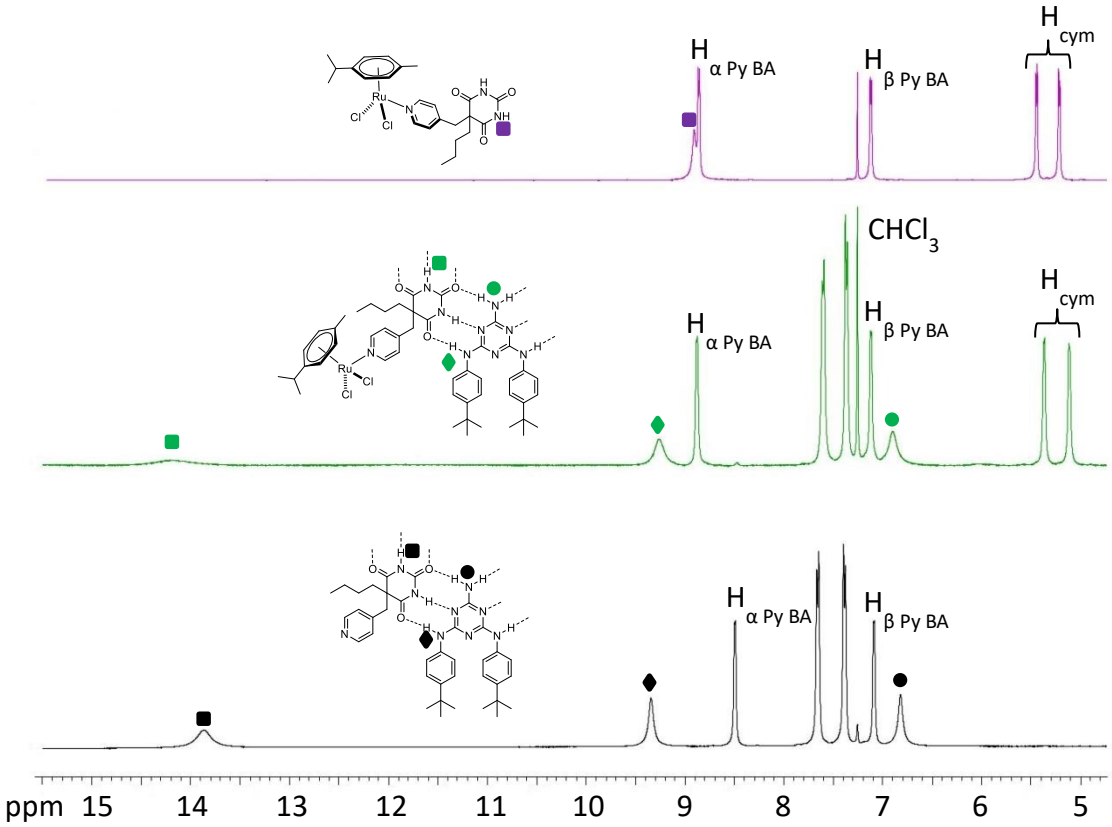

Figure 51: ^{1}H NMR spectra of BApyRu, $(ME)_3 \cdot (BApyRu)_3$ and $(ME)_3 \cdot (BApy)_3$ ($CDCl_3$, 25 ℃)

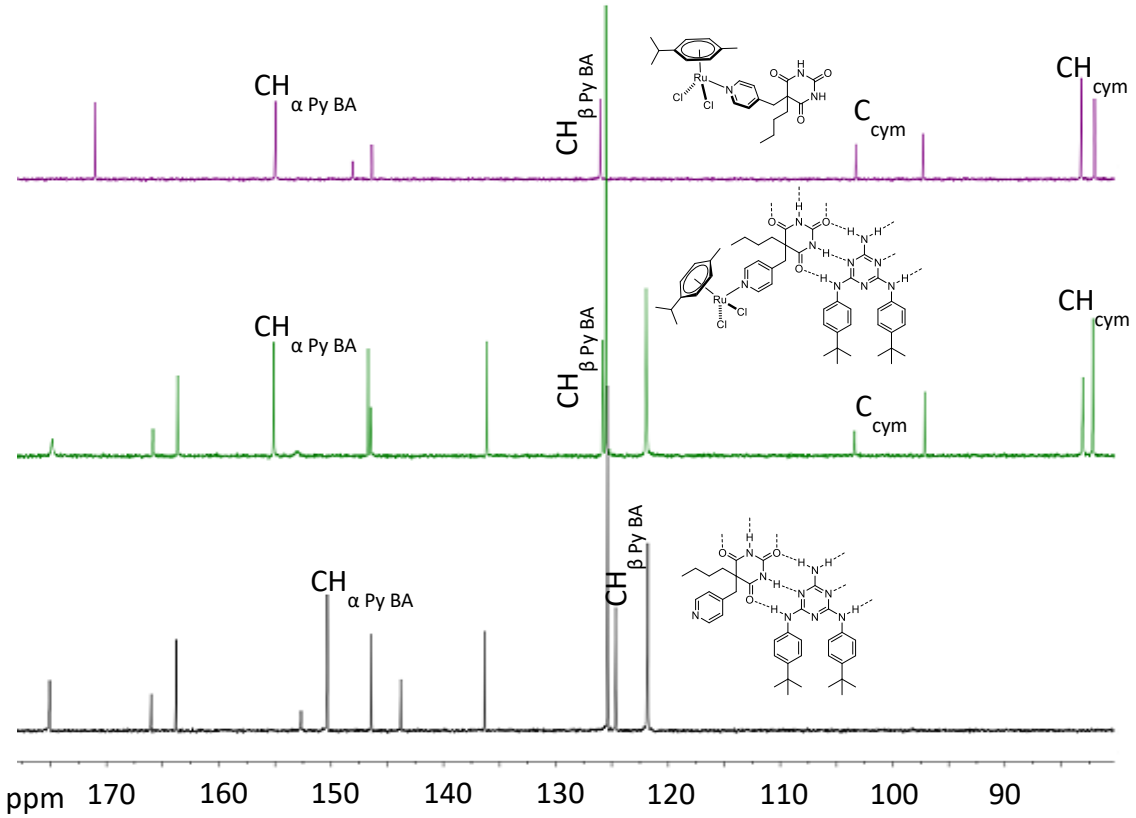

Figure 52: ^{13}C NMR spectra of BApyRu, $(ME)_3 \cdot (BApyRu)_3$ and $(ME)_3 \cdot (BApy)_3$ ($CDCl_3$, 25 °C)

For the ^{1}H NMR spectra of cationic trinuclear hydrogen-bonded metalla-assemblies, as in the neutral metalla-assemblies, a chemical shift is observed for the pyridyl protons and the protons involved in the hydrogen-bonding network. However, additional multiplets can be seen at 7.3 ppm, which corresponds to the protons of the triphenylphosphine ligand. Moreover, the chirality at the metal centers is confirmed in $\{(ME)_3 \cdot [(BApy)Ru(cym)(PPh_3)Cl]_3\} \cdot (3CF_3SO_3)$ by the occurrence of four doublets for the aromatic protons of the para-cymene ligand (Figure 53), while in the two other systems some signals tend to broaden.

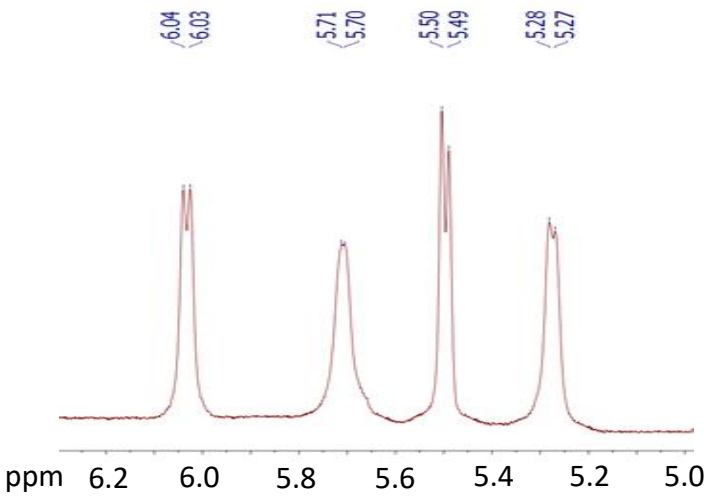

Figure 53: ^{1}H para-cymene signals of $\{(ME)_3 \cdot [(BApy)Ru(cym)(PPh_3)Cl]_3\} \cdot (3CF_3SO_3)$ ($CDCl_3$, 25 ℃)

Theoretically, the presence of three stereogenic centers should give rise to eight isomers. However, upon formation of the rosette, the (*S*,*R*,*R*), (*R*,*S*,*R*), and (*R*,*R*,*S*) isomers are identical to their enantiomers (*R*,*S*,*S*), (*S*,*R*,*S*), and (*S*,*S*,*R*), thus only four isomers are obtained (Figure 54). In addition, due to the lability of the chloride, inversion of the chirality at the arene ruthenium centers is fast in solution,[219] thus limiting the resolution of the diastereotopic signals.

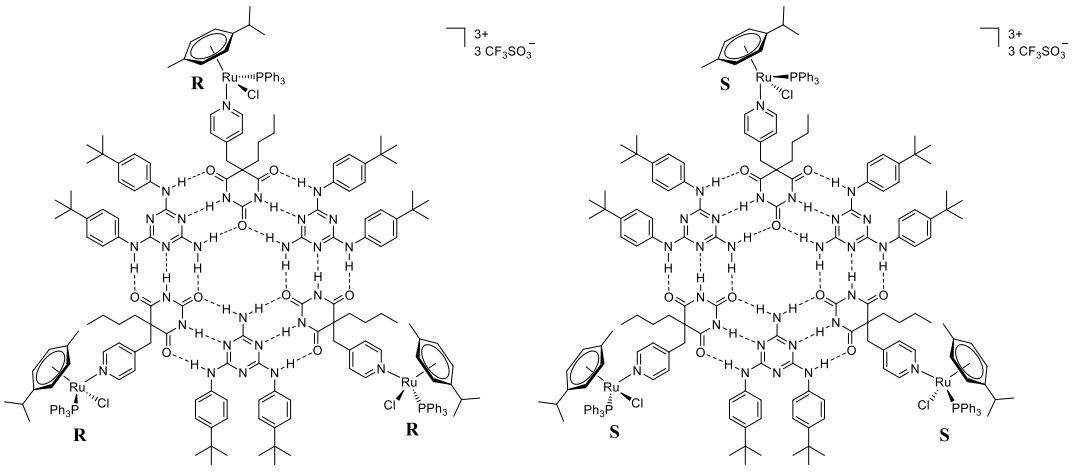

(*R*,*R*,*R*) (*S*,*S*,*S*)

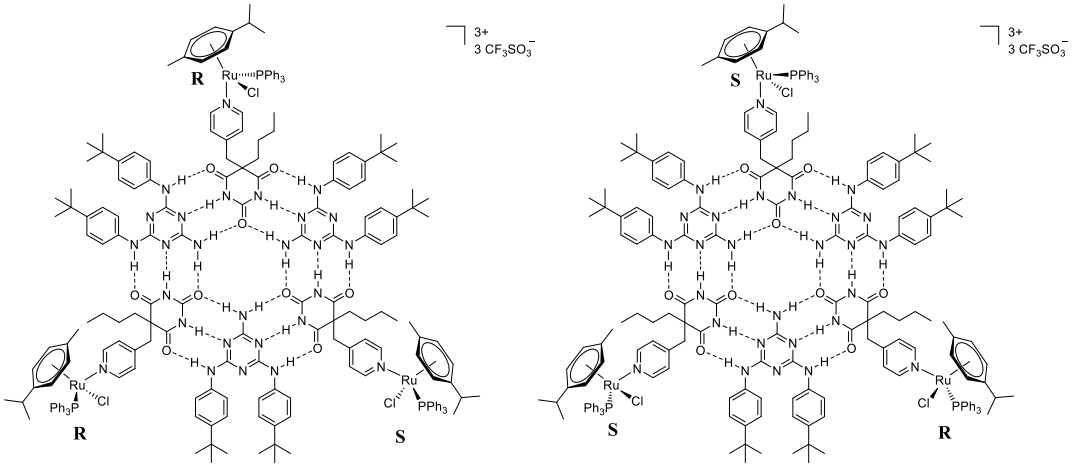

(*R*,*R*,*S*) (*S*,*S*,*R*)

Figure 54: The four isomers of $\{(ME)_3 \cdot [(BApy)Ru(cym)(PPh_3)Cl]_3\} \cdot (3CF_3SO_3)$

The presence of the PPh_3 ligand can also be confirmed by the ^{31}P NMR spectra. Typical signals, 37.4 ppm for Ph_3P-Ru and 8.8 ppm for Ph_3P-Ir, are observed. A doublet at 33.6 ppm is observed for the rhodium derivative due to Rh-P coupling ($^1J_{Rh\text{-}P}$ = 142 Hz) (Figure 55).

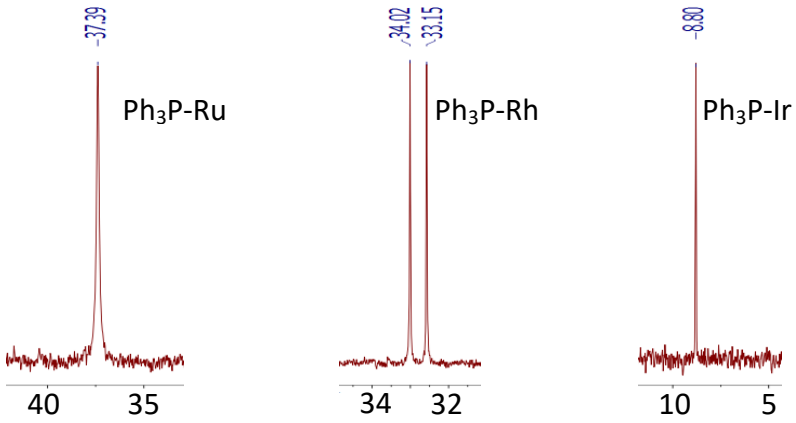

Figure 55: ^{31}P signals of the cationic trinuclear hydrogen-bonded metalla-assemblies ($CDCl_3$, 25 ℃)

2.3.2 DOSY NMR spectroscopy

DOSY (diffusion ordered spectroscopy) NMR experiment was designed by Morris and Johnson in 1992.[220] This NMR technique is a 2D-NMR experiment that detects the diffusion coefficients of species in solution. This method can be used to provide a global view of particle sizes and detect impurities in samples. It can also be used to separate different proton signals in a mixture through different diffusion coefficients of different molecules. The principle is similar to that of chromatograms, and it also provides NMR informations to analyze each individual molecule in a mixture.[221]

After DOSY measurements, diffusion coefficients can be extracted, which give the hydrodynamic radius of the molecule. The diffusion coefficient depends on physical parameters, like the size and shape of molecules, the temperature, and the viscosity of the solvent. It can be determined from the Stokes-Einstein equation.

$$D = \frac{KT}{6\pi\eta r}$$

D: Diffusion Coefficient ($m^2\ s^{-1}$)

K: Boltzmann Constant ($1.38064852*10^{-23}\ m^2\ kg\ s^{-2}\ k^{-1}$)

T: Absolute temperature (k)

η: Viscosity ($kg\ m^{-1}\ s^{-1}$)

r: Radius hydrodynamic (m)

All molecules and rosettes were analyzed by DOSY NMR to confirm the formation of rosette-type metalla-assemblies. The DOSY NMR experiments were performed in chloroform at room temperature. The results are listed in Table 4, and the hydrodynamic radius were calculated to estimate the size of the compounds.

Name	Diffusion coefficient [log(m^2/s)]	Diffusion coefficient (m^2/s)	Hydrodynamic radius (m)
BApy	-9.02	9.55×10^{-10}	4.18×10^{-10}
ME	-9.08	8.32×10^{-10}	4.80×10^{-10}
BApyRu	-9.31	4.90×10^{-10}	8.15×10^{-10}
BApyRh	-9.27	5.37×10^{-10}	7.44×10^{-10}
$(ME)_3 \cdot (BApy)_3$	-9.45	3.55×10^{-10}	1.13×10^{-9}
$(ME)_3 \cdot (BApyRu)_3$	-9.49	3.24×10^{-10}	1.23×10^{-9}
$(ME)_3 \cdot (BApyRh)_3$	-9.46	3.47×10^{-10}	1.15×10^{-9}
$(ME)_3 \cdot (BApyIr)_3$	-9.49	3.24×10^{-10}	1.23×10^{-9}
$\{(ME)_3 \cdot [(BApy)Ru(cym)(PPh_3)Cl]_3\} \cdot (3CF_3SO_3)$	-9.52	3.02×10^{-10}	1.32×10^{-9}
$\{(ME)_3 \cdot [(BApy)Rh(Cp^*)(PPh_3)Cl]_3\} \cdot (3CF_3SO_3)$	-9.48	3.31×10^{-10}	1.21×10^{-9}
$\{(ME)_3 \cdot [(BApy)Ir(Cp^*)(PPh_3)Cl]_3\} \cdot (3CF_3SO_3)$	-9.50	3.16×10^{-10}	1.26×10^{-9}

Table 4: Diffusion coefficients and hydrodynamic radius for molecules synthesized

Comparison of the DOSY NMR data show clear differences between $(ME)_3 \cdot (BApy)_3$ and BApy or ME. The radius value of $(ME)_3 \cdot (BApy)_3$ is 1.13×10^{-9} m, while BApy and ME possess radius values of 4.18×10^{-10} m and 4.80×10^{-10} m, respectively. All the neutral rosette-type metalla-assemblies show radius values [$(ME)_3 \cdot (BApyRu)_3$: 1.23×10^{-9} m; $(ME)_3 \cdot (BApyRh)_3$: 1.15×10^{-9} m; $(ME)_3 \cdot (BApyIr)_3$: 1.23×10^{-9} m] slightly higher than that of $(ME)_3 \cdot (BApy)_3$ (1.13×10^{-9} m). Additionally, radius values of $(ME)_3 \cdot (BApyRu)_3$ and $(ME)_3 \cdot (BApyRh)_3$ are higher than those of individual BApyRu (8.15×10^{-10} m) or BApyRh (7.44×10^{-10} m). For all cationic rosette-type metalla-assemblies, radius values are between 1.21×10^{-9} m and 1.32×10^{-9} m, thus being similar to those observed for the neutral rosette-type metalla-assemblies

and slightly higher than that of $(ME)_3 \cdot (BApy)_3$. In summary, all the DOSY NMR results confirm the formation of rosette-type metalla-assemblies.

Moreover, all compounds show single diffusion coefficient in their DOSY NMR spectra, indicating the formation of single species without impurities. The superimposed spectra of BApy, ME, BApyRu, $(ME)_3 \cdot (BApy)_3$, $(ME)_3 \cdot (BApyRu)_3$ and $\{(ME)_3 \cdot [(BApy)Ru(cym)(PPh_3)Cl]_3\} \cdot (3CF_3SO_3)$ are shown in Figure 56.

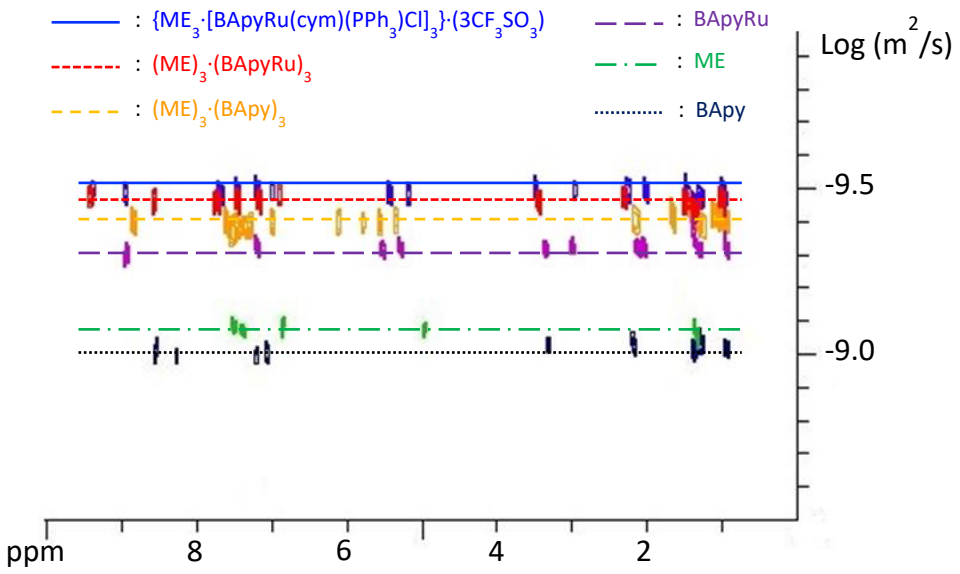

Figure 56: DOSY NMR superimposed spectra ($CDCl_3$, 25 ℃) of BApy, ME, BApyRu, $(ME)_3 \cdot (BApy)_3$, $(ME)_3 \cdot (BApyRu)_3$ and $\{(ME)_3 \cdot [(BApy)Ru(cym)(PPh_3)Cl]_3\} \cdot (3CF_3SO_3)$

2.3.3 IR spectroscopy

In the IR spectra of rosette-type assemblies, the band associated with the NH stretching vibration of the barbituric acid and melamine moieties is broadened and shifted by about 200 cm^{-1}. This important redshift correlates with the lengthening of the NH bonds.[10] Thus, the formation of the $(ME)_3 \cdot (BApy)_3$ rosette structure was also confirmed by IR spectroscopy.

After the coordination of metals, the infrared absorptions of the rosette-type complexes are only slightly shifted. Additionally, the infrared absorptions of the trifluoromethanesulfonate anions are observed at 1248 cm^{-1} for $\{(ME)_3 \cdot [(BApy)Ru(cym)(PPh_3)Cl]_3\} \cdot (3CF_3SO_3)$, 1245 cm^{-1} for $\{(ME)_3 \cdot [(BApy)Rh(Cp^*)(PPh_3)Cl]_3\} \cdot (3CF_3SO_3)$ and 1245 cm^{-1}

$\{(ME)_3 \cdot [(BApy)Ir(Cp^*)(PPh_3)Cl]_3\} \cdot (3CF_3SO_3)$, that also confirm the presence of cationic complexes.

2.3.4 UV spectroscopy

Rosette-type assemblies were studied by UV-visible spectroscopy; the spectra were obtained in chloroform at 1.0×10^{-5} M concentrations in the range 200 nm to 800 nm. In the spectrum of rosette-type ligand $(ME)_3 \cdot (BApy)_3$, a high energy absorption band is observed at 271 nm, which may be attributed to ligand π,π* transitions.[222] This band is also observed in other rosette-type metalla-assemblies, the bands are however slightly shifted for $(ME)_3 \cdot (BApyRu)_3$ (272 nm), $(ME)_3 \cdot (BApyRh)_3$ (270 nm), $(ME)_3 \cdot (BApyIr)_3$ (273 nm), $\{(ME)_3 \cdot [(BApy)Ru(cym)(PPh_3)Cl]_3\} \cdot (3CF_3SO_3)$ (270 nm), $\{(ME)_3 \cdot [(BApy)Rh(Cp^*)(PPh_3)Cl]_3\} \cdot (3CF_3SO_3)$ (268 nm) and $\{(ME)_3 \cdot [(BApy)Ir(Cp^*)(PPh_3)Cl]_3\} \cdot (3CF_3SO_3)$ (270 nm). The intensities of these bands are in the range from 1.16×10^5 M^{-1} cm^{-1} to 1.39×10^5 M^{-1} cm^{-1}, being almost identical (Figure 57).

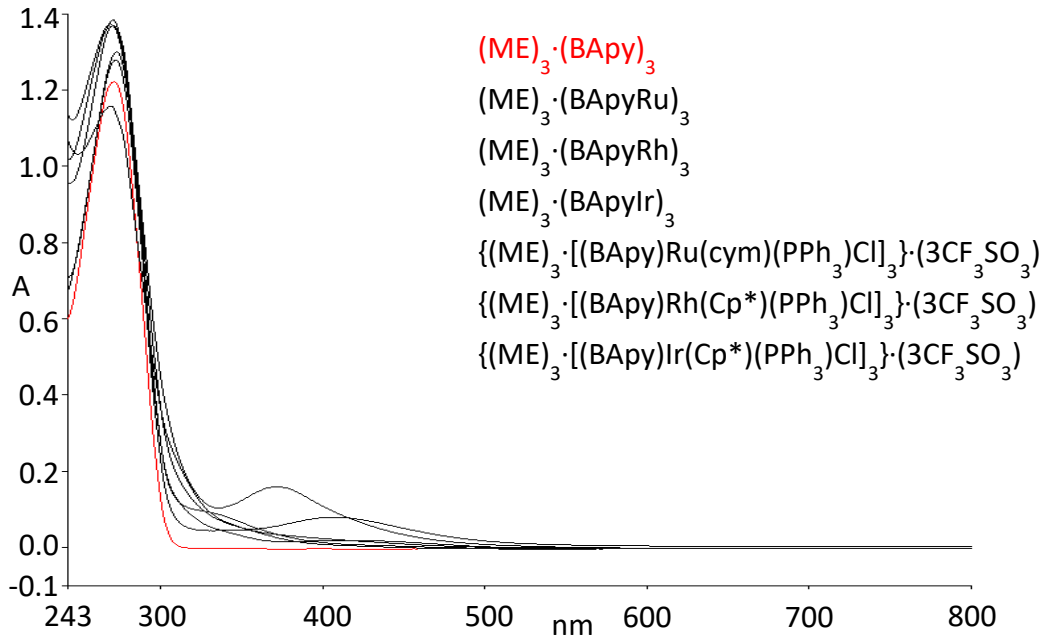

Figure 57: UV spectra of rosette-type metalla-assemblies synthesized in comparison with the rosette-type ligand $(ME)_3 \cdot (BApy)_3$ ($CHCl_3$, 25 ℃)

The UV-vis spectra of mononuclear complexes BApyRu and BApyRh were performed in chloroform at 5 $\times 10^{-5}$ M in the range 200 nm to 800 nm. The high energy absorption band observed at 241 nm is attributed to ligand-localized transition. The broad low-energy band observed at 411 nm for BApyRu and 406 nm for BApyRh, may be associated to metal-to-ligand charge transfer (MLCT) transitions. They possess moderate intensities, 8.57 $\times 10^{2}$ M^{-1} cm^{-1} for BApyRu and 2.38 $\times 10^{3}$ M^{-1} cm^{-1} for BApyRh. Similar absorption bands are observed in the visible region at 434 nm for $(ME)_3 \cdot (BApyRu)_3$ and at 408 nm for $(ME)_3 \cdot (BApyRh)_3$. Another absorption band is observed at 297 nm for BApyRu, which may be assigned to intra-ligand charge transfer (ILCT) transitions (Figure 58).

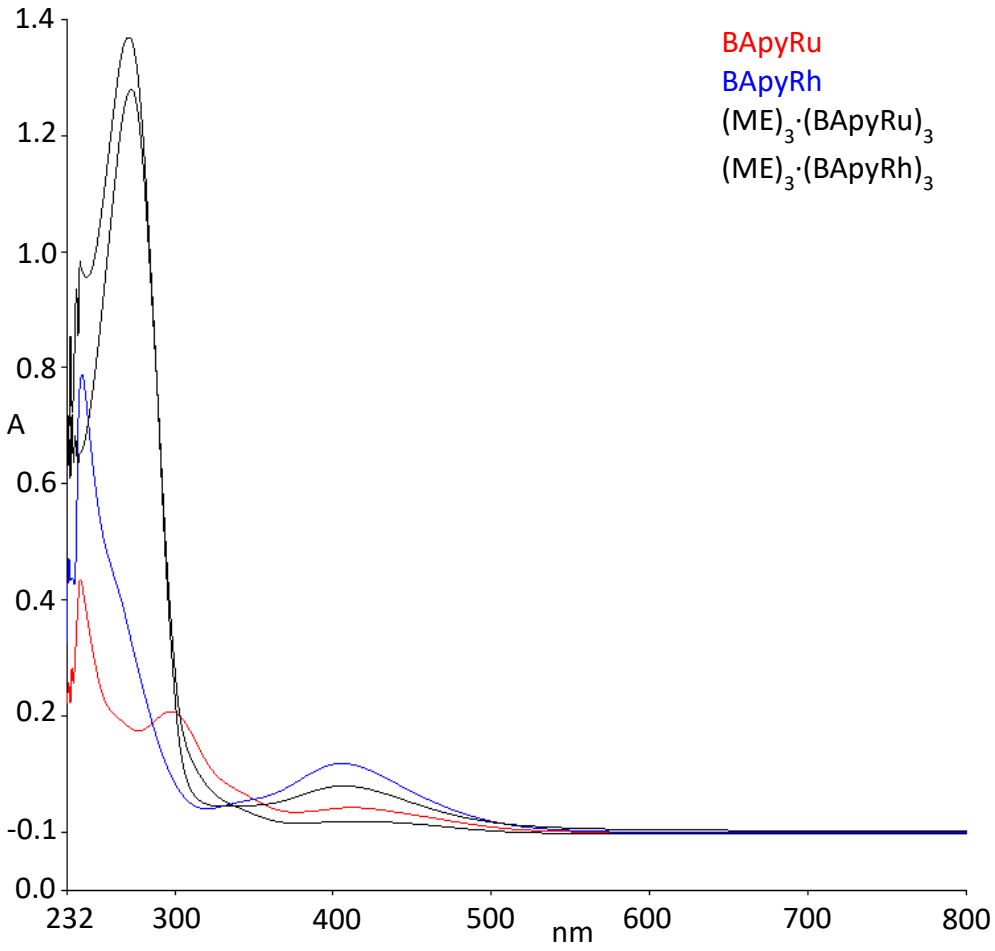

Figure 58: UV spectra of rosette-type assemblies $(ME)_3 \cdot (BApyRu)_3$ and $(ME)_3 \cdot (BApyRh)_3$ in comparison with mononuclear complexes BApyRu and BApyRh ($CHCl_3$, 25 ℃)

Furthermore, a broad moderately intense band at 371 nm for $\{(ME)_3 \cdot [(BApy)Ir(Cp^*)(PPh_3)Cl]_3\} \cdot (3CF_3SO_3)$ is assigned to mixed metal-to-ligand

charge transfer (MLCT), intra-ligand charge transfer (ILCT) and the [dσ*, π*] transition due to metal-metal interactions (Figure 57).[223]

2.3.5 RX spectroscopy

The coordination of the pyridyl nitrogen atom to the metal centers was also confirmed by single crystal X-ray diffraction structure analysis of the complex BApyRh (Figure 59). This mononuclear complex crystallized in the centrosymmetric space group $P2_1/c$ with two independent molecules per unit cell. The two molecules are almost identical, showing similar parametrical data, which are typical for pyridyl-Rh(Cp*)Cl_2 complexes.[224-225] Despite having high rotational freedom, the barbituric ring points in the direction of the pentamethylcyclopentadienyl moiety, thus creating a relatively compact environment between the complex and the BA ligand. In the crystal packing, only weak interactions can be observed between neighboring molecules, mainly involving the two chloride ions with, however, no meaningful hydrogen bonds.

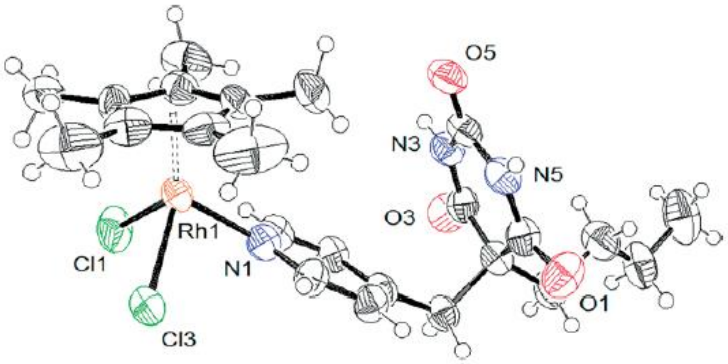

Figure 59: ORTEP representation of BApyRh at 50 % probability level ellipsoids. Selected bond lengths [Å] and angles [°]: Rh1-N1 2.109(6), Rh1-Cl1 2.400(2), Rh1-Cl3 2.425(2), Rh1-centroid 1.755; Cl1-Rh1-N1 87.94 (14), Cl3-Rh1-N1 89.89(17), C3-C6-C7 115.0(6)

2.3.6 Mass spectroscopy

The mass spectrum of BApy was performed under electrospray ionization in positive and negative modes. The highest signal is observed at *m/z* = 276.1 or 274.0 corresponding to $[M + H]^+$ or $[M - H]^-$. The mass spectra of BApyRu and BApyRh were performed by electrospray ionization in positive mode. The parent peak is observed at *m/z* = 546.1 corresponding to $[M - Cl]^+$ for BApyRu, and at *m/z* = 548.1 corresponding to $[M - Cl]^+$ for BApyRh.

All attempts to obtain the mass spetra of the intact rosette or metal-containing rosettes were unsuccessful (ESI, MALDI-TOF), even after applying the Ag^+ labeling technique, which has shown great results with analogous rosettes.[226-227]

2.4 Conclusion

Rosette-type assemblies mixing covalent, coordination, hydrogen-bonding, and ionic interactions have been synthesized and characterized. Coordination of metal centers at the periphery of the rosette was performed either prior to or after the formation of the hydrogen-bonded assembly, thus providing synthetic flexibility. Neutral and ionic systems were obtained, depending on the nature of the metal complex used. Overall, we have demonstrated that such supramolecular systems are easy to prepare, and functionality can be added to design complex structures.

Chapter 3

Using a hydrogen-bonded rosette-type scaffold to generate heteronuclear metalla-assemblies

3.1 General introduction

In the first part of the thesis (Chapter II), we used a pyridyl-containing barbituric acid derivative, 5-butyl-5-(pyridin-4-ylmethyl)pyrimidine-2,4,6-trione (BApy),[228] in combination with *N,N'*-bis(4-*tert*butylphenyl) melamine (ME),[76] to generate a $(ME)_3{\cdot}(BApy)_3$ rosette structure with three coordination sites at the periphery of the

hexameric rosette.[228] Arene ruthenium and cyclopentadienyl rhodium/iridium piano-stool complexes were coordinated to the rosette, giving rise to neutral and cationic trinuclear systems (Figure 60).

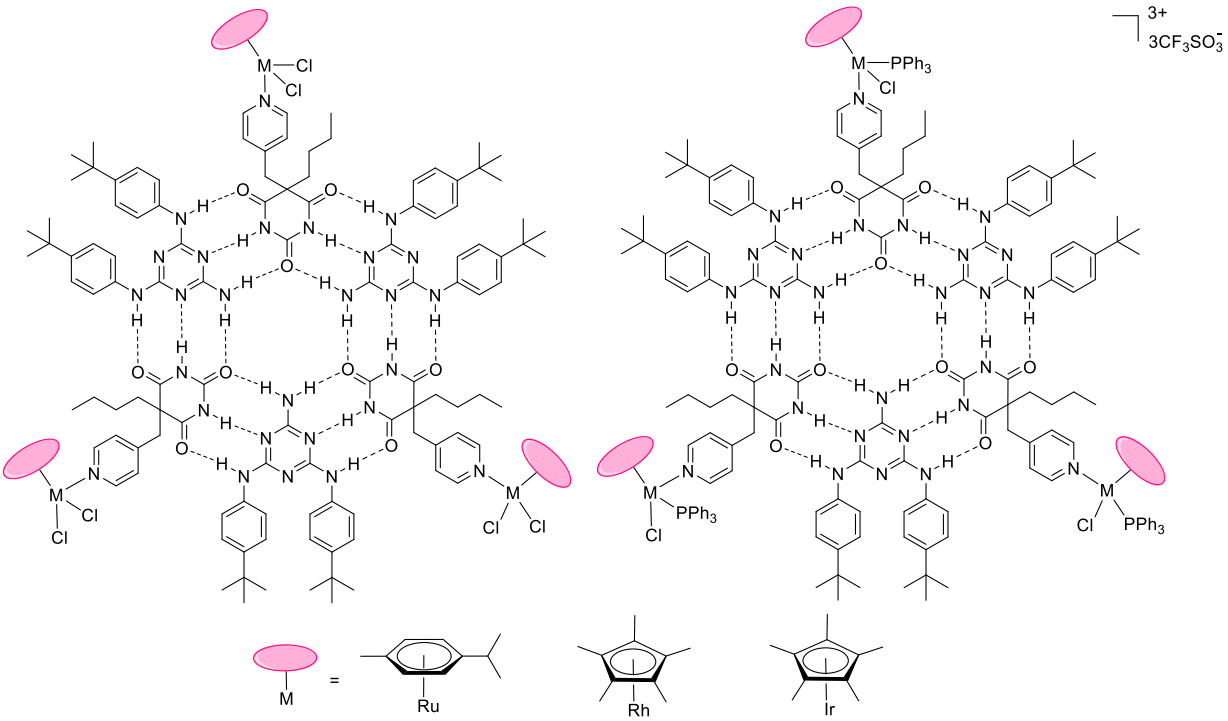

Figure 60: Molecular structures of neutral (left) and ionic (right) hexameric rosettes incorporating three piano-stool complexes

With the view of increasing the nuclearity of these systems and generating heteronuclear rosette-type assemblies, a pyridyl group has now been introduced to the melamine unit, thus providing six coordination sites to the $(MEpy)_3{\cdot}(BApy)_3$ rosette. Coordination of piano-stool complexes on the MEpy and BApy units, prior to the formation of the rosette, allows controlled formation of the desired heteronuclear system. These hexameric hexanuclear metalla-assemblies show good stability in solution, as demonstrated by various NMR spectroscopic experiments.

3.2 Synthesis

3.2.1 Synthesis of rosette-type ligands

In this section, two building blocks were used to prepare the $(MEpy)_3{\cdot}(BApy)_3$ rosettes *N*-(4-*tert*-butylphenyl)-*N'*-(pyridine-4-ylmethyl)melamine (MEpy) and 5-butyl-5-(pyridine-4-ylmethyl)pyrimidine-2,4,6-trione (BApy). Then MEpy unit was obtained in three synthetic steps, starting from 4-(*tert*-butyl)aniline and cyanuric chloride, following the procedure published by the group of Li.[93] $(MEpy)_3{\cdot}(BApy)_3$ is obtained by mixing equivalent amount of MEpy and BApy. The reaction is straightforward and fast, as for the preparation of $(ME)_3{\cdot}(BApy)_3$ (chloroform, 25 ℃ for 30 min). The apolar and aprotic solvent chloroform is necessary, and the concentrations of MEpy and BApy need to be higher than 4 mM, otherwise no rosette structure is obtained (Scheme 22).[80]

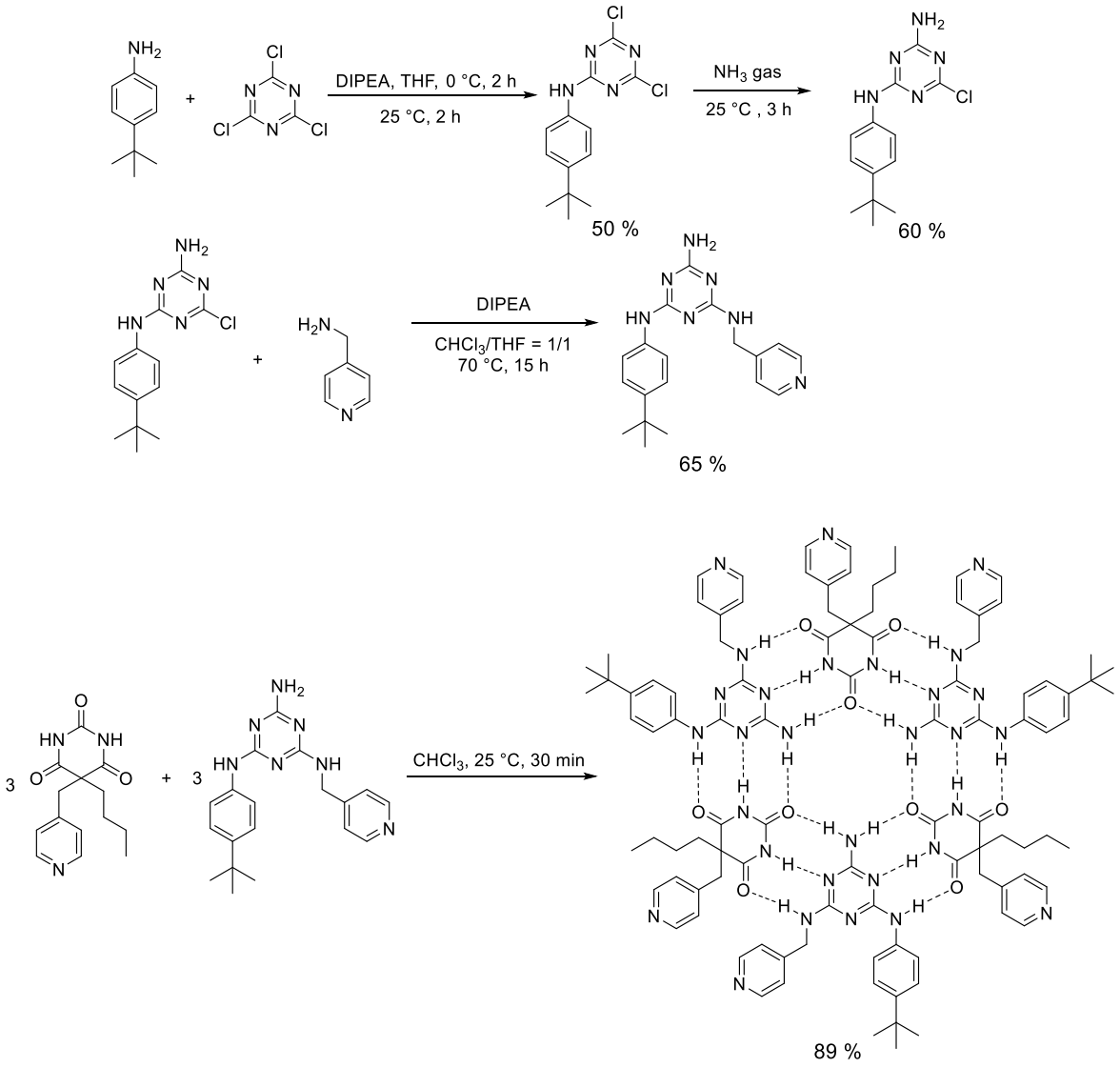

Scheme 22: Synthesis of rosette-type assembly $(MEpy)_3 \cdot (BApy)_3$

3.2.2 Synthesis of trinuclear hydrogen-bonded metalla-assemblies

First of all, coordination of the MEpy unit to the metal centers was realized by adding 0.5 equivalent of $[Ru(cym)Cl_2]_2$ or $[Rh(Cp^*)Cl_2]_2$ to a solution of MEpy in tetrahydrofuran. The corresponding mononuclear piano-stool complexes MEpyRu and MEpyRh were obtained after stirring the mixture at 25 ℃ for 16 h (Scheme 23). The synthetic route follows the same principle as that of complexes BApyRu and BApyRh.

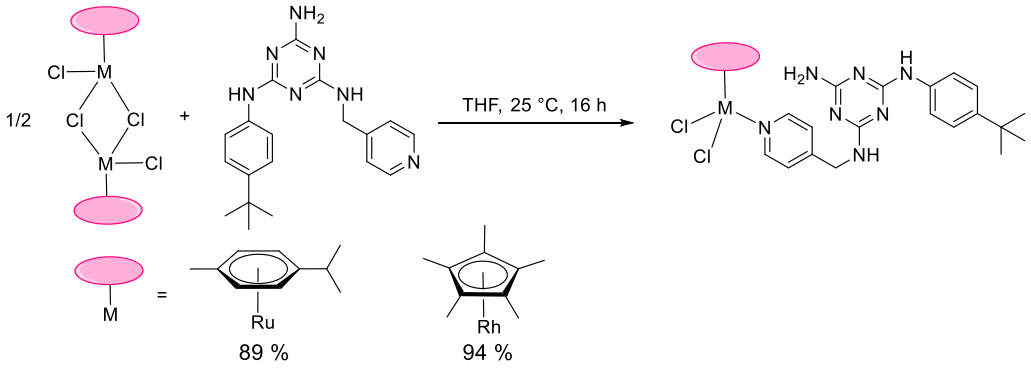

Scheme 23: Synthesis of mononuclear piano-stool complexes MEpyRu and MEpyRh

As previously shown,[228] trinuclear systems can be prepared by mixing a metal-containing unit with the corresponding metal-free component. Here, equimolar amounts of MEpyRu or MEpyRh and BApy reacted in chloroform at 25 ℃ for 30 min, giving rise to the corresponding trinuclear rosettes: $(MEpyRu)_3{\cdot}(BApy)_3$ and $(MEpyRh)_3{\cdot}(BApy)_3$. Similarly, mixtures of BApyRu or BApyRh and MEpy generate the trinuclear rosettes $(MEpy)_3{\cdot}(BApyRu)_3$ and $(MEpy)_3{\cdot}(BApyRh)_3$ respectively (Scheme 24).

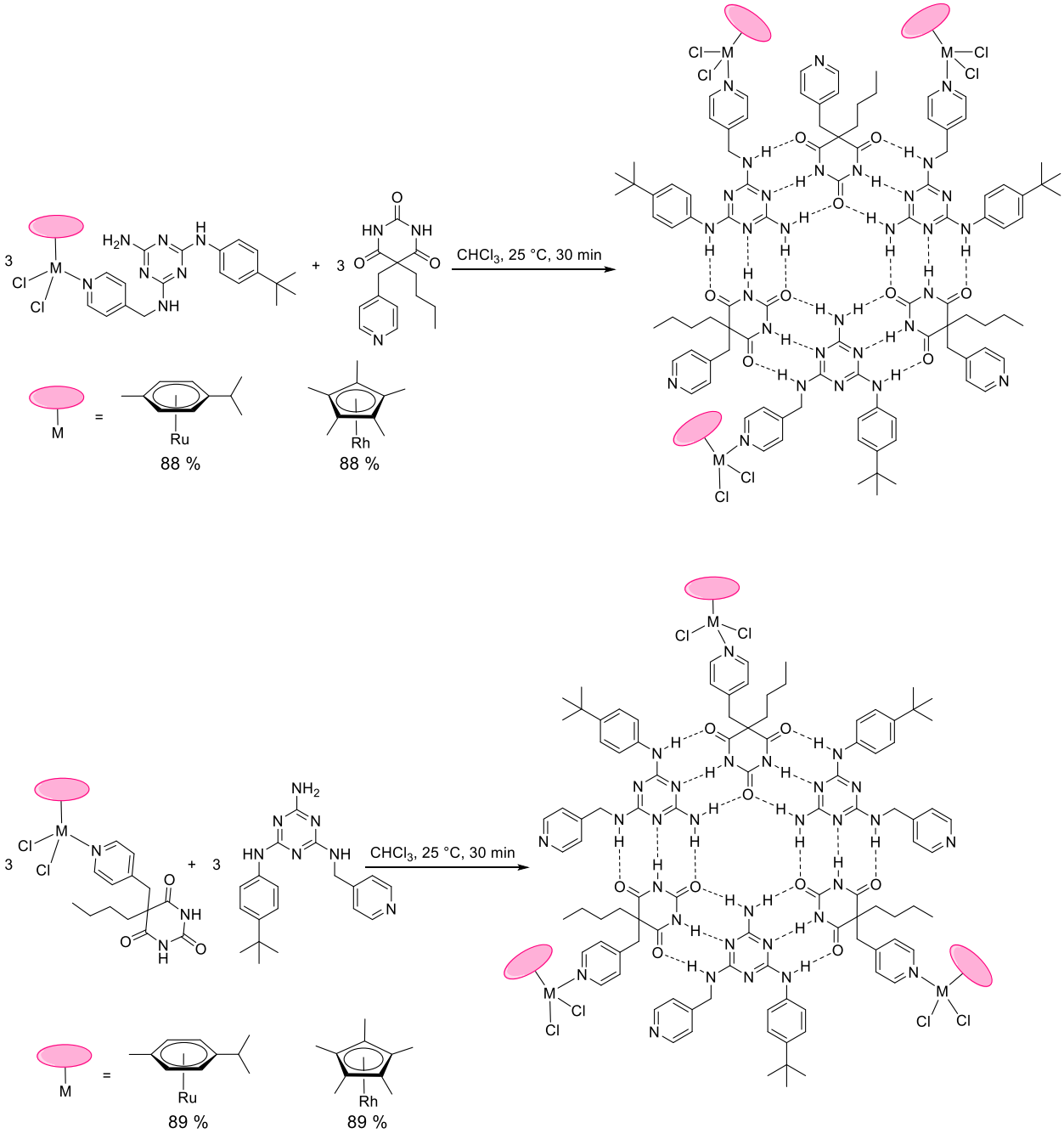

Scheme 24: Syntheses of trinuclear hydrogen-bonded rosettes

3.2.3 Synthesis of hexanuclear hydrogen-bonded metalla-assemblies

Two methods were used to synthesize the hexanuclear hydrogen-bonded metalla-assembly $(MEpyRu)_3{\cdot}(BApyRu)_3$. The addition of three equivalents of

$[Ru(cym)Cl_2]_2$ in chloroform to the rosette-type ligand $(MEpy)_3{\cdot}(BApy)_3$ afforded the desired hexanuclear complex $(MEpyRu)_3{\cdot}(BApyRu)_3$. The other method involves mixing the MEpyRu and BApyRu in chloroform, and stirring at 25 ℃ for 30 min (Scheme 25).

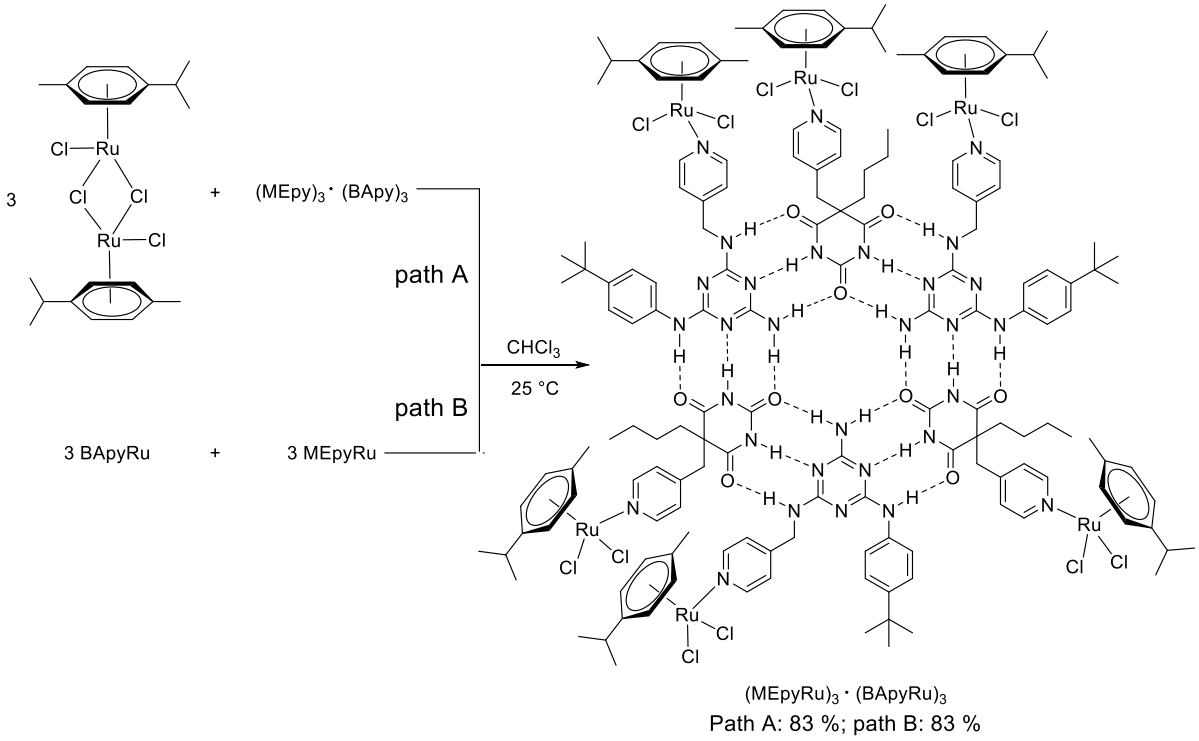

Scheme 25: Synthesis of the metalla-assembly $(MEpyRu)_3{\cdot}(BApyRu)_3$ (Paths A and B)

From the trinuclear systems, $(MEpy)_3{\cdot}(BApyRu)_3$, $(MEpyRu)_3{\cdot}(BApy)_3$, $(MEpy)_3{\cdot}(BApyRh)_3$ and $(MEpyRh)_3{\cdot}(BApy)_3$, hexameric hexanuclear assemblies can be obtained by addition of 1.5 equivalent of $[Ru(cym)Cl_2]_2$ or $[Rh(Cp^*)Cl_2]_2$ (Path A, Scheme 26). The same hexanuclear rosette-type metalla-assemblies can also be prepared by mixing in chloroform equimolar amounts of the mononuclear piano-stool complexes MEpyM and BApyM' (Path B, Scheme 26). Both strategies provide the desired hexanuclear rosette $(MEpyRu)_3{\cdot}(BApyRh)_3$ and $(MEpyRh)_3{\cdot}(BApyRu)_3$ in excellent yield (ca. 90 %).

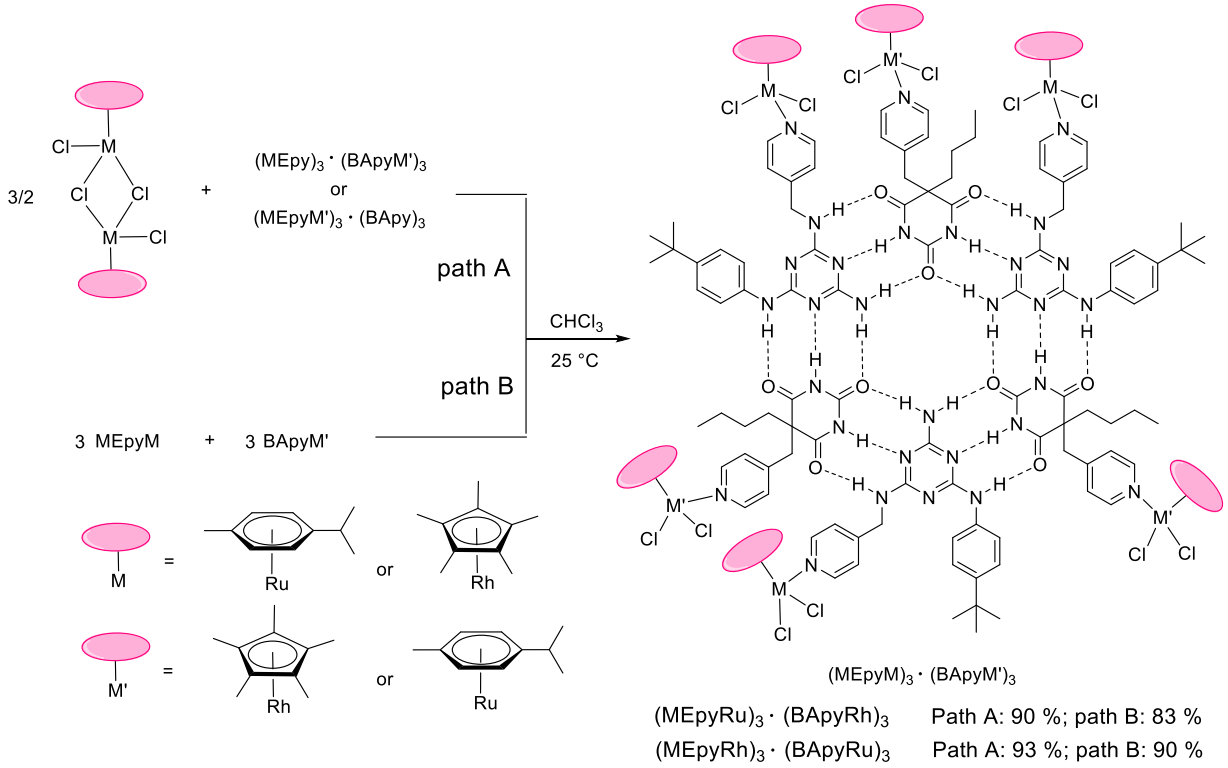

Scheme 26: Syntheses of metalla-assemblies $(MEpyRu)_3{\cdot}(BApyRh)_3$ and $(MEpyRh)_3{\cdot}(BApyRu)_3$ (Paths A and B)

3.3 Characterizations

3.3.1 Proton and carbon NMR spectroscopy

All rosettes were fully characterized by NMR spectroscopy. As mentioned in the second chapter, the most evident signal is at about 14.0 ppm. This signal, which is the NH protons of the BApy units, was observed for all the rosette-type metalla-assemblies. By comparing spectra of BApyRu and MEpyRh with that of the $(MEpyRh)_3{\cdot}(BApyRu)_3$ rosette, the NH signal of BApy is shifted by ca. 5.3 ppm, while for the ME units, the signals are shifted by ca. 0.7 ppm (NHC_{ar}), ca. 1.7 ppm ($NHCH_2$) and 0.7 ppm (NH_2) respectively (Figure 61). The broadening of the signals can be attributed to the presence of isomers. These isomers cannot be identified due to the complexity of the system. Other protons are relatively unaffected. All datas support the formation of the hexameric heteronuclear structures.

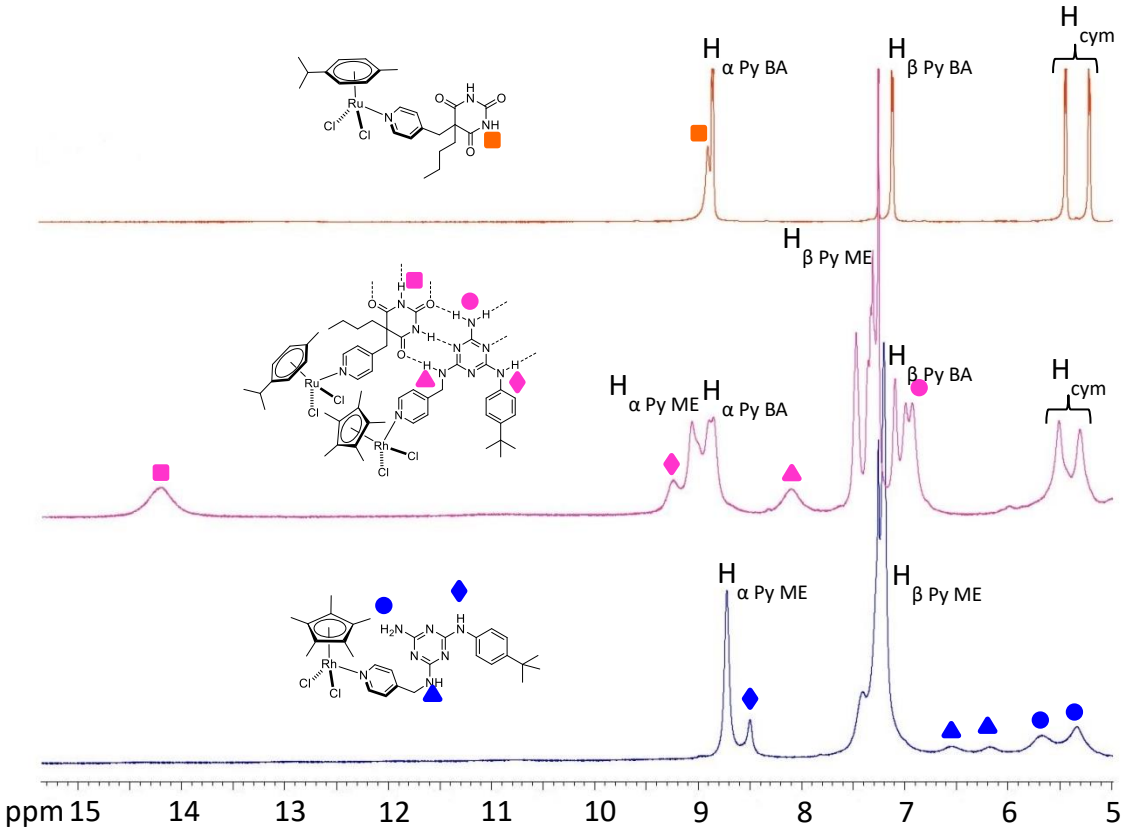

Figure 61: ^{1}H NMR spectra of BApyRu, $(MEpyRh)_3 \cdot (BApyRu)_3$, MEpyRh, with an emphasis on the chemical shifts of the different NH protons ($CDCl_3$, 25 ℃)

By comparing spectra of $(MEpyRh)_3 \cdot (BApyRu)_3$, $(MEpyRh)_3 \cdot (BApy)_3$ and $(MEpy)_3 \cdot (BApyRu)_3$ with that of $(MEpy)_3 \cdot (BApy)_3$, the proton of NH···N is shifted by about 0.6 ppm after coordination to metals. Other protons are almost unaffected (Figure 62). Additionally, the signals for the protons of the pyridyl groups have changed from one singlet to two singlets after the coordination.

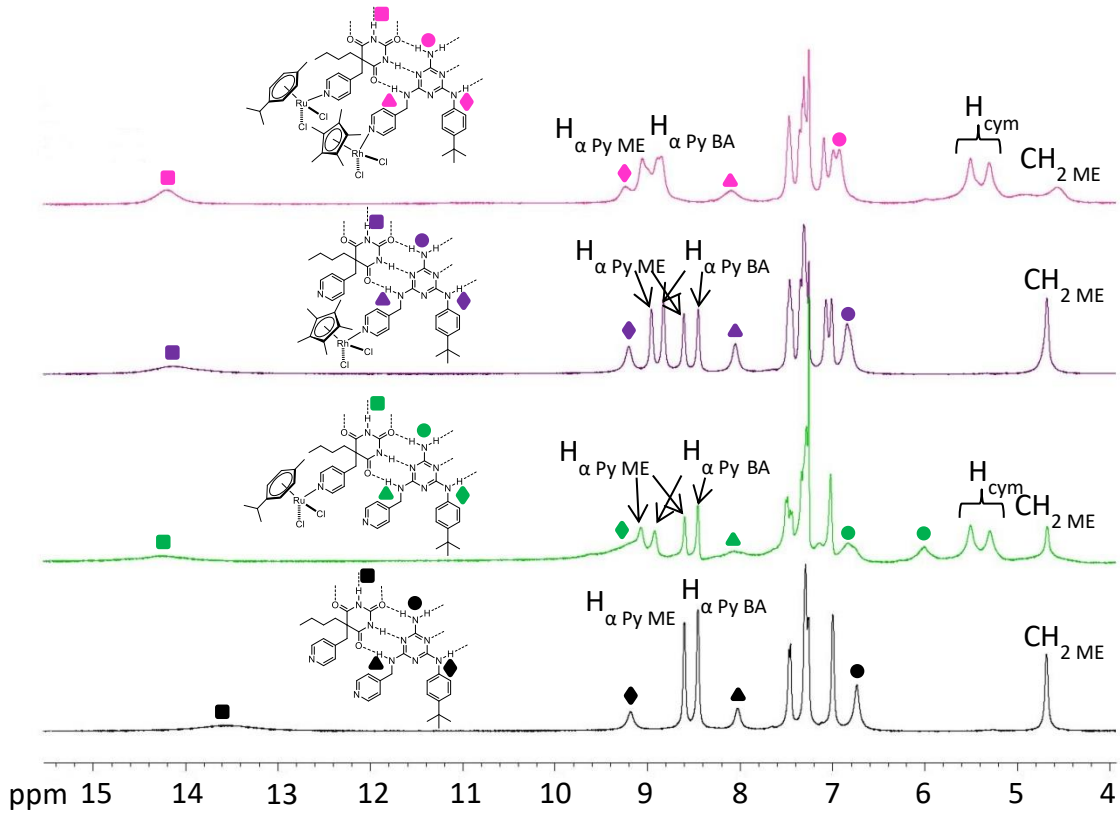

Figure 62: ^{1}H NMR spectra of $(MEpyRh)_3 \cdot (BApyRu)_3$, $(MEpyRh)_3 \cdot (BApy)_3$, $(MEpy)_3 \cdot (BApyRu)_3$ and $(MEpy)_3 \cdot (BApy)_3$ ($CDCl_3$, 25 ℃)

Temperature dependence spectra were measured to determine the stability of the rosette-type metalla-assemblies (Figure 63). The assemblies were stable at room temperature in chloroform. To ensure a wide range of temperatures, 1,1,2,2-tetrachloroethane-d_2 was chosen as deuterated solvent. The temperature varied from 20 ℃ to 120 ℃. After increasing the temperature, the O···H-N and NH_2···O protons are downfield shifted, suggesting disassembly of the rosette structure.

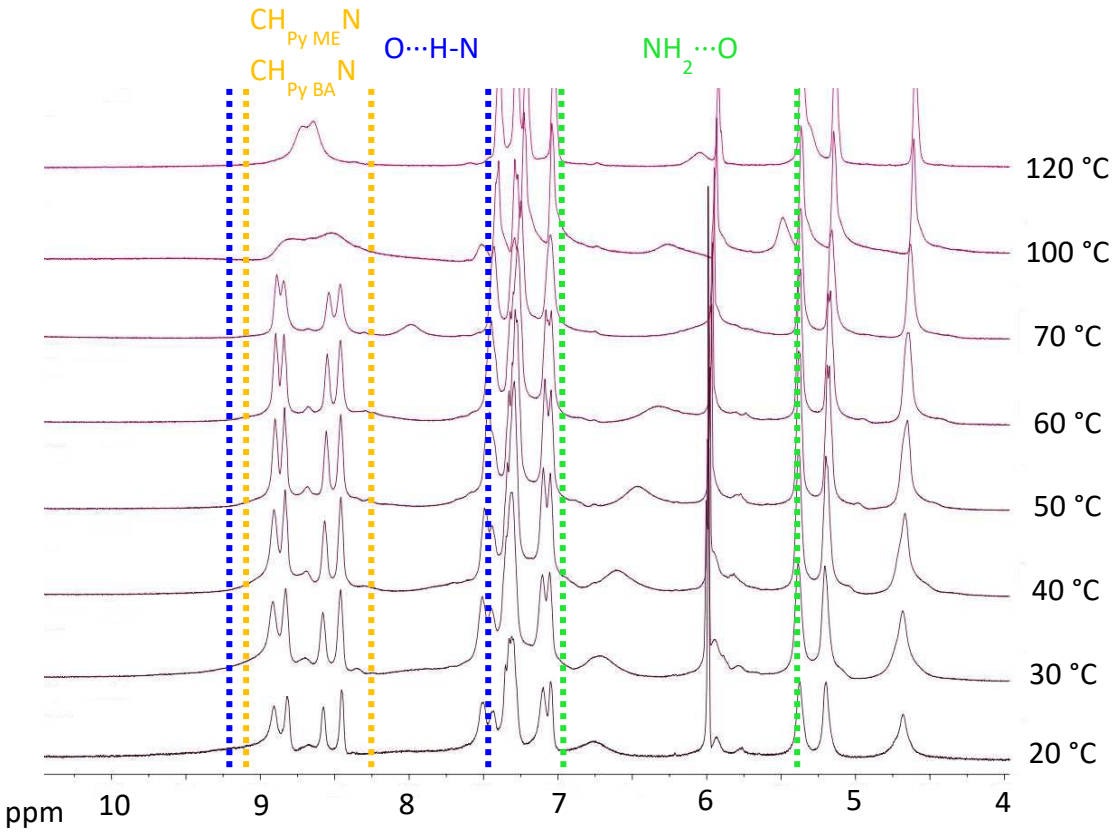

Figure 63: Temperature dependence spectra of $(MEpy)_3{\cdot}(BApyRu)_3$ from 4.0 ppm to 10.5 ppm ($Cl_2CDCDCl_2$).

The same observation was made for the NH···N proton. This proton is downfield shifted, when the temperature increases. Interestingly, the signal of the NH protons at 14.3 ppm remains visible up to 70 °C. However, a significant chemical shift is observed around 50 °C, showing the limit of the stability of the rosette. The superimposed spectra and the different chemical shifts are presented in Figure 64.

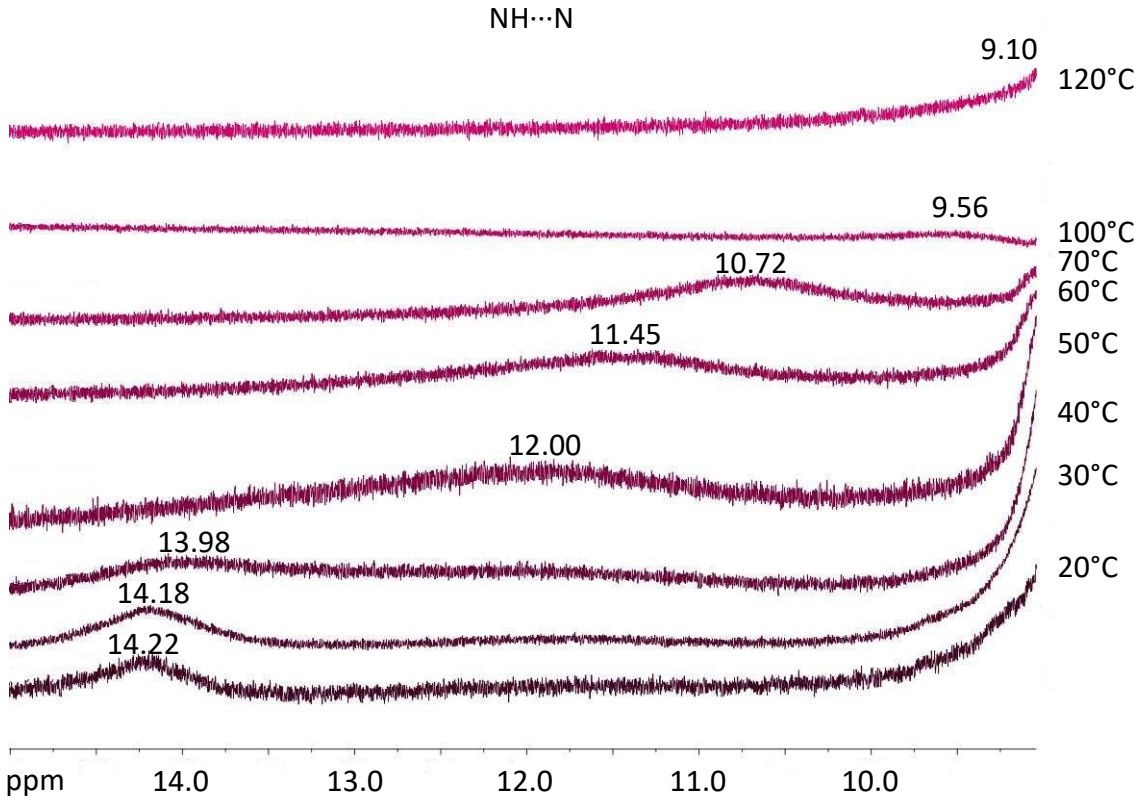

Figure 64: Temperature dependence spectra of $(MEpy)_3 \cdot (BApyRu)_3$ from 9.0 ppm to 15.0 ppm ($Cl_2CDCDCl_2$)

The temperature-dependence experiment provides thermodynamic data on the system.[229-230] An equilibrium constant of 4400 s^{-1} is associated to the assembly-disassembly process, which corresponds to a chemical stability for the supramolecular rosette structure of approximately 13.5 kJ. This value is in agreement with those found by Timmerman, de Jong et al. for analogous $(ME)_3 \cdot (BA)_3$ rosettes.[85]

Calculations of the equilibrium constant and chemical stability by Dynamic NMR have been performed. The coalescence temperature and frequency difference were obtained from Figure 64, while the equilibrium constant was calculated by the equation[229]:

$k = \pi \Delta v / 2^{1/2} \approx 2.22 \Delta v$

k: Equilibrium constant (s^{-1})

π: 3.1415926

Δv: Frequency difference (Hz)

Then free energy of activation was calculated by the equation[231]:

$$\Delta G^{\neq} = \Delta H^{\neq} - T\Delta S^{\neq} = -RT\ ln\ \frac{k\ h}{K\ T} = 1.987\ T\ (23.760 + ln\ (T/k))$$

$\Delta G^{\neq}$: Free energies of activation (J)

R: Gas constant (8.3144598 J mol^{-1} K^{-1})

T: Temperature (K)

h: Planck's constant (6.626070040 $\times 10^{-34}$ J s)

K: Boltzmann constant (1.38064852 $\times 10^{-23}$ m^2 kg s^{-2} K^{-1})

k: Equilibrium constant (s^{-1})

The solution stability of piano-stool complexes is crucial for various applications.[133-134, 215-216] It is well known that chloro ligands of piano-stool complexes are easily exchanged by water (aquation) or by other coordinating solvent molecules.[232-234] Moreover, even monodentate pyridyl-based ligands can be removed from the coordination sphere and replaced by dmso molecules.[235] Therefore, the stability in solution of the mononuclear pyridyl-based complexes and of the rosettes was evaluated.

The mononuclear pyridyl-based complexes are stable in solution for weeks as demonstrated by ^{1}H NMR experiments. Similarly, when the hexanuclear rosettes, $(MEpyRu)_3{\cdot}(BApyRh)_3$ and $(MEpyRh)_3{\cdot}(BApyRu)_3$, are left in chloroform-d_1 for a long period of time (up to two weeks), all signals remain intact (chemical shift and integration), and no additional signals are observed. Thus, a good solution stability of the mononuclear complexes and of the rosettes was demonstrated (Figure 65).

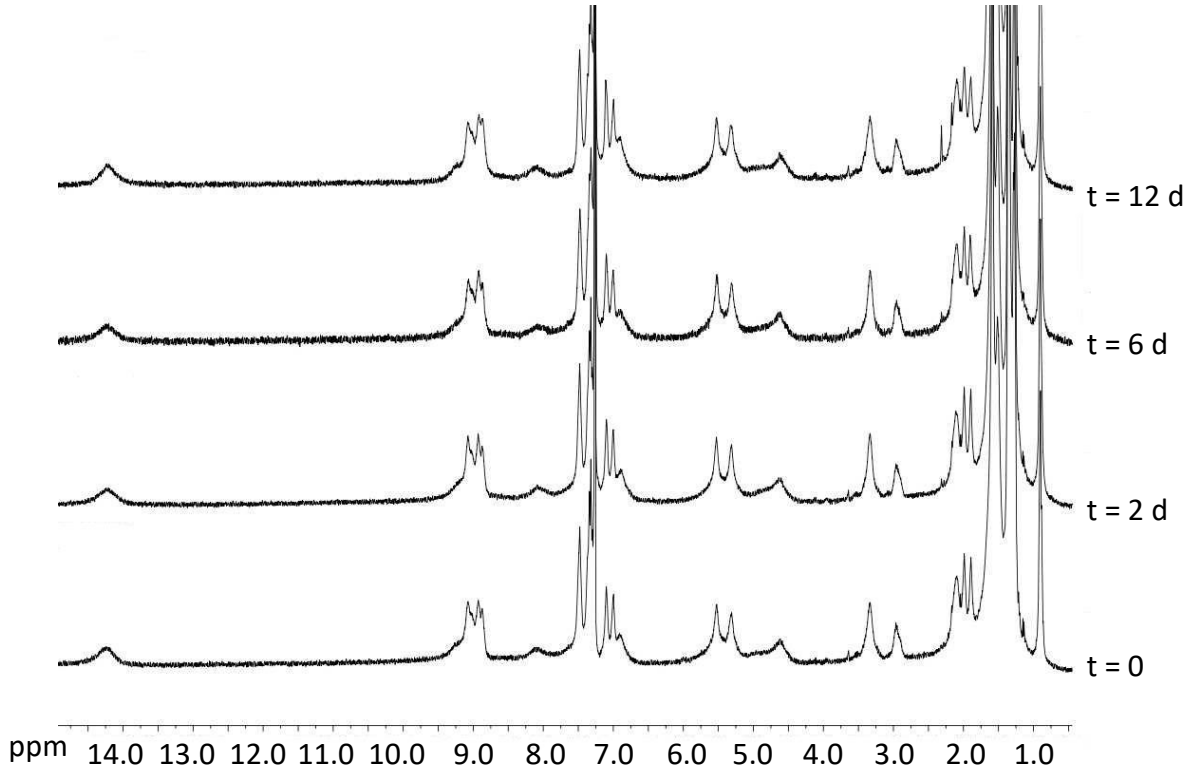

Figure 65: Evolution of the ^{1}H NMR spectra of $(MEpyRh)_3 \cdot (BApyRu)_3$ over a period of 12 days ($CDCl_3$, 25 ℃)

3.3.2 DOSY NMR spectroscopy

All synthesized molecules were analyzed by DOSY NMR to confirm the formation of the rosette-type metalla-assemblies. The DOSY NMR experiments were performed in chloroform at room temperature. All results are listed in Table 5, and the calculated hydrodynamic radius provide an estimation of the size of the molecules.

Name	Diffusion coefficient [log(m^2/s)]	Diffusion coefficient (m^2/s)	Hydrodynamic radius (m)
MEpy	-9.10	7.94×10^{-10}	5.03×10^{-10}
MEpyRu	-9.30	5.01×10^{-10}	7.98×10^{-10}
MEpyRh	-9.14	7.24×10^{-10}	5.52×10^{-10}
$(MEpy)_3 \cdot (BApy)_3$	-9.40	3.98×10^{-10}	1.00×10^{-9}
$(MEpy)_3 \cdot (BApyRu)_3$	-9.41	3.89×10^{-10}	1.03×10^{-9}
$(MEpyRu)_3 \cdot (BApy)_3$	-9.53	2.95×10^{-10}	1.35×10^{-9}
$(MEpy)_3 \cdot (BApyRh)_3$	-9.41	3.89×10^{-10}	1.03×10^{-9}
$(MEpyRh)_3 \cdot (BApy)_3$	-9.43	3.72×10^{-10}	1.07×10^{-9}
$(MEpyRu)_3 \cdot (BApyRu)_3$	-9.48	3.31×10^{-10}	1.21×10^{-9}
$(MEpyRu)_3 \cdot (BApyRh)_3$	-9.53	2.95×10^{-10}	1.35×10^{-9}
$(MEpyRh)_3 \cdot (BApyRu)_3$	-9.45	3.55×10^{-10}	1.13×10^{-9}

Table 5: Diffusion coefficients and hydrodynamic radius

Comparison of the DOSY NMR data of $(MEpy)_3 \cdot (BApy)_3$ and BApy or MEpy shows differences. The radius value of $(MEpy)_3 \cdot (BApy)_3$ is 1.00×10^{-9} m, while BApy and MEpy possess radius values of 4.18×10^{-10} m and 5.03×10^{-10} m, respectively. Like $(ME)_3 \cdot (BApy)_3$, the diffusion coefficient of these trinuclear systems are about 4×10^{-1} m^2 s^{-1}, which correspond to a hydrodynamic radius of more than 10 Å.

As deduced by DOSY NMR spectroscopy, the average hydrodynamic radius of the hexameric hexanuclear rosettes is 12.4 Å, which is slightly larger than those found for the trinuclear species $(MEpy)_3 \cdot (BApyRu)_3$, $(MEpyRu)_3 \cdot (BApy)_3$, $(MEpy)_3 \cdot (BApyRh)_3$ and $(MEpyRh)_3 \cdot (BApy)_3$ (Chapter II).

Moreover, all compounds have shown single diffusion coefficient in their DOSY spectra, indicating the formation of single species. The superimposed spectra of MEpy, MEpyRh, $(MEpy)_3 \cdot (BApy)_3$, $(MEpy)_3 \cdot (BApyRu)_3$ and $(MEpyRh)_3 \cdot (BApyRu)_3$ are shown in Figure 66.

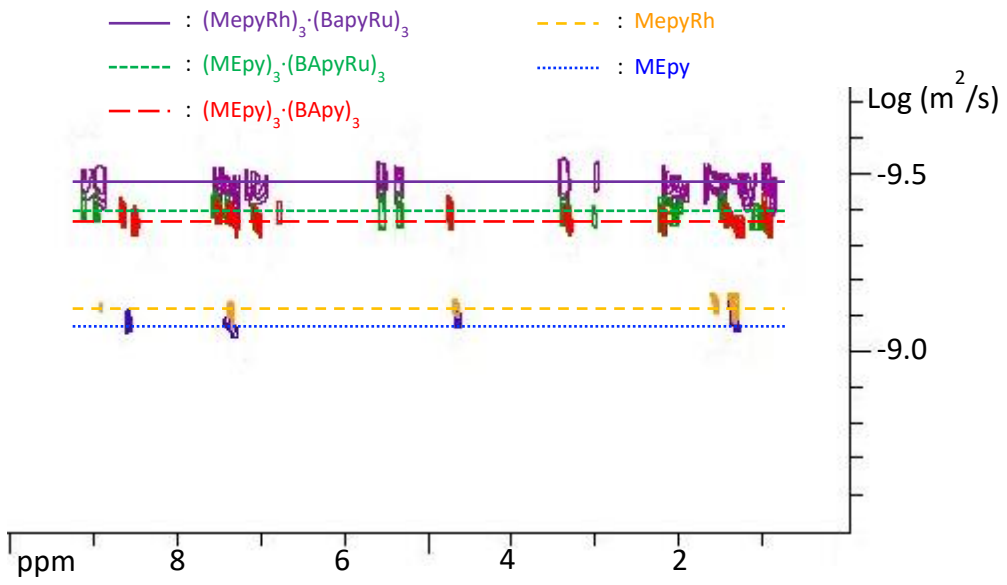

Figure 66: Superimposed DOSY NMR spectra ($CDCl_3$, 25 ℃) of compounds MEpy, MEpyRh, $(MEpy)_3$·$(BApy)_3$, $(MEpy)_3$·$(BApyRu)_3$ and $(MEpyRh)_3$·$(BApyRu)_3$

3.3.3 NOESY NMR spectroscopy

In the NOESY NMR spectrum of $(MEpy)_3$·$(BApyRu)_3$, cross peaks between the protons of the NH groups of BApyRu and the protons of the NH_2 and NH groups of MEpy are observed (Figure 67). Thus, the presence of hydrogen-bond interactions between the MEpy and BApy units is confirmed.

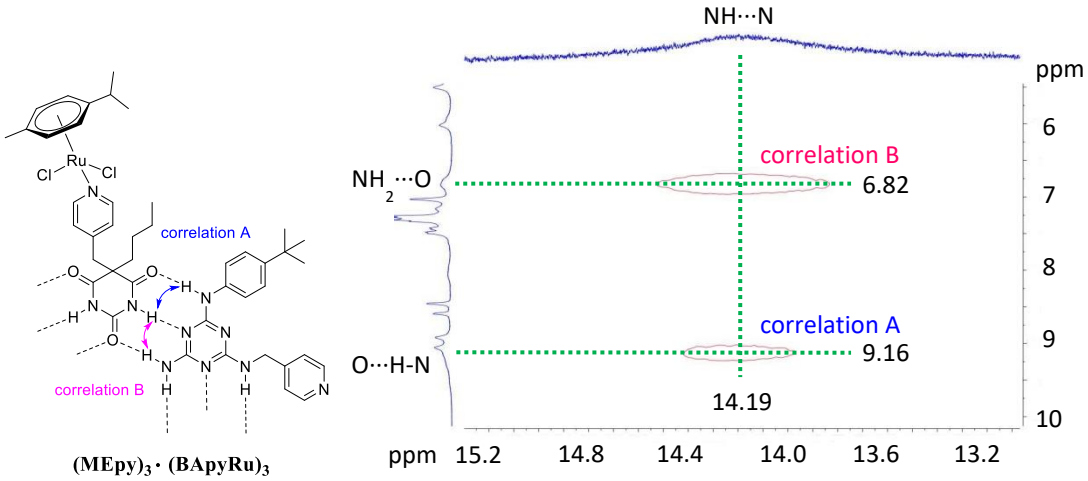

Figure 67: NOESY NMR spectrum of $(MEpy)_3$·$(BApyRu)_3$, showing the NH hydrogen-bond cross peaks ($CDCl_3$, 25 ℃)

3.3.4 IR spectroscopy

Upon formation of six triple ME-BA hydrogen-bonds (NH···O, N···HN, NH···O), the stretching vibrations of NH broadened and shifted by almost 200 cm^{-1} in the infrared spectra, as compare with pure MEpy and BApy. Similar absorption bands are also observed in the trinuclear complexes and rosette-type ligand. After the coordination of metals, the infrared spectra of the rosette-type complexes are almost identical.

3.3.5 UV spectroscopy

The rosette-type assemblies were studied by UV-visible spectroscopy. The spectra were recorded in chloroform at 1.0×10^{-5} M concentrations in the range 200 nm to 800 nm. The spectrum of the rosette-type ligand $(MEpy)_3 \cdot (BApy)_3$ shows a high energy absorption band at 265 nm, which may be attributed to ligand π,π* transitions,[222] and the value is close to that of rosette-type ligand $(ME)_3 \cdot (BApy)_3$. This band is also observed in the rosette-type metalla-assemblies, $(MEpy)_3 \cdot (BApyRu)_3$ (267 nm) and $(MEpyRu)_3 \cdot (BApy)_3$ (267 nm). The intensities of these bands are in the range 8.00×10^4 M^{-1} cm^{-1} to 1.02×10^5 M^{-1} cm^{-1} (Figure 68).

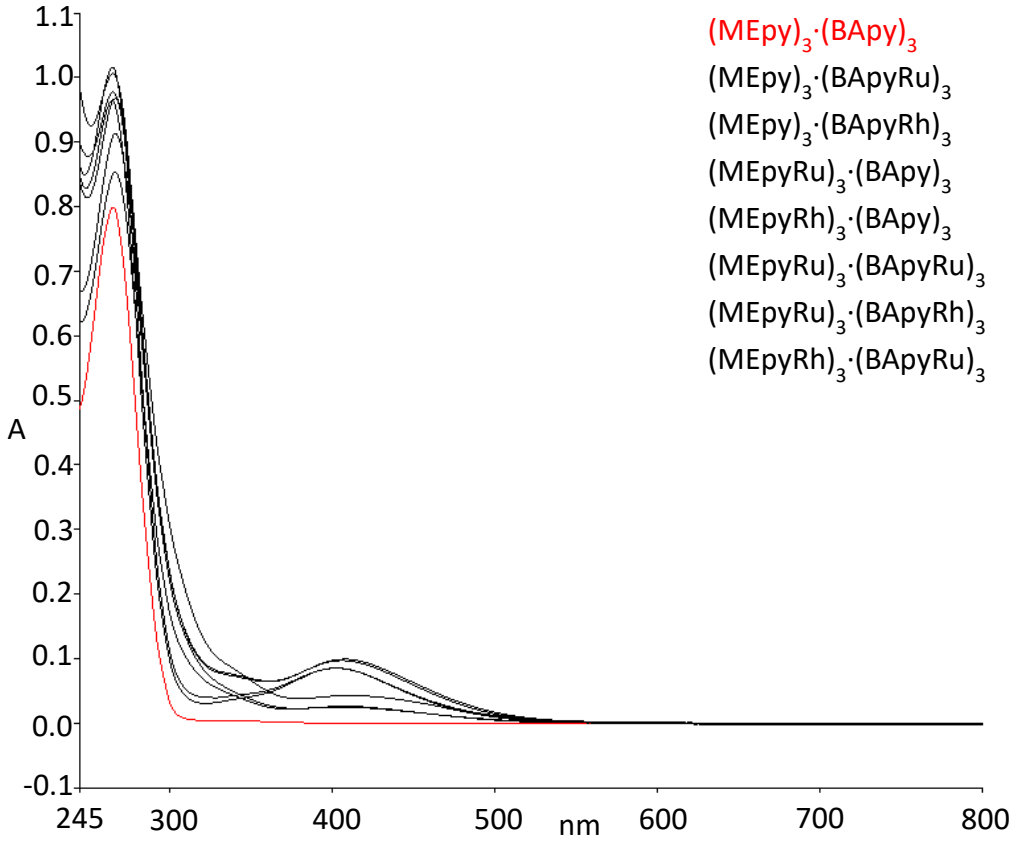

Figure 68: UV spectra of rosette-type metalla-assemblies synthesized in comparison with the rosette-type ligand $(MEpy)_3 \cdot (BApy)_3$ ($CHCl_3$, 25 ℃)

Moreover, the UV-vis spectra of mononuclear complexes MEpyRu and MEpyRh were performed in chloroform at 5×10^{-5} M in the range 200 nm to 800 nm. A high energy absorption band is observed at 267 nm for MEpyRu and 265 nm for MEpyRh, which may be attributed to ligand-localized transition. The broad low-energy band observed at 422 nm for MEpyRu and 407 nm for MEpyRh, is associated to metal-to-ligand charge transfer (MLCT) transitions. They are of moderate intensity, 7.48×10^2 M^{-1} cm^{-1} for MEpyRu and 2.78×10^3 M^{-1} cm^{-1} for MEpyRh (Figure 69).

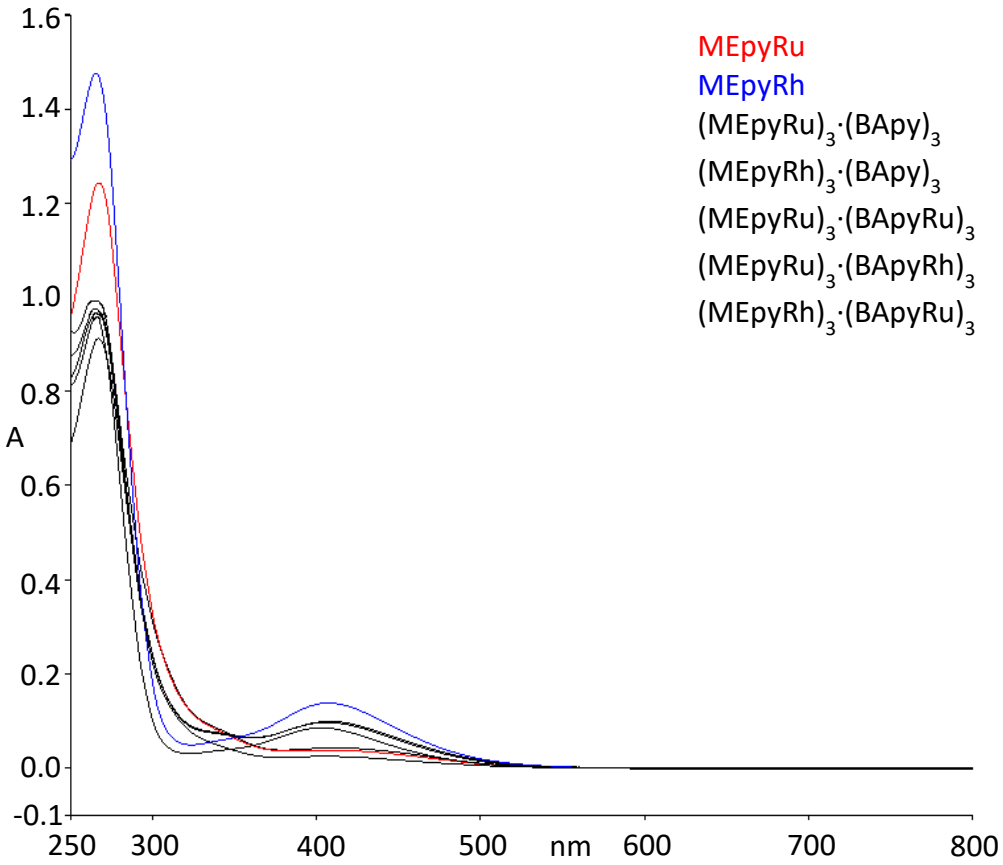

Figure 69: UV spectra of rosette-type assemblies $(MEpyRu)_3 \cdot (BApy)_3$, $(MEpyRh)_3 \cdot (BApy)_3$, $(MEpyRu)_3 \cdot (BApyRu)_3$, $(MEpyRu)_3 \cdot (BApyRh)_3$, $(MEpyRh)_3 \cdot (BApyRu)_3$ in comparison with mononuclear complexes MEpyRu and MEpyRh ($CHCl_3$, 25 ℃)

3.3.6 Mass spectroscopy

The mass spectra of MEpyRu and MEpyRh were performed by using electrospray ionization in a positive mode. The parent peak is observed at *m/z* = 620.1 corresponding to $[M - Cl]^+$ for MEpyRu, and at *m/z* = 622.1 corresponding to $[M - Cl]^+$ for MEpyRh. As often encountered in such neutral dichloro piano-stool complexes,[73, 236-238] a peak corresponding to the cationic $[M - Cl]^+$ species is observed in their ESI mass spectrum (positive mode).

The electrospray ionization mass spectra (ESI-MS) of the hexameric hexanuclear rosettes show, in both cases, a parent peak at *m/z* = 580.9, together with other metal-containing fragments of lower intensities. This main peak corresponds to the trichloro-bridged dinuclear complex $[Rh_2(Cp^*)_2(\mu\text{-}Cl)_3]^+$, a cationic trichloro-bridged dinuclear complex that is often produced upon decomposition of piano-stool

complexes.[239] The decomposition occurs during the ionization process, as the ^{1}H NMR spectra of the rosettes in chloroform-d_1 suggest high stability in solution.

3.4 Conclusion

In conclusion, two heterohexanuclear and four homotrinuclear rosette-type assemblies have been prepared and characterized. The combination of pyridyl-functionalized melamine and barbituric acid derivatives allows a controlled synthesis of the designed heteronuclear systems. The rosette-type assemblies are stable in solution at room temperature, showing an equilibrium constant of 4400 s^{-1} and a stability constant of approximately 13.5 kJ in 1,1,2,2-tetrachloroethane-d_2. In the future, we would like to insert additional complexity to such supramolecular assemblies, and expand, in a controlled manner, the system to the third dimension.

Chapter 4

Coordination of dinuclear complexes to a hydrogen-bonded rosette-type assembly

4.1 General introduction

Supramolecular interactions are powerful tools to design complicated complexes such as rosette-type assemblies.[204, 206] Rosette-type assemblies can be designed by directional multi-hydrogen-bonded systems[10, 80-81, 84] and the metal ligand coordination can be used to modify their properties. Only limited examples have been reported in the area of rosette-type metalla-assemblies,[90-93] thus it is still an emerging area. Arene

ruthenium and cyclopentadienyl rhodium/iridium complexes show great biological potential in medical applications.[133, 186, 191, 201-202, 240-243] Thus, addition of piano-stool complexes can offer new perspectives in the area of rosette-type metalla-assemblies.

Pyridyl groups were successfully added at either the barbituric acid part or the melamine part.[244] As previously seen, two different substituents can be inserted on the melamine unit. However, two identical substituents can also be added on melamine. Thus, the modifications of the melamine units can offer new opportunities to develop rosette-type metalla-assemblies. For example, additional groups with π-π stacking interactions were introduced by Yagai, providing π-conjugated rosette-type assemblies with stimuli-responsive properties.[95-98]

The π-π stacking interactions can play a key role for the controlled formation of metalla-assemblies. This concept was widely used for the formation of metalla-rectangles,[180-181] metalla-prisms[184, 190] and metalla-cubes.[189, 191] Indeed, two pyridyl groups showing π-π stacking interactions were added at the periphery of the melamine unit. Then addition of metalla-clips with long chains can modify the solubility of the rosettes.[202, 245] Accordingly, a series of cationic hexanuclear rosette-type metalla-assemblies were synthesize and characterized.

4.2 Synthesis

4.2.1 Synthesis of the bis-functionalized melamine ligand

The synthesis of the bis-functionalized melamine ligand can be divided in three steps. The first step was the formation of *N,N'*-bis(4-iodophenyl)melamine which was obtained in two synthetic steps, starting from 4-iodoaniline and cyanuric chloride. In parallel, 3-ethynyl-5-methoxypyridine was prepared in two synthetic steps, starting from 3-bromo-5-methoxypyridine and ethynyltrimethylsilane (Scheme 27).

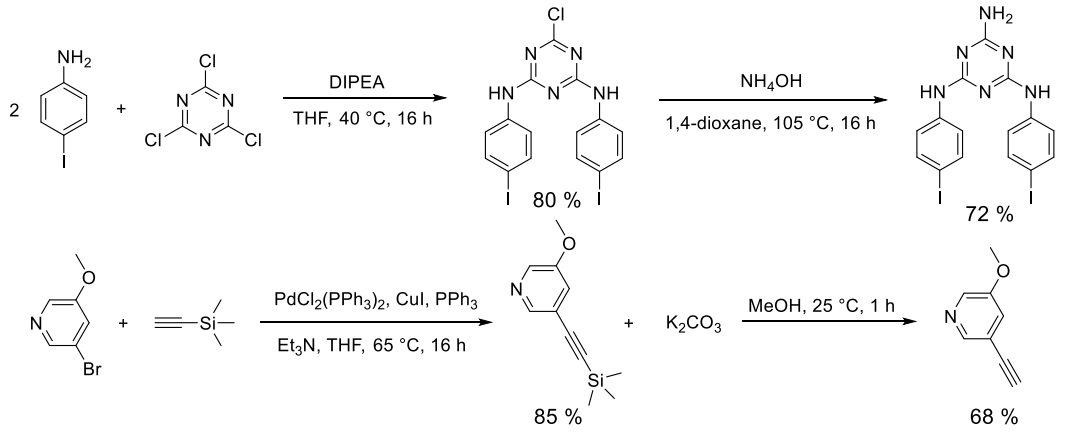

Scheme 27: Syntheses of two reactants *N,N'*-bis(4-iodophenyl)melamine (top) and 3-ethynyl-5-methoxypyridine (bottom)

Then the formation of the new melamine ligand was achieved by combining the two previously mentioned products. This final step was performed by a Sonogashira coupling in the presence of $PdCl_2(PPh_3)_2$ catalyst and CuI co-catalyst (Scheme 28).[98]

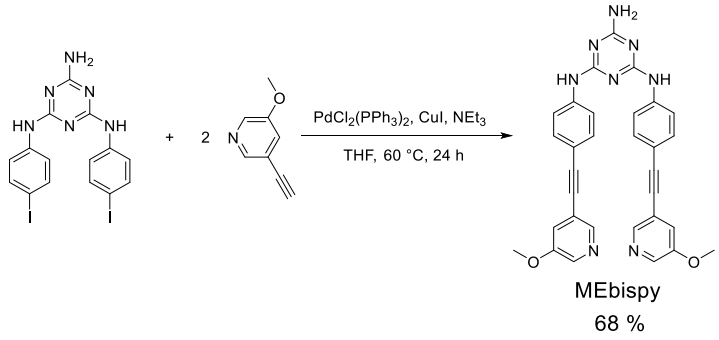

Scheme 28: Synthesis of the melamine ligand MEbispy

To prepare the bis-functionalized ligand, the first reaction was performed between 4-ethynylpyridine and *N,N'*-bis(4-iodophenyl)melamine (Scheme 29). But, the desired product was not obtained because of the poor solubility of 4-ethynylpyridine in the selected solvent. Then, the 3-ethynyl-5-methoxypyridine was used to modify the solubility and to give the desired melamine product (MEbispy).

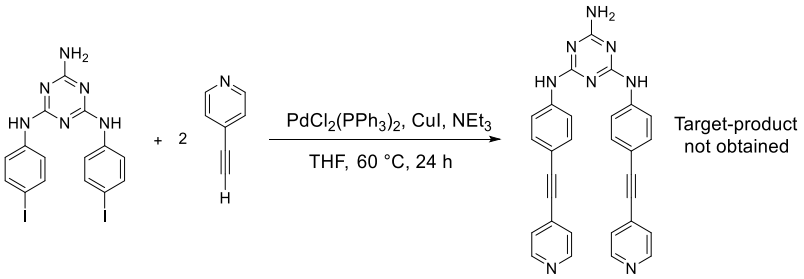

Scheme 29: Synthesis of the melamine ligand MEbispy

4.2.2 Synthesis of dinuclear melamine-type metalla-assemblies

Dinuclear melamine-type metalla-assemblies can be obtained starting from the dinuclear metalla-clips and MEbispy, as the distance between the two N-pyridyl coordinating sites in MEbispy is optimal for bis-coordination. Two dinuclear metalla-clips (oxalamide clip and benzoquinone clip) were used based on the length of the metalla-clips. A solvent mixture (methanol/tetrahydrofuran) was used to ensure that both reactants were soluble. After removal of silver chloride, addition of MEbispy gave the desired dinuclear melamine-type unit in excellent yields (> 86 %) (Scheme 30).

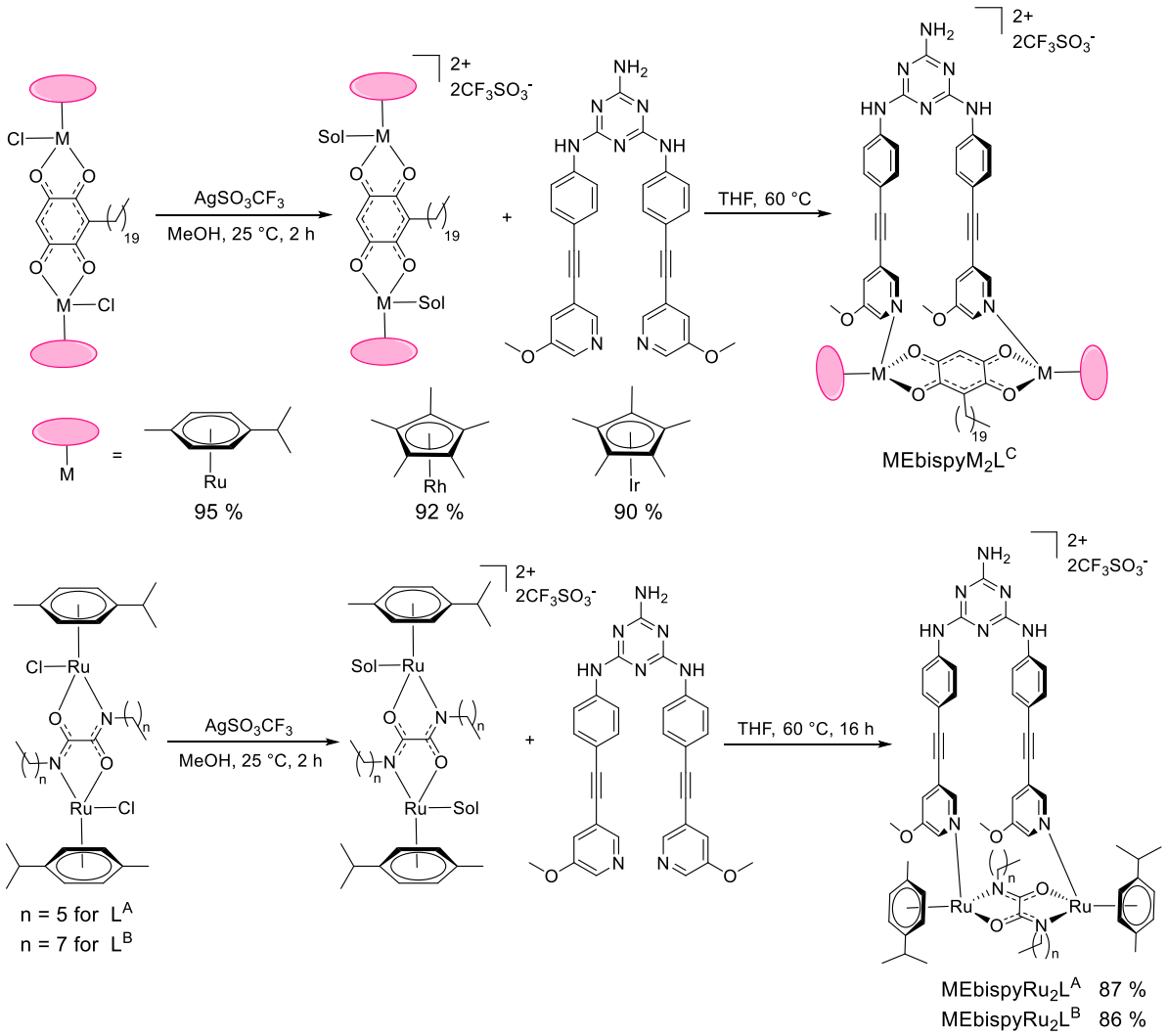

Scheme 30: Syntheses of cationic dinuclear melamine-type units

4.2.3 Synthesis of cationic hexanuclear hydrogen-bonded metalla-assemblies

The cationic hexanuclear metalla-assembly $(MEbispyRu_2L^C)_3{\cdot}(BA)_3$ [Ru_2: $Ru_2(cym)_2$, H_2L^C: 2,5-dihydroxy-3-icosyl-2,5-diene-1,4-dione] was prepared by mixing in chloroform equimolar amounts of the dinuclear melamine-type unit ($MEbispyRu_2L^C$) and 5,5-diethylbarbituric acid (BA). The reaction mixture was stirred at 25 ℃ for 48 h. The expected rosette $(MEbispyRu_2L^C)_3{\cdot}(BA)_3$ was obtained in high yield (80 %).

Then the same method was used to prepare other cationic hexanuclear metalla-assemblies. Unfortunately, the rosette assemblies were not obtained because of the poor solubility of the melamine-type unit. Thus, a different mixture of solvents

(chloroform/dichloromethane) was used. Indeed, different metalla-assemblies have been synthesized by varying the reaction conditions. These cationic hexanuclear metalla-assemblies are all obtained in excellent yields (> 86 %) (Scheme 31).

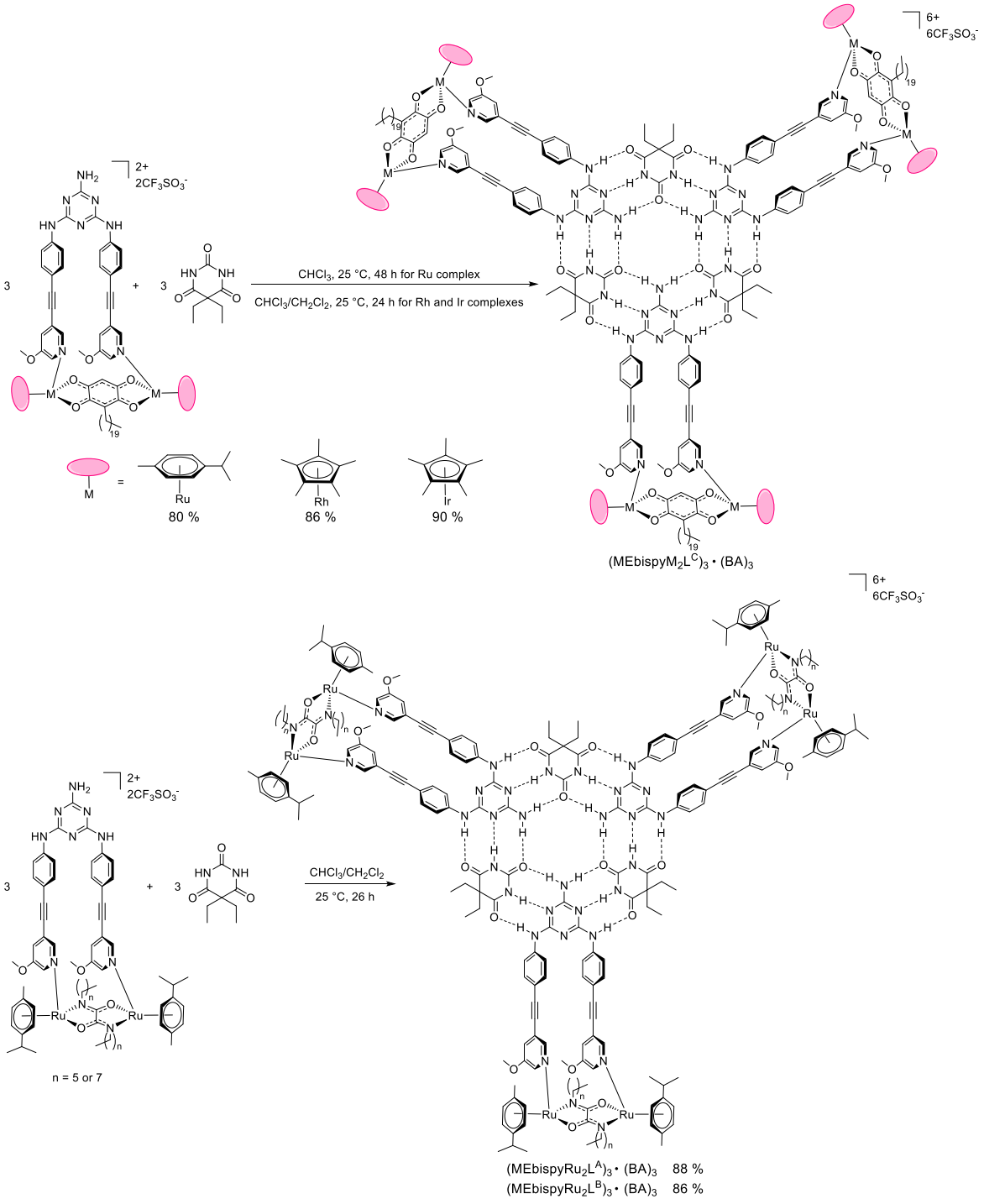

Scheme 31: Syntheses of cationic hexanuclear hydrogen-bonded metalla-assemblies

4.3 Characterizations

4.3.1 Proton and carbon NMR spectroscopy

The new cationic rosettes were fully characterized by NMR spectroscopy. Due to the poor solubility of the rosettes, dichloromethane-d_2 was used, which do not allow a clear detection of the typical N-H signal (around 14.0 ppm) of the hydrogen-bonded systems. This characteristic signal was only observed for $(MEbispyRu_2L^C)_3{\cdot}(BA)_3$ and $(MEbispyIr_2L^C)_3{\cdot}(BA)_3$, and in both cases as broad signals. To solve this problem, a ^1H NMR spectrum at low temperature was performed. The selected temperature was based on published results, saying that the characteristic signal of rosette structures are only present in the -60 ℃ to -30 ℃ range.[91] Indeed, a sharp signal was observed at 14.2 ppm for $(MEbispyRu_2L^C)_3{\cdot}(BA)_3$ at -30 ℃. The signals of hydrogen bonds are slightly upfield shifted, when the temperature decreases (Figure 70). The same phenomenon is observed for the temperature dependence spectra of the trinuclear metalla-assembly $(MEpy)_3{\cdot}(BApyRu)_3$ (Chapter III).

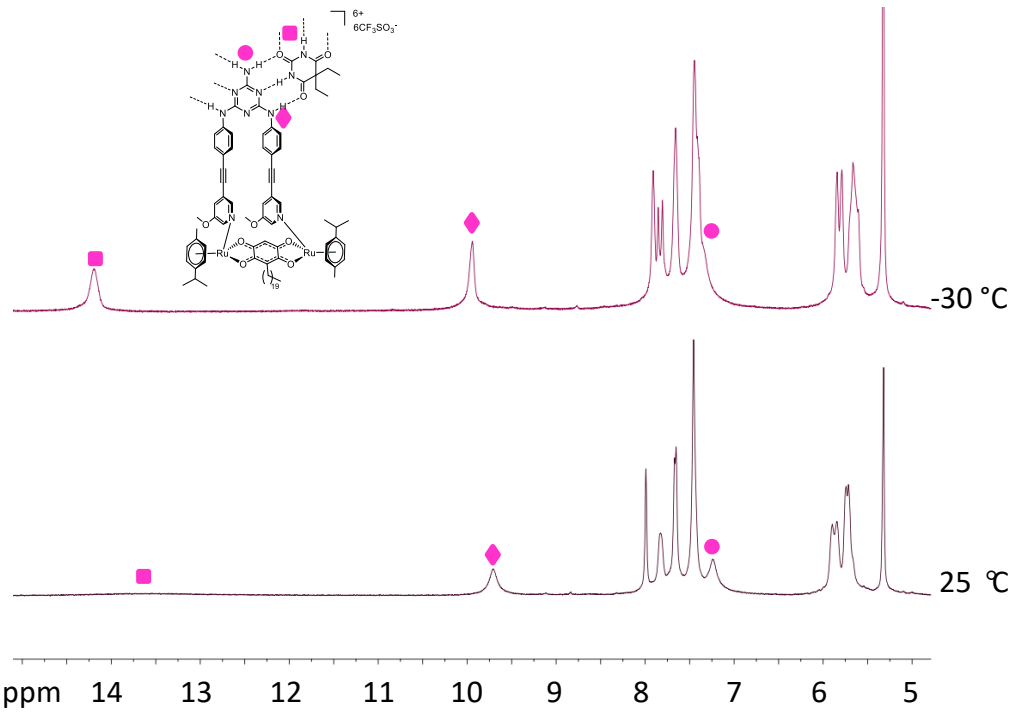

Figure 70: Temperature dependence spectra of $(MEbispyRu_2L^C)_3{\cdot}(BA)_3$ from 5.0 ppm to 15.0 ppm (CD_2Cl_2)

By comparing spectra of BA and MEbispyRu$_2$L^C with the (MEbispyRu$_2$L^C)$_3$·(BA)$_3$ rosette, the NH signal of the BA units is shifted by 5.6 ppm, while for the MEbispy units the signals are shifted by 1.3 ppm (NHC$_{ar}$) and 1.0 ppm (NH$_2$). These results are quite similar to those observed in the previous chapters. Other protons remain unaffected (Figure 71). All these informations support the formation of the cationic hexanuclear hydrogen-bonded metalla-assemblies.

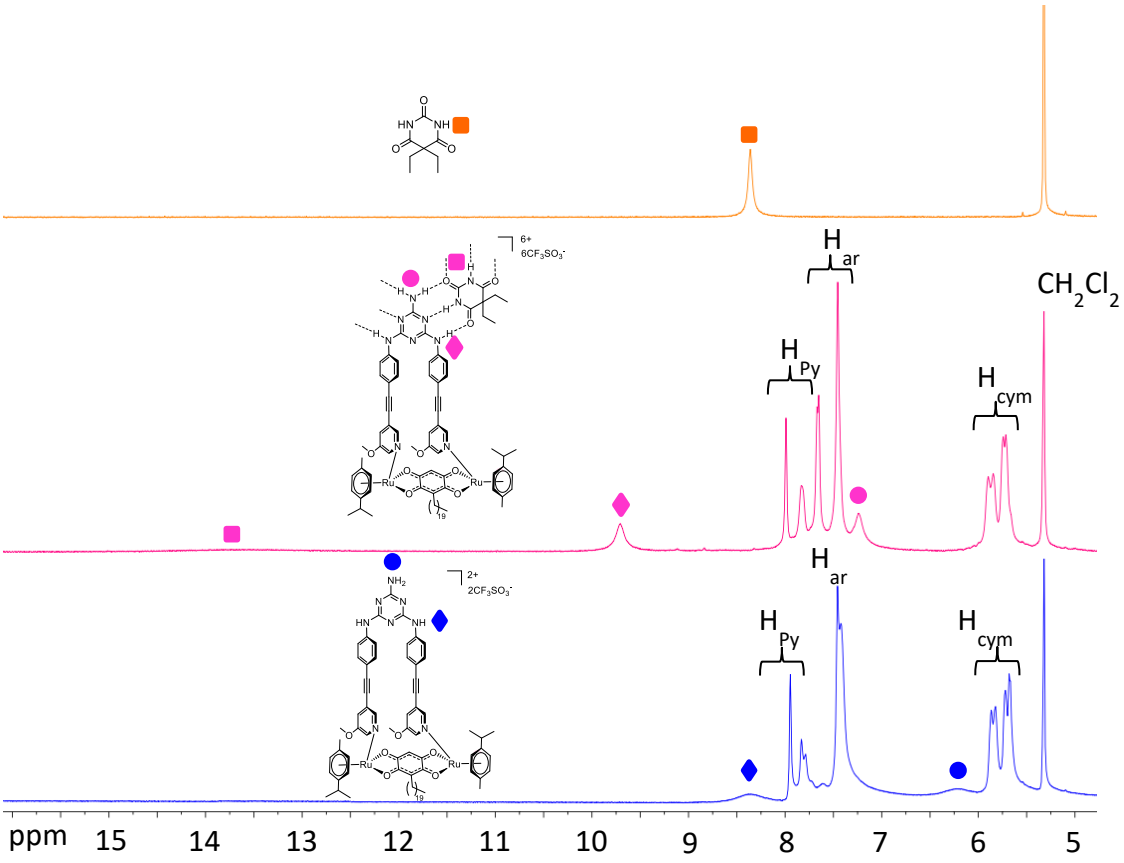

Figure 71: ^{1}H NMR spectra of BA, (MEbispyRu$_2$L^C)$_3$·(BA)$_3$, MEbispyRu$_2$L^C, with an emphasis on the chemical shifts of the different NH protons (CD_2Cl_2, 25 ℃)

The formation of (MEbispy)$_3$·(BA)$_3$ was also confirmed by ^{1}H NMR in chloroform-d_1, in which the signal of the NH protons of the BA units was observed at 13.5 ppm. Because of the poor solubility of (MEbispyRu$_2$L^C)$_3$·(BA)$_3$ in chloroform-d_1, the superimposition of the spectra was done in dichloromethane-d_2. The coordination of metalla-clips can be confirmed by the additional signals of the para-cymene ligands at 5.9 ppm and 5.7 ppm. Important chemical shifts are observed for the signals of the

pyridyl protons. One of the signal of the pyridyl groups is upfield shifted, and two other signals are downfield shifted (Figure 72).

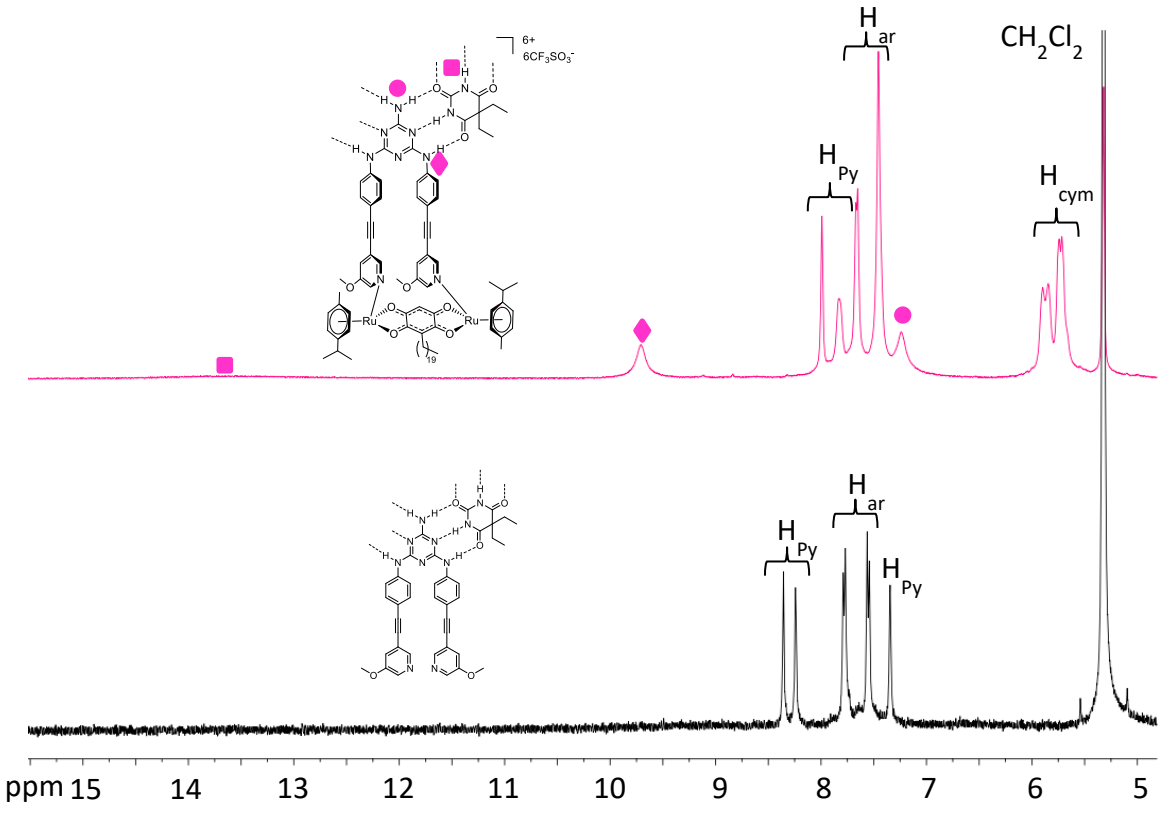

Figure 72: ^{1}H NMR spectra of (MEbispyRu$_2$L^{C})$_3$·(BA)$_3$ and (MEbispy)$_3$·(BA)$_3$ (CD_2Cl_2, 25 ℃)

4.3.2 DOSY NMR spectroscopy

As suggested in the third chapter, the assembly/disassembly process will occur in chloroform, if the temperature is higher than 50 ℃. The cationic hexanuclear metalla-assemblies cannot be solubilized in chloroform, thus all the NMR spectra were performed in dichloromethane-d_2. Unfortunately, the disassembly occurred at room temperature in dichloromethane-d_2. As shown in the ^{1}H NMR spectra of the rosettes, only broad signals were observed at room temperature. The same conclusion was made from the DOSY NMR experiments, as the proton signals of the rosette-type metalla-assemblies were not on the same line in the DOSY NMR spectra, confirming the presence of two species.

To solve this problem, a DOSY NMR spectrum was performed at -30 ℃ in dichloromethane-d_2 for (MEbispyRu$_2$L^{C})$_3$·(BA)$_3$. At low temperature, all proton signals

were observed on the same line (Figure 73). The large signals observed are due to the difficulties of maintaining the temperature at exactly -30 °C during the measurement. The diffusion coefficient obtained is 1.38×10^{-10} m^2 s^{-1}, and the calculated hydrodynamic radius is 1.92×10^{-9} m. The radius of the cationic rosette-type metalla-assembly $(MEbispyRu_2L^C)_3 \cdot (BA)_3$ is higher than that of the neutral hexanuclear rosette-type metalla-assemblies. However, these results suggest the formation of the rosette.

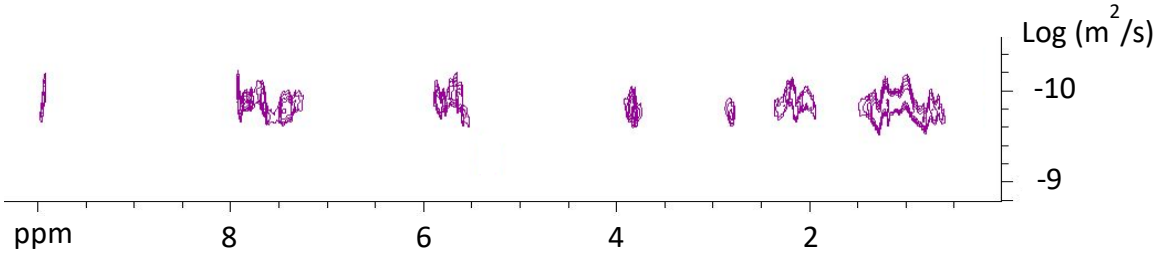

Figure 73: DOSY spectrum (CD_2Cl_2, -30 °C) of $(MEbispyRu_2L^C)_3 \cdot (BA)_3$

4.3.3 IR spectroscopy

All products were analyzed by IR spectroscopy. In the IR spectra of the rosettes, a significant band associated with the NH stretching vibration of BA and MEbispy is shifted and broadened by about 200 cm^{-1}. This important redshift correlates with the lengthening of the NH bonds.[10] Thus, the formations of the rosette-type metalla-assemblies was also confirmed by IR spectroscopy.

Bands associated to the presence of the trifluoromethanesulfonate anions are observed at 1223 cm^{-1} to 1255 cm^{-1}. These typical peaks suggest the presence of cationic complexes and support the formation of melamine-type metalla-assemblies and rosette-type metalla-assemblies.

4.3.4 UV spectroscopy

Rosette-type assemblies were studied by UV-visible spectroscopy. All spectra were measured in dichloromethane at 1.0×10^{-5} M concentrations in the range 200 nm to 800 nm. The spectrum of the rosette-type ligand $(MEbispy)_3 \cdot (BA)_3$ shows two energy absorption bands at 230 nm and 323 nm, which may be attributed to ligand π,π* transitions.[222] These bands are also observed in the rosette-type metalla-assemblies, the

bands being however slightly shifted. The intensities of these bands varied from 1.51 × 10^5 M^{-1} cm^{-1} to 2.32 × 10^5 M^{-1} cm^{-1} for the band at 230 nm, while the intensities of the band around 323 nm varied from 1.57 × 10^5 M^{-1} cm^{-1} to 1.91 × 10^5 M^{-1} cm^{-1} (Figure 74).

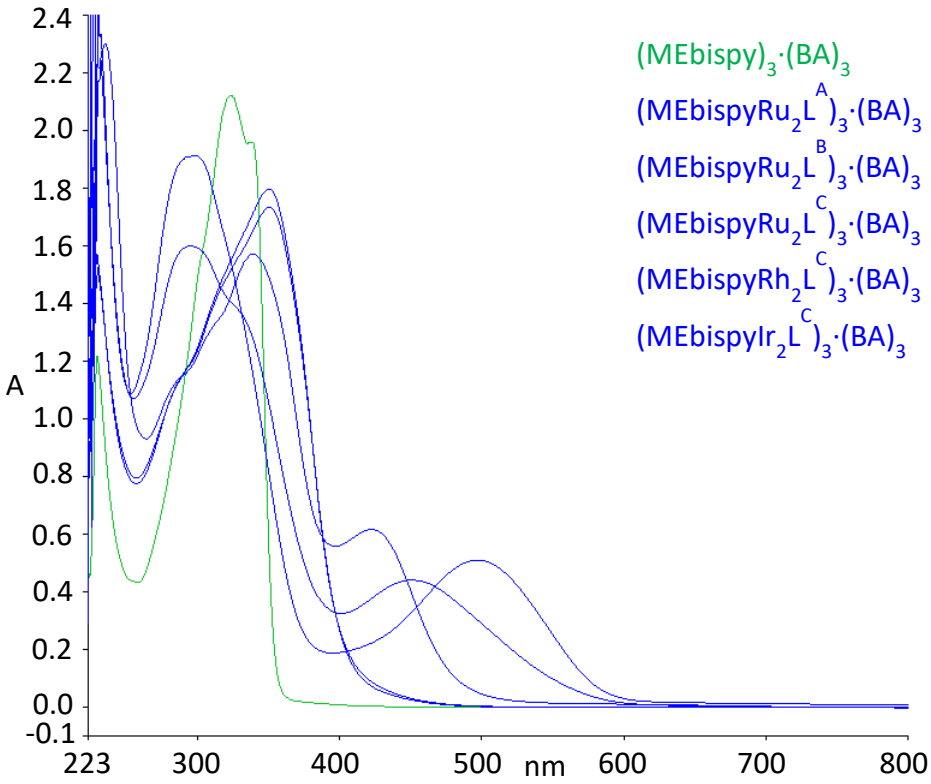

Figure 74: UV spectra of rosette-type metalla-assemblies synthesized in comparison with the rosette-type ligand $(MEbispy)_3{\cdot}(BA)_3$ ($CHCl_3$, 25 ℃)

These bands around 230 nm and 323 nm are also observed for the melamine-type metalla-assemblies. Thus, these two bands may be attributed to ligand π,π* transitions of the melamine parts. The intensities of these bands in the rosette-type metalla-assemblies are three times higher than those of the melamine-type complexes. This is in agreement with a three times higher concentration of the melamine-type complex in the corresponding rosette.

An additional band observed in the visible region at 496 nm for $(MEbispyRu_2L^C)_3{\cdot}(BA)_3$, at 422 nm for $(MEbispyRh_2L^C)_3{\cdot}(BA)_3$ and at 451 nm for $(MEbispyIr_2L^C)_3{\cdot}(BA)_3$ is attributed to metal-to-ligand charge transfer (MLCT) transitions (Figure 75). Similar absorption bands are also observed for the corresponding melamine-type metalla-assemblies, but with less intensity.

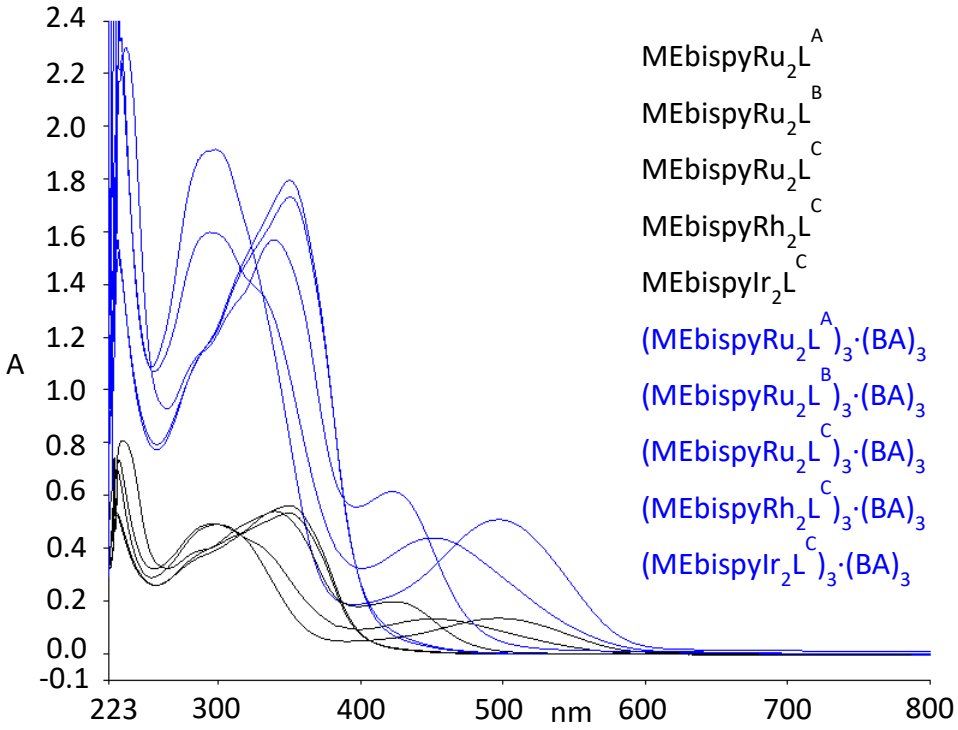

Figure 75: UV spectra of melamine-type metalla-assemblies synthesized in comparison with rosette-type metalla-assemblies synthesized ($CHCl_3$, 25 °C)

4.3.5 Mass spectroscopy

The mass spectra of $[Rh_2(Cp^*)_2(L^C)Cl_2]$ and $[Ir_2(Cp^*)_2(L^C)Cl_2]$ were measured by electrospray ionization technique in a positive mode. The parent peak is observed at *m/z* = 929.2 and 1109.2, which correspond to $[M - Cl]^+$ cations, as often encountered in such dinuclear metalla-clips.[202, 245]

The mass spectrum of *N,N'*-bis{4-[(5-methoxypyridin-3-yl)ethynyl]phenyl}melamine (MEbispy) was also performed in positive mode, showing a parent peak at *m/z* = 541.1 corresponding to the $[MEbispy + H]^+$ cation.

The reaction between the melamine unit and the dinuclear clip can in principle give [1 + 1] or [2 + 2] metalla-assemblies (Figure 76). Thus, to confirm the structure of the melamine-type metalla-assemblies, electrospray ionization mass spectra were performed (positive mode). Two signals were observed for each melamine-type metalla-assemblies, at *m/z* = 1579.0 corresponding to $[M - CF_3SO_3]^+$ and at *m/z* = 715.2 corresponding to $[M - 2\ CF_3SO_3]^{2+}$ for $MEbispyRu_2L^C$, *m/z* = 1582.9 and *m/z* = 717.3

for MEbispyRh$_2$L^C, *m/z* = 1760.9 and *m/z* = 807.3 for MEbispyIr$_2$L^C, *m/z* = 1415.0 and *m/z* = 633.4 for MEbispyRu$_2$L^A, and *m/z* = 1470.0 and *m/z* = 660.8 for MEbispyRu$_2$L^B.

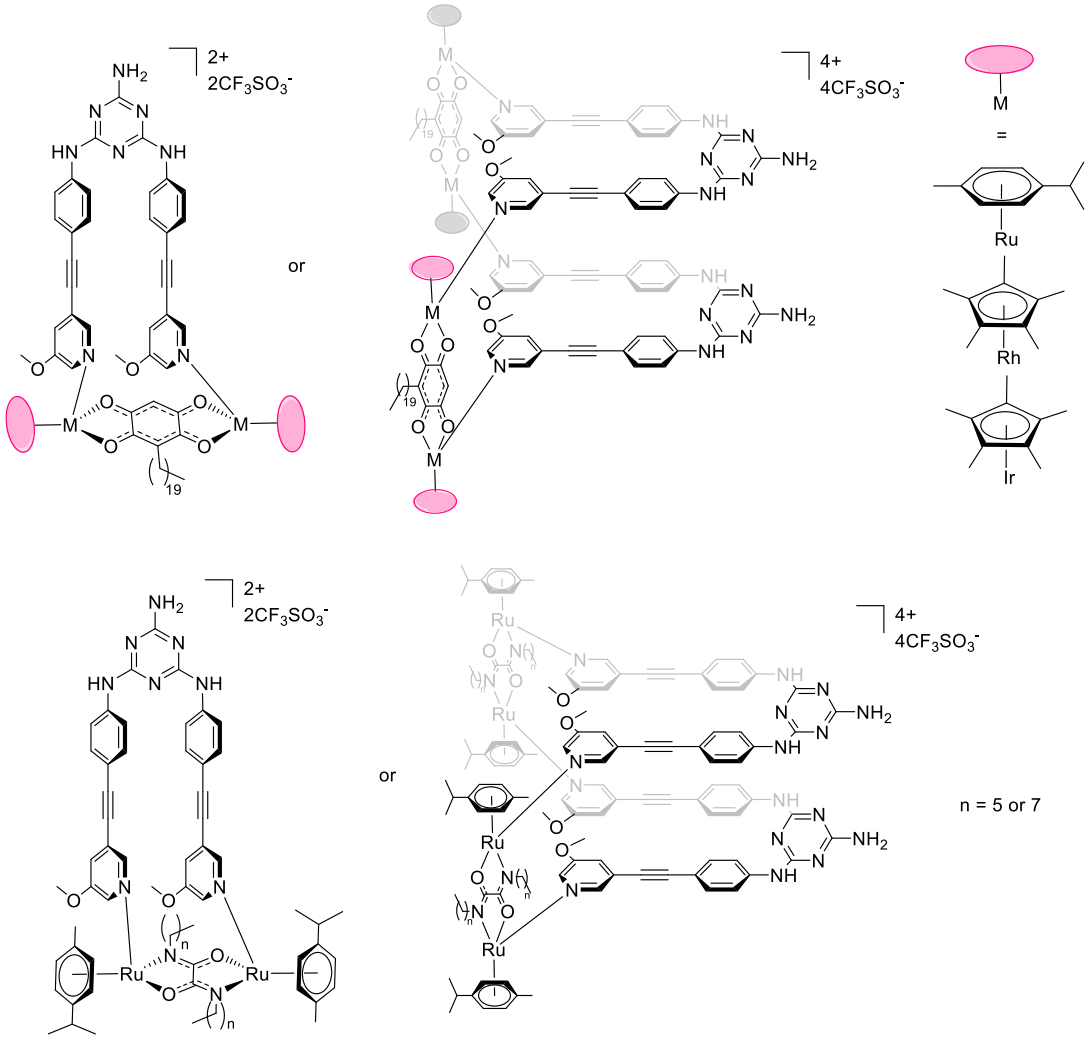

Figure 76: [1 + 1] and [2 + 2] melamine-derived metalla-assemblies

The isotopic patterns of these two signals have been compared to those of the calculated patterns for [1 + 1] and [2 + 2] metalla-assemblies. The results show that the measured spectra match perfectly with the [1 + 1] calculated patterns, but they are different in comparison with the [2 + 2] metalla-assemblies. The values of the mass being the same but the patterns being different. For example, the superimposed spectra of MEbispyRu$_2$L^C are shown in Figure 77. The measured pattern of the signal at *m/z* = 715.2 (top) matches perfectly with the calculated pattern for [M – 2 CF_3SO_3]$^{2+}$ of the [1 + 1] metalla-assemblies (bottom). But the measured pattern of the signal at *m/z* = 1579.0

(top) does not match with the calculated pattern for $[M - 2\ CF_3SO_3]^{2+}$ of the [2 + 2] metalla-assemblies (bottom).

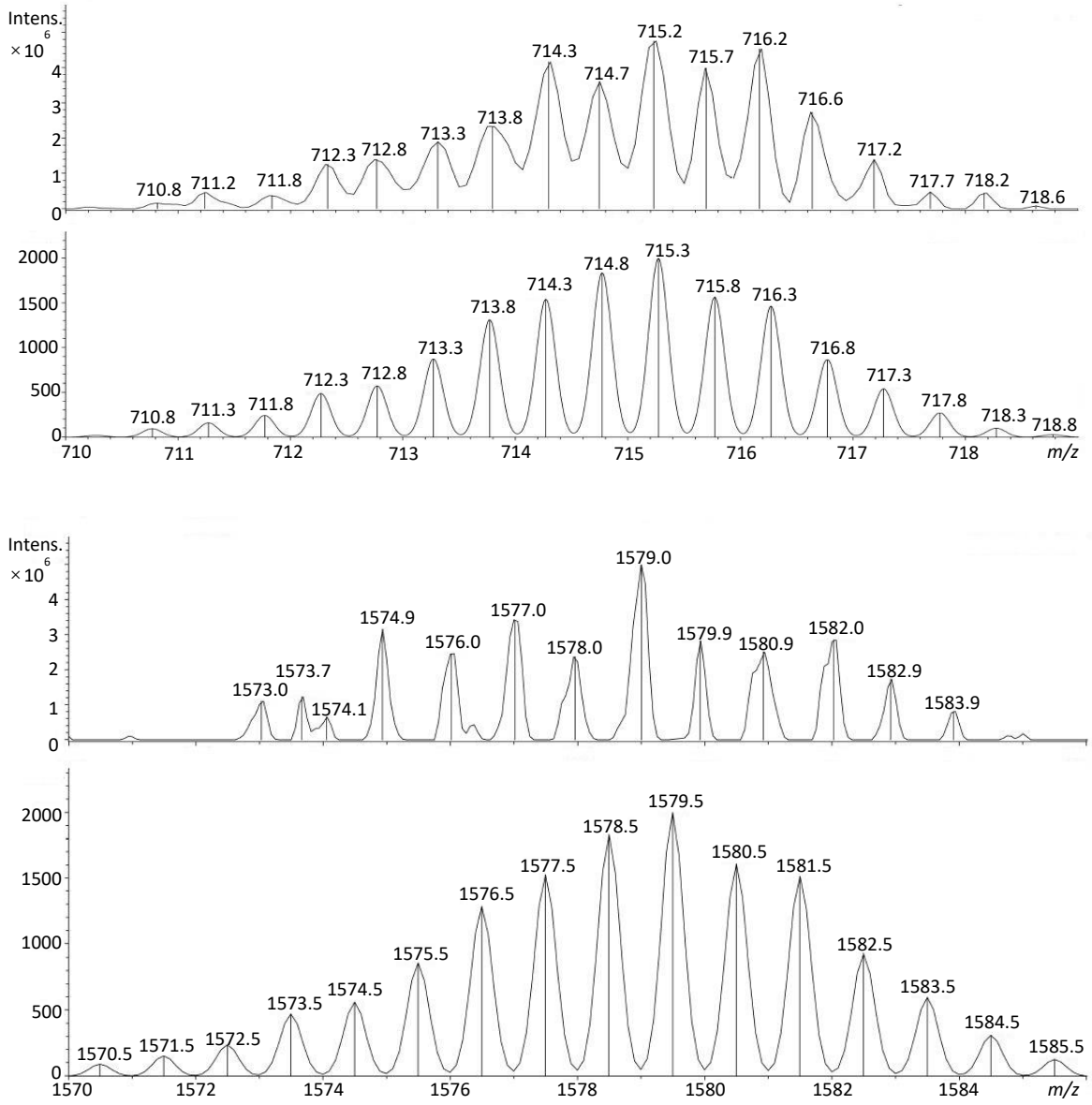

Figure 77: Measured isotopic patterns and calculated isotopic patterns for the metalla-assembly $MEbispyRu_2L^C$

4.3.6 Concentration effects

A concentration dependence experiment was performed to study the stability of the rosette-type assembly. This study followed the method published by Whitesides.[80] This experiment was performed on the $(MEbispy)_3{\cdot}(BApy)_3$ rosette. The chemical shifts of the melamine NH protons were measured in chloroform-d_1 at different concentrations.

The results are shown in Figure 78 and the corresponding data listed in Table 6. The melamine (MEbispy) alone shows a chemical shift of the NH proton at 8.0 ppm. When the concentrations of the two rosette components reach 2.5 mM, the formation of the rosette-type structure increases rapidly, until it reaches a plateau at 20 mM. When the concentration is higher than 20 mM, the rosette-type structure is stable. These results are similar to those observed by Whitesides with the $(ME)_3 \cdot (BA)_3$ rosette.

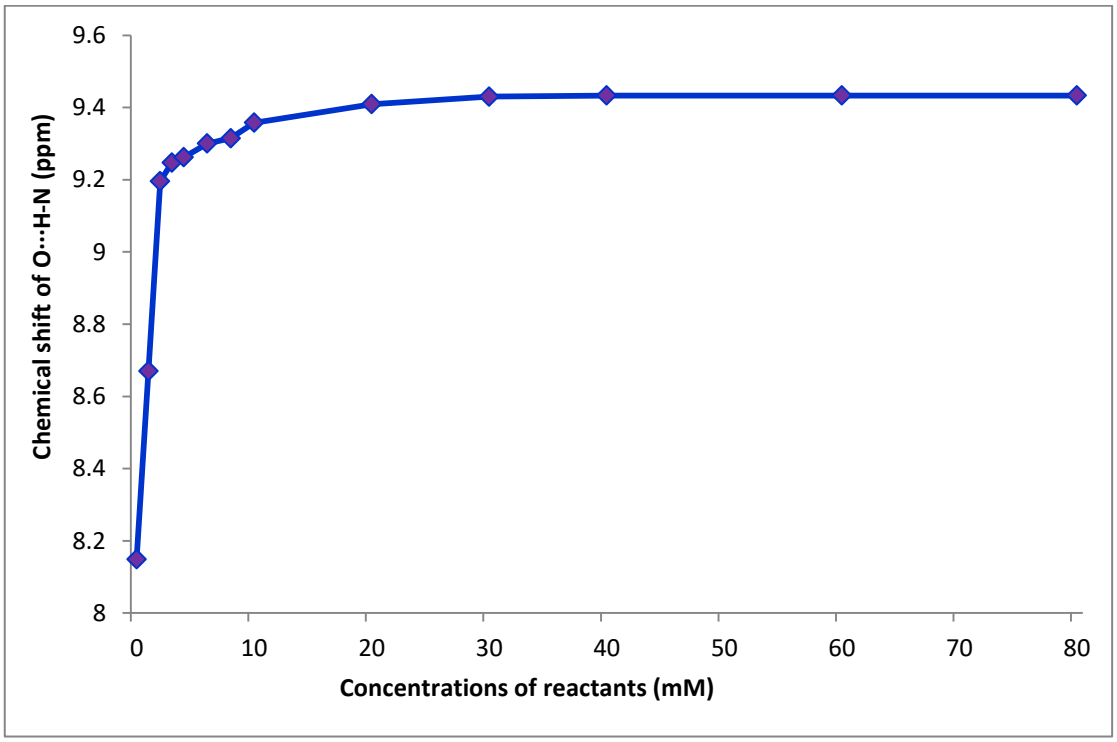

Figure 78: Concentration dependence curve

Concentration (mM)	**MEbispy BApy**	**0.5 0**	**0.5 0.5**	**1.5 1.5**	**2.5 2.5**	**3.5 3.5**	**4 4**	**6 6**
Chemical shift of O···H-N (ppm)		8.04	8.15	8.67	9.20	9.25	9.26	9.30
Concentration (mM)	**MEbispy BApy**	**8 8**	**10 10**	**20 20**	**30 30**	**40 40**	**60 60**	**80 80**
Chemical shift of O···H-N (ppm)		9.32	9.36	9.41	9.43	9.43	9.43	9.43

Table 6: Concentration dependence data of the O···HN proton chemical shifts

4.4 Conclusion

Two pyridyl groups have been inserted on the melamine unit, thus generating additional π-π stacking interactions within the rosette-type metalla-assemblies. Coordination of metalla-clips to the melamine units was performed showing [1 + 1] addition of metalla-clips, which was confirmed by mass spectroscopy. Five rosette-type metalla-assemblies with different metalla-clips were synthesized and characterized. The cationic hexanuclear metalla-assemblies were not stable in dichloromethane at room temperature, thus NMR spectra at low temperature was performed to establish their structures. In the following work, the solubility of the rosette-type metalla-assemblies in water needs to be adjusted to evaluate possible biological applications.

Chapter 5

Conclusions and perspectives

5.1 Conclusions

The combination of hydrogen bonds and metal coordinations to design supramolecular assemblies remains unexplored. The objective of my thesis was to exploit hydrogen-bonded systems to form in combination with piano-stool complexes, 2D and 3D metalla-assemblies. To achieve these goals, a rosette-type scaffold was used, more specifically the melamine barbituric acid pairing system. Overall, the thesis can be divided in three parts, with a general strategy, which is described in Scheme 32.

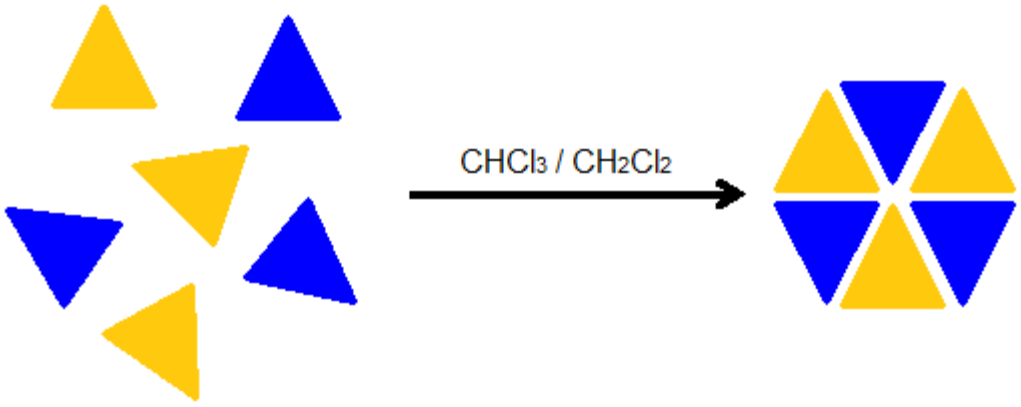

Scheme 32: General strategy for the formation of rosette-type metalla-assemblies

In the first section, the possibility of coordinating piano-stool complexes to a hydrogen-bonded rosette-type assembly was confirmed through the formation of trinuclear rosette-type metalla-assemblies. Neutral and cationic trinuclear rosette-type metalla-assemblies were synthesized and characterized. Two different methods were used to obtain the neutral trinuclear rosette-type metalla-assemblies. In the first method, after formation of the rosette, the coordination to the pyridyl groups was performed. In the second method, the coordination of the metal centers was done prior to the rosette formation.

In the second part of my thesis, neutral hexanuclear rosette-type metalla-assemblies incorporating homo- and hetero-metallic units have been synthesized and characterized. BA and ME ligands offer great flexibility to connect different metals. Thus, heteronuclear metalla-assemblies were generated with success, and they have showed good stability in chloroform.

Finally, cationic hexanuclear metalla-assemblies were synthesized and characterized, using dinuclear piano-stool complexes. This strategy has allowed the insertion of three metalla-clips at the periphery of the rosette, thus generating large rosette-type metalla-assemblies.

5.2 Perspectives

Different supramolecular interactions were introduced in the same rosette-type metalla-assembly. Hydrogen bonds are crucial for the formation of rosettes, while π-π stacking, electrostatic, metal-ligand and other weak interactions can be used to add functionality to these supramolecular systems. In the future work, more supramolecular interactions can be used in the rosette-type systems to increase complexity and diversity.

A series of cationic hexanuclear metalla-assemblies based on metalla-clips has been synthesized (Chapter IV). But the stability of these cationic hexanuclear metalla-assemblies in dichloromethane at room temperature became a challenge for their characterization. Thus, their stability needs to be modified in the future. Moreover, addition of nine metallic centers can be an idea: Both mononuclear piano-stool complexes or dinuclear metalla-clips can be added at the periphery of the rosettes for the formation of nona-nuclear rosette-type metalla-assemblies. Three types of nona-nuclear rosette-type metalla-assemblies can be prepared: A metalla-assembly with nine identical piano-stool complexes, a metalla-assembly with six identical piano-stool complexes at the melamine part and three other piano-stool complexes on the barbituric acid part and finally, a metalla-assembly with three metalla-clips at the melamine part and three piano-stool complexes on the barbituric acid part (Figure 79).

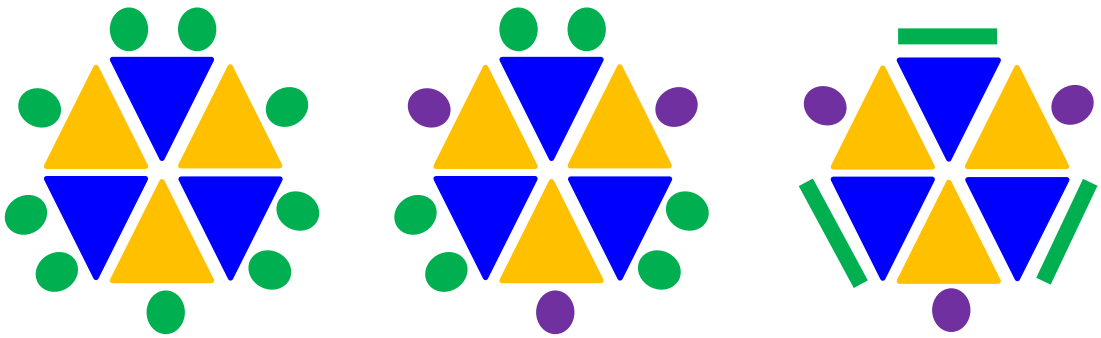

Figure 79 : Three types of nona-nuclear rosette-type metalla-assemblies

The synthesis of double-decker rosette systems may be a target in the future. Several arene ruthenium metalla-cages have been synthesized by our group. They were used for the encapsulation of planar aromatic molecules, and these molecular-cages can be used to transport unsoluble molecules to cells. If metalla-cages based on hydrogen bonds are obtained, they can be used to encapsulate non-planar molecules, actually most

of pharmaceutical drugs are non-planar. Hydrogen-bonded metalla-cages can in principle be more biocompatible than coordination-driven metalla-cages, and they can be pH-dependent, thus seeking more medical applications. Two strategies can be considered for the formation of hydrogen-bonded metalla-cages (Scheme 33): The formation of a rosette structure, followed by the addition of metalla-clips (Route A, Scheme 33); or by mixing melamine-based dinuclear clips with barbituric acid (Route B, Scheme 33). Additionally, the limit of solubility of the rosette assemblies, their stability and their selectivity need to be considered for the design of hydrogen-bonded metalla-cages.

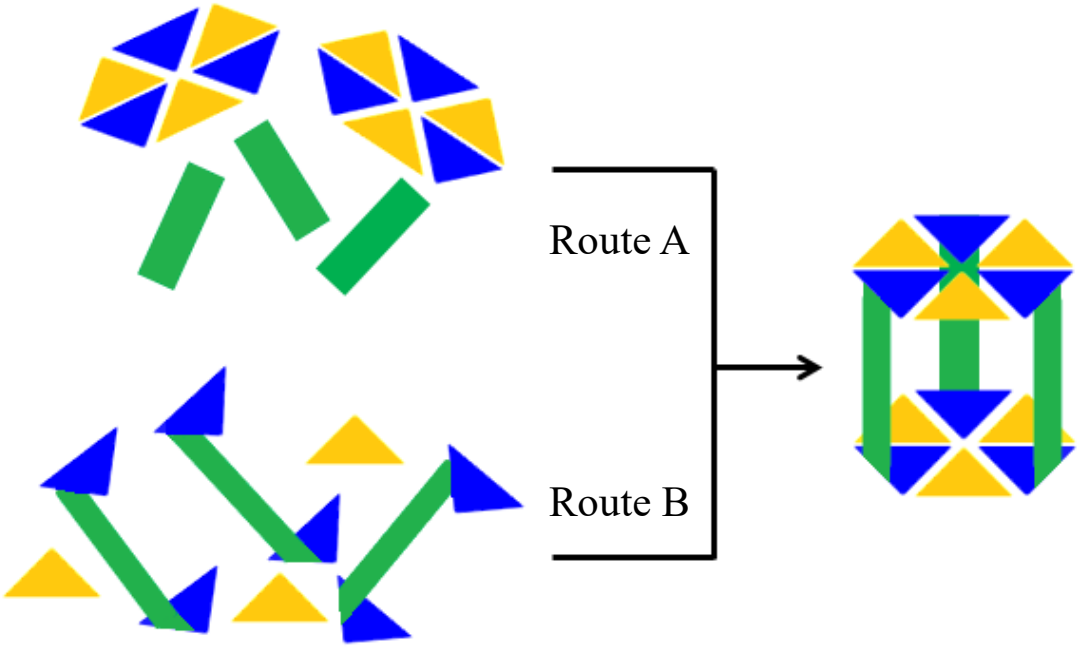

Scheme 33: Two general strategies for the formation of hydrogen-bonded metalla-cages

All attempts to obtain the mass spectra of rosette-type metalla-assemblies were unsuccessful (Chapter II). Thus, vapor pressure osmometry (VPO) can be applied in the future to determine the molecular weight of rosettes. This method was already used by researchers to determine the molecular weight of rosette-type assemblies.[246],[80] Moreover, atomic force microscopy (AFM) can also be used to determine the three-dimensional surface profile of the rosette-type metalla-assemblies, thus potentially excluding the formation of the other structures, the linear and crinkled tapes.[98]

Chapter 6

Experimental

6.1 General remarks

All solvents were dried before use following standard procedures and all reactions were manipulated under an inert atmosphere. 3-Ethynyl-5-methoxypyridine,[247] *N,N'*-bis(4-iodophenyl)melamine,[82] *N,N'*-bis(4-*tert*-butylphenyl)melamine (ME),[80] *N*-(4-tert-butylphenyl)-*N'*-(pyridin-4-

ylmethyl)melamine (MEpy),[93] 5-butyl-5-(pyridin-4-ylmethyl)pyrimidine-2,4,6-trione (BApy),[228] $[Ru(cym)Cl_2]_2$,[248] $[Rh(Cp^*)Cl_2]_2$,[249] $[Ir(Cp^*)Cl_2]_2$,[250] $[Ru(cym)(PPh_3)Cl_2]$,[144] $[Rh(Cp^*)(PPh_3)Cl_2]$,[251] $[Ir(Cp^*)(PPh_3)Cl_2]$,[250] 2,5-dihydroxy-3-icosylcyclohexa-2,5-diene-1,4-dione (H_2L^C),[170] $[Ru_2(cym)_2(L^A)Cl_2]$ (H_2L^A: *N,N'*-dihexyloxalamide) (Ru_2L^A), $[Ru_2(cym)_2(L^B)Cl_2]$ (H_2L^B: *N,N'*-dioctyloxalamide) (Ru_2L^B), and $[Ru_2(cym)_2(L^C)Cl_2]$ (Ru_2L^C)[170] were prepared according to published methods. All other reagents were commercially available and used as received. NMR spectra were recorded with a Bruker Avance II 400 spectrometer. The chemical shifts are referenced to deuterated solvent residual peaks [$CDCl_3$: δ = 7.26 ppm; CD_2Cl_2 : δ = 5.32 ppm; $(CD_3)_2SO$: δ = 2.50 ppm and CD_3OD = 3.31 ppm]. DOSY experiments were conducted using standard parameters.[167] UV/Vis absorption spectra were recorded with a Perkin-Elmer UV/Vis spectrophotometer. Infrared spectra were recorded with a Perkin-Elmer FTIR spectrometer. Electrospray mass spectra were obtained in the positive mode with an LCQ Finnigan mass spectrometer (University of Fribourg, Switzerland). Microanalyses were carried out by the Mikroelementaranalytisches Laoratorium (ETH Zürich, Switzerland).

6.2 Syntheses and characterizations

6.2.1 Neutral and cationic trinuclear metalla-assemblies

Diethyl 2-butyl-2-(pyridin-4-ylmethyl)malonate

Sodium hydride (1.10 g, 27.44 mmol) was added to a solution of diethyl 2-butylmalonate (2.69 g, 12.30 mmol) in dry tetrahydrofuran (100 mL). After stirring for 30 min, 4-(chloromethyl)pyridine (1.60 g, 9.46 mmol) was added progressively. The mixture was stirred at reflux for 16 h, and then the solvent was evaporated. The residue was triturated with diethyl ether, and the organic phase was washed with water and brine and dried with magnesium sulfate. After evaporation of the solvent and column chromatography (CH_2Cl_2/EtOAc, 15:1), the desired product was obtained.

Diethyl 2-butyl-2-(pyridin-4-ylmethyl)malonate: Colorless oil, yield 80 % (2.32 g, 7.53 mmol).

^{1}H NMR (400 MHz, $CDCl_3$): δ = 8.45 (d, $^{3}J_{H,H}$ = 5.7 Hz, 2 H, $CH_{Py}N$), 6.99 (d, $^{3}J_{H,H}$ = 5.7 Hz, 2 H, $CH_{Py}C$), 4.14 (m, 4 H, CH_2O), 3.18 (s, 2 H, CH_2C_{Py}), 1.75 (m, 2 H, CH_2C), 1.28 (m, 4 H, CH_2 and CH_2CH_3), 1.20 (t, $^{3}J_{H,H}$ = 7.0 Hz, 6 H, CH_3CH_2O), 0.87 (t, $^{3}J_{H,H}$ = 7.2 Hz, 3 H, CH_3) ppm.

^{13}C NMR (100 MHz, $CDCl_3$): δ = 170.95 (CO); 149.77 ($CH_{Py}N$); 145.69 (C_{Py}); 125.27 ($CH_{Py}C$); 61.47(CH_2O); 58.47 (C); 37.62 (CH_2C_{Py}); 31.97 (CH_2C); 26.35 (CH_2); 22.88 (CH_2CH_3); 14.10 (CH_3CH_2O); 13.96 (CH_3) ppm.

5-Butyl-5-(pyridin-4-ylmethyl)pyrimidine-2,4,6-trione (BApy)

Urea (0.50 g, 8.28 mmol) and sodium ethoxide (5.62 mL, 15.06 mmol) were added to a solution of diethyl 2-butyl-2-(pyridin-4-ylmethyl)malonate (2.32 g, 7.53 mmol) in dry ethanol (30 mL). The reaction mixture was heated under reflux for 16 h and then the solvent was evaporated. After column chromatography (CH_2Cl_2/MeOH, 15:1), and recrystallization from ethanol, the pure product was obtained.

BApy: White solid, yield 35 % (0.73 g, 2.64 mmol).

^{1}H NMR [400 MHz, $(CD_3)_2SO$]: δ = 11.51 (br., 2 H, NH), 8.46 (d, $^{3}J_{H,H}$ = 5.5 Hz, 2 H, $CH_{Py}N$), 6.99 (d, $^{3}J_{H,H}$ = 5.5 Hz, 2 H, $CH_{Py}C$), 3.13 (s, 2 H, CH_2C_{Py}), 1.95 (m, 2 H, CH_2C_{BA}), 1.24 (m, 2 H, CH_2), 1.09 (m, 2 H, CH_2CH_3), 0.82 (t, $^{3}J_{H,H}$ = 7.2 Hz, 3 H, CH_3) ppm.

^{13}C NMR [100 MHz, $(CD_3)_2SO$]: δ = 172.27 (CO); 149.79 ($CH_{Py}N$); 149.33 (HNCONH); 144.32 (C_{Py}); 124.57 ($CH_{Py}C$); 56.35 (C_{BA}); 42.45 (CH_2C_{Py}); 38.40 (CH_2C_{BA}); 26.56 (CH_2); 22.12 (CH_2CH_3); 13.64 (CH_3) ppm.

UV/Vis (DMF, 1.0×10^{-4} M): λ_{max} (ε) = 257 nm (3.99×10^{3} M^{-1} cm^{-1}).

IR: $\tilde{\nu}$ = 3225 (br., NH), 2937 (br., CH aromatic), 1716 (s, NH), 1696 (s, C=O), 1607 (s, C⋯N), 1406 (s, C⋯C) cm^{-1}.

D ($CDCl_3$): 9.5×10^{-10} m^2 s^{-1}.

$C_{14}H_{17}N_3O_3$ (275.3): calcd. C 61.08, H 6.22, N 15.26; found: C 61.04, H 6.22, N 15.07.

ESI-MS: *m/z* = 276.1 $[M + H]^+$.

BApyRu and BApyRh

A mixture of BApy (0.18 g, 0.65 mmol) and $[Ru(cym)Cl_2]_2$ or $[Rh(Cp^*)Cl_2]_2$ (0.20 g, 0.33 mmol) in dry tetrahydrofuran (10 mL) was stirred at 70 °C for 16 h. Then the solvent was evaporated, the residue was solubilized in dichloromethane (5 mL), and pentane was added to precipitate the product.

BApyRu: Yellow solid, yield 92 % (0.35 g, 0.60 mmol).

^{1}H NMR (400 MHz, $CDCl_3$): δ = 8.91 (br., 2 H, NH), 8.86 (d, $^3J_{H,H}$ = 5.9 Hz, 2 H, $CH_{Py}N$), 7.12 (d, $^3J_{H,H}$ = 5.9 Hz, 2 H, $CH_{Py}C$), 5.45 (d, $^3J_{H,H}$ = 5.7 Hz, 2 H, CH_{cym}), 5.22 (d, $^3J_{H,H}$ = 5.7 Hz, 2 H, CH_{cym}), 3.29 (s, 2 H, CH_2C_{Py}), 2.93 (m, 1 H, CH), 2.05 (m, 2H, CH_2C_{BA}), 1.97 (s, 3 H, CH_3C_{cym}), 1.29 (m, 4 H, CH_2 and CH_2CH_3), 1.27 (d, $^3J_{H,H}$ = 6.8 Hz, 6 H, CH_3CH), 0.87 (t, $^3J_{H,H}$ = 6.6 Hz, 3 H, CH_3) ppm.

^{13}C NMR (100 MHz, $CDCl_3$): δ = 171.09 (CO), 155.07 ($CH_{Py}N$), 148.19 (HNCONH), 146.49 (C_{Py}), 126.14 ($CH_{Py}C$), 103.37 ($C_{cym}CH$), 97.40 ($C_{cym}CH_3$), 83.31 (CH_{cym}), 82.13 (CH_{cym}), 57.59 (C_{BA}), 41.14 (CH_2C_{Py}), 40.65 (CH_2C_{BA}), 30.81 (CH), 26.72 (CH_2), 22.63 (CH_2CH_3), 22.46 (CH_3CH), 18.25 (CH_3C_{cym}), 13.79 (CH_3) ppm.

UV/Vis ($CHCl_3$, 5.0 × 10^{-5} M): λ_{max} (ε) = 241 (8.72 × 10^3), 297 (4.17 × 10^3), 411 nm (8.57 × 10^2 M^{-1} cm^{-1}).

IR: $\tilde{\nu}$ = 3185 (br., NH), 2960 (br., CH aromatic), 1722 (s, NH), 1700 (s, C=O), 1616 (s, C··N), 1404 (s, C··C) cm^{-1}.

D ($CDCl_3$): 4.9 × 10^{-10} m^2 s^{-1}.

$C_{24}H_{31}Cl_2N_3O_3Ru$ (581.5): calcd. C 49.57, H 5.37, N 7.23; found C 48.89, H 5.57, N 7.32.

ESI-MS: *m/z* = 546.1 $[M - Cl]^+$.

BApyRh: Orange solid, yield 88 % (0.34 g, 0.57 mmol).

^{1}H NMR (400 MHz, $CDCl_3$): δ = 8.84 (br., 2 H, NH), 8.83 (d, $^3J_{H,H}$ = 5.3 Hz, 2 H, $CH_{Py}N$), 7.18 (d, $^3J_{H,H}$ = 5.3 Hz, 2 H, $CH_{Py}C$), 3.30 (s, 2 H, CH_2C_{Py}), 2.07 (m, 2 H, CH_2C_{BA}), 1.51 (s, 15 H, $CH_3C_{Cp^*}$), 1.28 (m, 4 H, CH_2 and CH_2CH_3), 0.87 (t, $^3J_{H,H}$ = 7.0 Hz, 3 H, CH_3) ppm.

^{13}C NMR (100 MHz, $CDCl_3$): δ = 171.07 (CO), 153.65 ($CH_{Py}N$), 148.04 (HNCONH), 146.74 (C_{Py}), 126.87 ($CH_{Py}C$), 94.25 (C_{Cp*}), 57.64 (C_{BA}), 41.22 (CH_2C_{Py}), 40.65 (CH_2C_{BA}), 26.77 (CH_2), 22.61 (CH_2CH_3), 13.80 (CH_3), 8.94 (CH_3C_{Cp*}) ppm.

UV/Vis ($CHCl_3$, 5.0 × 10^{-5} M): λ_{max} (ε) = 241 (1.58 × 10^4), 406 nm (2.38 × 10^3 M^{-1} cm^{-1}).

IR: $\tilde{\nu}$ = 3190 (br., NH), 2959 (br., CH aromatic), 1724 (s, NH), 1699 (s, C=O), 1614 (s, C⋯N), 1403 (s, C⋯C) cm^{-1}.

D ($CDCl_3$): 5.4 × 10^{-10} m^2 s^{-1}.

$C_{24}H_{31}Cl_2N_3O_3Ru$ (584.4): calcd. C 49.33, H 5.52, N 7.19; found C 49.10, H 5.80, N 7.06.

ESI-MS: *m/z* 548.1 $[M - Cl]^+$.

$(ME)_3$·$(BApy)_3$

A mixture of BApy (50.0 mg, 0.18 mmol) and ME (70.9 mg, 0.18 mmol) in dry chloroform (1.5 mL) was stirred at 25 ℃ for 30 min. Then pentane was added to precipitate the product as a white solid.

$(ME)_3$·$(BApy)_3$: White solid, yield 89 % (0.11 g, 0.05 mmol).

^{1}H NMR (400 MHz, $CDCl_3$): δ = 13.87 (br., 6 H, NH⋯N), 9.35 (br., 6 H, O⋯HN), 8.49 (d, $^3J_{H,H}$ = 4.2 Hz, 6 H, $CH_{Py}N$), 7.66 (d, $^3J_{H,H}$ = 8.1 Hz, 12 H, $CH_{ar}CC$), 7.39 (d, $^3J_{H,H}$ = 8.1 Hz, 12 H, $CH_{ar}CN$), 7.09 (d, $^3J_{H,H}$ = 4.2 Hz, 6 H, $CH_{Py}C$), 6.83 (br., 6 H, NH_2⋯O), 3.37 (s, 6 H, CH_2C_{Py}), 2.23 (m, 6 H, CH_2C_{BA}), 1.39 [s, 66 H, CH_2, CH_2CH_3 and $C(CH_3)_3$], 0.93 (t, $^3J_{H,H}$ = 5.6 Hz, 9 H, CH_3) ppm.

^{13}C NMR (100 MHz, $CDCl_3$): δ = 175.18 (CO), 166.13 (CNH_2), 163.91 (CNH), 152.78 (HNCONH), 150.46 ($CH_{Py}N$), 146.52 ($C_{ar}C$), 143.90 (C_{Py}), 136.43 ($C_{ar}NH$), 125.49 ($CH_{ar}CN$), 124.76 (CH_{Py}), 121.92 ($CH_{ar}CC$), 57.72 (C_{BA}), 42.92 (CH_2C_{Py}), 40.04 (CH_2C_{BA}), 34.49 [$C(CH_3)_3$], 31.61 [$C(CH_3)_3$], 27.13 (CH_2), 22.74 (CH_2CH_3), 13.78 (CH_3) ppm.

UV/Vis ($CDCl_3$, 1.0 × 10^{-5} M): λ_{max} (ε) = 271 nm (1.22 × 10^5 M^{-1} cm^{-1}).

IR: $\tilde{\nu}$ = 3302 (br., NH), 2959 (br., CH aromatic), 1724 (s, NH), 1693 (s, C=O), 1613 (s, C⋯N), 1565 (s, C=N), 1506 (s, CN), 1410 (s, C⋯C) cm^{-1}.

D ($CDCl_3$): 3.6 × 10^{-10} m^2 s^{-1}.

$C_{111}H_{141}N_{27}O_9$ (1997.5): calcd. C 66.74, H 7.11, N 18.93; found C 66.23, H 7.06, N 18.63.

$(ME)_3$·$(BApyRu)_3$ and $(ME)_3$·$(BApyM)_3$ (M = Rh, Ir)

Method 1: A mixture of BApy (0.09 g, 0.33 mmol) and ME (0.13 g, 0.33 mmol) in dry chloroform (5 mL) was stirred at 25 ℃. After 30 min, $[Ru(cym)Cl_2]_2$ (0.10 g, 0.17 mmol) or $[M(Cp^*)Cl_2]_2$ (Rh, 0.10 g; Ir, 0.13 g; 0.17 mmol)was added, and the mixture was stirred at 25 ℃ for 16 h. Then the mixture was concentrated, and pentane was added to precipitate the product.

Method 2: A mixture of BApyRu or BApyRh (Ru 0.19 g, Rh 0.19 g; 0.33 mmol) and ME (0.13 g, 0.33 mmol) in dry chloroform (5 mL) was stirred at 25 ℃ for 30 min. Then the mixture was concentrated and pentane was added to precipitate the product.

$(ME)_3$·$(BApyRu)_3$: Orange solid, yield 90 % (Method 1: 0.29 g, 0.10 mmol); 88 % (Method 2: 0.28 g, 0.10 mmol).

^{1}H NMR (400 MHz, $CDCl_3$): δ = 14.18 (br., 6 H, NH⋯N), 9.27 (br., 6 H, O⋯HN), 8.88 (d, $^3J_{H,H}$ = 4.9 Hz, 6 H, $CH_{Py}N$), 7.60 (d, $^3J_{H,H}$ = 7.8 Hz, 12 H, $CH_{ar}CC$), 7.37 (d, $^3J_{H,H}$ = 7.8 Hz, 12 H, $CH_{ar}CN$), 7.12 (d, $^3J_{H,H}$ = 4.9 Hz, 6 H, $CH_{Py}C$), 6.90 (br., 6 H, NH_2⋯O), 5.37 (d, $^3J_{H,H}$ = 4.6 Hz, 6 H, CH_{cym}), 5.11 (d, $^3J_{H,H}$ = 4.6 Hz, 6 H, CH_{cym}), 3.40 (s, 6 H, CH_2C_{Py}), 2.90 (m, 3 H, CH), 2.17 (m, 6 H, CH_2C_{BA}), 1.95 (s, 9 H, CH_3C_{cym}), 1.37 [s, 66 H, CH_2, CH_2CH_3 and $C(CH_3)_3$], 1.23 (d, $^3J_{H,H}$ = 6.8 Hz, 18H, CH_3CH), 0.91 (t, $^3J_{H,H}$ = 5.6 Hz, 9 H, CH_3) ppm.

^{13}C NMR (100 MHz, $CDCl_3$): δ = 174.87 (CO), 165.87 (CNH_2), 163.68 (CNH), 155.12 ($CH_{Py}N$), 153.01 (HNCONH), 146.71 ($C_{ar}C$), 146.48 (C_{Py}), 136.13 ($C_{ar}NH$), 125.81 (CH_{Py}), 125.53 ($CH_{ar}CN$), 121.95 ($CH_{ar}CC$), 103.39 ($C_{cym}CH$), 97.14 ($C_{cym}CH_3$), 83.07 (CH_{cym}), 82.18 (CH_{cym}), 57.53 (C_{BA}), 41.06 (CH_2C_{Py}), 41.00 (CH_2C_{BA}), 34.48 [$C(CH_3)_3$], 31.58 [$C(CH_3)_3$], 30.77 (CH), 26.79 (CH_2), 22.61 (CH_2CH_3), 22.35 (CH_3CH), 18.09 (CH_3C_{cym}), 13.75 (CH_3) ppm.

UV/Vis ($CDCl_3$, 1.0 $\times 10^{-5}$ M): λ_{max} (ε) = 272 (1.28 $\times 10^5$), 434 nm (1.79 $\times 10^3$ M^{-1} cm^{-1}).

IR: $\tilde{\nu}$ = 3311 (br., NH), 2960 (br., CH aromatic), 1725 (s, NH), 1698 (s, C=O), 1614 (s, C⋯N), 1566 (s, C=N), 1498 (s, CN), 1410 (s, C⋯C) cm^{-1}.

D ($CDCl_3$): 3.2 $\times 10^{-10}$ m^2 s^{-1}.

$C_{141}H_{183}Cl_6N_{27}O_9Ru_3$ (2916.1): calcd. C 58.08, H 6.33, N 12.97; found C 57.11, H 6.35, N 12.64.

$(ME)_3$·$(BApyRh)_3$: Dark-orange solid, yield 93 % (Method 1: 0.30 g, 0.10 mmol); 90 % (Method 2: 0.29 g, 0.10 mmol).

^{1}H NMR (400 MHz, $CDCl_3$): δ = 14.16 (br., 6 H, NH···N), 9.29 (br., 6 H, O···HN), 8.84 (d, $^3J_{H,H}$ = 4.2 Hz, 6 H, $CH_{Py}N$), 7.61 (d, $^3J_{H,H}$ = 8.4 Hz, 12 H, $CH_{ar}CC$), 7.37 (d, $^3J_{H,H}$ = 8.4 Hz, 12 H, $CH_{ar}CN$), 7.17 (d, $^3J_{H,H}$ = 4.2 Hz, 6 H, $CH_{Py}C$), 6.87 (br., 6 H, NH_2···O), 3.42 (s, 6 H, CH_2C_{Py}), 2.20 (m, 6 H, CH_2C_{BA}), 1.45 (s, 45 H, $C_{Cp*}CH_3$), 1.38 [s, 66 H, CH_2, CH_2CH_3 and $C(CH_3)_3$], 0.91 (t, $^3J_{H,H}$ = 6.4 Hz, 9 H, CH_3) ppm.

^{13}C NMR (100 MHz, $CDCl_3$): δ = 174.96 (CO), 165.91 (CNH_2), 163.71 (CNH), 153.81 ($CH_{Py}N$), 152.94 (HNCONH), 146.73 ($C_{ar}C$), 146.66 (C_{Py}), 136.14 ($C_{ar}NH$), 126.51 (CH_{Py}), 125.56 ($CH_{ar}CN$), 121.92 ($CH_{ar}CC$), 94.23, 94.20 (C_{Cp*}), 57.69 (C_{BA}), 41.59 (CH_2C_{Py}), 40.87 (CH_2C_{BA}), 34.49 [$C(CH_3)_3$], 31.58 [$C(CH_3)_3$], 26.93 (CH_2), 22.63 (CH_2CH_3), 13.74 (CH_3), 8.80 (CH_3C_{Cp*}) ppm.

UV/Vis ($CDCl_3$, 1.0 $\times 10^{-5}$ M): λ_{max} (ε) = 270 (1.37 $\times 10^5$), 408 nm (8.01 $\times 10^3$ M^{-1} cm^{-1}).

IR: $\tilde{\nu}$ = 3315 (br., NH), 2960 (br., CH aromatic), 1726 (s, NH), 1698 (s, C=O), 1612 (s, C⋯N), 1564 (s, C=N), 1494 (s, CN), 1409 (s, C⋯C) cm^{-1}.

D ($CDCl_3$): 3.5 $\times 10^{-10}$ m^2 s^{-1}.

$C_{141}H_{186}Cl_6N_{27}O_9Rh_3$ (2924.6): calcd. C 57.91, H 6.41, N 12.93; found C 57.64, H 6.50, N 12.83.

$(ME)_3$·$(BApyIr)_3$: Yellow solid, yield 88 % (Method 1: 0.31 g, 0.10 mmol).

^{1}H NMR (400 MHz, $CDCl_3$): δ = 14.22 (br., 6 H, NH···N), 9.29 (br., 6 H, O···HN), 8.81 (d, $^3J_{H,H}$ = 5.1 Hz, 6 H, $CH_{Py}N$), 7.61 (d, $^3J_{H,H}$ = 8.1 Hz, 12 H, $CH_{ar}CC$), 7.37 (d, $^3J_{H,H}$ =

8.1 Hz, 12 H, $CH_{ar}CN$), 7.14 (d, $^3J_{H,H}$ = 5.1 Hz, 6 H, $CH_{Py}C$), 6.91 (br., 6 H, $NH_2\cdots O$), 3.44 (s, 6 H, CH_2C_{Py}), 2.20 (m, 6 H, CH_2C_{BA}), 1.42 (s, 45 H, $C_{Cp*}CH_3$), 1.38 [s, 66 H, CH_2, CH_2CH_3 and $C(CH_3)_3$], 0.91 (t, $^3J_{H,H}$ = 5.9 Hz, 9H, CH_3) ppm.

^{13}C NMR (100 MHz, $CDCl_3$): δ = 174.90 (CO), 165.81 (CNH_2), 163.64 (CNH), 153.68 ($CH_{Py}N$), 152.87 (HNCONH), 146.74 ($C_{ar}C$), 146.62 (C_{Py}), 136.11 ($C_{ar}NH$), 126.65 (CH_{Py}), 125.55 ($CH_{ar}CN$), 121.93 ($CH_{ar}CC$), 85.92 (C_{Cp*}), 57.70 (C_{BA}), 41.29 (CH_2C_{Py}), 40.96 (CH_2C_{BA}), 34.49 [$C(CH_3)_3$], 31.58 [$C(CH_3)_3$], 26.88 (CH_2), 22.61 (CH_2CH_3), 13.74 (CH_3), 8.49 (CH_3C_{Cp*}) ppm.

UV/Vis ($CDCl_3$, 1.0×10^{-5} M): λ_{max} (ε) = 273 nm (1.30×10^5 M^{-1} cm^{-1}).

IR: $\tilde{\nu}$ = 3321 (br., NH), 2960 (br., CH aromatic), 1727 (s, NH), 1699 (s, C=O), 1615 (s, C⋯N), 1564 (s, C=N), 1495 (s, CN), 1409 (s, C⋯C) cm^{-1}.

D ($CDCl_3$): 3.2×10^{-10} m^2 s^{-1}.

$C_{141}H_{186}Cl_6N_{27}O_9Ir_3 \cdot 2H_2O$ (3228.6): calcd. C 52.45, H 5.93, N 11.71; found C 51.71, H 5.85, N 11.41.

{(ME)$_3$·[(BApy)Ru(cym)(PPh$_3$)Cl]$_3$}·(3CF$_3$SO$_3$) and {(ME)$_3$·[(BApy)M(Cp*)(PPh$_3$)Cl]$_3$}·(3CF$_3$SO$_3$) (M = Rh, Ir)

A mixture of $[Ru(cym)(PPh_3)Cl_2]$ (45.5 mg, 0.08 mmol) or $[M(Cp^*)(PPh_3)Cl_2]$ (Rh 45.7 mg, Ir 52.9 mg; 0.08 mmol) and $AgSO_3CF_3$ (25.7 mg, 0.10 mmol) in dry chloroform (2 mL) was stirred at 25 ℃ for 2 h and filtered to remove AgCl. In parallel, a mixture of BApy (21.3 mg, 0.08 mmol) and ME (30.2 mg, 0.08 mmol) in dry chloroform (1 mL) was stirred at 25 ℃ for 30 min. The solution containing the $(ME)_3 \cdot (BA)_3$ rosette was added to the solution containing the complex, and the mixture was stirred at 25 ℃ for 16 h. Then the volume was reduced, and pentane was added to precipitate the product.

{(ME)$_3$·[(BApy)Ru(cym)(PPh$_3$)Cl]$_3$}·(3CF$_3$SO$_3$): Orange solid, yield 95 % (99.0 mg, 0.02 mmol).

^{1}H NMR (400 MHz, $CDCl_3$): δ = 8.76 (d, $^3J_{H,H}$ = 5.3 Hz, 6 H, $CH_{Py}N$), 7.52 (d, $^3J_{H,H}$ = 8.0 Hz, 12 H, $CH_{ar}CC$), 7.33 (d, $^3J_{H,H}$ = 8.0 Hz, 12 H, $CH_{ar}CN$), 7.32 (m, 45 H, CH_{Ph}),

6.91 (d, $^{3}J_{H,H}$ = 5.3 Hz, 6 H, $CH_{Py}C$), 6.03 (d, $^{3}J_{H,H}$ = 5.9 Hz, 3 H, CH_{cym}), 5.71 (d, $^{3}J_{H,H}$ = 4.5 Hz, 3 H, CH_{cym}), 5.49 (d, $^{3}J_{H,H}$ = 5.9 Hz, 3 H, CH_{cym}), 5.27 (d, $^{3}J_{H,H}$ = 4.5 Hz, 3 H, CH_{cym}), 3.24 (d, $^{2}J_{H,H}$ = 12.3 Hz, 3 H, CH_2C_{Py}), 3.14 (d, $^{2}J_{H,H}$ = 12.3 Hz, 3 H, CH_2C_{Py}), 2.09 (m, 9 H, CH and CH_2C_{BA}), 1.58 (s, 9 H, CH_3C_{cym}), 1.32 [s, 66 H, CH_2, CH_2CH_3 and $C(CH_3)_3$], 1.03 (d, $^{3}J_{H,H}$ = 5.3 Hz, 9 H, CH_3CH), 0.98 (d, $^{3}J_{H,H}$ = 6.6 Hz, 9 H, CH_3CH), 0.86 (t, $^{3}J_{H,H}$ = 6.6 Hz, 9 H, CH_3) ppm.

^{13}C NMR (100 MHz, $CDCl_3$): δ = 173.70 (CO), 164.16 (CNH_2), 162.51 (CNH), 156.80 ($CH_{Py}N$), 151.16 (HNCONH), 147.35 (C_{Py}), 147.17 ($C_{ar}C$), 135.44 ($C_{ar}NH$), 134.21 ($CH_{Ph\text{-}ortho}$), 131.24 ($CH_{Ph\text{-}para}$), 129.26 (C_{Ph}), 128.72 ($CH_{Ph\text{-}meta}$), 126.63 (CH_{Py}), 125.61 ($CH_{ar}CN$), 121.89 ($CH_{ar}CC$), 113.63 ($C_{cym}CH$), 104.33 ($C_{p\text{-}cym}CH_3$), 93.62 (CH_{cym}), 90.27 (CH_{cym}), 89.45 (CH_{cym}), 84.89 (CH_{cym}), 57.19 (C_{BA}), 41.68 (CH_2C_{Py}), 39.89 (CH_2C_{BA}), 34.47 [$C(CH_3)_3$], 31.52 [$C(CH_3)_3$], 30.82 (CH), 26.89 (CH_2), 22.77 (CH_3CH), 22.61 (CH_2CH_3), 21.30 (CH_3CH), 18.00 (CH_3C_{cym}), 13.73 (CH_3) ppm.

^{31}P NMR (162 MHz, $CDCl_3$, 298 K): δ = 37.38 (s, PPh_3) ppm.

UV/Vis ($CDCl_3$, 1.0 × 10^{-5} M): λ_{max} (ε) = 270 nm (1.39 × 10^{5} M^{-1} cm^{-1}).

IR: $\tilde{\nu}$ = 3315 (br., NH), 2961 (br., CH aromatic), 1729 (s, NH), 1699 (s, C=O), 1615 (s, C⋯N), 1565 (s, C=N), 1506 (s, CN), 1411 (s, C⋯C), 1248 (s, CF_3) cm^{-1}.

D ($CDCl_3$): 3.0 × 10^{-10} m^2 s^{-1}.

$C_{198}H_{228}Cl_3F_9N_{27}O_{18}P_3S_3Ru_3 \cdot CHCl_3 \cdot H_2O$ (4181.2): calcd. C 57.17, H 5.57, N 9.04; found C 56.35, H 5.51, N 8.42.

$\{(ME)_3 \cdot [(BApy)Rh(Cp^*)(PPh_3)Cl]_3\} \cdot (3CF_3SO_3)$ Dark-orange solid, yield 96 % (0.10 g, 0.02 mmol).

^{1}H NMR (400 MHz, $CDCl_3$): δ = 11.59 (br., 3 H, NH⋯N), 10.95 (br., 3 H, NH⋯N), 8.86 (br., 3 H, O⋯HN), 8.69 (d, $^{3}J_{H,H}$ = 5.3 Hz, 6 H, $CH_{Py}N$), 8.38 (br., 3 H, O⋯H-N), 7.50 (d, $^{3}J_{H,H}$ = 8.4 Hz, 12 H, $CH_{ar}CC$), 7.33 (d, $^{3}J_{H,H}$ = 8.4 Hz, 12 H, $CH_{ar}CN$), 7.32 (m, 45 H, CH_{Ph}), 7.08 (d, $^{3}J_{H,H}$ = 5.3 Hz, 6 H, $CH_{Py}C$), 6.91 (br., 6 H, NH_2⋯O), 3.31 (d, $^{2}J_{H,H}$ = 12.3 Hz, 3 H, CH_2C_{Py}), 3.12 (d, $^{2}J_{H,H}$ = 12.3 Hz, 3 H, CH_2C_{Py}), 2.11 (m, 6 H, CH_2C_{BA}), 1.52 (d, $^{2}J_{H,H}$ = 17.8 Hz, 6 H, CH_2), 1.33 (s, 45 H, $CH_3C_{Cp^*}$), 1.28 [d, $^{2}J_{H,H}$ = 12.3 Hz, 60 H, CH_2CH_3 and $C(CH_3)_3$], 0.85 (t, $^{3}J_{H,H}$ = 7.0 Hz, 9 H, CH_3) ppm.

^{13}C NMR (100 MHz, $CDCl_3$): δ = 173.49 (CO), 163.41 (CNH_2), 161.97 (CNH), 156.07 ($CH_{Py}N$), 150.48 (HNCONH), 147.69 (C_{Py}), 147.51 ($C_{ar}C$), 135.07 ($C_{ar}NH$), 134.05 ($CH_{Ph\text{-}ortho}$), 131.84 ($CH_{Ph\text{-}para}$), 128.90 (C_{Ph}), 128.73 ($CH_{Ph\text{-}meta}$), 127.77 (CH_{Py}), 125.75 ($CH_{ar}CN$), 121.83 ($CH_{ar}CC$), 101.45 (C_{Cp*}), 57.40 (C_{BA}), 42.83 (CH_2C_{Py}), 39.04 (CH_2C_{BA}), 34.52 [$C(CH_3)_3$], 31.52 [$C(CH_3)_3$], 27.13 (CH_2), 22.69 (CH_2CH_3), 13.78 (CH_3), 8.81 (CH_3C_{Cp*}) ppm.

^{31}P NMR (162 MHz, $CDCl_3$, 298 K): δ = 33.58 (d, $^1J_{P\text{-}Rh}$ = 141.7 Hz, PPh_3) ppm.

UV/Vis ($CDCl_3$, 1.0 × 10^{-5} M): λ_{max} (ε) = 268 (1.37 × 10^5), 371 nm (1.60 × 10^4 M^{-1} cm^{-1}).

IR: ṽ = 3316 (br., NH), 2961 (br., CH aromatic), 1729 (s, NH), 1704 (s, C=O), 1614 (s, C⋯N), 1567 (s, C=N), 1503 (s, CN), 1411 (s, C⋯C), 1245 (s, CF_3) cm^{-1}.

D ($CDCl_3$): 3.9 × 10^{-10} m^2 s^{-1}.

$C_{198}H_{231}Cl_3F_9N_{27}O_{18}P_3S_3Rh_3 \cdot 2CHCl_3$ (4291.1): calcd. C 55.98, H 5.47, N 8.81; found C 55.47, H 5.49, N 8.12.

{(ME)$_3$·[(BApy)Ir(Cp*)(PPh$_3$)Cl]$_3$}·(3CF$_3$SO$_3$): Yellow solid, yield 94 % (0.10 g, 0.02 mmol).

^{1}H NMR (400 MHz, $CDCl_3$): δ = 10.50 (br., 6 H, NH⋯N), 8.77 (br., 6 H, O⋯HN), 8.50 (d, $^3J_{H,H}$ = 5.3 Hz, 6 H, $CH_{Py}N$), 7.47 (d, $^3J_{H,H}$ = 8.4 Hz, 12 H, $CH_{ar}CC$), 7.34 (d, $^3J_{H,H}$ = 8.4 Hz, 12 H, $CH_{ar}CN$), 7.30 (m, 45 H, CH_{Ph}), 7.00 (d, $^3J_{H,H}$ = 5.3 Hz, 6 H, $CH_{Py}C$), 6.54 (br., 6 H, NH_2⋯O), 3.31 (d, $^2J_{H,H}$ = 12.3 Hz, 3 H, CH_2C_{Py}), 3.08 (d, $^2J_{H,H}$ = 12.3 Hz, 3 H, CH_2C_{Py}), 2.16 (m, 3 H, CH_2C_{BA}), 2.05 (m, 3 H, CH_2C_{BA}), 1.36 (s, 6 H, CH_2), 1.33 [s, 60 H, CH_2CH_3 and $C(CH_3)_3$], 1.28 (s, 45 H, CH_3C_{Cp*}), 0.86 (t, $^3J_{H,H}$ = 7.0 Hz, 9 H, CH_3) ppm.

^{13}C NMR (100 MHz, $CDCl_3$): δ = 173.00 (CO), 159.87 (CNH_2), 158.97 (CNH), 153.17 ($CH_{Py}N$), 150.02 (HNCONH), 148.27 (C_{Py}), 147.88 ($C_{ar}C$), 134.93 ($C_{ar}NH$), 133.70 ($CH_{Ph\text{-}ortho}$), 132.70 ($CH_{Ph\text{-}para}$), 129.39 (C_{Ph}), 128.58 (CH_{Py}), 127.98 ($CH_{Ph\text{-}meta}$), 125.78 ($CH_{ar}CN$), 122.22 ($CH_{ar}CC$), 94.94 (C_{Cp*}), 57.42 (C_{BA}), 42.61 (CH_2C_{Py}), 39.11 (CH_2C_{BA}), 34.57 [$C(CH_3)_3$], 31.47 [$C(CH_3)_3$], 27.08 (CH_2), 22.66 (CH_2CH_3), 13.75 (CH_3), 8.22 (CH_3C_{Cp*}) ppm.

^{31}P NMR (162 MHz, $CDCl_3$, 298 K): δ = 8.80 (s, PPh_3) ppm.

UV/Vis ($CDCl_3$, 1.0 × 10^{-5} M): λ_{max} (ε) = 270 nm (1.16 × 10^5 M^{-1} cm^{-1}).

IR: $\tilde{\nu}$ = 3321 (br., NH), 2961 (br., CH aromatic), 1729 (s, NH), 1699 (s, C=O), 1617 (s, C⋯N), 1568 (s, C=N), 1505 (s, CN), 1412 (s, C⋯C), 1245 (s, CF_3) cm^{-1}.

D ($CDCl_3$): 3.8 × 10^{-10} m^2 s^{-1}.

$C_{198}H_{231}Cl_3$ $F_9N_{27}O_{18}P_3S_3Ir_3 \cdot 2CHCl_3 \cdot H_2O$ (4577.0): calcd. C 52.48, H 5.18, N 8.26; found C 51.68, H 5.17, N 7.80.

6.2.2 Neutral hexanuclear metalla-assemblies

MEpyRu and MEpyRh

A mixture of MEpy (91.3 mg, 0.26 mmol) and $[Ru(cym)Cl_2]_2$ (80.0 mg, 0.13 mmol) or $[Rh(Cp^*)Cl_2]_2$ (80.7 mg, 0.13 mmol) in dry tetrahydrofuran (7 mL) was stirred at 25 ℃ for 16 h. Then the solvent was evaporated, the residue was solubilized in chloroform (2 mL), and pentane was added to precipitate the product.

MEpyRu: Orange solid, yield 89 % (0.15 g, 0.23 mmol).

^{1}H NMR (400 MHz, $CDCl_3$): δ = 8.77 (br., 2 H, $CH_{Py}N$), 7.40 (br., 2 H, $CH_{ar}CC$), 7.22 (br., 2 H, $CH_{ar}CN$), 7.13 (br., 2 H, $CH_{Py}C$), 5.38 (br., 2 H, CH_{cym}), 5.15 (br., 2 H, CH_{cym}), 4.45 (br., 2 H, CH_2), 2.89 (br., 1 H, CH), 1.90 (br., 3 H, CH_3C_{cym}), 1.26 [s, 9 H, $C(CH_3)_3$], 1.22 [m, 6 H, $(CH_3)_2CH$] ppm.

^{13}C NMR (100 MHz, $CDCl_3$): δ = 165.73 (*C*$NHCH_2$), 165.53 (CNH_2), 163.74 (*C*NHC), 154.40 ($CH_{Py}N$), 151.63 (C_{Py}), 146.13 ($C_{ar}C$), 136.07 ($C_{ar}NH$), 125.62 (*C*$H_{ar}CN$), 123.32 (*C*$H_{Py}C$), 120.54 (*C*$H_{ar}CC$), 103.33 ($C_{cym}CH$), 97.24 ($C_{cym}CH_3$), 83.04 (CH_{cym}), 82.10 (CH_{cym}), 43.07 (CH_2), 34.39 [*C*$(CH_3)_3$], 31.57 [$C(CH_3)_3$], 30.75 (CH), 22.41 [$(CH_3)_2CH$], 18.24 (CH_3C_{cym}) ppm.

UV/Vis ($CHCl_3$, 5.0 × 10^{-5} M): λ_{max} (ε) = 267 (2.49 × 10^4), 422 nm (7.48 × 10^2 M^{-1} cm^{-1}).

IR: $\tilde{\nu}$ = 3311 (br., NH), 2960 (br., CH aromatic), 1590 (s, C⋯N), 1567 (s, C=N), 1497 (s, CN), 1412 (s, C⋯C) cm^{-1}.

D ($CDCl_3$): 5.0 × 10^{-10} m^2 s^{-1}.

$C_{29}H_{37}Cl_2N_7Ru \cdot H_2O$ (673.7): calcd. C 51.71, H 5.84, N 14.55; found C 51.20, H 5.72, N 14.12.

ESI-MS: *m/z* = 620.1 $[M - Cl]^+$.

MEpyRh: Dark orange solid, yield 94 % (0.16 g, 0.25 mmol).

^{1}H NMR (400 MHz, $CDCl_3$): δ = 8.73 (br., 2 H, $CH_{Py}N$), 8.51 (br., 1 H, NHC_{ar}), 7.42 (br., 2 H, $CH_{ar}CC$), 7.21 (br., 4 H, $CH_{ar}CN$ and $CH_{Py}C$), 6.25 (br., 1 H, $NHCH_2$), 5.46 (br., 2 H, NH_2), 4.47 (br., 2 H, CH_2), 1.47 (s, 15 H, CH_3C_{Cp*}), 1.27 (s, 9 H, CH_3) ppm. ^{13}C NMR (100 MHz, $CDCl_3$): δ = 166.97 (*C*$NHCH_2$), 166.22 (CNH_2), 164.41 (*C*NHC), 152.90 ($CH_{Py}N$), 152.17 (C_{Py}), 145.98 ($C_{ar}C$), 136.31 ($C_{ar}NH$), 125.59 (*C*$H_{ar}CN$), 123.97 (*C*$H_{Py}C$), 120.33 (*C*$H_{ar}CC$), 94.13 (C_{Cp*}), 43.27 (CH_2), 34.36 [*C*$(CH_3)_3$], 31.55 [C(*C*$H_3)_3$], 8.92 (*C*H_3C_{Cp*}) ppm.

UV/Vis ($CHCl_3$, 5.0 × 10^{-5} M): λ_{max} (ε) = 265 (2.95 × 10^4), 407 nm (2.78 × 10^3 M^{-1} cm^{-1}).

IR: $\tilde{\nu}$ = 3310 (br., NH), 2961 (br, CH aromatic), 1597 (s, C⋯N), 1568 (s, C=N), 1504 (s, CN), 1414 (s, C⋯C) cm^{-1}.

D ($CDCl_3$): 7.2 × 10^{-10} m^2 s^{-1}.

$C_{29}H_{38}Cl_2N_7Rh \cdot 2H_2O$ (694.5): calcd. C 50.15, H 6.10, N 14.12; found C 49.76, H 5.88, N 13.31.

ESI-MS: *m/z* = 622.1 $[M - Cl]^+$.

$(MEpy)_3 \cdot (BApy)_3$

A mixture of (BApy) (39.4 mg, 0.14 mmol) and (MEpy) (50.0 mg, 0.14 mmol) in dry chloroform (1 mL) was stirred at 25 ℃ for 30 min. Then pentane was added to precipitate the product.

$(MEpy)_3 \cdot (BApy)_3$: White solid, yield 89 % (79.6 mg, 0.04 mmol).

^{1}H NMR (400 MHz, $CDCl_3$): δ = 13.59 (br., 6 H, NH···N), 9.19 (br., 3 H, O···H-N), 8.61 (d, $^{3}J_{H,H}$ = 3.3 Hz, 6 H, $CH_{Py\ ME}N$), 8.46 (d, $^{3}J_{H,H}$ = 3.1 Hz, 6 H, $CH_{Py\ BA}N$), 8.03 (br., 3 H, O···H-N), 7.48 (d, $^{3}J_{H,H}$ = 7.7 Hz, 6 H, $CH_{ar}CC$), 7.29 (d, $^{3}J_{H,H}$ = 3.3 Hz, 6 H, $CH_{Py\ ME}C$), 7.26 (d, $^{3}J_{H,H}$ = 7.7 Hz, 6 H, $CH_{ar}CN$), 7.00 (d, $^{3}J_{H,H}$ = 3.1 Hz, 6 H, $CH_{Py\ BA}C$), 6.74 (br., 6 H, NH_2···O), 4.69 (s, 6 H, $CH_{2\ ME}$), 3.28 (s, 6 H, $CH_{2\ BA}$), 2.14 (s, 6 H, CH_2C_{BA}), 1.33 [s, 27 H, $C(CH_3)_3$], 1.30 (m, 12 H, CH_2 and CH_2CH_3), 0.90 (t, $^{3}J_{H,H}$ = 6.4 Hz, 9 H, CH_3) ppm.

^{13}C NMR (100 MHz, $CDCl_3$): δ = 174.67 (CO), 166.00 (CNHCH$_2$), 165.67 (CNH_2), 163.58 (CNHC), 152.28 (HNCONH), 150.34 ($CH_{Py\ BA}N$), 149.91 ($CH_{Py\ ME}N$), 148.98 ($C_{Py\ ME}$), 146.21 ($C_{ar}C$), 144.02 ($C_{Py\ BA}$), 136.55 ($C_{ar}NH$), 125.54 ($CH_{ar}CN$), 124.74 ($CH_{Py\ BA}C$), 122.35 ($CH_{Py\ ME}C$), 120.75 ($CH_{ar}CC$), 57.73 (C_{BA}), 43.97 ($CH_{2\ ME}$), 42.87 ($CH_{2\ BA}$), 40.04 (CH_2C_{BA}), 34.46 [$C(CH_3)_3$], 31.60 [$C(CH_3)_3$], 27.12 (CH_2), 22.73 (CH_2CH_3), 13.80 (CH_3) ppm.

UV/Vis ($CHCl_3$, 1.0 × 10^{-5} M): λ_{max} (ε) = 265 nm (8.00 × 10^{4} M^{-1} cm^{-1}).

IR: $\tilde{\nu}$ = 3344 (br., NH), 2961 (br., CH aromatic), 1720 (s, NH), 1685 (s, C=O), 1602 (s, C⋯N), 1571 (s, C=N), 1520 (s, CN), 1411 (s, C⋯C) cm^{-1}.

D ($CDCl_3$): 4.0 × 10^{-10} m^2 s^{-1}.

$C_{99}H_{120}N_{30}O_9 \cdot H_2O$ (1892.3): calcd. C 62.84, H 6.50, N 22.21; found C 62.18, H 6.36, N 21.24.

$(MEpy)_3 \cdot (BApyRu)_3$ and $(MEpy)_3 \cdot (BApyRh)_3$

A mixture of BApyRu (50.0 mg, 0.09 mmol) or BApyRh (50.3 mg; 0.09 mmol) and MEpy (30.1 mg, 0.09 mmol) in dry chloroform (1 mL) was stirred at 25 ℃ for 30 min. Then pentane was added to precipitate the product.

$(MEpy)_3 \cdot (BApyRu)_3$: Yellow solid, yield 89 % (71.3 mg, 0.03 mmol).

^{1}H NMR (400 MHz, $CDCl_3$): δ = 14.26 (br., 6 H, NH···N), 9.26 (br., 3 H, O···H-N), 9.07 (br., 3 H, $CH_{Py\ ME}N$), 8.92 (br., 3 H, $CH_{Py\ BA}N$), 8.60 (br., 3 H, $CH_{Py\ ME}$'N), 8.47 (br., 3 H, $CH_{Py\ BA}$'N), 8.10 (br., 3 H, O···H'-N), 7.48 (m, 6 H, $CH_{ar}CC$), 7.34 (m, 6 H, $CH_{ar}CN$), 7.29 (br., 6 H, $CH_{Py\ ME}C$), 7.03 (br., 6 H, $CH_{Py\ BA}C$), 6.84 (br., 3 H, NH_2···O),

6.02 (br., 3 H, NH_2'···O), 5.52 (br., 6 H, CH_{cym}), 5.30 (br., 6 H, CH_{cym}), 4.68 (br., 6 H, $CH_{2\ ME}$), 3.30 (br., 6 H, $CH_{2\ BA}$), 2.97 (m, 3 H, CH), 2.15 (br., 3 H, CH_2C_{BA}), 2.10 (br., 3 H, CH_2'C_{BA}), 1.95 (m, 9 H, CH_3C_{cym}), 1.36 [br., 27 H, $C(CH_3)_3$], 1.32 (m, 12 H, CH_2 and CH_2CH_3), 1.28 [m, 18 H, $(CH_3)_2CH$], 0.89 (t, $^3J_{H,H}$ = 6.6 Hz, 9 H, CH_3) ppm.

^{13}C NMR (100 MHz, $CDCl_3$): δ = 174.81 (CO), 165.84 (CNHCH$_2$), 165.54 (CNH_2), 165.41(CNH_2'), 163.43 (CNHC), 155.27 ($CH_{Py\ BA}N$), 154.91 ($CH_{Py\ ME}N$), 152.63 (HNCONH), 151.53 (HNC'ONH), 150.36 ($CH_{Py\ BA}$'N), 149.93 ($CH_{Py\ ME}$'N), 148.88 ($C_{Py\ ME}$), 146.55 (C_{ar}C), 146.23 (C_{ar}'C), 143.96 ($C_{Py\ BA}$), 136.65 (C_{ar}NH), 136.44 (C_{ar}'NH), 125.92 (CH$_{Py\ BA}$C), 125.53 (CH$_{ar}$CN), 124.71 (CH$_{Py\ BA}$'C), 122.73 (CH$_{Py\ ME}$C), 122.35 (CH$_{Py\ ME}$'C), 120.77 (CH$_{ar}$CC), 120.63 (CH$_{ar}$'CC), 103.33 (C_{cym}CH), 97.36 ($C_{cym}CH_3$), 83.35 (CH_{cym}), 81.93 (CH_{cym}), 57.68 (C_{BA}), 57.40 (C_{BA}'), 43.97 ($CH_{2\ ME}$), 43.37 ($CH_{2\ ME}$'), 43.35 ($CH_{2\ BA}$), 42.76 ($CH_{2\ BA}$'), 39.99 (CH$_2C_{BA}$), 34.50 [$C(CH_3)_3$], 34.44 [C'$(CH_3)_3$], 31.67 [$(CH_3)_3$], 31.58 [C(C'$H_3)_3$], 30.84 (CH), 27.07 (CH_2), 26.69 (CH_2'), 22.68 (CH$_2$CH$_3$), 22.50 [$(CH_3)_2$CH], 18.40 (CH$_3C_{cym}$), 18.19 (CH$_3$'C_{cym}), 13.79 (CH_3) ppm.

UV/Vis ($CHCl_3$, 1.0 × 10^{-5} M): λ_{max} (ε) = 267 (8.55 × 10^4), 413 nm (2.67 × 10^3 M^{-1} cm^{-1}).

IR: $\tilde{\nu}$ = 3326 (br., NH), 2961 (br., CH aromatic), 1725 (s, NH), 1698 (s, C=O), 1601 (s, C⋯N), 1570 (s, C=N), 1512 (s, CN), 1413 (s, C⋯C).

D ($CDCl_3$): 3.9 × 10^{-10} m^2 s^{-1}.

$C_{129}H_{162}Cl_6N_{30}O_9Ru_3 \cdot 3H_2O$ (2846.9): calcd. C 54.43, H 5.95, N 14.76; found C 53.47, H 5.82, N 13.89.

$(MEpy)_3$·$(BApyRh)_3$: Orange solid, yield 89 % (71.5 mg, 0.03 mmol).

^{1}H NMR (400 MHz, $CDCl_3$): δ = 14.17 (br., 6 H, NH···N), 9.20 (br., 3 H, O···H-N), 8.96 (br., 3 H, $CH_{Py\ ME}N$), 8.83 (br., 3 H, $CH_{Py\ BA}N$), 8.61 (br., 3 H, $CH_{Py\ ME}$'N), 8.46 (br., 3 H, $CH_{Py\ BA}$'N), 8.06 (br., 3 H, O···H'-N), 7.46 (br., 6 H, $CH_{ar}CC$), 7.32 (br., 6 H, $CH_{Py\ ME}C$), 7.29 (br., 6 H, $CH_{ar}CN$), 7.08 (br., 3 H, $CH_{Py\ BA}C$), 7.01 (br., 3 H, $CH_{Py\ BA}$'C), 6.83 (br., 3 H, NH_2···O), 4.69 (br., 6 H, $CH_{2\ ME}$), 3.29 (br., 6 H, $CH_{2\ BA}$), 2.13 (br., 6 H, CH_2C_{BA}), 1.53 (m, 45 H, CH_3C_{Cp*}), 1.33 [br., 27 H, $C(CH_3)_3$], 1.30 (m, 12 H, CH_2 and CH_2CH_3), 0.89 (t, $^3J_{H,H}$ = 6.4 Hz, 9 H, CH_3) ppm.

^{13}C NMR (100 MHz, $CDCl_3$): δ = 175.01 (CO), 165.53 (*C*NHCH$_2$), 165.28 (CNH$_2$), 163.26 (*C*NHC), 153.73 (CH$_{Py\ BA}$N), 153.33 (CH$_{Py\ ME}$N), 152.90 (HNCONH), 151.55 (HNC'ONH), 150.27 (CH$_{Py\ BA}$'N), 149.56 (CH$_{Py\ ME}$'N), 149.25 (C$_{Py\ ME}$), 146.80 (*C*$_{ar}$C), 146.31 (*C*$_{ar}$'C), 144.03 (C$_{Py\ BA}$), 136.47 (C$_{ar}$NH), 136.30 (C$_{ar}$'NH), 126.56 (*C*H$_{Py\ BA}$C), 125.51 (*C*H$_{ar}$CN), 124.70 (*C*H$_{Py\ BA}$'C), 123.73 (*C*H$_{Py\ ME}$C), 122.44 (*C*H$_{Py\ ME}$'C), 120.80 (*C*H$_{ar}$CC), 120.66 (*C*H$_{ar}$'CC), 94.16 (C$_{Cp*}$), 57.62 (C$_{BA}$), 57.45 (C$_{BA}$'), 43.97 (CH$_{2\ ME}$), 43.61 (CH$_{2\ ME}$'), 42.72 (CH$_{2\ BA}$), 41.06 (CH$_{2\ BA}$'), 39.95 (*C*H$_2$C$_{BA}$), 34.44 [*C*(CH$_3$)$_3$], 31.57 [C(*C*H$_3$)$_3$], 27.04 (CH$_2$), 26.82 (CH$_2$'), 22.61 (*C*H$_2$CH$_3$), 13.78 (CH$_3$), 8.99 (*C*H$_3$C$_{Cp*}$), 8.90 (*C*H$_3$'C$_{Cp*}$) ppm.

UV/Vis ($CHCl_3$, 1.0 × 10^{-5} M): λ_{max} (ε) = 265 (1.02 × 10^5), 402 nm (8.59 × 10^3 M^{-1} cm^{-1}).

IR: $\tilde{\nu}$ = 3327 (br., NH), 2960 (br., CH aromatic), 1726 (s, NH), 1698 (s, C=O), 1601 (s, C⋯N), 1570 (s, C=N), 1512 (s, CN), 1413 (s, C⋯C) cm^{-1}.

D ($CDCl_3$): 3.9 × 10^{-10} m^2 s^{-1}.

$C_{129}H_{165}Cl_6N_{30}O_9Rh_3 \cdot 3H_2O$ (2855.4): calcd. C 54.26, H 6.04, N 14.72; found C 53.42, H 6.07, N 14.46.

(MEpyRu)$_3$·(BApy)$_3$ and (MEpyRh)$_3$·(BApy)$_3$

A mixture of BApy (30.0 mg, 0.11 mmol) and MEpyRu (71.4 mg, 0.11 mmol) or MEpyRh (71.8 mg, 0.11 mmol) in dry chloroform (1 mL) was stirred at 25 ℃ for 30 min. Then pentane was added to precipitate the product.

(MEpyRu)$_3$·(BApy)$_3$: Yellow solid, yield 88 % (89.3 mg, 0.03 mmol).

^{1}H NMR (400 MHz, $CDCl_3$): δ = 14.18 (br., 6 H, NH⋯N), 9.20 (br., 3 H, O⋯H-N), 9.07 (br., 3 H, CH$_{Py\ ME}$N), 8.92 (br., 3 H, CH$_{Py\ BA}$N), 8.60 (br., 3 H, CH$_{Py\ ME}$'N), 8.45 (br., 3 H, CH$_{Py\ BA}$'N), 8.10 (br., 3 H, O⋯H'-N), 7.47 (m, 6 H, CH$_{ar}$CC), 7.33 (m, 6 H, CH$_{ar}$CN), 7.28 (br., 6 H, CH$_{Py\ ME}$C), 7.02 (br., 6 H, CH$_{Py\ BA}$C), 6.85 (br., 3 H, NH$_2$⋯O), 6.03 (br., 3 H, NH$_2$'⋯O), 5.50 (br., 6 H, CH$_{cym}$), 5.30 (br., 6 H, CH$_{cym}$), 4.68 (br., 6 H, CH$_{2\ ME}$), 3.30 (br., 6 H, CH$_{2\ BA}$), 2.96 (m, 3 H, CH), 2.11 (br., 6 H, CH$_2$C$_{BA}$), 1.96 (m, 9

H, CH_3C_{cym}), 1.35 [br., 27 H, $C(CH_3)_3$], 1.32 (m, 12 H, CH_2 and CH_2CH_3), 1.28 [m, 18 H, $(CH_3)_2CH$], 0.88 (t, $^3J_{H,H}$ = 6.4 Hz, 9 H, CH_3) ppm.

^{13}C NMR (100 MHz, $CDCl_3$): δ = 174.83 (CO), 165.73 (*C*NHCH$_2$), 165.43 (CNH_2), 165.33 (C'NH_2), 163.34 (*C*NHC), 155.23 ($CH_{Py\ BA}N$), 154.87 ($CH_{Py\ ME}N$), 152.69 (HNCONH), 151.51 (HNC'ONH), 150.24 ($CH_{Py\ BA}$'N), 149.76 ($CH_{Py\ ME}$'N), 149.02 ($C_{Py\ ME}$), 146.56 ($C_{ar}C$), 146.23 (C_{ar}'C), 144.05 ($C_{Py\ BA}$), 136.59 ($C_{ar}NH$), 136.39 (C_{ar}'NH), 125.92 ($CH_{Py\ BA}C$), 125.51 ($CH_{ar}CN$), 124.73 ($CH_{Py\ BA}$'C), 122.76 ($CH_{Py\ ME}C$), 122.37 ($CH_{Py\ ME}$'C), 120.76 ($CH_{ar}CC$), 120.61 (CH_{ar}'CC), 103.30 ($C_{cym}CH$), 102.98 (C_{cym}'CH), 97.60 ($C_{cym}CH_3$), 97.36 (C_{cym}'CH_3), 83.33 (CH_{cym}), 81.93 (CH_{cym}), 57.63 (C_{BA}), 57.36 (C_{BA}'), 43.94 ($CH_{2\ ME}$), 43.35 ($CH_{2\ ME}$'), 43.34 ($CH_{2\ BA}$), 43.71 ($CH_{2\ BA}$'), 39.97 (CH_2C_{BA}), 34.47 [$C(CH_3)_3$], 34.42 [$C'(CH_3)_3$], 31.64 [$C(CH_3)_3$], 31.55 [$C(CH_3')_3$], 30.81 (CH), 27.03 (CH_2), 26.67 (CH_2'), 22.65 (CH_2CH_3), 22.57 ($CH_2'CH_3$), 22.47 [$(CH_3)_2CH$], 18.38 (CH_3C_{cym}), 18.18 ($CH_3'C_{cym}$), 13.78 (CH_3) ppm.

UV/Vis ($CHCl_3$, 1.0 × 10^{-5} M): λ_{max} (ε) = 267 (9.14 × 10^4), 407 nm (2.55 × 10^3 M^{-1} cm^{-1}).

IR: $\tilde{\nu}$ = 3324 (br., NH), 2960 (br., CH aromatic), 1725 (s, NH), 1698 (s, C=O), 1614 (s, C···N), 1570 (s, C=N), 1512 (s, CN), 1414 (s, C···C) cm^{-1}.

D ($CDCl_3$): 3.0 × 10^{-10} m^2 s^{-1}.

$C_{129}H_{162}Cl_6N_{30}O_9Ru_3 \cdot CHCl_3 \cdot H_2O$ (2930.2): calcd. C 53.29, H 5.68, N 14.34; found C 52.46, H 5.83, N 13.85.

(MEpyRh)$_3$·(BApy)$_3$: orange solid, yield 88 % (89.5 mg, 0.03 mmol).

^{1}H NMR (400 MHz, $CDCl_3$): δ = 14.15 (br., 6 H, NH···N), 9.21 (br., 3 H, O···H-N), 8.96 (br., 3 H, $CH_{Py\ ME}N$), 8.83 (br., 3 H, $CH_{Py\ BA}N$), 8.61 (br., 3 H, $CH_{Py\ ME}$'N), 8.46 (br., 3 H, $CH_{Py\ BA}$'N), 8.06 (br., 3 H, O···H'-N), 7.47 (br., 6 H, $CH_{ar}CC$), 7.35 (br., 6 H, $CH_{Py\ ME}C$), 7.31 (br., 6 H, $CH_{ar}CN$), 7.08 (br., 3 H, $CH_{Py\ BA}C$), 7.02 (br., 3 H, $CH_{Py\ BA}$'C), 6.85 (br., 6 H, NH_2···O), 4.69 (br., 6 H, $CH_{2\ ME}$), 3.29 (br., 6 H, $CH_{2\ BA}$), 2.13 (br., 6 H, CH_2C_{BA}), 1.53 (m, 45 H, CH_3C_{Cp*}), 1.34 [br., 27 H, $C(CH_3)_3$], 1.30 (m, 12 H, CH_2 and CH_2CH_3), 0.89 (t, $^3J_{H,H}$ = 6.4 Hz, 9 H, CH_3) ppm.

^{13}C NMR (100 MHz, $CDCl_3$): δ = 174.87 (CO), 165.69 (*C*NHCH$_2$), 165.39 (CNH_2), 163.32 (*C*NHC), 153.73 ($CH_{Py\ BA}N$), 153.35 ($CH_{Py\ ME}N$), 151.55 (HNCONH), 150.26

($CH_{Py\ BA}$'N), 149.72 ($CH_{Py\ ME}$'N), 149.05 ($C_{Py\ ME}$), 146.82 (C_{ar}C), 146.25 (C_{ar}'C), 144.05 ($C_{Py\ BA}$), 136.54 (C_{ar}NH), 136.37 (C_{ar}'NH), 126.55 ($CH_{Py\ BA}$C), 125.51 (CH_{ar}CN), 124.70 ($CH_{Py\ BA}$'C), 123.72 ($CH_{Py\ ME}$C), 122.38 ($CH_{Py\ ME}$'C), 120.77 (CH_{ar}CC), 120.63 (CH_{ar}'CC), 94.18 (C_{Cp*}), 57.63 (C_{BA}), 57.47 (C_{BA}'), 43.95 ($CH_{2\ ME}$), 43.62 ($CH_{2\ ME}$'), 42.72 ($CH_{2\ BA}$), 41.07 ($CH_{2\ BA}$'), 39.96 (CH_2C_{BA}), 34.43 [$C(CH_3)_3$], 31.58 [$C(CH_3)_3$], 27.03 (CH_2), 26.81 (CH_2'), 22.60 (CH_2CH_3), 13.78 (CH_3), 9.01 (CH_3C_{Cp*}), 8.90 (CH_3'C_{Cp*}) ppm.

UV/Vis ($CHCl_3$, 1.0×10^{-5} M): λ_{max} (ε) = 265 (9.65×10^4), 403 nm (8.61×10^3 M^{-1} cm^{-1}).

IR: $\tilde{\nu}$ = 3329 (br., NH), 2960 (br., CH aromatic), 1726 (s, NH), 1698 (s, C=O), 1602 (s, C⋯N), 1570 (s, C=N), 1513 (s, CN), 1414 (s, C⋯C) cm^{-1}.

D ($CDCl_3$): 3.7×10^{-10} m^2 s^{-1}.

$C_{129}H_{165}Cl_6N_{30}O_9Rh_3 \cdot CHCl_3 \cdot H_2O$ (2938.7): calcd. C 53.13, H 5.76, N 14.30; found C 52.31, H 5.90, N 13.62.

$(MEpyRu)_3 \cdot (BApyRu)_3$

Method 1: A mixture of BApy (39.4 mg, 0.14 mmol) and MEpy (50.0 mg, 0.14 mmol) in dry chloroform (1.5 mL) was stirred at 25 ℃. After 30 min, $[Ru(cym)Cl_2]_2$ (87.6 mg, 0.14 mmol) was added, and the mixture was stirred at 25 ℃ for 16 h. Then the mixture was concentrated, and pentane was added to precipitate the product.

Method 2: A mixture of (BApyRu) (44.4 mg, 0.08 mmol) and (MEpyRu) (50.0 mg, 0.08 mmol) in dry chloroform (2 mL) was stirred at 25 ℃ for 30 min. Then pentane was added to precipitate the product.

$(MEpyRu)_3 \cdot (BApyRu)_3$: orange solid, yield 83 % (Method 1: 0.15 g, 0.04 mmol); 83 % (Method 2: 78.3 mg, 0.02 mmol).

^{1}H NMR (400 MHz, $CDCl_3$): δ = 14.23 (br., 6 H, NH⋯N), 9.21 (br., 3 H, O⋯H-N), 9.07 (br., 6 H, $CH_{Py\ ME}$N), 8.92 (br., 6 H, $CH_{Py\ BA}$N), 8.09 (br., 3 H, O⋯H'-N), 7.47 (d, $^3J_{H,H}$ = 7.5 Hz, 6 H, CH_{ar}CC), 7.31 (d, $^3J_{H,H}$ = 7.5 Hz, 6 H, CH_{ar}CN), 7.27 (br., 6 H, $CH_{Py\ ME}$C), 7.01 (br., 6 H, $CH_{Py\ BA}$C), 6.89 (br., 6 H, NH_2⋯O), 5.52 (br., 12 H, CH_{cym}), 5.31

(br., 12 H, CH_{cym}), 4.56 (br., 6 H, $CH_{2\ ME}$), 3.32 (br., 6 H, $CH_{2\ BA}$), 2.95 (m, 6 H, CH), 2.09 (br., 6 H, CH_2C_{BA}), 1.99 (br., 9 H, CH_3C_{cym}), 1.88 (br., 9 H, CH_3'C_{cym}), 1.35 [br., 27 H, $C(CH_3)_3$], 1.32 (m, 12 H, CH_2 and CH_2CH_3), 1.26 [m, 36 H, $(CH_3)_2CH$], 0.88 (t, $^3J_{H,H}$ = 6.4 Hz, 9 H, CH_3) ppm.

^{13}C NMR (100 MHz, $CDCl_3$): δ = 175.02 (CO), 165.47 (CNHCH$_2$), 165.15 (CNH_2), 163.18 (CNHC), 155.25 ($CH_{Py\ BA}N$), 154.86 ($CH_{Py\ ME}N$), 153.06 (HNCONH), 151.45 ($C_{Py\ ME}$), 146.47 ($C_{Py\ BA}$), 146.24 ($C_{ar}C$), 136.43 ($C_{ar}NH$), 125.87 ($CH_{Py\ BA}C$), 125.50 ($CH_{ar}CN$), 122.68 ($CH_{Py\ ME}C$), 120.60 ($CH_{ar}CC$), 103.20 ($C_{cym}CH$), 102.72 (C_{cym}'CH), 97.67 ($C_{cym}CH_3$), 97.39 (C_{cym}'CH_3), 83.66 (CH_{cym}), 81.85 (CH_{cym}), 57.37 (C_{BA}), 43.27 ($CH_{2\ ME}$), 41.35 (CH_2C_{BA}), 40.36 ($CH_{2\ BA}$), 34.44 [$C(CH_3)_3$], 31.59 [$C(CH_3)_3$], 30.78 (CH), 26.62 (CH_2), 22.46 (CH_2CH_3), 22.46 [$(CH_3)_2CH$], 18.37 (CH_3C_{cym}), 18.11 (CH_3'C_{cym}), 13.73 (CH_3) ppm.

UV/Vis ($CHCl_3$, 1.0 × 10^{-5} M): λ_{max} (ε) = 266 (9.68 × 10^4), 419 nm (4.31 × 10^3 M^{-1} cm^{-1}).

IR: $\tilde{\nu}$ = 3325 (br., NH), 2961 (br., CH aromatic), 1726 (s, NH), 1699 (s, C=O), 1615 (s, C⋯N), 1569 (s, C=N), 1512 (s, CN), 1414 (s, C⋯C) cm^{-1}.

D ($CDCl_3$): 3.3 × 10^{-10} m^2 s^{-1}.

$C_{159}H_{204}Cl_{12}N_{30}O_9Ru_6$ (3711.4): calcd. C 51.46, H 5.54, N 11.32; found C 50.54, H 5.70, N 11.43.

$(MEpyRh)_3$·$(BApyRu)_3$ and $(MEpyRu)_3$·$(BApyRh)_3$

Method 1: A mixture of BApyRu (83.2 mg, 0.14 mmol) or BApyRh (83.6 mg, 0.14 mmol) and MEpy (50.0 mg, 0.14 mmol) in dry chloroform (3 mL) was stirred at 25 ℃. After 30 min, $[Rh(Cp^*)Cl_2]_2$ (44.2 mg, 0.07 mmol) or $[Ru(cym)Cl_2]_2$ (43.8 mg, 0.07 mmol) was added, and the mixture was stirred at 25 ℃ for 16 h. Then the mixture was concentrated, and pentane was added to precipitate the product.

Method 2: A mixture of BApyRu (44.2 mg, 0.08 mmol) or BApyRh (44.6 mg, 0.08 mmol) and MEpyRh (50.0 mg, 0.08 mmol) or MEpyRu (50.0 mg, 0.08 mmol) in dry chloroform (2 mL) was stirred at 25 ℃ for 30 min. Then pentane was added to precipitate the product.

$(MEpyRh)_3$·$(BApyRu)_3$: Orange solid, yield 93 % (Method 1: 0.17 g, 0.04 mmol); 90 % (Method 2: 89.3 mg, 0.02 mmol).

^{1}H NMR (400 MHz, $CDCl_3$): δ = 14.20 (br., 6 H, NH···N), 9.25 (br., 3 H, O···H-N), 9.06 (br., 6 H, $CH_{Py\ ME}N$), 8.88 (br., 6 H, $CH_{Py\ BA}N$), 8.10 (br., 3 H, O···H'-N), 7.48 (br., 6 H, $CH_{ar}CC$), 7.34 (m, 6 H, $CH_{Py\ ME}C$), 7.32 (m, 6 H, $CH_{ar}CN$), 7.10 (br., 6 H, $CH_{Py\ BA}C$), 7.00 (br., 3 H, NH_2···O), 6.93 (br., 3 H, NH_2'···O), 5.51 (br., 6 H, CH_{cym}), 5.31 (br., 6 H, CH_{cym}), 4.93 (br., 3 H, $CH_{2\ ME}$), 4.58 (br., 3 H, CH_2'$_{ME}$), 3.34 (br., 6 H, $CH_{2\ BA}$), 2.94 (br., 3 H, CH), 2.09 (br., 6 H, CH_2C_{BA}), 1.94 (m., 9 H, CH_3C_{cym}), 1.54 (m, 45 H, CH_3C_{Cp*}), 1.35 [m, 27 H, $C(CH_3)_3$], 1.32 (m, 12 H, CH_2 and CH_2CH_3), 1.26 [m, 18 H, $(CH_3)_2CH$], 0.89 (t, $^3J_{H,H}$ = 6.2 Hz, 9 H, CH_3) ppm.

^{13}C NMR (100 MHz, $CDCl_3$): δ = 174.93 (CO), 165.60 (CNHCH$_2$), 165.22 (CNH_2), 163.20 (CNHC), 155.27 ($CH_{Py\ ME}N$), 154.90 ($CH_{Py\ ME}$'N), 154.09 (HNCONH), 153.77 ($CH_{Py\ BA}N$), 153.48 ($CH_{Py\ BA}$'N), 153.11 ($C_{Py\ ME}$), 152.98 ($C_{Py\ ME}$'), 151.53 ($C_{Py\ BA}$), 151.36 ($C_{Py\ BA}$'), 146.50 ($C_{ar}C$), 146.29 (C_{ar}'C), 136.47 ($C_{ar}NH$), 126.52 ($CH_{Py\ BA}C$), 126.02 ($CH_{Py\ BA}$'C), 125.51 ($CH_{ar}CN$), 123.60 ($CH_{Py\ ME}C$), 122.77 ($CH_{Py\ ME}$'C), 120.64 ($CH_{ar}CC$), 103.17 ($C_{cym}CH$), 97.39 ($C_{cym}CH_3$), 94.21 (C_{Cp*}), 83.48 (CH_{cym}), 82.07 (CH_{cym}), 57.44 (C_{BA}), 43.38 ($CH_{2\ ME}$), 41.67 (CH_2C_{BA}), 40.85 ($CH_{2\ BA}$), 34.46 [$C(CH_3)_3$], 31.62 [$C(CH_3)_3$], 30.81 (CH), 26.61 (CH_2), 22.55 (CH_2CH_3), 22.48 [$(CH_3)_2CH$], 18.37 (CH_3C_{cym}), 18.14 (CH_3'C_{cym}), 13.78 (CH_3), 9.09 (CH_3C_{Cp*}), 8.95 (CH_3'C_{Cp*}) ppm.

UV/Vis ($CHCl_3$, 1.0 × 10^{-5} M): λ_{max} (ε) = 265 (1.01 × 10^5), 409 nm (9.97 × 10^3 M^{-1} cm^{-1}).

IR: $\tilde{\nu}$ = 3318 (br., NH), 2960 (br., CH aromatic), 1726 (s, NH), 1699 (s, C=O), 1614 (s, C⋯N), 1570 (s, C=N), 1512 (s, CN), 1417 (s, C⋯C) cm^{-1}.

D ($CDCl_3$): 3.6 × 10^{-10} m^2 s^{-1}.

$C_{159}H_{207}Cl_{12}N_{30}O_9Ru_3Rh_3 \cdot 3H_2O$ (3774.0): calcd. C 50.60, H 5.69, N 11.13; found C 49.77, H 5.74, N 10.87.

$(MEpyRu)_3$·$(BApyRh)_3$: Orange solid, yield 90 % (Method 1: 0.16 g, 0.04 mmol); 87 % (Method 2: 86.3 mg, 0.02 mmol).

^{1}H NMR (400 MHz, $CDCl_3$): δ = 14.22 (br., 6 H, NH···N), 9.25 (br., 3 H, O···H-N), 9.08 (br., 6 H, $CH_{Py\ ME}N$), 8.86 (br., 6 H, $CH_{Py\ BA}N$), 8.11 (br., 3 H, O···H'-N), 7.48 (br., 6 H, $CH_{ar}CC$), 7.34 (m, 6 H, $CH_{Py\ ME}C$), 7.28 (m, 6 H, $CH_{ar}CN$), 7.09 (br., 6 H, $CH_{Py\ BA}C$), 6.99 (br., 3 H, NH_2···O), 6.92 (br., 3 H, NH_2'···O), 5.52 (br., 6 H, CH_{cym}), 5.33 (br., 6 H, CH_{cym}), 4.96 (br., 3 H, $CH_{2\ ME}$), 4.58 (br., 3 H, CH_2'$_{ME}$), 3.34 (br., 6 H, $CH_{2\ BA}$), 2.96 (br., 3 H, CH), 2.09 (br., 6 H, CH_2C_{BA}), 1.95 (br., 9 H, CH_3C_{cym}), 1.54 (m, 45 H, CH_3C_{Cp*}), 1.35 [m, 27 H, $C(CH_3)_3$], 1.32 (m, 12 H, CH_2 and CH_2CH_3), 1.27 [m, 18 H, $(CH_3)_2CH$], 0.89 (t, $^{3}J_{H,H}$ = 6.4 Hz, 9 H, CH_3) ppm.

^{13}C NMR (100 MHz, $CDCl_3$): δ = 174.91 (CO), 165.65 (*C*NHCH$_2$), 165.30 (CNH_2), 163.23 (*C*NHC), 155.22 ($CH_{Py\ ME}N$), 154.88 ($CH_{Py\ ME}$'N), 154.29 (HNCONH), 153.73 ($CH_{Py\ BA}N$), 153.46 ($CH_{Py\ BA}$'N), 153.22 ($C_{Py\ ME}$), 152.84 ($C_{Py\ ME}$'), 151.61 ($C_{Py\ BA}$), 151.39 ($C_{Py\ BA}$'), 146.47 ($C_{ar}C$), 146.23 (C_{ar}'C), 136.50 ($C_{ar}NH$), 126.56 ($CH_{Py\ BA}C$), 126.00 ($CH_{Py\ BA}$'C), 125.49 ($CH_{ar}CN$), 123.55 ($CH_{Py\ ME}C$), 122.72 ($CH_{Py\ ME}$'C), 120.61 ($CH_{ar}CC$), 103.14 ($C_{cym}CH$), 97.38 ($C_{cym}CH_3$), 94.20 (C_{Cp*}), 83.47 (CH_{cym}), 81.81 (CH_{cym}), 57.44 (C_{BA}), 43.37 ($CH_{2\ ME}$), 41.41 (CH_2C_{BA}), 40.51 ($CH_{2\ BA}$), 34.44 [$C(CH_3)_3$], 31.59 [$C(CH_3)_3$], 30.79 (CH), 26.61 (CH_2), 22.52 (CH_2CH_3), 22.47 [$(CH_3)_2CH$], 18.33 (CH_3C_{cym}), 18.12 (CH_3'C_{cym}), 13.75 (CH_3), 9.07 (CH_3C_{Cp*}), 8.93 (CH_3'C_{Cp*}) ppm.

UV/Vis ($CHCl_3$, 1.0 × 10^{-5} M): λ_{max} (ε) = 265 (9.77 × 10^{4}), 406 nm (9.77 × 10^{3} M^{-1} cm^{-1}).

IR: $\tilde{\nu}$ = 3325 (br., NH), 2960 (br., CH aromatic), 1726 (s, NH), 1699 (s, C=O), 1614 (s, C··N), 1570 (s, C=N), 1513 (s, CN), 1417 (s, C··C) cm^{-1}.

D ($CDCl_3$): 3.0 × 10^{-10} m^2 s^{-1}.

$C_{159}H_{207}Cl_{12}N_{30}O_9Ru_3Rh_3 \cdot 3H_2O$ (3774.0): calcd. C 50.60, H 5.69, N 11.13; found C 49.73, H 5.81, N 10.90.

6.2.3 Cationic hexanuclear metalla-assemblies

$[Rh_2(Cp^*)_2(L^C)Cl_2]$ (Rh_2L^C) and $[Ir_2(Cp^*)_2(L^C)Cl_2]$ (Ir_2L^C)

Sodium acetate (73.4 mg, 0.90 mmol) was added to a solution of 2,5-dihydroxy-3-icosylcyclohexa-2,5-diene-1,4-dione (0.18 g, 0.43 mmol) in methanol (20 mL). After stirring for 1 h, $[Rh(Cp^*)Cl_2]_2$ (0.25 g, 0.40 mmol) or $[Ir(Cp^*)Cl_2]_2$ (0.31 g, 0.40 mmol) was added. The mixture was stirred at 25 ℃ for 16 h, and then the solvent was evaporated. The residue was washed with water to give the product.

Rh_2L^C: Brown solid, yield 75 % (0.29 g, 0.30 mmol).

^{1}H NMR (400 MHz, $CDCl_3$): δ = 5.63 (s, 1 H, CH_{dobq}), 2.35 (m, 2 H, CH_2C_{dobq}), 1.71 (s, 30 H, $CH_3C_{Cp^*}$), 1.41 (m, 2 H, CH_2), 1.25 (m, 34 H, CH_2), 0.87 (t, $^3J_{H,H}$ = 6.0 Hz, 3 H, CH_3) ppm.

^{13}C NMR (100 MHz, $CDCl_3$): δ = 184.04 (CO_{dobq}), 181.37 (CO_{dobq}), 115.18 (C_{dobq}), 101.10 (CH_{dobq}), 92.70 (C_{Cp^*}), 32.05 (CH_2), 30.12 (CH_2), 29.84 (CH_2), 29.49 (CH_2), 28.44 (CH_2), 22.82 (CH_2), 22.49 (CH_2C_{dobq}), 14.24 (CH_3), 9.11 ($CH_3C_{Cp^*}$) ppm.

UV/Vis (CH_2Cl_2, 1.0 × 10^{-5} M): λ_{max} (ε) = 243 (3.74 × 10^4), 308 nm (1.27 × 10^4), 436 nm (2.08 × 10^4 M^{-1} cm^{-1}).

IR: $\tilde{\nu}$ = 2920 (s, CH aromatic), 1519 (s, C⋯O) cm^{-1}.

$C_{46}H_{72}O_4Cl_2Rh_2 \cdot H_2O$ (983.8): calcd. C 56.16, H 7.58; found C 55.95, H 7.33.

ESI-MS: *m/z* = 929.2 $[M - Cl]^+$.

Ir_2L^C: Red-brown solid, yield 70 % (0.32 g, 0.28 mmol).

^{1}H NMR (400 MHz, $CDCl_3$): δ = 5.82 (s, 1 H, CH_{dobq}), 2.42 (m, 2 H, CH_2C_{dobq}), 1.71 (s, 30 H, $CH_3C_{Cp^*}$), 1.45 (m, 2 H, CH_2), 1.25 (m, 34 H, CH_2), 0.87 (t, $^3J_{H,H}$ = 6.8 Hz, 3 H, CH_3) ppm.

^{13}C NMR (100 MHz, $CDCl_3$): δ = 185.50 (CO_{dobq}), 182.90 (CO_{dobq}), 115.27 (C_{dobq}), 100.92 (CH_{dobq}), 84.23 (C_{Cp^*}), 32.06 (CH_2), 29.85 (CH_2), 29.65 (CH_2), 29.49 (CH_2), 28.18 (CH_2), 22.82 (CH_2), 22.44 (CH_2C_{dobq}), 14.24 (CH_3), 9.38 ($CH_3C_{Cp^*}$) ppm.

UV/Vis ($CHCl_3$, 1.0×10^{-5} M): λ_{max} (ε) = 230 (3.60×10^4), 310 nm (1.54×10^4), 460 nm (1.76×10^4 M^{-1} cm^{-1}).

IR: $\tilde{\nu}$ = 2920 (s, CH aromatic), 1523 (s, C⋯O) cm^{-1}.

$C_{46}H_{72}O_4Cl_2Ir_2$ (1144.4): calcd. C 48.28, H 6.34; found C 49.27, H 6.59.

ESI-MS: *m/z* = 1109.2 $[M - Cl]^+$.

N,N'-bis{4-[(5-methoxypyridin-3-yl)ethynyl]phenyl}melamine (MEbispy)

3-ethynyl-5-methoxypyridine (0.40 g, 3.00 mmol), $[PdCl_2(PPh_3)_2]$ (0.10 g, 0.15 mmol) and copper iodide (28.1 mg, 0.15 mmol) were added to a solution of *N,N'*-bis(4-iodophenyl)melamine (0.78 g, 1.47 mmol) in dry tetrahydrofuran (20 mL). Then triethylamine (20 mL, 0.27 mol) was added progressively, and the mixture was stirred at 60 ℃. After 24 h, the mixture was filtered and washed with H_2O, THF, AcOEt and MeOH to give the product.

MEbispy: Yellow solid, yield 68 % (0.54 g, 1.00 mmol).

^{1}H NMR [400 MHz, $(CD_3)_2SO$]: δ = 9.45 (br., 2 H, NH), 8.33 (br., 2 H, CH_{Py}), 8.31 (br., 2 H, CH_{Py}), 7.92 (d, $^3J_{H,H}$ = 7.8 Hz, 4 H, CH_{ar}), 7.55 (s, 2 H, CH_{Py}), 7.49 (d, $^3J_{H,H}$ = 7.8 Hz, 4 H, CH_{ar}), 6.80 (br., 2 H, NH_2), 3.86 (s, 6 H, CH_3O) ppm.

^{13}C NMR [100 MHz, $(CD_3)_2SO$]: δ = 166.70 (CNH_2), 164.19 (CNH), 155.05 ($C_{Py}OCH_3$), 143.48 (CH_{Py}), 141.23 (C_{ar}), 137.34 (CH_{Py}), 131.76 (CH_{ar}), 121.69 (CH_{Py}), 120.23 (C_{Py}), 119.43 (CH_{ar}), 114.00 (C_{ar}), 92.87 (C), 84.93 (C), 55.64 (CH_3O) ppm.

UV/Vis (THF, 1.0×10^{-5} M): λ_{max} (ε) = 210 (5.29×10^4), 329 nm (7.76×10^4 M^{-1} cm^{-1}).

IR: $\tilde{\nu}$ = 3276 (br., NH), 2963 (br., CH aromatic), 2209 (s, C≡C), 1584 (s, C⋯N), 1498 (s, C=N), 1432 (s, C⋯C) cm^{-1}.

$C_{31}H_{24}N_8O_2 \cdot CH_3OH$ (572.6): calcd. C 67.12, H 4.93, N 19.57; found C 68.02, H 4.77, N 19.51.

ESI-MS: *m/z* = 541.1 $[M + H]^+$.

$(MEbispy)_3 \cdot (BA)_3$

A mixture of MEbispy (0.15 g, 0.27 mmol) and BA (50.0 mg, 0.27 mmol) in dry chloroform (5 mL) was stirred at 25 ℃ for 30 min. Then the mixture was filtered over celite, and washed with chloroform. The residue was concentrated, and pentane was added to precipitate the product.

$(MEbispy)_3 \cdot (BA)_3$: Light yellow solid, yield 50 % (98.4 mg, 0.05 mmol).

^{1}H NMR (400 MHz, $CDCl_3$): δ = 13.36 (br., 6 H, NH···N), 9.53 (br., 6 H, O···H-N), 8.41 (s, 6 H, CH_{Py}), 8.27 (s, 6 H, CH_{Py}), 7.79 (br., 12 H, CH_{ar}), 7.56 (br., 12 H, CH_{ar}), 7.33 (s, 6 H, CH_{Py}), 7.04 (br., 6 H, NH_2···O), 3.88 (s, 18 H, CH_3O), 2.18 (m, 12 H, $CH_{2\ BA}$), 1.01 (m, 18 H, $CH_{3\ BA}$) ppm.

^{13}C NMR (100 MHz, $CDCl_3$): δ = 175.97 (CO_{BA}), 166.35 (CNH_2), 163.81 (CNH), 155.24 ($C_{Py}OCH_3$), 153.30 (NHCONH), 144.66 (CH_{Py}), 139.72 (C_{ar}), 137.23 (CH_{Py}), 132.41 (CH_{ar}), 122.38 (CH_{Py}), 121.91 (C_{Py}), 121.07 (CH_{ar}), 117.13 (C_{ar}), 92.84 (C), 85.62 (C), 58.09 (C_{BA}), 55.77 (CH_3O), 32.26 ($CH_{2\ BA}$), 9.89 ($CH_{3\ BA}$) ppm.

UV/Vis (CH_2Cl_2, 1.0×10^{-5} M): λ_{max} (ε) = 230 (1.21×10^5), 323 nm (2.12×10^5 M^{-1} cm^{-1}).

IR: $\tilde{\nu}$ = 3298 (br., NH), 2973 (br., CH aromatic), 2204 (s, C≡C), 1715 (s, NH), 1562 (s, C··N), 1497 (s, C··O), 1456 (s, C=N), 1420 (s, C··C) cm^{-1}.

$C_{117}H_{108}N_{30}O_{15} \cdot 3H_2O$ (2228.4): calcd. C 63.06, H 5.16, N 18.86; found C 63.49, H 5.08, N 18.03.

$MEbispyRu_2L^C$

A mixture of Ru_2L^C (0.25 g, 0.26 mmol) and $AgSO_3CF_3$ (0.20 g, 0.78 mmol) in dry methanol (20 mL) was stirred at 25 ℃ for 2 h and filtered to remove AgCl. The solution of MEbispy (0.14 g, 0.26 mmol) in dry tetrahydrofuran (12 mL) was added to the residue. The mixture was stirred at 60 ℃ for 40 h, and then the solvent was evaporated. The residue was solubilized in dichloromethane, and diethyl ether was added to precipitate the product.

MEbispyRu$_2$L^C: Red-brown solid, yield 95 % (0.43 g, 0.25 mmol).

^{1}H NMR (400 MHz, CD_2Cl_2): δ = 8.39 (br., 2 H, NH), 7.95 (s, 2 H, CH_{Py}), 7.83 (s, 2 H, CH_{Py}), 7.79 (s, 2 H, CH_{Py}), 7.46 (br., 4 H, CH_{ar}), 7.42 (br., 4 H, CH_{ar}), 6.23 (br., 2 H, NH_2), 5.84 (br., 4 H, CH_{cym}), 5.70 (br., 4 H, CH_{cym}), 5.64 (br., 1 H, CH_{dobq}), 3.86 (s, 6 H, CH_3O), 2.85 (m, 2 H, CH), 2.36 (m, 2 H, CH_2C_{dobq}), 2.21 (s, 6 H, CH_3C_{cym}), 1.36 [m, 12 H, $(CH_3)_2CH$], 1.26 (m, 36 H, CH_2), 0.87 (t, $^3J_{H,H}$ = 6.6 Hz, 3 H, CH_3) ppm.

^{13}C NMR (100 MHz, CD_2Cl_2): δ = 184.75 (CO), 182.31 (CO), 166.38 (CNH_2), 161.87 (CNH), 157.09 ($C_{Py}OCH_3$), 146.43 (CH_{Py}), 141.41 (CH_{Py}), 138.67 (C_{ar}), 132.42 (CH_{ar}), 125.68 (CH_{Py}), 123.44 (CH_{ar}), 122.74 (C_{Py}), 119.56 (C_{ar}), 117.70, (C_{dobq}), 104.45 (C_{cym}), 101.64 (CH_{dobq}), 98.60 (C_{cym}), 95.21 (C), 83.79 (CH_{cym}), 83.22 (C), 82.70 (CH_{cym}), 56.90 (CH_3O), 32.31 (CH_2), 31.81 (CH), 30.12 (CH_2), 29.75 (CH_2), 29.00 (CH_2), 23.08 (CH_2), 22.27 [(CH_3)$_2$CH], 22.10 (CH_2C_{dobq}), 18.39 (CH_3C_{cym}), 14.29 (CH_3) ppm.

UV/Vis (CH_2Cl_2, 1.0 × 10^{-5} M): λ_{max} (ε) = 228 (6.77 × 10^4), 298 nm (4.91 × 10^4), 496 nm (1.35 × 10^4 M^{-1} cm^{-1}).

IR: $\tilde{\nu}$ = 3287 (br., NH), 2924 (br., CH aromatic), 2219 (s, C≡C), 1580 (s, C⋯N), 1512 (s, C⋯O), 1474 (s, C=N), 1415 (s, C⋯C), 1223 (s, CF_3) cm^{-1}.

$C_{79}H_{94}N_8O_{12}F_6S_2Ru_2 \cdot 2CH_2Cl_2$ (1897.8): calcd. C 51.26, H 5.21, N 5.90; found C 50.73, H 5.10, N 5.60.

ESI-MS: *m/z* = 1579.0 [M – CF_3SO_3]$^+$, 715.2 [M - 2 CF_3SO_3]$^{2+}$.

MEbispyRh$_2$L^C and MEbispyIr$_2$L^C

A mixture of Rh$_2$L^C (0.25 g, 0.26 mmol) or Ir$_2$L^C (0.30 g, 0.26 mmol) and $AgSO_3CF_3$ (0.20 g, 0.78 mmol) in dry methanol (20 mL) was stirred at 25 ℃ for 2 h and filtered to remove AgCl. The solution of MEbispy (0.14 g, 0.26 mmol) in dry tetrahydrofuran (12 mL) was added to the residue. The mixture was stirred at 60 ℃ for 20 h, and then the solvent was evaporated. The residue was solubilized in dichloromethane, and diethyl ether was added to precipitate the product.

MEbispyRh$_2$L^C: Green solid, yield 92 % (0.41 g, 0.24 mmol).

^{1}H NMR (400 MHz, CD_3OD): δ = 8.05 (s, 2 H, CH_{Py}), 7.95 (s, 2 H, CH_{Py}), 7.70 (s, 2 H, CH_{Py}), 7.57 (br., 4 H, CH_{ar}), 7.43 (br., 4 H, CH_{ar}), 5.59 (br., 1 H, CH_{dobq}), 3.88 (s, 6 H, CH_3O), 2.45 (m, 2 H, CH_2C_{dobq}), 1.70 (s, 30 H, CH_3C_{Cp*}), 1.28 (m, 36 H, CH_2), 0.90 (t, $^{3}J_{H,H}$ = 6.2 Hz, 3 H, CH_3) ppm.

^{13}C NMR (100 MHz, CD_3OD): δ = 185.05 (CO), 182.49 (CO), 164.07 (CNH_2), 161.84 (CNH), 158.81 ($C_{Py}OCH_3$), 145.72 (CH_{Py}), 140.65 (CH_{Py}), 135.79 (C_{ar}), 133.20 (CH_{ar}), 126.59 (CH_{Py}), 124.43 (CH_{ar}), 123.41 (C_{Py}), 120.26 (C_{ar}), 117.02, (C_{dobq}), 102.29 (CH_{dobq}), 97.16 (C_{Cp*}), 95.55 (C), 84.38 (C), 57.08 (CH_3O), 33.07 (CH_2), 30.80 (CH_2), 30.50 (CH_2), 23.72 (CH_2), 22.81 (CH_2C_{dobq}), 14.46 (CH_3), 8.67 (CH_3C_{Cp*}) ppm.

UV/Vis (CH_2Cl_2, 1.0 × 10^{-5} M): λ_{max} (ε) = 234 (8.08 × 10^4), 339 nm (5.41 × 10^4), 422 nm (1.99 × 10^4 M^{-1} cm^{-1}).

IR: $\tilde{\nu}$ = 3319 (br., NH), 2924 (br., CH aromatic), 2214 (s, C≡C), 1577 (s, C⋯N), 1511 (s, C⋯O), 1483 (s, C=N), 1413 (s, C⋯C), 1223 (s, CF_3) cm^{-1}.

$C_{79}H_{96}N_8O_{12}F_6S_2Rh_2 \cdot 4CH_2Cl_2$ (2073.3): calcd. C 48.08, H 5.06, N 5.40; found C 48.49, H 5.04, N 5.40.

ESI-MS: *m/z* = 1582.9 $[M - CF_3SO_3]^+$, 717.3 $[M - 2\ CF_3SO_3]^{2+}$.

MEbispyIr$_2$L^C: Red-brown solid, yield 90 % (0.45 g, 0.23 mmol).

^{1}H NMR (400 MHz, CD_3OD): δ = 8.07 (s, 2 H, CH_{Py}), 7.95 (s, 2 H, CH_{Py}), 7.72 (s, 2 H, CH_{Py}), 7.51 (br., 4 H, CH_{ar}), 7.49 (br., 4 H, CH_{ar}), 5.80 (br., 1 H, CH_{dobq}), 3.90 (s, 6 H, CH_3O), 2.50 (m, 2 H, CH_2C_{dobq}), 1.67 (s, 30 H, CH_3C_{Cp*}), 1.28 (m, 36 H, CH_2), 0.90 (t, $^{3}J_{H,H}$ = 6.2 Hz, 3 H, CH_3) ppm.

^{13}C NMR (100 MHz, CD_3OD): δ = 186.79 (CO), 184.09 (CO), 163.02 (CNH_2), 161.41 (CNH), 159.32 ($C_{Py}OCH_3$), 146.09 (CH_{Py}), 141.80 (CH_{Py}), 139.71 (C_{ar}), 133.24 (CH_{ar}), 127.10 (CH_{Py}), 124.74 (CH_{ar}), 123.41 (C_{Py}), 120.24 (C_{ar}), 117.08, (C_{dobq}), 101.47 (CH_{dobq}), 95.66 (C), 88.70 (C_{Cp*}), 84.00 (C), 57.25 (CH_3O), 33.07 (CH_2), 30.77 (CH_2), 30.47 (CH_2), 23.72 (CH_2), 22.83 (CH_2C_{dobq}), 14.44 (CH_3), 8.78 (CH_3C_{Cp*}) ppm.

UV/Vis (CH_2Cl_2, 1.0 × 10^{-5} M): λ_{max} (ε) = 230 (7.34 × 10^4), 296 (4.94 × 10^4), 451 nm (1.33 × 10^4 M^{-1} cm^{-1}).

IR: $\tilde{\nu}$ = 3310 (br., NH), 2924 (br., CH aromatic), 2217 (s, C≡C), 1580 (s, C⋯N), 1515 (s, C⋯O), 1459 (s, C=N), 1416 (s, C⋯C), 1223 (s, CF_3) cm^{-1}.

$C_{79}H_{96}N_8O_{12}F_6S_2Ir_2 \cdot 4CH_2Cl_2$ (2251.9): calcd. C 44.27, H 4.66, N 4.98; found C 43.42, H 4.47, N 4.94.

ESI-MS: *m/z* = 1760.9 $[M - CF_3SO_3]^+$, 807.3 $[M - 2\ CF_3SO_3]^{2+}$.

MEbispyRu$_2$L^A and MEbispyIr$_2$L^B

A mixture of Ru_2L^A (0.30 g, 0.38 mmol) or Ru_2L^B (0.32 g, 0.38 mmol) and $AgSO_3CF_3$ (0.29 g, 1.13 mmol) in dry methanol (26 mL) was stirred at 25 ℃ for 2 h and filtered to remove AgCl. The solution of MEbispy (0.21 g, 0.38 mmol) in dry tetrahydrofuran (14 mL) was added to the residue. The mixture was stirred at 60 ℃ for 16 h, and then the solvent was evaporated. The residue was solubilized in dichloromethane, and diethyl ether was added to precipitate the product.

MEbispyRu$_2$L^A: Light green solid, yield 87 % (0.52 g, 0.33 mmol).

^{1}H NMR (400 MHz, CD_3OD): δ = 7.87 (br., 2 H, CH_{Py}), 7.77 (br., 2 H, CH_{Py}), 7.69 (br., 2 H, CH_{Py}), 7.57 (br., 4 H, CH_{ar}), 7.23 (br., 4 H, CH_{ar}), 5.94 (br., 4 H, CH_{cym}), 5.53 (br., 4 H, CH_{cym}), 3.90 (s, 6 H, CH_3O), 3.69 (m, 4 H, CH_2N), 2.75 (m, 2 H, CH), 1.97 (m, 4 H, CH_2), 1.74 (s, 6 H, CH_3C_{cym}) 1.53 (m, 12 H, CH_2), 1.27 [m, 12 H, $(CH_3)_2CH$], 1.04 (m, 6 H, CH_3) ppm.

^{13}C NMR (100 MHz, CD_3OD): δ = 172.12 (CO), 162.82 (CNH_2), 159.91 (CNH), 157.55 ($C_{Py}OCH_3$), 148.48 (CH_{Py}), 139.26 (CH_{Py}), 135.73 (C_{ar}), 133.42 (CH_{ar}), 126.65 (CH_{Py}), 124.65 (C_{Py}), 123.48 (C), 121.34 (CH_{ar}), 120.31 (C), 118.12 (C_{ar}), 104.40 (C_{cym}), 100.49 (C_{cym}), 87.71 (CH_{cym}), 80.44 (CH_{cym}), 57.07 (CH_3O), 54.12 (NCH_2), 33.02 (CH_2), 32.53 (CH), 31.15 (CH_2), 28.34 (CH_2), 23.75 (CH_2), 23.01 (CH_2), 22.29 [(CH_3)$_2$CH], 17.82 (CH_3C_{cym}), 14.50 (CH_3) ppm.

UV/Vis (CH_2Cl_2, 1.0 × 10^{-5} M): λ_{max} (ε) = 228 (5.21 × 10^4), 350 nm (5.35 × 10^4 M^{-1} cm^{-1}).

IR: $\tilde{\nu}$ = 3310 (br., NH), 2931 (br., CH aromatic), 2214 (s, C≡C), 1595 (s, C⋯N), 1510 (s, C⋯O), 1462 (s, C=N), 1416 (s, C⋯C), 1254 (s, CF_3) cm^{-1}.

$C_{67}H_{78}N_{10}O_{10}F_6S_2Ru_2 \cdot 2CH_2Cl_2$ (1733.5): calcd. C 47.81, H 4.77, N 8.08; found C 47.14, H 4.69, N 7.66.

ESI-MS: *m/z* = 1415.0 $[M - CF_3SO_3]^+$, 633.4 $[M - 2\ CF_3SO_3]^{2+}$.

MEbispyIr$_2$L^B: Light yellow solid, yield 86 % (0.53 g, 0.33 mmol).

^{1}H NMR (400 MHz, CD_3OD): δ = 7.90 (br., 2 H, CH_{Py}), 7.79 (br., 2 H, CH_{Py}), 7.73 (br., 2 H, CH_{Py}), 7.60 (br., 4 H, CH_{ar}), 7.24 (br., 4 H, CH_{ar}), 5.96 (br., 4 H, CH_{cym}), 5.55 (br., 4 H, CH_{cym}), 3.93 (s, 6 H, CH_3O), 3.68 (m, 4 H, CH_2N), 2.78 (m, 2 H, CH), 2.01 (m, 4 H, CH_2), 1.76 (s, 6 H, CH_3C_{cym}) 1.45 (m, 20 H, CH_2), 1.30 [m, 12 H, $(CH_3)_2CH$], 0.99 (m, 6 H, CH_3) ppm.

^{13}C NMR (100 MHz, CD_3OD): δ = 172.36 (CO), 163.40 (CNH_2), 161.62 (CNH), 157.64 ($C_{Py}OCH_3$), 148.07 (CH_{Py}), 140.25 (CH_{Py}), 135.79 (C_{ar}), 133.59 (CH_{ar}), 126.65 (CH_{Py}), 124.75 (C_{Py}), 123.48 (C), 121.23 (CH_{ar}), 120.31 (C), 117.34 (C_{ar}), 104.13 (C_{cym}), 100.54 (C_{cym}), 87.53 (CH_{cym}), 80.35 (CH_{cym}), 57.11 (CH_3O), 54.17 (NCH_2), 33.11 (CH_2), 32.59 (CH), 31.27 (CH_2), 30.82 (CH_2), 30.54 (CH_2), 28.77 (CH_2), 23.82 (CH_2), 23.23 [(CH_3)$_2$CH], 17.83 (CH_3C_{cym}), 14.50 (CH_3) ppm.

UV/Vis (CH_2Cl_2, 1.0 × 10^{-5} M): λ_{max} (ε) = 229 (5.34 × 10^4), 349 nm (5.63 × 10^4 M^{-1} cm^{-1}).

IR: $\tilde{\nu}$ = 3313 (br., NH), 2928 (br., CH aromatic), 2214 (s, C≡C), 1596 (s, C⋯N), 1510 (s, C⋯O), 1465 (s, C=N), 1416 (s, C⋯C), 1255 (s, CF_3) cm^{-1}.

$C_{71}H_{86}N_{10}O_{10}F_6S_2Ru_2 \cdot 2CH_2Cl_2$ (1789.6): calcd. C 48.99, H 5.07, N 7.83; found C 48.57, H 5.01, N 7.58.

ESI-MS: *m/z* = 1470.0 $[M - CF_3SO_3]^+$, 660.8 $[M - 2\ CF_3SO_3]^{2+}$.

(MEbispyRu$_2$L^C)$_3$·(BA)$_3$

A mixture of MEbispyRu$_2$L^C (0.14 g, 0.08 mmol) and BA (14.9 mg, 0.08 mmol) in dry chloroform (3 mL) was stirred at 25 ℃ for 48 h. Then the mixture was filtered over celite, and washed with chloroform. The residue was concentrated, and pentane was added to precipitate the product.

(MEbispyRu$_2$L^C)$_3$·(BA)$_3$: Dark purple solid, yield 80 % (0.12 g, 0.02 mmol).

^{1}H NMR (400 MHz, CD_2Cl_2): δ = 13.73 (br., 6 H, NH···N), 9.71 (br., 6 H, O···H-N), 7.99 (s, 6 H, CH_{Py}), 7.84 (br., 6 H, CH_{Py}), 7.81 (br., 6 H, CH_{Py}), 7.66 (br., 12 H, CH_{ar}), 7.46 (br., 12 H, CH_{ar}), 7.24 (br., 6 H, NH_2···O), 5.87 (br., 12 H, CH_{cym}), 5.73 (br., 12 H, CH_{cym}), 5.57 (br., 3 H, CH_{dobq}), 3.88 (s, 18 H, CH_3O), 2.87 (m, 6 H, CH), 2.39 (m, 6 H, CH_2C_{dobq}), 2.23 (s, 18 H, CH_3C_{cym}), 2.15 (m, 12 H, $CH_{2\ BA}$), 1.38 [m, 36 H, $(CH_3)_2CH$], 1.26 (m, 108 H, CH_2), 0.99 (t, $^3J_{H,H}$ = 6.6 Hz, 18 H, $CH_{3\ BA}$), 0.86 (m, 9 H, CH_3) ppm.

^{13}C NMR (100 MHz, CD_2Cl_2): δ = 184.93 (CO), 182.45 (CO), 175.82 (CO_{BA}), 166.76 (CNH_2), 163.94 (CNH), 157.23 ($C_{Py}OCH_3$), 153.00 (NHCONH), 146.48 (CH_{Py}), 141.43 (CH_{Py}), 140.33 (C_{ar}), 132.44 (CH_{ar}), 125.93 (CH_{Py}), 123.69 (C_{Py}), 123.08 (CH_{ar}), 119.85 (C_{ar}), 116.71 (C_{dobq}), 104.99 (C_{cym}), 101.59 (CH_{dobq}), 98.72 (C_{cym}), 95.70 (C), 83.86 (CH_{cym}), 83.37 (CH_{cym}), 82.73 (C), 58.46 (C_{BA}), 57.04 (CH_3O), 32.54 ($CH_{2\ BA}$), 32.38 ($CH_{2\ BA}$), 31.90 (CH), 30.19 (CH_2), 29.82 (CH_2), 23.14 (CH_2), 22.46 [(CH_3)$_2$CH], 22.18 (CH_2C_{dobq}), 18.46 (CH_3C_{cym}), 14.30 (CH_3), 9.86 ($CH_{3\ BA}$) ppm.

UV/Vis (CH_2Cl_2, 1.0 × 10^{-5} M): λ_{max} (ε) = 230 (2.32 × 10^5), 297 (1.91 × 10^5), 496 nm (5.10 × 10^4 M^{-1} cm^{-1}).

IR: $\tilde{\nu}$ = 3290 (br., NH), 2924 (br., CH aromatic), 2216 (s, C≡C), 1715 (s, NH), 1580 (s, C···N), 1513 (s, C···O), 1453 (s, C=N), 1423 (s, C···C), 1241 (s, CF_3) cm^{-1}.

$C_{261}H_{318}N_{30}O_{45}F_{18}S_6Ru_6$ (5736.3): calcd. C 54.65, H 5.59, N 7.33; found C 53.87, H 5.59, N 7.13.

(MEbispyRh$_2$L^C)$_3$·(BA)$_3$ and (MEbispyIr$_2$L^C)$_3$·(BA)$_3$

A mixture of MEbispyRh$_2$L^C (0.14 g, 0.08 mmol) or MEbispyIr$_2$L^C (0.15 g, 0.08 mmol) and BA (15.0 mg, 0.08 mmol) in dry chloroform/dichloromethane (2 mL/1 mL) was stirred at 25 ℃ for 24 h. Then the mixture was filtered over celite, and washed with chloroform. The residue was concentrated, and pentane was added to precipitate the product.

(MEbispyRh$_2$L^C)$_3$·(BA)$_3$: Green solid, yield 86 % (0.13 g, 0.02 mmol).

^{1}H NMR (400 MHz, CD_2Cl_2): δ = 9.58 (br., 6 H, O···H-N), 7.89 (br., 6 H, CH_{Py}), 7.85 (br., 6 H, CH_{Py}), 7.73 (br., 6 H, CH_{Py}), 7.58 (br., 12 H, CH_{ar}), 7.45 (br., 12 H, CH_{ar}), 7.22 (br., 6 H, NH_2···O), 5.60 (br., 3 H, CH_{dobq}), 3.88 (s, 18 H, CH_3O), 2.37 (m, 6 H, CH_2C_{dobq}), 2.04 (m, 12 H, $CH_{2\ BA}$), 1.67 (s, 90 H, CH_3C_{Cp*}), 1.26 (m, 108 H, CH_2), 0.90 (m, 18 H, $CH_{3\ BA}$), 0.89 (m, 9 H, CH_3) ppm.

^{13}C NMR (100 MHz, CD_2Cl_2): δ = 184.31 (CO), 181.90 (CO), 173.61 (CO_{BA}), 168.61 (CNH_2), 164.03 (CNH), 157.68 ($C_{Py}OCH_3$), 150.79 (NHCONH), 144.89 (CH_{Py}), 139.78 (CH_{Py}), 134.83 (C_{ar}), 132.35 (CH_{ar}), 130.91 (CH_{Py}), 124.83 (CH_{ar}), 123.10 (C_{Py}), 119.65 (C_{ar}), 116.71 (C_{dobq}), 105.43 (CH_{dobq}), 101.78 (C), 96.05 (C_{Cp*}), 82.92 (C), 58.35 (C_{BA}), 56.96 (CH_3O), 32.34 ($CH_{2\ BA}$), 30.13 (CH_2), 29.77 (CH_2), 29.04 (CH_2), 23.10 (CH_2), 22.31 (CH_2C_{dobq}), 14.29 (CH_3), 9.71 ($CH_{3\ BA}$), 9.05 (CH_3C_{Cp*}) ppm.

UV/Vis (CH_2Cl_2, 1.0 × 10^{-5} M): λ_{max} (ε) = 234 (2.29 × 10^5), 339 (1.57 × 10^5), 422 nm (6.16 × 10^4 M^{-1} cm^{-1}).

IR: $\tilde{\nu}$ = 3313 (br., NH), 2924 (br., CH aromatic), 2214 (s, C≡C), 1709 (s, NH), 1578 (s, C··N), 1512 (s, C··O), 1486 (s, C=N), 1413 (s, C··C), 1223 (s, CF_3) cm^{-1}.

$C_{261}H_{324}N_{30}O_{45}F_{18}S_6Rh_6 \cdot 5CHCl_3$ (6350.2): calcd. C 50.31, H 5.22, N 6.62; found C 49.51, H 5.35, N 6.23.

$(MEbispyIr_2L^C)_3 \cdot (BA)_3$: Red solid, yield 90 % (0.15 g, 0.02 mmol).

^{1}H NMR (400 MHz, CD_2Cl_2): δ = 13.91 (br., 6 H, NH···N), 8.95 (br., 6 H, O···H-N), 8.54 (br., 6 H, CH_{Py}), 7.89 (br., 6 H, CH_{Py}), 7.84 (br., 6 H, CH_{Py}), 7.56 (br., 12 H, CH_{ar}), 7.46 (br., 12 H, CH_{ar}), 6.61 (br., 6 H, NH_2···O), 5.83 (br., 3 H, CH_{dobq}), 3.89 (s, 18 H, CH_3O), 2.42 (m, 6 H, CH_2C_{dobq}), 2.01 (m, 12 H, $CH_{2\ BA}$), 1.64 (s, 90 H, CH_3C_{Cp*}), 1.26 (m, 108 H, CH_2), 0.90 (m, 18 H, $CH_{3\ BA}$), 0.88 (m, 9 H, CH_3) ppm.

^{13}C NMR (100 MHz, CD_2Cl_2): δ = 185.86 (CO), 183.62 (CO), 173.71 (CO_{BA}), 165.16 (CNH_2), 162.50 (CNH), 158.20 ($C_{Py}OCH_3$), 150.64 (NHCONH), 145.43 (CH_{Py}), 140.66 (CH_{Py}), 139.46 (C_{ar}), 132.43 (CH_{ar}), 125.93 (CH_{Py}), 123.37 (CH_{ar}), 122.76 (C_{Py}), 119.57 (C_{ar}), 117.26 (C_{dobq}), 101.62 (CH_{dobq}), 96.06 (C), 87.66 (C_{Cp*}), 82.76 (C), 58.32 (C_{BA}), 57.13 (CH_3O), 32.32 ($CH_{2\ BA}$), 30.11 (CH_2), 29.75 (CH_2), 28.85 (CH_2), 23.08 (CH_2), 22.38 (CH_2C_{dobq}), 14.28 (CH_3), 9.66 ($CH_{3\ BA}$), 9.10 (CH_3C_{Cp*}) ppm.

UV/Vis (CH_2Cl_2, 1.0 × 10^{-5} M): λ_{max} (ε) = 232 (2.23 × 10^5), 295 (1.60 × 10^5), 451 nm (4.40 × 10^4 M^{-1} cm^{-1}).

IR: $\tilde{\nu}$ = 3302 (br., NH), 2925 (br., CH aromatic), 2216 (s, C≡C), 1711 (s, NH), 1580 (s, C⋯N), 1515 (s, C⋯O), 1458 (s, C=N), 1417 (s, C⋯C), 1241 (s, CF_3) cm^{-1}.

$C_{261}H_{324}N_{30}O_{45}F_{18}S_6Ir_6 \cdot 5CHCl_3$ (6886.1): calcd. C 46.40, H 4.82, N 6.10; found C 45.60, H 4.75, N 6.02.

$(MEbispyRu_2L^A)_3 \cdot (BA)_3$ and $(MEbispyRu_2L^B)_3 \cdot (BA)_3$

A mixture of $MEbispyRu_2L^A$ (0.13 g, 0.08 mmol) or $MEbispyRu_2L^B$ (0.13 g, 0.08 mmol) and BA (15.0 mg, 0.08 mmol) in dry chloroform/dichloromethane (2 mL/1 mL) was stirred at 25 ℃ for 26 h. Then the mixture was filtered over celite, and washed with chloroform. The residue was concentrated, and pentane was added to precipitate the product.

$(MEbispyRu_2L^A)_3 \cdot (BA)_3$: Light yellow solid, yield 88 % (0.12 g, 0.02 mmol).

^{1}H NMR (400 MHz, CD_2Cl_2): δ = 9.17 (br., 6 H, NH⋯N), 8.71 (br., 6 H, O⋯H-N), 7.65 (br., 6 H, CH_{Py}), 7.56 (br., 6 H, CH_{Py}), 7.48 (br., 6 H, CH_{Py}), 7.39 (br., 12 H, CH_{ar}), 7.20 (br., 12 H, CH_{ar}), 6.46 (br., 6 H, NH_2⋯O), 5.76 (br., 12 H, CH_{cym}), 5.48 (br., 12 H, CH_{cym}), 3.89 (s, 18 H, CH_3O), 3.70 (br., 12 H, NCH_2), 2.72 (m, 6 H, CH), 2.02 (m, 12 H, $CH_{2\ BA}$), 1.80 (s, 18 H, CH_3C_{cym}), 1.50 (m, 48 H, CH_2), 1.27 [m, 36 H, $(CH_3)_2CH$], 1.03 (m, 18 H, CH_3), 0.91 (m, 18 H, $CH_{3\ BA}$) ppm.

^{13}C NMR (100 MHz, CD_2Cl_2): δ = 173.17 (CO_{BA}), 170.94 (CO), 164.78 (CNH_2), 162.19 (CNH), 156.45 ($C_{Py}OCH_3$), 149.84 (NHCONH), 146.96 (CH_{Py}), 138.38 (CH_{Py}), 136.25 (C_{ar}), 133.07 (CH_{ar}), 126.02 (CH_{Py}), 124.16 (C_{Py}), 122.83 (C), 120.75 (CH_{ar}), 119.65 (C), 116.47 (C_{ar}), 103.46 (C_{cym}), 98.12 (C_{cym}), 84.96 (CH_{cym}), 81.59 (CH_{cym}), 58.30 (C_{BA}), 56.88 (CH_3O), 53.28 (NCH_2), 32.29 (CH_2), 31.73 (CH), 30.53 ($CH_{2\ BA}$), 27.50 (CH_2), 23.10 (CH_2), 22.72 [$(CH_3)_2CH$], 18.03 (CH_3C_{cym}), 14.35 (CH_3), 9.66 ($CH_{3\ BA}$) ppm.

UV/Vis (CH_2Cl_2, 1.0 × 10^{-5} M): λ_{max} (ε) = 230 (1.51 × 10^5), 350 nm (1.80 × 10^5 M^{-1} cm^{-1}).

IR: $\tilde{\nu}$ = 3310 (br., NH), 2966 (br., CH aromatic), 2214 (s, C≡C), 1708 (s, NH), 1597 (s, C⋯N), 1511 (s, C⋯O), 1459 (s, C=N), 1417 (s, C⋯C), 1254 (s, CF_3) cm^{-1}.

$C_{225}H_{270}N_{36}O_{39}F_{18}S_6Ru_6 \cdot 3CHCl_3$ (5601.7): calcd. C 48.89, H 4.91, N 9.00; found C 48.32, H 4.95, N 8.60.

$(MEbispyRu_2L^B)_3 \cdot (BA)_3$: Yellow solid, yield 86 % (0.12 g, 0.02 mmol).

^{1}H NMR (400 MHz, CD_2Cl_2): δ = 9.35 (br., 6 H, NH···N), 8.76 (br., 6 H, O···H-N), 7.72 (br., 6 H, CH_{Py}), 7.62 (br., 6 H, CH_{Py}), 7.47 (br., 6 H, CH_{Py}), 7.29 (br., 12 H, CH_{ar}), 7.17 (br., 12 H, CH_{ar}), 6.55 (br., 6 H, NH_2···O), 5.76 (br., 12 H, CH_{cym}), 5.51 (br., 12 H, CH_{cym}), 3.89 (s, 18 H, CH_3O), 3.71 (br., 12 H, NCH_2), 2.73 (m, 6 H, CH), 2.05 (m, 12 H, $CH_{2\ BA}$), 1.80 (s, 18 H, CH_3C_{cym}), 1.41 (m, 72 H, CH_2), 1.27 [m, 36 H, $(CH_3)_2CH$], 0.99 (m, 18 H, CH_3), 0.96 (m, 18 H, $CH_{3\ BA}$) ppm.

^{13}C NMR (100 MHz, CD_2Cl_2): δ = 173.24 (CO_{BA}), 171.02 (CO), 163.85 (CNH_2), 162.48 (CNH), 156.33 ($C_{Py}OCH_3$), 150.60 (NHCONH), 147.29 (CH_{Py}), 138.35 (CH_{Py}), 134.81 (C_{ar}), 133.07 (CH_{ar}), 126.07 (CH_{Py}), 123.77 (C_{Py}), 122.89 (C), 120.38 (CH_{ar}), 119.70 (C), 116.51 (C_{ar}), 103.83 (C_{cym}), 98.25 (C_{cym}), 84.66 (CH_{cym}), 81.58 (CH_{cym}), 58.24 (C_{BA}), 57.01 (CH_3O), 53.19 (NCH_2), 32.37 (CH_2), 31.74 (CH), 30.60 ($CH_{2\ BA}$), 30.18 (CH_2), 29.78 (CH_2), 27.87 (CH_2), 23.18 (CH_2), 22.76 (CH_2), 22.47 [(CH_3)$_2$CH], 18.04 (CH_3C_{cym}), 14.36 (CH_3), 9.69 ($CH_{3\ BA}$) ppm.

UV/Vis (CH_2Cl_2, 1.0 × 10^{-5} M): λ_{max} (ε) = 229 (1.56 × 10^5), 351 nm (1.73 × 10^5 M^{-1} cm^{-1}).

IR: $\tilde{\nu}$ = 3307 (br., NH), 2929 (br., CH aromatic), 2214 (s, C≡C), 1711 (s, NH), 1596 (s, C⋯N), 1510 (s, C⋯O), 1456 (s, C=N), 1416 (s, C⋯C), 1254 (s, CF_3) cm^{-1}.

$C_{237}H_{294}N_{36}O_{39}F_{18}S_6Ru_6 \cdot 2CHCl_3$ (5650.7): calcd. C 50.80, H 5.28, N 8.92; found C 50,30 H 5.24, N 8.46.

6.2.4 Crystal data

A crystal of BApyRh was mounted on a Stoe Mark II-Image Plate Diffraction System, using Mo-K_α graphite-monochromated radiation, image plate distance 135 nm, 2θ range 2.4-51.3 °, D_{max} - D_{min} = 16.029-0.836 Å.

Empirical formula	$C_{24}H_{32}Cl_2N_3O_3Rh_1$
Formula mass [g mol^{-1}]	584.33
Crystal system	monoclinic
Space group	$P2_1/c$
Crystal size [nm]	0.18 × 0.17 × 0.14
Crystal color and shape	orange block
a [Å]	16.3767(9)
b [Å]	12.7685(6)
c [Å]	25.0841(11)
α [°]	90
β [°]	103.962(4)
γ [°]	90
Cell volume [Å^3]	5090.3(4)
T [K]	203(2)
Z	8
Scan range [°]	$1.80 < \theta < 29.25$
$\varrho_{calcd.}$ [g cm^{-3}]	1.525
μ [mm^{-1}]	0.911
Unique reflections	13485
Reflections used [$I > 2\sigma(I)$]	6261
R_{int}	0.1261
Final R indices [$I > 2\sigma(I)$] [a]	0.0747, wR_2 0.1610
R indices (all data)[b]	0.1555, wR_2 0.1878
GOF[c]	0.927
Max, min $\Delta\varrho$/e [Å^{-3}]	1.787, -1.718

[a] $R_1 = \Sigma||F_o| - |F_c||/\Sigma|F_o|$. [b] $wR_2 = \{\Sigma[w(F_o^2 - F_c^2)^2]/\Sigma[w(F_o^2)^2]\}^{1/2}$. [c] $GOF = \{\Sigma[w(F_o^2 - F_c^2)^2]/(n - p)\}^{1/2}$, where n is the number of reflections and p is the total number of parameters refined.

Table 7: Crystallographic data and structure refinement parameters for BApyRh

The structure was solved by direct methods using the program SHELXS-97.[252] Refinement and all further calculations were carried out using SHELXL-97.[252] The H

atoms were included in calculated positions and treated as riding atoms using the SHELXL default parameters. The non-H atoms were refined anisotropically, using weighted full-matrix least squares on F^2. The electron densities higher than 1 e $Å^{-3}$ were all located at less than 1 Å from the rhodium atoms. Crystallographic details are summarized in Table 1, and Figure 5 was drawn with ORTEP32.[253] CCDC 1545897 (for BApyRh) contains the supplementary crystallographic data for this paper. These data can be obtained free of charge from The Cambridge Crystallographic Data Centre.

Chapter 7

References

[1] J. D. Bernal, H. D. Megaw, *Proceedings of the Royal Society of London. Series A - Mathematical and Physical Sciences* **1935**, *151*, 384-420.
[2] M. L. Huggins, *The Journal of Organic Chemistry* **1936**, *01*, 407-456.
[3] L. Pauling, *The Nature of the Chemical Bond*, Cornell University Press, Ithaca, **1939**.
[4] P. A. Kollman, L. C. Allen, *Chemical Reviews* **1972**, *72*, 283-303.
[5] *Monatshefte für Chemie / Chemical Monthly* **1999**, *130*, 945-946.
[6] IUPAC, *Compendium of Chemical Terminology*, The online version (http://old.iupac.org/publications/compendium/) mostly corresponds to the second

edition, compiled by A. D. McNaught and A. Wilkinson of the Royal Society of Chemistry. The definition of the term hydrogen bond is given at http://goldbook.iupac.org/pdf/goldbook.pdf, consulted 25/05/2018, Royal Society of Chemistry, Cambridge, **1997**.

[7] E. Arunan, R. Desiraju Gautam, A. Klein Roger, J. Sadlej, S. Scheiner, I. Alkorta, C. Clary David, H. Crabtree Robert, J. Dannenberg Joseph, P. Hobza, G. Kjaergaard Henrik, C. Legon Anthony, B. Mennucci, J. Nesbitt David, in *Pure and Applied Chemistry, Vol. 83*, **2011**, p. 1637.

[8] X. W. H. Hirao, *The Chemical Bond: Chemical Bonding Across the Periodic Table*, Wiley-VCH, Weinheim, **2014**.

[9] J. W. S. a. J. L. Atwood, *Supramolecular Chemistry*, John Wiley and Sons, Ltd, **2009**.

[10] L. J. Prins, D. N. Reinhoudt, P. Timmerman, *Angewandte Chemie International Edition* **2001**, *40*, 2382-2426.

[11] J. Reedijk, *Platinum Metals Review* **2008**, *52*, 2-11.

[12] G. A. Jeffrey, *An Introduction to Hydrogen Bonding*, Oxford University Press, New York, **1997**.

[13] J. W. Larson, T. B. McMahon, *Inorganic Chemistry* **1984**, *23*, 2029-2033.

[14] S. T. Desiraju Gautam, *The Weak Hydrogen Bond*, Oxford Scholarship Online, **2010**.

[15] J. L. Cook, C. A. Hunter, C. M. R. Low, A. Perez-Velasco, J. G. Vinter, *Angewandte Chemie International Edition* **2007**, *46*, 3706-3709.

[16] P. S. C. S.C. Zimmerman, *Structure and Bonding, Vol. 96*, Springer-Verlag Berlin Heidelberg New York, **2000**.

[17] T. Rehm, C. Schmuck, *Chemical Communications* **2008**, 801-813.

[18] R. P. Sijbesma, E. W. Meijer, *Chemical Communications* **2003**, 5-16.

[19] C. A. Hunter, *Angewandte Chemie International Edition* **2004**, *43*, 5310-5324.

[20] A. J. Wilson, *Soft Matter* **2007**, *3*, 409-425.

[21] W. L. Jorgensen, J. Pranata, *Journal of the American Chemical Society* **1990**, *112*, 2008-2010.

[22] J. Pranata, S. G. Wierschke, W. L. Jorgensen, *Journal of the American Chemical Society* **1991**, *113*, 2810-2819.

[23] J. Sartorius, H.-J. Schneider, *Chemistry – A European Journal* **1996**, *2*, 1446-1452.

[24] J. H. E. L. T. L. Brown, B. E. Bursten, C. J. Murphy, P. M. Woodward, *Chemistry: The Central Science*, Pearson Prentice Hall, Boston, **2012**.

[25] C. a. T. Branden, J., *Introduction to Protein Structure*, Garland Science, New York, **1999**.

[26] J. D. Watson, F. H. C. Crick, *Nature* **1953**, *171*, 737-738.

[27] C. R. Calladine, Drew, H. R., Luisi, B. and Travers, A. , *Understanding DNA: The Molecule and how it Works*, Academic Press: New York, **2004**.

[28] L. Pauling, R. B. Corey, H. R. Branson, *Proceedings of the National Academy of Sciences* **1951**, *37*, 205-211.

[29] W. Kabsch, C. Sander, *Biopolymers* **1983**, *22*, 2577-2637.

[30] https://alevelnotes.com/Protein-Structure/61, consulted 25/05/2018.

[31] M. Gellert, M. N. Lipsett, D. R. Davies, *Proceedings of the National Academy of Sciences* **1962**, *48*, 2013-2018.

[32] S. Arnott, R. Chandrasekaran, C. M. Marttila, *Biochemical Journal* **1974**, *141*, 537-543.

[33] in *Quadruplex Nucleic Acids* (Eds.: S. Neidle, S. Balasubramanian), The Royal Society of Chemistry, **2006**, pp. 1-30.

[34] S. Burge, G. N. Parkinson, P. Hazel, A. K. Todd, S. Neidle, *Nucleic Acids Research* **2006**, *34*, 5402-5415.

[35] E. H. Blackburn, *Angewandte Chemie International Edition* **2010**, *49*, 7405-7421.

[36] Y. Ducharme, J. D. Wuest, *The Journal of Organic Chemistry* **1988**, *53*, 5787-5789.

[37] B. Feibush, A. Figueroa, R. Charles, K. D. Onan, P. Feibush, B. L. Karger, *Journal of the American Chemical Society* **1986**, *108*, 3310-3318.
[38] M. C. Etter, Z. Urbanczyk-Lipkowska, M. Zia-Ebrahimi, T. W. Panunto, *Journal of the American Chemical Society* **1990**, *112*, 8415-8426.
[39] F. H. Beijer, R. P. Sijbesma, H. Kooijman, A. L. Spek, E. W. Meijer, *Journal of the American Chemical Society* **1998**, *120*, 6761-6769.
[40] M. C. Etter, S. M. Reutzel, *Journal of the American Chemical Society* **1991**, *113*, 2586-2598.
[41] J. Hine, S. Hahn, J. Hwang, *The Journal of Organic Chemistry* **1988**, *53*, 884-887.
[42] C. Fouquey, J.-M. Lehn, A.-M. Levelut, *Advanced Materials* **1990**, *2*, 254-257.
[43] J.-M. Lehn, *Makromolekulare Chemie. Macromolecular Symposia* **1993**, *69*, 1-17.
[44] S. K. Chang, A. D. Hamilton, *Journal of the American Chemical Society* **1988**, *110*, 1318-1319.
[45] S. K. Chang, D. Van Engen, E. Fan, A. D. Hamilton, *Journal of the American Chemical Society* **1991**, *113*, 7640-7645.
[46] Y. Hisamatsu, Y. Fukumi, N. Shirai, S.-i. Ikeda, K. Odashima, *Tetrahedron Letters* **2008**, *49*, 2005-2009.
[47] A. M. McGhee, C. Kilner, A. J. Wilson, *Chemical Communications* **2008**, 344-346.
[48] A. Gooch, A. M. McGhee, M. L. Pellizzaro, C. I. Lindsay, A. J. Wilson, *Organic Letters* **2011**, *13*, 240-243.
[49] T. J. Murray, S. C. Zimmerman, S. V. Kolotuchin, *Tetrahedron* **1995**, *51*, 635-648.
[50] D. A. Bell, E. V. Anslyn, *Tetrahedron* **1995**, *51*, 7161-7172.
[51] S. Djurdjevic, D. A. Leigh, H. McNab, S. Parsons, G. Teobaldi, F. Zerbetto, *Journal of the American Chemical Society* **2007**, *129*, 476-477.
[52] B. A. Blight, A. Camara-Campos, S. Djurdjevic, M. Kaller, D. A. Leigh, F. M. McMillan, H. McNab, A. M. Z. Slawin, *Journal of the American Chemical Society* **2009**, *131*, 14116-14122.
[53] F. H. Beijer, R. P. Sijbesma, J. A. J. M. Vekemans, E. W. Meijer, H. Kooijman, A. L. Spek, *The Journal of Organic Chemistry* **1996**, *61*, 6371-6380.
[54] F. H. Beijer, H. Kooijman, A. L. Spek, R. P. Sijbesma, E. W. Meijer, *Angewandte Chemie International Edition* **1998**, *37*, 75-78.
[55] P. S. Corbin, S. C. Zimmerman, *Journal of the American Chemical Society* **1998**, *120*, 9710-9711.
[56] T. Park, S. C. Zimmerman, S. Nakashima, *Journal of the American Chemical Society* **2005**, *127*, 6520-6521.
[57] T. Park, E. M. Todd, S. Nakashima, S. C. Zimmerman, *Journal of the American Chemical Society* **2005**, *127*, 18133-18142.
[58] H. C. Ong, S. C. Zimmerman, *Organic Letters* **2006**, *8*, 1589-1592.
[59] D. W. Kuykendall, C. A. Anderson, S. C. Zimmerman, *Organic Letters* **2009**, *11*, 61-64.
[60] R. P. Sijbesma, F. H. Beijer, L. Brunsveld, B. J. B. Folmer, J. H. K. K. Hirschberg, R. F. M. Lange, J. K. L. Lowe, E. W. Meijer, *Science* **1997**, *278*, 1601-1604.
[61] Henk M. Keizer, Rint P. Sijbesma, E. W. Meijer, *European Journal of Organic Chemistry* **2004**, *2004*, 2553-2555.
[62] L. Sánchez, N. Martín, D. M. Guldi, *Angewandte Chemie International Edition* **2005**, *44*, 5374-5382.
[63] S. K. Sommer, L. N. Zakharov, M. D. Pluth, *Inorganic Chemistry* **2015**, *54*, 1912-1918.
[64] A. D. Burrows, C.-W. Chan, M. M. Chowdhry, J. E. McGrady, D. M. P. Mingos, *Chemical Society Reviews* **1995**, *24*, 329-339.
[65] C.-W. Chan, D. M. P. Mingos, A. J. P. White, D. J. Williams, *Chemical Communications* **1996**, 81-83.

[66] O. M. Yaghi, H. Li, T. L. Groy, *Journal of the American Chemical Society* **1996**, *118*, 9096-9101.
[67] L. J. Marshall, J. de Mendoza, *Organic Letters* **2013**, *15*, 1548-1551.
[68] M. H. Keefe, K. D. Benkstein, J. T. Hupp, *Coordination Chemistry Reviews* **2000**, *205*, 201-228.
[69] P. A. Gale, N. Busschaert, C. J. E. Haynes, L. E. Karagiannidis, I. L. Kirby, *Chemical Society Reviews* **2014**, *43*, 205-241.
[70] X. Yan, S. Li, J. B. Pollock, T. R. Cook, J. Chen, Y. Zhang, X. Ji, Y. Yu, F. Huang, P. J. Stang, *Proceedings of the National Academy of Sciences* **2013**, *110*, 15585-15590.
[71] Z. Zhou, X. Yan, T. R. Cook, M. L. Saha, P. J. Stang, *Journal of the American Chemical Society* **2016**, *138*, 806-809.
[72] D. Appavoo, N. Raja, R. Deschenaux, B. Therrien, D. Carnevale, *Dalton Transactions* **2016**, *45*, 1410-1421.
[73] D. Appavoo, D. Carnevale, R. Deschenaux, B. Therrien, *Journal of Organometallic Chemistry* **2016**, *824*, 80-87.
[74] M. H. Kazuo, K.; Koichiso, Y.; Junichi, N., *Jpn. Kokai Tokkyo Koho* **1979**, *79*, 588.
[75] C. T. Seto, G. M. Whitesides, *Journal of the American Chemical Society* **1990**, *112*, 6409-6411.
[76] J. A. Zerkowski, C. T. Seto, G. M. Whitesides, *Journal of the American Chemical Society* **1992**, *114*, 5473-5475.
[77] C. M. Drain, K. C. Russell, J.-M. Lehn, *Chemical Communications* **1996**, 337-338.
[78] J. A. Zerkowski, C. T. Seto, D. A. Wierda, G. M. Whitesides, *Journal of the American Chemical Society* **1990**, *112*, 9025-9026.
[79] J.-M. Lehn, M. Mascal, A. Decian, J. Fischer, *Journal of the Chemical Society, Chemical Communications* **1990**, 479-481.
[80] J. P. Mathias, E. E. Simanek, J. A. Zerkowski, C. T. Seto, G. M. Whitesides, *Journal of the American Chemical Society* **1994**, *116*, 4316-4325.
[81] E. E. Simanek, M. I. M. Wazeer, J. P. Mathias, G. M. Whitesides, *The Journal of Organic Chemistry* **1994**, *59*, 4904-4909.
[82] J. A. Zerkowski, J. C. MacDonald, C. T. Seto, D. A. Wierda, G. M. Whitesides, *Journal of the American Chemical Society* **1994**, *116*, 2382-2391.
[83] G. M. Whitesides, E. E. Simanek, J. P. Mathias, C. T. Seto, D. Chin, M. Mammen, D. M. Gordon, *Accounts of Chemical Research* **1995**, *28*, 37-44.
[84] J. P. Mathias, E. E. Simanek, G. M. Whitesides, *Journal of the American Chemical Society* **1994**, *116*, 4326-4340.
[85] A. G. Bielejewska, C. E. Marjo, L. J. Prins, P. Timmerman, F. de Jong, D. N. Reinhoudt, *Journal of the American Chemical Society* **2001**, *123*, 7518-7533.
[86] P. Timmerman, Leonard J. Prins, *European Journal of Organic Chemistry* **2001**, *2001*, 3191-3205.
[87] *Chemical Communications* **2017**, *53*, 9651-9651.
[88] S. C. Zimmerman, B. F. Duerr, *The Journal of Organic Chemistry* **1992**, *57*, 2215-2217.
[89] C. T. Seto, J. P. Mathias, G. M. Whitesides, *Journal of the American Chemical Society* **1993**, *115*, 1321-1329.
[90] E. E. Simanek, L. Isaacs, X. Li, C. C. C. Wang, G. M. Whitesides, *The Journal of Organic Chemistry* **1997**, *62*, 8994-9000.
[91] W. T. S. Huck, R. Hulst, P. Timmerman, F. C. J. M. van Veggel, D. N. Reinhoudt, *Angewandte Chemie International Edition in English* **1997**, *36*, 1006-1008.
[92] H.-J. van Manen, V. Paraschiv, J. J. García-López, H. Schönherr, S. Zapotoczny, G. J. Vancso, M. Crego-Calama, D. N. Reinhoudt, *Nano Letters* **2004**, *4*, 441-446.
[93] X.-B. Shao, X.-K. Jiang, S.-Z. Zhu, Z.-T. Li, *Tetrahedron* **2004**, *60*, 9155-9162.
[94] S. Yagai, T. Karatsu, A. Kitamura, *Chemical Communications* **2003**, 1844-1845.

[95] S. Yagai, T. Nakajima, T. Karatsu, K.-i. Saitow, A. Kitamura, *Journal of the American Chemical Society* **2004**, *126*, 11500-11508.
[96] S. Yagai, T. Nakajima, K. Kishikawa, S. Kohmoto, T. Karatsu, A. Kitamura, *Journal of the American Chemical Society* **2005**, *127*, 11134-11139.
[97] S. Yagai, M. Usui, T. Seki, H. Murayama, Y. Kikkawa, S. Uemura, T. Karatsu, A. Kitamura, A. Asano, S. Seki, *Journal of the American Chemical Society* **2012**, *134*, 7983-7994.
[98] S. Yagai, S. Mahesh, Y. Kikkawa, K. Unoike, T. Karatsu, A. Kitamura, A. Ajayaghosh, *Angewandte Chemie International Edition* **2008**, *47*, 4691-4694.
[99] https://www.nobelprize.org/nobel_prizes/chemistry/laureates/1987/, consulted 25/05/2018.
[100] https://www.nobelprize.org/nobel_prizes/chemistry/laureates/2016/, consulted 25/05/2018.
[101] J.-M. Lehn, *Supramolecular Chemistry*, **1995**.
[102] J. Lehn, *Science* **1993**, *260*, 1762-1763.
[103] J. Reedijk, *Platinum Metals Rev.* **2008**, *52*, 2-11.
[104] D. R. T. Jonathan W. Steed, Karl J. Wallace, *Core concepts in supramolecular chemistry and nanochemistry*, **2007**.
[105] D. J. Cram, J. M. Cram, *Complexes between organic compounds simulate the substrate selectivity of enzymes* **1974**, *183*, 803-809.
[106] E. P. Kyba, R. C. Helgeson, K. Madan, G. W. Gokel, T. L. Tarnowski, S. S. Moore, D. J. Cram, *Journal of the American Chemical Society* **1977**, *99*, 2564-2571.
[107] C. J. Pedersen, *Journal of the American Chemical Society* **1967**, *89*, 2495-2496.
[108] C. J. Pedersen, *Journal of the American Chemical Society* **1967**, *89*, 7017-7036.
[109] B. Dietrich, J. M. Lehn, J. P. Sauvage, *Tetrahedron Letters* **1969**, *10*, 2885-2888.
[110] B. Dietrich, J. M. Lehn, J. P. Sauvage, *Tetrahedron Letters* **1969**, *10*, 2889-2892.
[111] J. R. Moran, S. Karbach, D. J. Cram, *Journal of the American Chemical Society* **1982**, *104*, 5826-5828.
[112] D. J. Cram, G. M. Lein, *Journal of the American Chemical Society* **1985**, *107*, 3657-3668.
[113] http://lcco.u-strasbg.fr/wp-content/uploads/2011/09/Cours-Supramol-copie.pdf, consulted 25/05/2018.
[114] E. C. C. a. D. Smith, *Chem. Br.* **1995**, *33*.
[115] A. W. Maverick, F. E. Klavetter, *Inorganic Chemistry* **1984**, *23*, 4129-4130.
[116] A. W. Maverick, S. C. Buckingham, Q. Yao, J. R. Bradbury, G. G. Stanley, *Journal of the American Chemical Society* **1986**, *108*, 7430-7431.
[117] R. W. Saalfrank, B. Hörner, D. Stalke, J. Salbeck, *Angewandte Chemie International Edition in English* **1993**, *32*, 1179-1182.
[118] P. Baxter, J.-M. Lehn, A. DeCian, J. Fischer, *Angewandte Chemie International Edition in English* **1993**, *32*, 69-72.
[119] M. Fujita, J. Yazaki, K. Ogura, *Journal of the American Chemical Society* **1990**, *112*, 5645-5647.
[120] S. Roche, C. Haslam, S. L. Heath, J. A. Thomas, *Chemical Communications* **1998**, 1681-1682.
[121] C. A. Hunter, *Angewandte Chemie International Edition in English* **1995**, *34*, 1079-1081.
[122] R. Wyler, J. de Mendoza, J. Rebek, *Angewandte Chemie International Edition in English* **1993**, *32*, 1699-1701.
[123] R. M. Grotzfeld, N. Branda, J. Rebek, *Science* **1996**, *271*, 487-489.
[124] M. M. Conn, J. Rebek, *Chemical Reviews* **1997**, *97*, 1647-1668.
[125] J. Chen, J. Rebek, *Organic Letters* **2002**, *4*, 327-329.
[126] R. H. Vreekamp, W. Verboom, D. N. Reinhoudt, *The Journal of Organic Chemistry* **1996**, *61*, 4282-4288.

[127] C. B. Aakeroy, A. Rajbanshi, J. Desper, *Chemical Communications* **2011**, *47*, 11411-11413.
[128] V. N. Pitchkov, *Platinum Metals Rev.* **1996**, *40*, 8.
[129] J. e. a. Meija, *Pure and Applied Chemistry* **2016**, *88*, 27.
[130] D. R. Lide, ed., *Magnetic susceptibility of the elements and inorganic compounds*, CRC Handbook of Chemistry and Physics (PDF) (86th ed.), **2005**.
[131] T. Naota, H. Takaya, S.-I. Murahashi, *Chemical Reviews* **1998**, *98*, 2599-2660.
[132] N. N. G. a. A. EARNSHAW, *Chemistry of the elements*, Butterworth Heinemann, **1998**.
[133] B. Therrien, *Coordination Chemistry Reviews* **2009**, *253*, 493-519.
[134] A. K. Singh, D. S. Pandey, Q. Xu, P. Braunstein, *Coordination Chemistry Reviews* **2014**, *270–271*, 31-56.
[135] A. Kisova, L. Zerzankova, A. Habtemariam, P. J. Sadler, V. Brabec, J. Kasparkova, *Molecular Pharmaceutics* **2011**, *8*, 949-957.
[136] M. Fujita, M. Tominaga, A. Hori, B. Therrien, *Accounts of Chemical Research* **2005**, *38*, 369-378.
[137] M. A. Bennett, *Coordination Chemistry Reviews* **1997**, *166*, 225-254.
[138] A. M. Pizarro, A. Habtemariam, P. J. Sadler, in *Medicinal Organometallic Chemistry* (Eds.: G. Jaouen, N. Metzler-Nolte), Springer Berlin Heidelberg, Berlin, Heidelberg, **2010**, pp. 21-56.
[139] E. O. Fischer, R. Böttcher, *Zeitschrift für anorganische und allgemeine Chemie* **1957**, *291*, 305-309.
[140] T. A. Stephenson, E. Switkes, *Inorganic and Nuclear Chemistry Letters* **1971**, *7*, 805-809.
[141] G. Winkhaus, H. Singer, *Journal of Organometallic Chemistry* **1967**, *7*, 487-491.
[142] R. A. Zelonka, M. C. Baird, *Journal of Organometallic Chemistry* **1972**, *35*, C43-C46.
[143] M. A. Bennett, G. B. Robertson, A. K. Smith, *Journal of Organometallic Chemistry* **1972**, *43*, C41-C43.
[144] M. A. Bennett, A. K. Smith, *Journal of the Chemical Society, Dalton Transactions* **1974**, 233-241.
[145] M. A. Bennett, L. Y. Goh, I. J. McMahon, T. R. B. Mitchell, G. B. Robertson, T. W. Turney, A. Wickramasinghe Wasantha, *Organometallics* **1992**, *11*, 3069-3085.
[146] P. Kumar, R. K. Gupta, D. S. Pandey, *Chemical Society Reviews* **2014**, *43*, 707-733.
[147] C. G. Hartinger, P. J. Dyson, *Chemical Society Reviews* **2009**, *38*, 391-401.
[148] N. P. E. Barry, P. J. Sadler, *Chemical Communications* **2013**, *49*, 5106-5131.
[149] P. C. A. Bruijnincx, P. J. Sadler, *Current Opinion in Chemical Biology* **2008**, *12*, 197-206.
[150] B. S. Murray, M. V. Babak, C. G. Hartinger, P. J. Dyson, *Coordination Chemistry Reviews* **2016**, *306*, 86-114.
[151] C. S. Allardyce, P. J. Dyson, D. J. Ellis, S. L. Heath, *Chemical Communications* **2001**, 1396-1397.
[152] G. Suss-Fink, *Dalton Transactions* **2010**, *39*, 1673-1688.
[153] C. Scolaro, A. Bergamo, L. Brescacin, R. Delfino, M. Cocchietto, G. Laurenczy, T. J. Geldbach, G. Sava, P. J. Dyson, *Journal of Medicinal Chemistry* **2005**, *48*, 4161-4171.
[154] A. Weiss, R. H. Berndsen, M. Dubois, C. Muller, R. Schibli, A. W. Griffioen, P. J. Dyson, P. Nowak-Sliwinska, *Chemical Science* **2014**, *5*, 4742-4748.
[155] A. Weiss, X. Ding, J. R. van Beijnum, I. Wong, T. J. Wong, R. H. Berndsen, O. Dormond, M. Dallinga, L. Shen, R. O. Schlingemann, R. Pili, C.-M. Ho, P. J. Dyson, H. van den Bergh, A. W. Griffioen, P. Nowak-Sliwinska, *Angiogenesis* **2015**, *18*, 233-244.
[156] R. E. Morris, R. E. Aird, P. del Socorro Murdoch, H. Chen, J. Cummings, N. D. Hughes, S. Parsons, A. Parkin, G. Boyd, D. I. Jodrell, P. J. Sadler, *Journal of Medicinal Chemistry* **2001**, *44*, 3616-3621.
[157] R. E. Aird, J. Cummings, A. A. Ritchie, M. Muir, R. E. Morris, H. Chen, P. J. Sadler, D. I. Jodrell, *British Journal of Cancer* **2002**, *86*, 1652-1657.

[158] F. Wang, A. Habtemariam, E. P. L. van der Geer, R. Fernández, M. Melchart, R. J. Deeth, R. Aird, S. Guichard, F. P. A. Fabbiani, P. Lozano-Casal, I. D. H. Oswald, D. I. Jodrell, S. Parsons, P. J. Sadler, *Proceedings of the National Academy of Sciences of the United States of America* **2005**, *102*, 18269-18274.
[159] H. Yan, G. Suss-Fink, A. Neels, H. Stoeckli-Evans, *Journal of the Chemical Society, Dalton Transactions* **1997**, 4345-4350.
[160] B. Therrien, *European Journal of Inorganic Chemistry* **2009**, *2009*, 2445-2453.
[161] A. Mishra, S. C. Kang, K.-W. Chi, *European Journal of Inorganic Chemistry* **2013**, *2013*, 5222-5232.
[162] S. Mirtschin, A. Slabon-Turski, R. Scopelliti, A. H. Velders, K. Severin, *Journal of the American Chemical Society* **2010**, *132*, 14004-14005.
[163] B. Therrien, G. Süss-Fink, P. Govindaswamy, A. K. Renfrew, P. J. Dyson, *Angewandte Chemie International Edition* **2008**, *47*, 3773-3776.
[164] J. Mattsson, P. Govindaswamy, J. Furrer, Y. Sei, K. Yamaguchi, G. Süss-Fink, B. Therrien, *Organometallics* **2008**, *27*, 4346-4356.
[165] N. P. E. Barry, B. Therrien, *European Journal of Inorganic Chemistry* **2009**, *2009*, 4695-4700.
[166] F. Kühlwein, K. Polborn, W. Beck, *Zeitschrift für anorganische und allgemeine Chemie* **1997**, *623*, 1931-1944.
[167] N. P. E. Barry, J. Furrer, B. Therrien, *Helvetica Chimica Acta* **2010**, *93*, 1313-1328.
[168] E. Orhan, A. Garci, T. Riedel, M. Soudani, P. J. Dyson, B. Therrien, *Journal of Organometallic Chemistry* **2016**, *803*, 39-44.
[169] A. Garci, A. A. Dobrov, T. Riedel, E. Orhan, P. J. Dyson, V. B. Arion, B. Therrien, *Organometallics* **2014**, *33*, 3813-3822.
[170] V. Mannancherril, B. Therrien, *Inorganic Chemistry* **2017**.
[171] B. Kilbas, S. Mirtschin, T. Riis-Johannessen, R. Scopelliti, K. Severin, *Inorganic Chemistry* **2012**, *51*, 5795-5804.
[172] B. Kilbas, S. Mirtschin, R. Scopelliti, K. Severin, *Chemical Science* **2012**, *3*, 701-704.
[173] S. R. Seidel, P. J. Stang, *Accounts of Chemical Research* **2002**, *35*, 972-983.
[174] M. Fujita, M. Yoshizawa, in *Modern Supramolecular Chemistry*, Wiley-VCH Verlag GmbH & Co. KGaA, **2008**, pp. 277-313.
[175] M. Fujita, D. Oguro, M. Miyazawa, H. Oka, K. Yamaguchi, K. Ogura, *Nature* **1995**, *378*, 469.
[176] F. Ibukuro, T. Kusukawa, M. Fujita, *Journal of the American Chemical Society* **1998**, *120*, 8561-8562.
[177] R. Chakrabarty, P. S. Mukherjee, P. J. Stang, *Chemical Reviews* **2011**, *111*, 6810-6918.
[178] S. Leininger, B. Olenyuk, P. J. Stang, *Chemical Reviews* **2000**, *100*, 853-908.
[179] B. Therrien, *Coordination Chemistry Reviews* **2009**, *253*, 493-519.
[180] J. Mattsson, P. Govindaswamy, A. K. Renfrew, P. J. Dyson, P. Štěpnička, G. Süss-Fink, B. Therrien, *Organometallics* **2009**, *28*, 4350-4357.
[181] A. Garci, G. Gupta, C. Dalvit, B. Therrien, *European Journal of Inorganic Chemistry* **2014**, *2014*, 5626-5626.
[182] P. Govindaswamy, D. Linder, J. Lacour, G. Suss-Fink, B. Therrien, *Chemical Communications* **2006**, 4691-4693.
[183] P. Govindaswamy, G. Süss-Fink, B. Therrien, *Organometallics* **2007**, *26*, 915-924.
[184] B. Therrien, G. Süss‐Fink, P. Govindaswamy, A. K. Renfrew, P. J. Dyson, *Angewandte Chemie International Edition* **2008**, *47*, 3773-3776.
[185] J. Mattsson, O. Zava, A. K. Renfrew, Y. Sei, K. Yamaguchi, P. J. Dyson, B. Therrien, *Dalton Transactions* **2010**, *39*, 8248-8255.
[186] B. Therrien, in *Chemistry of Nanocontainers* (Eds.: M. Albrecht, E. Hahn), Springer Berlin Heidelberg, Berlin, Heidelberg, **2012**, pp. 35-55.

[187] Y. Matsumura, H. Maeda, *Cancer Research* **1986**, *46*, 6387-6392.
[188] H. Maeda, G. Y. Bharate, J. Daruwalla, *European Journal of Pharmaceutics and Biopharmaceutics* **2009**, *71*, 409-419.
[189] B. Therrien, *Chemistry – A European Journal* **2013**, *19*, 8378-8386.
[190] F. Schmitt, J. Freudenreich, N. P. E. Barry, L. Juillerat-Jeanneret, G. Süss-Fink, B. Therrien, *Journal of the American Chemical Society* **2012**, *134*, 754-757.
[191] B. Therrien, J. Furrer, *Advances in Chemistry* **2014**, *2014*, 20.
[192] in *Ullmann's Encyclopedia of Industrial Chemistry*.
[193] K. Severin, R. Bergs, W. Beck, *Angewandte Chemie International Edition* **1998**, *37*, 1634-1654.
[194] G. Gupta, A. Garci, B. S. Murray, P. J. Dyson, G. Fabre, P. Trouillas, F. Giannini, J. Furrer, G. Suss-Fink, B. Therrien, *Dalton Transactions* **2013**, *42*, 15457-15463.
[195] A. Y. C. WHITE, * and P. M. MAITLIS*, C. b. D. M. HEINEKEYt, in *Inorganic Syntheses, Vol. 29*, **1992**, pp. 228-234.
[196] Z. Liu, A. Habtemariam, A. M. Pizarro, G. J. Clarkson, P. J. Sadler, *Organometallics* **2011**, *30*, 4702-4710.
[197] C.-H. Leung, H.-J. Zhong, D. S.-H. Chan, D.-L. Ma, *Coordination Chemistry Reviews* **2013**, *257*, 1764-1776.
[198] S. J. Lucas, R. M. Lord, R. L. Wilson, R. M. Phillips, V. Sridharan, P. C. McGowan, *Dalton Transactions* **2012**, *41*, 13800-13802.
[199] R. Payne, P. Govender, B. Therrien, C. M. Clavel, P. J. Dyson, G. S. Smith, *Journal of Organometallic Chemistry* **2013**, *729*, 20-27.
[200] G. Gupta, B. S. Murray, P. J. Dyson, B. Therrien, *Journal of Organometallic Chemistry* **2014**, *767*, 78-82.
[201] G. Gupta, B. Murray, P. Dyson, B. Therrien, *Materials* **2013**, *6*, 5352.
[202] G. Gupta, J. M. Kumar, A. Garci, N. Rangaraj, N. Nagesh, B. Therrien, *ChemPlusChem* **2014**, *79*, 610-618.
[203] G. Gupta, G. S. Oggu, N. Nagesh, K. K. Bokara, B. Therrien, *CrystEngComm* **2016**, *18*, 4952-4957.
[204] J.-M. Lehn, *Science* **2002**, *295*, 2400-2403.
[205] J. D. Badjić, A. Nelson, S. J. Cantrill, W. B. Turnbull, J. F. Stoddart, *Accounts of Chemical Research* **2005**, *38*, 723-732.
[206] D. N. Reinhoudt, M. Crego-Calama, *Science* **2002**, *295*, 2403-2407.
[207] E. R. Kay, D. A. Leigh, F. Zerbetto, *Angewandte Chemie International Edition* **2007**, *46*, 72-191.
[208] H.-J. Schneider, *Angewandte Chemie International Edition* **2009**, *48*, 3924-3977.
[209] J.-M. Lehn, *Angewandte Chemie International Edition* **2013**, *52*, 2836-2850.
[210] M. Yoshizawa, J. K. Klosterman, M. Fujita, *Angewandte Chemie International Edition* **2009**, *48*, 3418-3438.
[211] H. Amouri, C. Guyard-Duhayon, J. Vaissermann, M. N. Rager, *Inorganic Chemistry* **2002**, *41*, 1397-1403.
[212] H. Amouri, C. Desmarets, J. Moussa, *Chemical Reviews* **2012**, *112*, 2015-2041.
[213] K. Severin, *Chemical Communications* **2006**, 3859-3867.
[214] A. Pitto-Barry, N. P. E. Barry, V. Russo, B. Heinrich, B. Donnio, B. Therrien, R. Deschenaux, *Journal of the American Chemical Society* **2014**, *136*, 17616-17625.
[215] T. R. Cook, V. Vajpayee, M. H. Lee, P. J. Stang, K.-W. Chi, *Accounts of Chemical Research* **2013**, *46*, 2464-2474.
[216] B. Therrien, *CrystEngComm* **2015**, *17*, 484-491.
[217] D. C. Sherrington, K. A. Taskinen, *Chemical Society Reviews* **2001**, *30*, 83-93.
[218] K. Aratsu, D. D. Prabhu, H. Iwawaki, X. Lin, M. Yamauchi, T. Karatsu, S. Yagai, *Chemical Communications* **2016**, *52*, 8211-8214.

[219] B. Therrien, T. R. Ward, *Angewandte Chemie International Edition* **1999**, *38*, 405-408.
[220] K. F. Morris, C. S. Johnson, *Journal of the American Chemical Society* **1992**, *114*, 3139-3141.
[221] D. T. Thierry Gostan, Emmanuel Brun, Yann Prigent, Marc-André Delsuc, *Spectra analyse*, *240*, 9.
[222] W. Sun, H. Zhu, P. M. Barron, *Chemistry of Materials* **2006**, *18*, 2602-2610.
[223] I. Mathew, Y. Li, Z. Li, W. Sun, *Dalton Transactions* **2010**, *39*, 11201-11209.
[224] G. Gupta, S. Gloria, S. L. Nongbri, B. Therrien, K. M. Rao, *Journal of Organometallic Chemistry* **2011**, *696*, 2014-2022.
[225] F. Schmitt, P. Govindaswamy, G. Süss-Fink, W. H. Ang, P. J. Dyson, L. Juillerat-Jeanneret, B. Therrien, *Journal of Medicinal Chemistry* **2008**, *51*, 1811-1816.
[226] P. Timmerman, K. A. Jolliffe, M. Crego Calama, J.-L. Weidmann, L. J. Prins, F. Cardullo, B. H. M. Snellink-Ruël, R. H. Fokkens, N. M. M. Nibbering, S. Shinkai, D. N. Reinhoudt, *Chemistry – A European Journal* **2000**, *6*, 4104-4115.
[227] K. A. Jolliffe, M. C. Calama, R. Fokkens, N. M. M. Nibbering, P. Timmerman, D. N. Reinhoudt, *Angewandte Chemie International Edition* **1998**, *37*, 1247-1251.
[228] F. Zhang, B. Therrien, *European Journal of Inorganic Chemistry* **2017**, *2017*, 3214-3221.
[229] D. Kost, E. H. Carlson, M. Raban, *Journal of the Chemical Society D: Chemical Communications* **1971**, 656-657.
[230] Y. Cohen, L. Avram, L. Frish, *Angewandte Chemie International Edition* **2005**, *44*, 520-554.
[231] H. Eyring, *The Journal of Chemical Physics* **1935**, *3*, 107-115.
[232] G. Süss-Fink, *Journal of Organometallic Chemistry* **2014**, *751*, 2-19.
[233] M. Patra, T. Joshi, V. Pierroz, K. Ingram, M. Kaiser, S. Ferrari, B. Spingler, J. Keiser, G. Gasser, *Chemistry – A European Journal* **2013**, *19*, 14768-14772.
[234] A. Bacchi, C. Loffi, P. Pagano, P. Pelagatti, F. Scè, *Journal of Organometallic Chemistry* **2015**, *778*, 1-9.
[235] A. Bacchi, D. Capucci, A. Gatti, C. Loffi, M. Pioli, D. Rogolino, F. Terenziani, P. Pelagatti, *ChemistrySelect* **2017**, *2*, 7000-7007.
[236] R. Pettinari, A. Petrini, F. Marchetti, C. Pettinari, T. Riedel, B. Therrien, P. J. Dyson, *European Journal of Inorganic Chemistry* **2017**, *2017*, 1800-1806.
[237] R. D. D. Appavoo, B. Therrien, *Studia UBB Chemia* **2015**, *4*, 10.
[238] M. Gras, B. Therrien, G. Süss-Fink, A. Casini, F. Edafe, P. J. Dyson, *Journal of Organometallic Chemistry* **2010**, *695*, 1119-1125.
[239] L. Ezzedinloo, S. Shrestha, M. Bhadbhade, S. Colbran, *Acta Crystallographica Section E* **2014**, *70*, m14-m15.
[240] L. E. H. Paul, B. Therrien, J. Furrer, *Inorganica Chimica Acta* **2018**, *469*, 1-10.
[241] G. S. Smith, B. Therrien, *Dalton Transactions* **2011**, *40*, 10793-10800.
[242] G. Gupta, E. Denoyelle-Di-Muro, J.-P. Mbakidi, S. Leroy-Lhez, V. Sol, B. Therrien, *Journal of Organometallic Chemistry* **2015**, *787*, 44-50.
[243] G. Gupta, J. Kumar, A. Garci, N. Nagesh, B. Therrien, *Molecules* **2014**, *19*, 6031.
[244] F. Zhang, B. Therrien, *European Journal of Inorganic Chemistry* **2018**, *2018*, 2399-2407.
[245] V. Mannancherril, B. Therrien, *Inorganic Chemistry* **2018**, *57*, 3626-3633.
[246] C. T. Seto, G. M. Whitesides, *Journal of the American Chemical Society* **1993**, *115*, 905-916.
[247] C. B. Aakeröy, N. Schultheiss, J. Desper, *Inorganic Chemistry* **2005**, *44*, 4983-4991.
[248] M. A. Bennett, T. N. Huang, T. W. Matheson, A. K. Smith, S. Ittel, W. Nickerson, in *Inorganic Syntheses*, John Wiley & Sons, Inc., **2007**, pp. 74-78.
[249] J. W. Kang, K. Moseley, P. M. Maitlis, *Journal of the American Chemical Society* **1969**, *91*, 5970-5977.

[250] B. L. Booth, R. N. Haszeldine, M. Hill, *Journal of Organometallic Chemistry* **1969**, *16*, 491-496.
[251] W. D. Jones, V. L. Kuykendall, *Inorganic Chemistry* **1991**, *30*, 2615-2622.
[252] G. Sheldrick, *Acta Crystallographica Section A* **2008**, *64*, 112-122.
[253] L. Farrugia, *Journal of Applied Crystallography* **1997**, *30*, 565.

List of abbreviations

IUPAC : International union of pure and applied chemistry

NMR : Nuclear magnetic resonance

DMSO : Dimethyl sulfoxide

THF : Tetrahydrofuran

UPy : Ureidopyrimidinone

G-C : Guanine-cytosine

A-T : Adenine-thymine

D : Donor

A : Acceptor

DNA : Deoxyribonucleic acid

G : Guanines

DeAP : Deazapterin

DAN : 2,7-Diamido-1,8-naphthyridine

UG : Butylurea of guanosine

DeUG : Ureido-7-deazaguanine

DFT : Density functional theory

CA: Isocyanuric acid

M : Melamine

BA : 5,5-Diethylbarbituric acid

VPO : Vapor pressure osmometry

GPC : Gel permeation chromatographic

TPP: Tetraphenyl porphyrin

NOESY : Nuclear overhauser effect spectroscopy

UV/Vis : Ultraviolet/visible

PBI : Perylene 3,4,9,10-tetracarboxylic acid bisimide

OPE : Oligo(*p*-phenyleneethynylene)

AFM : Atomic force microscopy

Et : Ethyl

PTA : 1,3,5-Triaza-7-phosphaadamantane

MCa : Mucinous carcinoma associated antigen

DIPEA : *N*,*N*-Diisopropylethylamine

dobq : 2,5-Dioxydo-1,4-benzoquinonato

dClobq : 2,5-Dichlorido-1,4-benzoquinonato

dhbq : 2,5-Dihydroxy-1,4-benzoquinonato

dchq : 2,5-Dichloro-1,4-benzoquinonato

dhnq: 5,8-Dihydroxy-1,4-naphthoquinonato

dhaq : 9,10-Dihydroxy-1,4-anthraquinonato

dhtq : 6,11-Dihydroxynaphthacene-5,12-dionato

cym : 1-Methyl-4-(propan-2-yl)benzene

3D : Three dimensional

2D : Two dimensional

Hmb : 1,2,3,4,5,6-Hexamethylbenzene

pyr : Pyrazine

bpy : 4-4'-Bipyridine

bpe : 1,2-Bis(4-pyridyl)ethylene

tpt : 2,4,6-Tri(pyridyl)-1,3,5-triazine

EPR : Enhanced permeability and retention

Cp* : 1,2,3,4,5-Pentamethylcyclopentadienyl

Cp : Cyclopentadienyl

ppy : 2-Phenylpyridine

pmp : 2-[(Propylimino)methyl]phenol

ctDNA : Circulating tumor DNA

ME : *N,N'*-bis(4-*tert*-butylphenyl)melamine

BApy : 5-Butyl-5-(pyridin-4-ylmethyl)pyrimidine-2,4,6-trione

Ph : Phenyl

DOSY : Diffusion ordered spectroscopy

IR : Infrared

MLCT : Metal-to-ligand charge transfer

ILCT : Intra-ligand charge transfer

RX : Rayon X

ESI : Electrospray ionization

MALDI-TOF : Matrix assisted laser desorption/ionization – time of flight

MEpy : *N*-(4-*tert*-butylphenyl)-*N'*-(pyridine-4-ylmethyl)melamine

Me : Methyl

MEbispy : *N,N'*-Bis{4-[(5-methoxypyridin-3-yl)ethynyl]phenyl}melamine

H_2L^A : *N,N'*-dihexyloxalamide

H_2L^B : *N,N'*-dioctyloxalamide

H_2L^C : 2,5-Dihydroxy-3-icosylcyclohexa-2,5-diene-1,4-dione

FTIR : Fourier-transform infrared spectroscopy

ETH : Swiss federal institute of technology

Sol : Solvent

ORTEP : Oak ridge thermal-ellipsoid plot program

List of structures

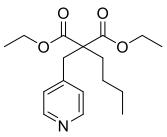

Diethyl 2-butyl-2-(pyridin-4-ylmethyl) malonate

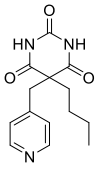

BApy

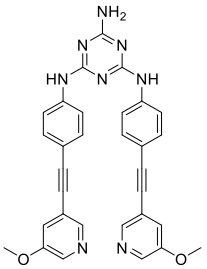

MEbispy

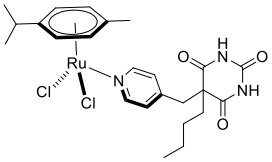

BApyRu

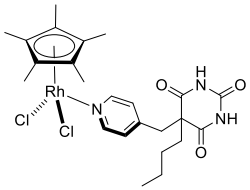

BApyRh

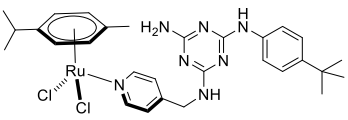

MEpyRu

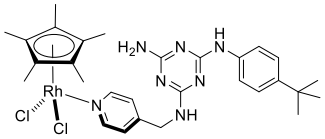

MEpyRh

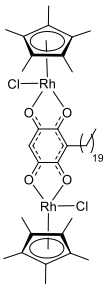

Rh_2L^C

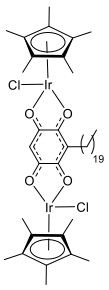

Ir_2L^C

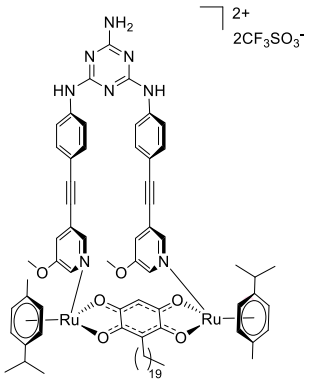

$MEbispyRu_2L^C$

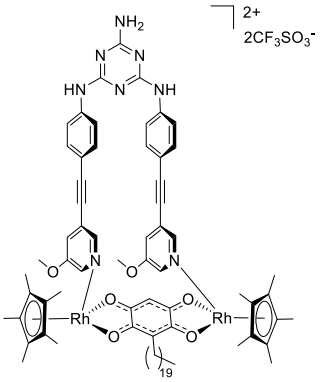

$MEbispyRh_2L^C$

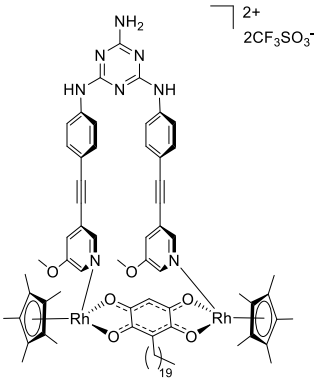

$MEbispyIr_2L^C$

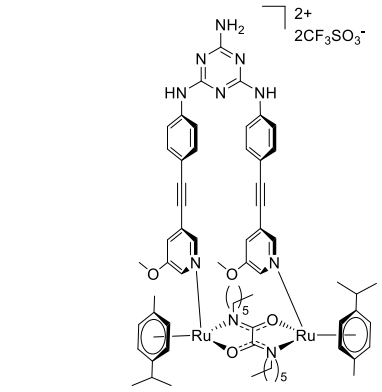

MEbispyRu$_2$L^A

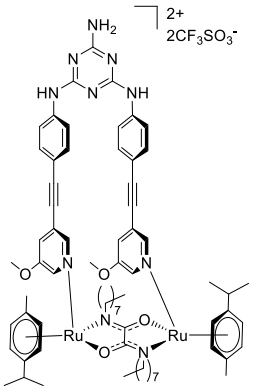

MEbispyRu$_2$L^B

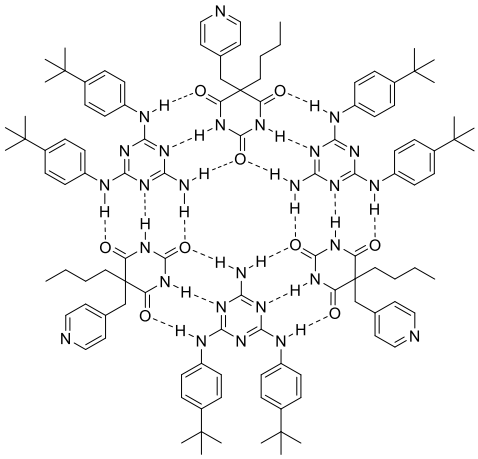

(ME)$_3$ · (BApy)$_3$

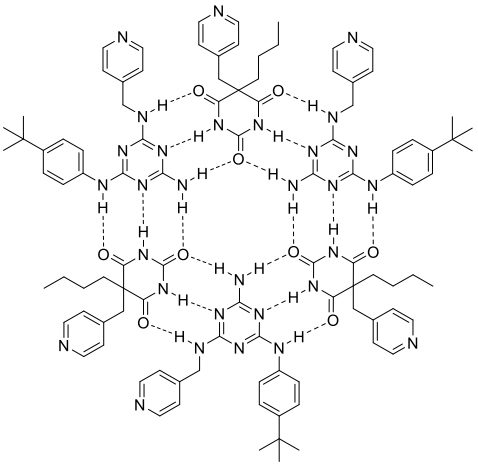

(MEpy)$_3$ · (BApy)$_3$

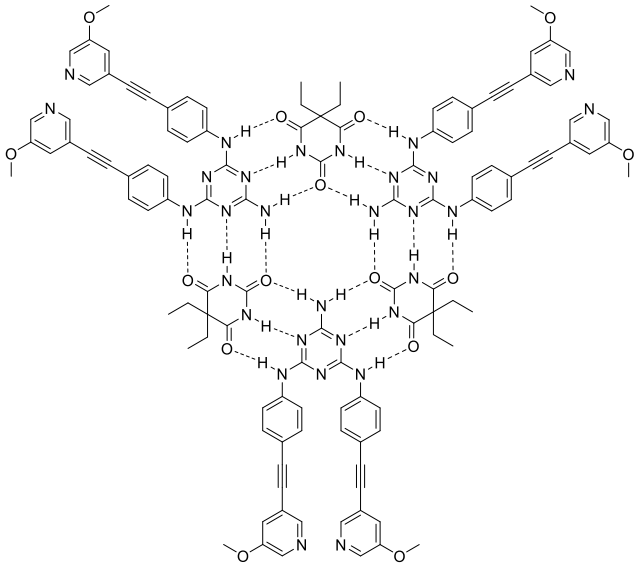

(MEbispy)$_3$ · (BA)$_3$

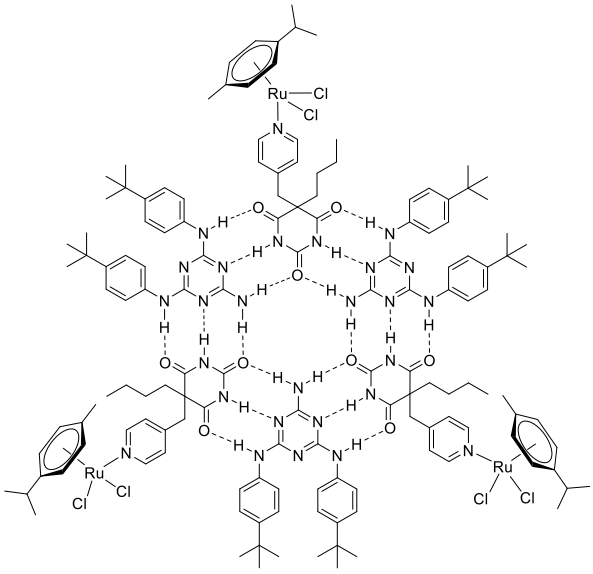

$(ME)_3 \cdot (BApyRu)_3$

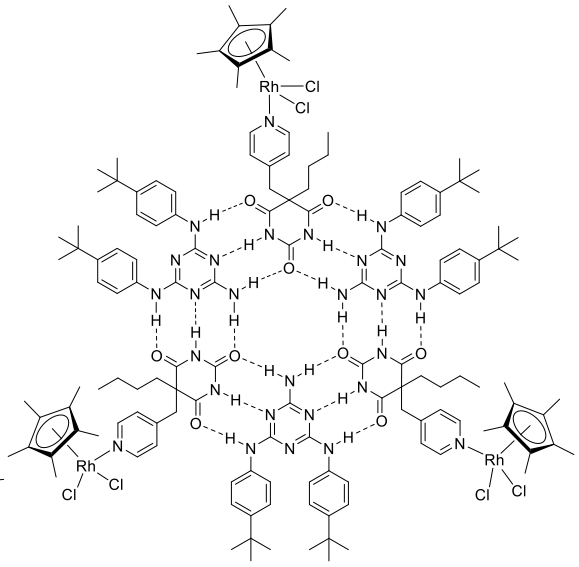

$(ME)_3 \cdot (BApyRh)_3$

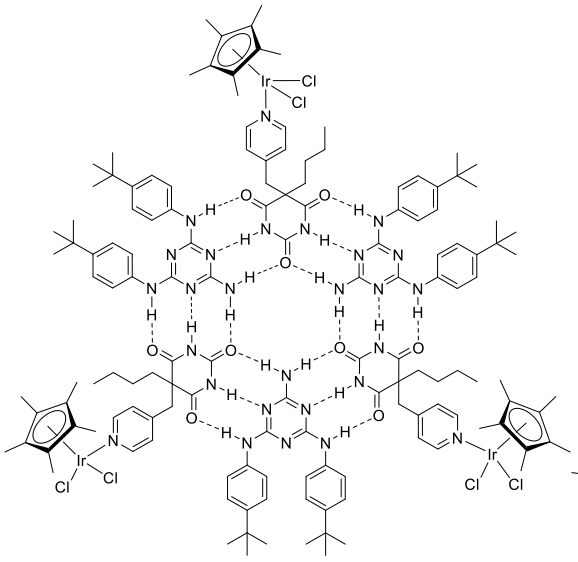

$(ME)_3 \cdot (BApyIr)_3$

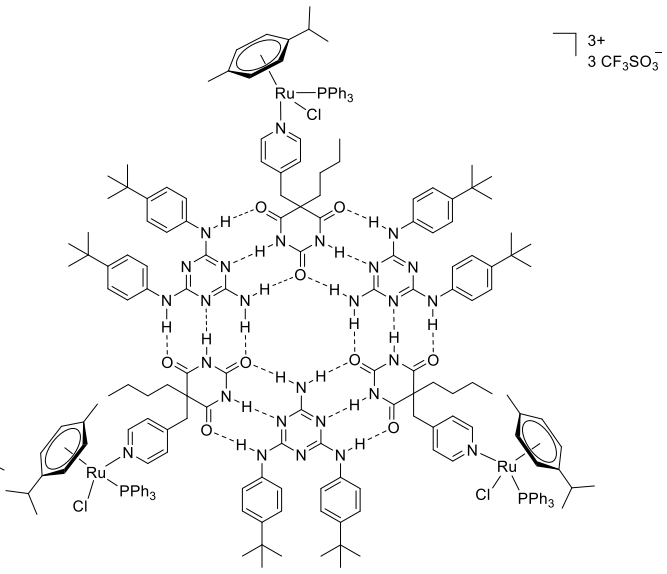

$\{(ME)_3 \cdot [(BApy)Ru(cym)(PPh_3)Cl]_3\} \cdot (3CF_3SO_3)$

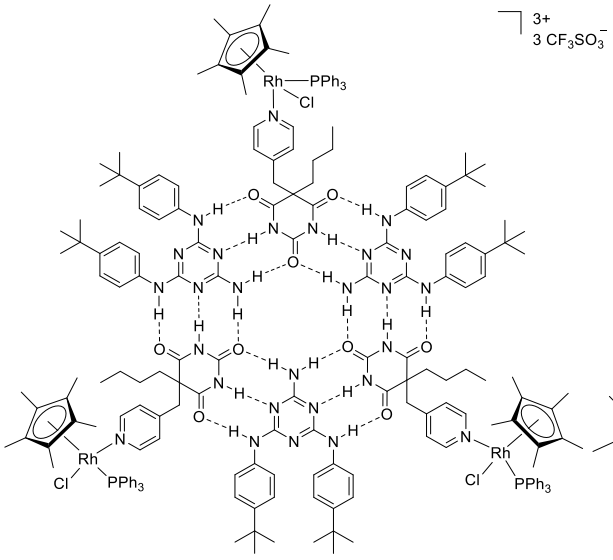

$\{(ME)_3 \cdot [(BApy)Rh(Cp^*)(PPh_3)Cl]_3\} \cdot (3CF_3SO_3)$

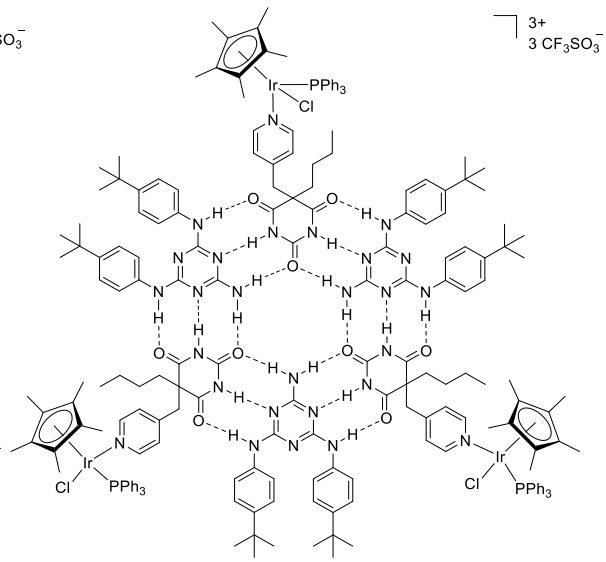

$\{(ME)_3 \cdot [(BApy)Ir(Cp^*)(PPh_3)Cl]_3\} \cdot (3CF_3SO_3)$

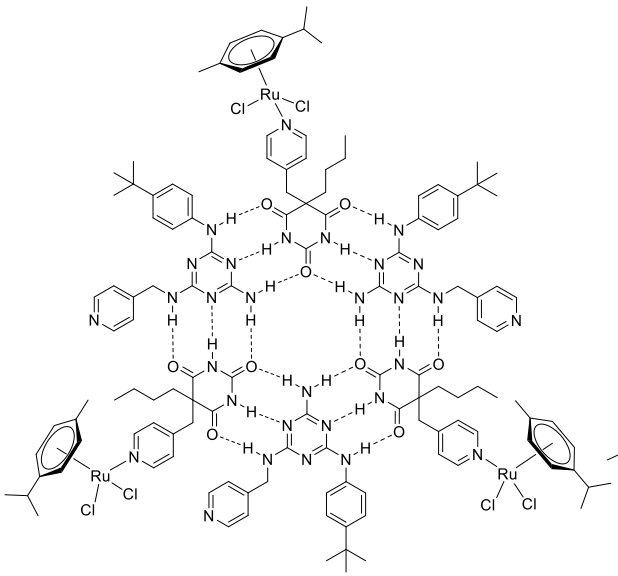

(MEpy)$_3$ · (BApyRu)$_3$

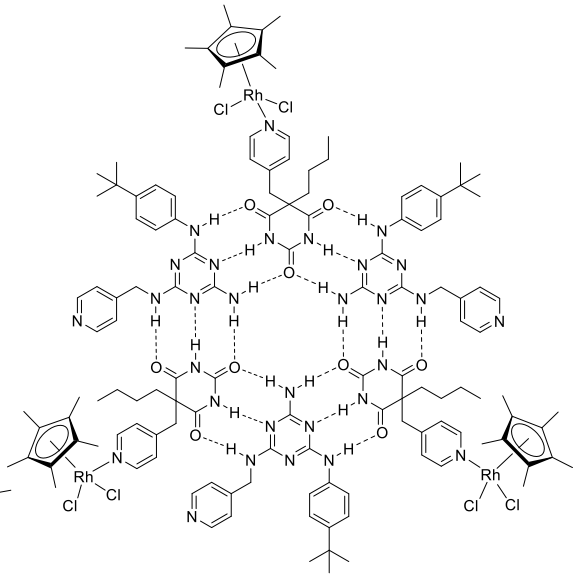

(MEpy)$_3$ · (BApyRh)$_3$

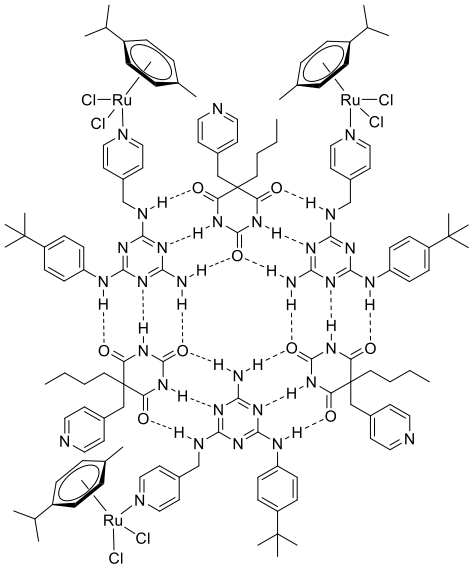

(MEpyRu)$_3$ · (BApy)$_3$

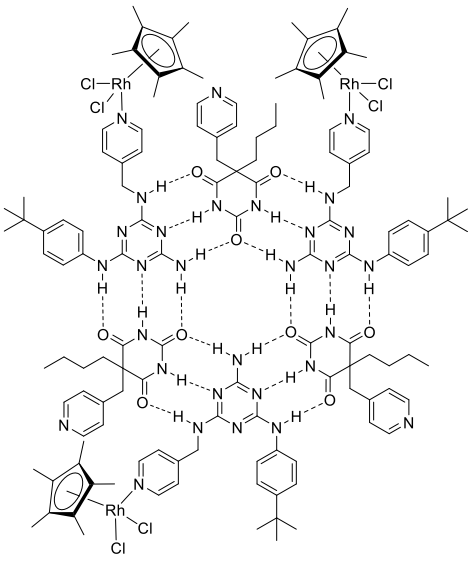

(MEpyRh)$_3$ · (BApy)$_3$

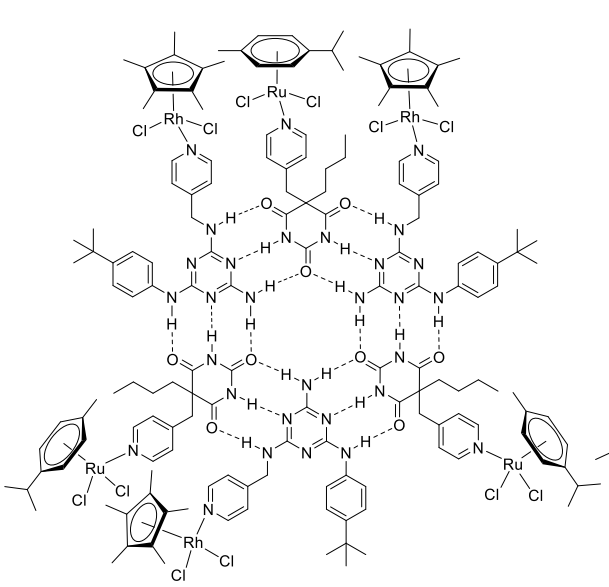

$(MEpyRh)_3 \cdot (BApyRu)_3$

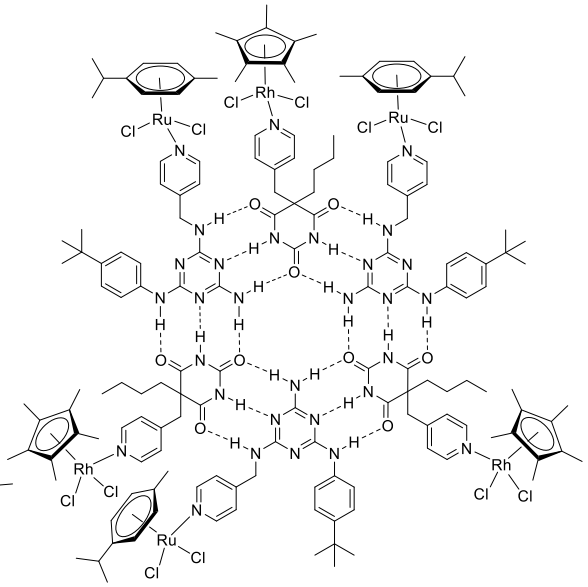

$(MEpyRu)_3 \cdot (BApyRh)_3$

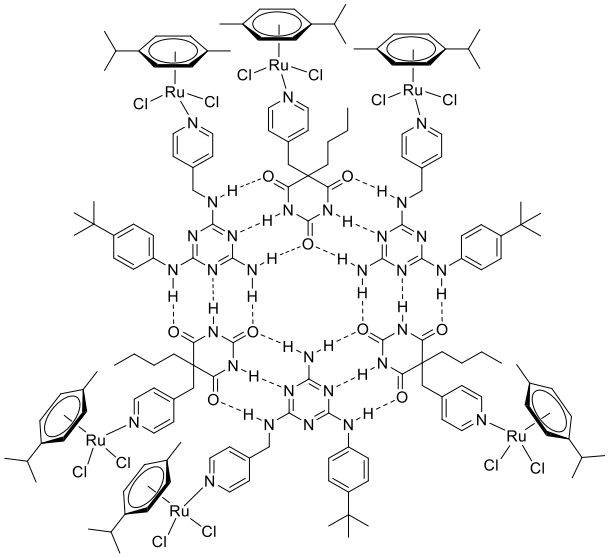

$(MEpyRu)_3 \cdot (BApyRu)_3$

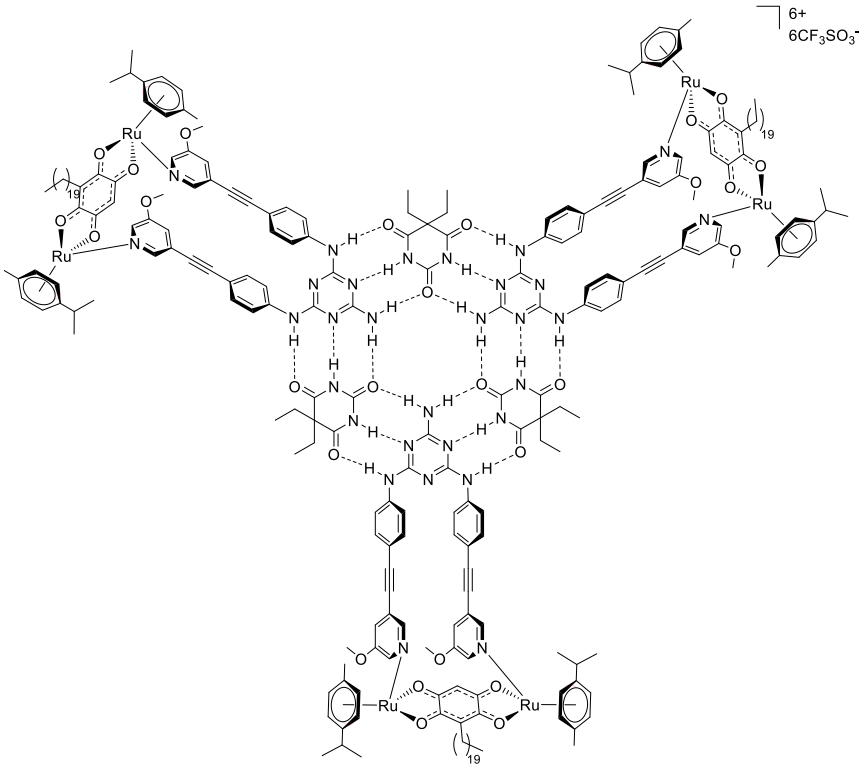

(MEbispyRu$_2$L^C)$_3$· (BA)$_3$

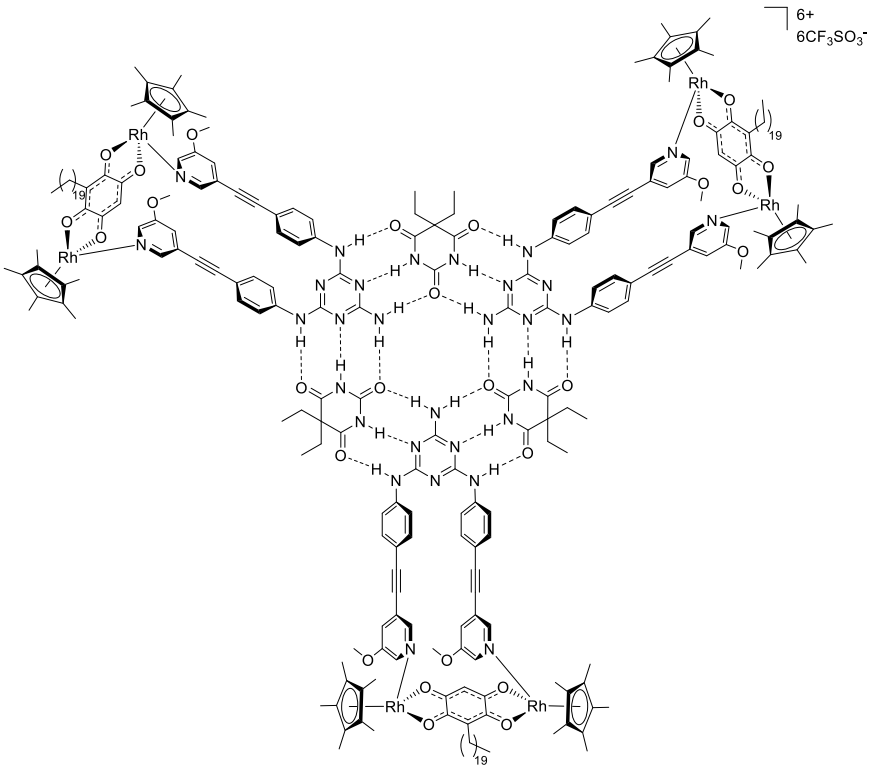

(MEbispyRh$_2$L^C)$_3$ · (BA)$_3$

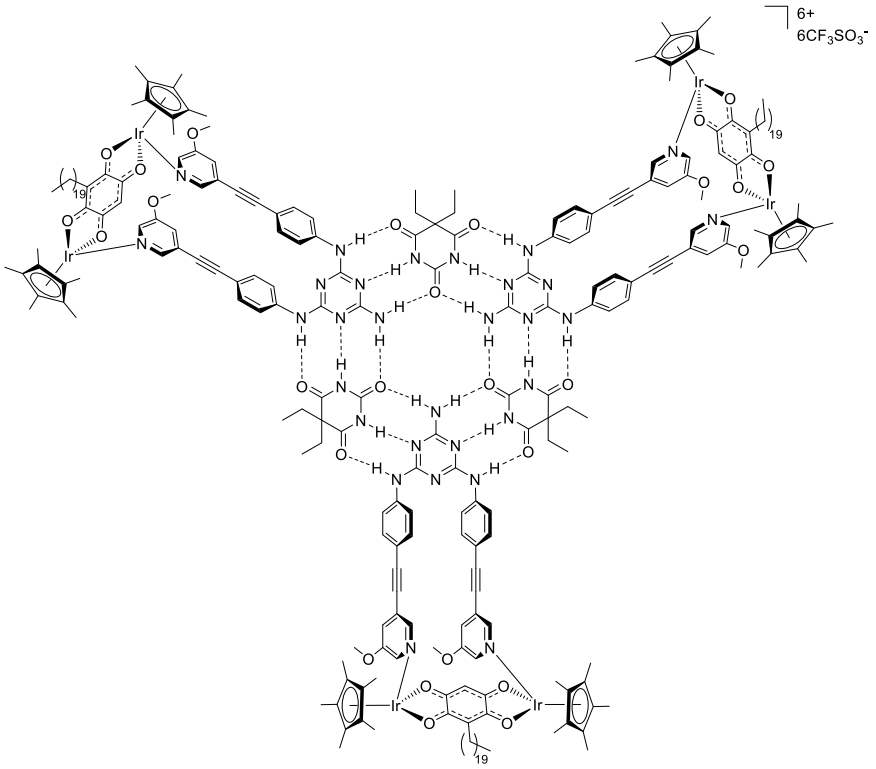

(MEbispyIr$_2$L^C)$_3$ · (BA)$_3$

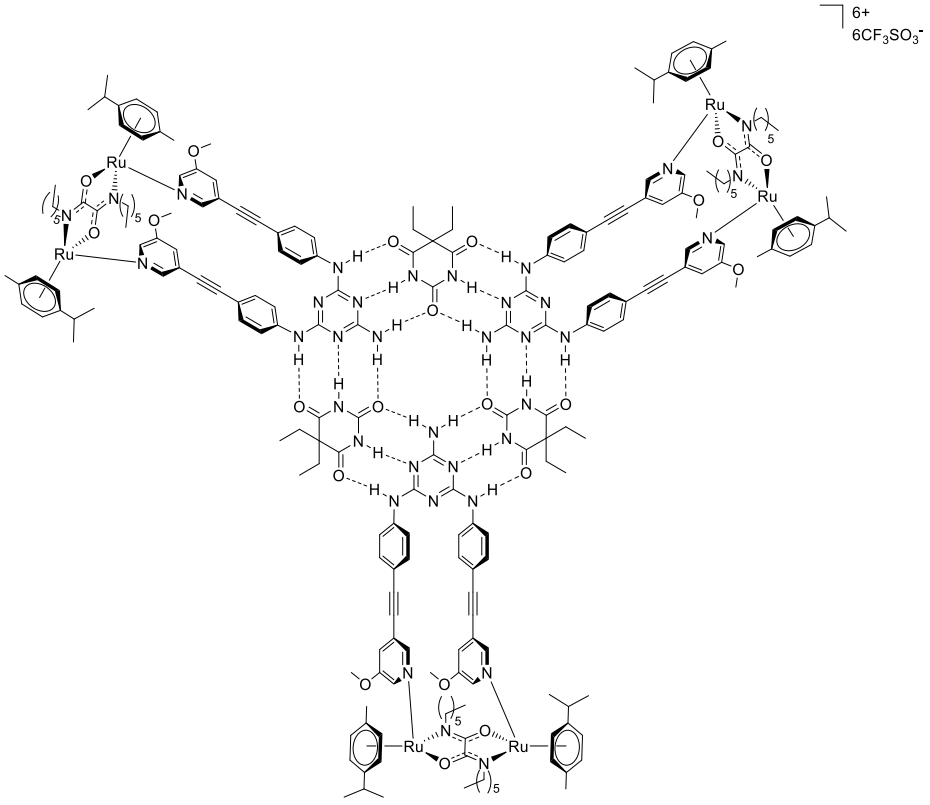

(MEbispyRu$_2$L^A)$_3$ · (BA)$_3$

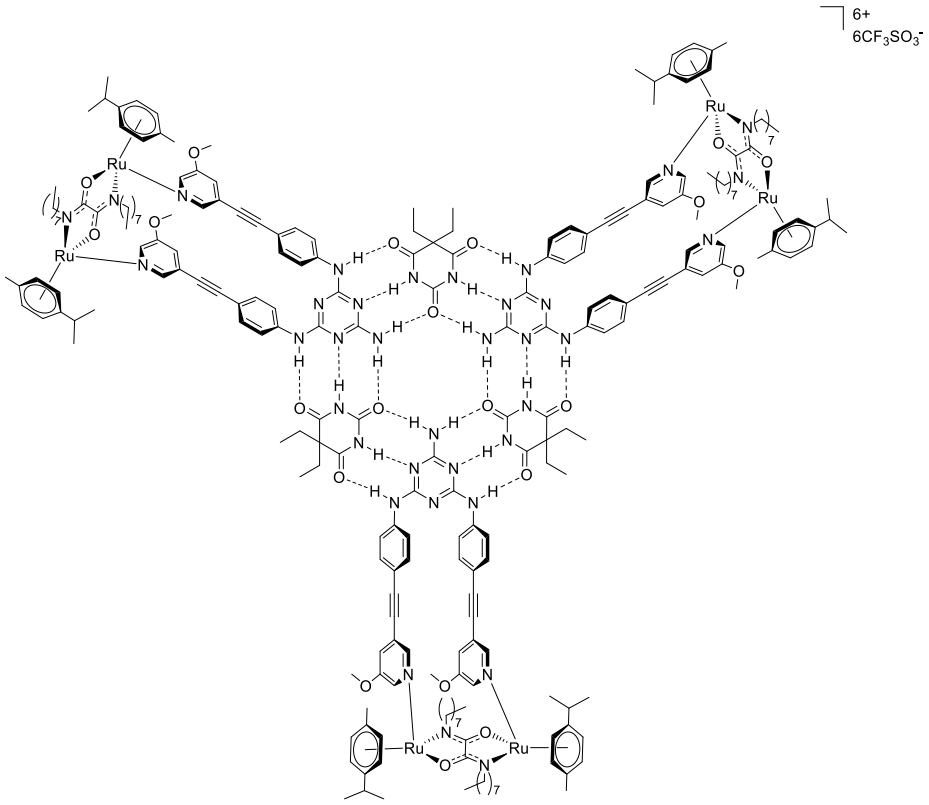

(MEbispyRu$_2$L^B)$_3$ · (BA)$_3$

List of figures

List of schemes

List of tables

List of publications and conference contributions

Publications during the PhD studies:

1. W. Aboura, T. Benabdallah, **F. Zhang**, B. Therrien, Alkoxylation of the imine carbon atom of a Schiff-base ligand upon coordination to arene ruthenium, *Inorganica Chimica Acta*, Submission no: ICA_2018_642.

2. **F. Zhang**, B. Therrien, Using a Hydrogen-Bonded Rosette-Type Scaffold to Generate Heteronuclear Metalla-Assemblies, *European Journal of Inorganic Chemistry* **2018**, 2399-2407.
3. **F. Zhang**, B. Therrien, Coordination of Piano-Stool Complexes to a Hydrogen-Bonded Rosette-Type Assembly, *European Journal of Inorganic Chemistry* **2017**, 3214-3221.

Publications of previous work:

1. C. Basmadjian, **F. Zhang**, L. Désaubry, Novel carbocationic rearrangements of 1-styrylpropargyl alcohols, *Beilstein Journal of Organic Chemistry*, **2015**, 11, 1017-1022.

Conference Contributions:

1. **SCS Fall Meeting 2018**, Lausanne, Switzerland, 07/09/2018, Poster
2. **SCS Spring Meeting 2018**, Neuchâtel, Switzerland, 06/04/2018
3. **SCS Fall Meeting 2017**, Bern, Switzerland, 21/08/2017-22/08/2017, Poster
4. **ICREA Conference on Functional Nanocontainers 2016**, Tarragona, Spain, 17/10/2016-20/10/2016, Poster
5. **SCS Fall Meeting 2016**, Zurich, Switzerland, 15/09/2016, Poster